The impact of cytomegalovirus infection and viral vector vaccination on human and mouse immune systems



Hannah Rosalind Sharpe
St Edmund Hall
University of Oxford

A thesis submitted for the degree of
Doctor of Philosophy

Trinity term 2021
Word count: ~50,000 (excluding tables, figures legends, references and appendix)

The impact of cytomegalovirus infection and viral vector vaccination on human and mouse immune systems

Hannah Rosalind Sharpe, St Edmund Hall, University of Oxford

Abstract

Viral vectors are a next-generation vaccine platform that elicit a robust response from the humoral and cellular arms of the immune system. The importance of this vaccine platform was demonstrated during this PhD with the emergence of SARS-CoV-2 and the development of the chimpanzee adenovirus-vectored vaccine ChAdOx1 nCoV-19. Although this vaccine is immunogenic, pre-existing infections such as cytomegalovirus have been shown to reduce antigen-specific vaccine immunogenicity in other vaccines. Cytomegalovirus is a chronic herpesvirus that is prevalent in ~40-100% adults worldwide, and although infection is often asymptomatic it can increase the frequency of terminally differentiated immune cells in healthy young adults.

This thesis aims to characterise the effect of viral vectored vaccines including ChAdOx1 on immune populations not traditionally studied in vaccinology, including NK cells. It also investigates how cytomegalovirus impacts the immune phenotype and vaccine immunogenicity in humans and mice. This thesis demonstrates that viral vector vaccination activates NK cells and induces robust cytokine secretion in both mouse and human studies, although can affect NK cell phenotype following vaccination with MVA. Furthermore, CMV seropositivity elicits a terminally differentiated phenotype on the immune system, but does not affect viral vector vaccine immunogenicity following a single dose or homologous boost of ChAdOx1. Overall, these findings which are especially important for the ongoing vaccination regimen against SARS-CoV-2, and provide further insight into the interplay of viral vectored vaccines and viral infection on the immune system.

Acknowledgements

First and foremost, I would like to thank my supervisors, Professors Teresa Lambe, Sarah Gilbert, and Paul Klenerman, for their supervision and guidance throughout this PhD. Thank you for giving me the opportunity to work in this field and for sharing your expertise with me. I never anticipated when starting this PhD that it would be encompassed by a pandemic, which took the work of our lab to international renown. I have been inspired and driven by the motivation, professionalism, and sheer hard work of my supervisors and colleagues that will be motivation for the rest of my career.

This PhD could not be possible without the support from many members of the Jenner Institute and beyond. Especially; Dr Nick Provine, for many hours of running Aurora samples, answering science questions, and insight into life in America. Also, Dr Sandra Belij-Rammerstorfer and Dr Alex Spencer for the help and invaluable advice they have provided.

Special thanks must also go to all the FGF, BSB and Jenner Institute staff, and all the volunteers who participated in the clinical trials within this thesis. Also, to the Wellcome trust, for funding my D.Phil., and to my college, St Edmund Hall, for funding several travel grants.

My whole PhD experience has been made richer through the friendships built with my colleagues in the Jenner Institute, of whom there are so many they would need a supplementary list to name them all. Thank you especially to Liz Allen, Cameron Bissett, Katie Ewer, Danny Wright, Jon Sheridan, Amy Flaxman, Marta Ulaszewska, Leila Godfrey, Francesca Donnellan, Amelia Lias, Claire Hutchings, Rebecca Makinson, Duncan Bellamy,

Jeremy Aboagye and Fede Cappuccini. Also thank you to Georgie Bowyer, for starting the CMV work that formed the foundation of this thesis. I cannot forget to mention the other PhD students in the Lambe lab, who began this journey at the same time as me and without whom, this PhD experience would not have been the same. Jyothi – thank you for keeping me company during long cytometer sample runs, and for your friendship, support, and pictures of cats. Ciaran – for always being there to encourage me, but also not letting me forget about the time I didn't add primers to my PCR. We never figured out which one of us was Pinky, and which one was the Brain?

Outside the lab, I am grateful for the friendship of so many people. Agata – for the nights out and consequential hungover brunches. Abi – for being my Somerville (and soon to be America) bestie. The Hot Slug crew (Sarah, Jenny, Jordan, Sofia, Simon, Ewen and Fraser) for over a decade of friendship. And my housemates, who put up with me for three whole pandemic lockdowns. Cara, for our shared love of police dramas and reality TV. And Mari, who somehow has put up with me from when we met on the first day of our PhD.

Finally, thank you to my family; my parents, grandma, and brother, for their everlasting love and encouragement.

Table of contents

ACKNOWLEDGEMENTS III

LIST OF FIGURES XI

LIST OF TABLES XIII

LIST OF ABBREVIATIONS XIV

STATEMENT OF AUTHORSHIP XVII

CHAPTER 1 INTRODUCTION 2

1.1. THE IMMUNE SYSTEM 2
1.2.1. NATURAL KILLER CELLS 3
1.2.1.1. Mechanisms of NK cell activation 4
1.2.1.2. NK cell maturation and functional changes 6
1.2.1.3. NK cell tissue residency in the liver 8
1.2.1.4. NK cell memory 10
1.3. THE ADAPTIVE IMMUNE SYSTEM 12
1.3.1. T CELLS 13
1.3.1.1. $CD8^+$ T cells 14
1.3.1.2. $CD4^+$ T cells 15
1.3.2. MAIT CELLS 17
1.3.3. B CELLS 19
1.4. OVERVIEW OF VACCINES 20
1.4.1. FIRST-GENERATION VACCINES 21
1.4.2. NEXT GENERATION VACCINE PLATFORM TECHNOLOGY: NUCLEIC ACID VACCINES 22
1.4.3. NEXT GENERATION VACCINE PLATFORM TECHNOLOGY: RECOMBINANT VIRAL VECTORED VACCINES 23
1.4.3.1. ChAdOx1 and MVA 25
1.4.4. VACCINE DEVELOPMENT FOR EMERGING PANDEMIC PATHOGENS 28
1.5. EPIDEMICS AND PANDEMICS FEATURED IN THIS THESIS 28
1.5.1. SARS-COV-2 28
1.5.1.1. Epidemiology 28
1.5.1.2. SARS-CoV-2 virology 29
1.5.1.3. Immune response to SARS-CoV-2 29
1.5.1.4. Vaccines against SARS-CoV-2 30
1.5.2. INFLUENZA A 31
1.5.2.1. Epidemiology 31
1.5.2.2. Virology and immunology 31
1.5.2.3. Vaccines against influenza A 32
1.5.3. EBOLAVIRUS 34
1.5.3.1. Epidemiology 34
1.5.3.2. Virology and immunology 34
1.5.3.3. Vaccines against ebolavirus 35
1.6. CYTOMEGALOVIRUS 35
1.6.1. EPIDEMIOLOGY 35
1.6.2. IMMUNOLOGY OF CYTOMEGALOVIRUS IN MICE AND HUMANS 37

1.6.2.1. NK cells 37
1.6.2.2. T cells 40
1.6.2.3. Memory inflation 41
1.6.2.4. CMV and immunosenescence 42
1.6.2.5. Functionality of T cells with CMV infection 42
1.6.2.6. Cytomegalovirus and vaccine immunogenicity in clinical trials 44
1.7. THESIS OUTLINE AND AIMS 45

CHAPTER 2 MATERIALS AND METHODS 48

2.1. MATERIALS AND REAGENTS 48
2.1.1. GENERAL MATERIALS AND REAGENTS 48
2.1.2. HUMAN ANTIBODIES AND TETRAMERS (BD BIOSCIENCES FORTESSA CYTOMETER) 50
2.1.5. MOUSE DEPLETION ANTIBODIES 53
2.2. SOLUTIONS 54
2.2.1. R0 MEDIA 54
2.2.2. COMPLETE α-MEM/ R10 MEDIA 54
2.2.3. FACS BUFFER 54
2.2.4. PERCOLL GRADIENT SOLUTION 54
2.2.5. NK CELL ISOLATION BUFFER 54
2.3. MOUSE IMMUNOLOGY 54
2.3.1. ANIMALS 54
2.3.2. INFECTIONS 55
2.3.3. ANAESTHESIA 55
2.3.4. VACCINATIONS 55
2.3.5. NK CELL DEPLETION 56
2.3.6. PEPTIDES 56
2.3.7. TAIL VEIN BLEED PBMC PREPARATION 57
2.3.8. SPLENOCYTE PREPARATION 57
2.3.9. INGUINAL LYMPH NODE PREPARATION 57
2.3.10. LIVER PREPARATION 58
2.3.11. LUNG PREPARATION 58
2.3.12. NK CELL ISOLATION 59
2.3.13. MURINE IFN-γ ELISPOT 59
2.3.14. CELL STIMULATION 60
2.3.15. TETRAMER STAINING 60
2.3.16. MURINE CELLULAR SURFACE STAINING 61
2.3.17. MURINE INTRACELLULAR CYTOKINE STAINING 61
2.4. HUMAN IMMUNOLOGY 65
2.4.1. CLINICAL TRIALS STUDIED DURING THIS PHD 65
2.4.1.1. EBL04 65
2.4.1.2. FLU005 65
2.4.1.3. COV001/COV002 66
2.4.1.4. AspiFlu 66
2.4.2. PBMC DEFROSTING 67
2.4.3. PBMC STIMULATION 68
2.4.4. BD FORTESSA AND LSR-II ANTIBODY PANELS 68
2.4.5. CYTEK® AURORA PANEL DESIGN 70
2.4.6. HUMAN CELLULAR SURFACE STAINING 71
2.4.7. INTRACELLULAR CYTOKINE STAINING 72
2.4.8. ANTI-CMV IGG ELISA 72

2.5. DATA ANALYSIS **73**
2.5.1. FLOW CYTOMETRY ANALYSIS 73
2.5.2. TSNE PLOTS 73
2.5.3. STATISTICAL ANALYSIS 73
2.6. COVID-19 PRE-CLINICAL AND CLINICAL TRIAL SAMPLE PROCESSING AND ASSAY SET UP. **74**
2.6.1. RHESUS MACAQUE AND FERRET PBMC SEPARATION 74
2.6.2. CLINICAL TRIAL PBMC SEPARATION 74
2.6.2.1. COV001/COV002 74
2.6.2.2. COV006 75
2.6.3. CLINICAL TRIAL ELISPOT SET UP 76
2.6.3.1. General protocol for COV001/COV002 and COV006 76
2.6.4. COV001/COV002 CLINICAL TRIAL INTRACELLULAR CYTOKINE STAINING (ICS) SET UP 76
2.6.5. PBMC SAMPLE FREEZE DOWN 77

CHAPTER 3 : VIRAL VECTOR VACCINATION AND THE MURINE NK CELL RESPONSE 79

3.1. INTRODUCTION AND AIMS **79**
3.2. RESULTS **82**
3.2.1. T CELL ACTIVATION AND MIGRATION FOLLOWING VIRAL VECTOR AND INACTIVATED VIRUS VACCINATION 82
3.2.2. T_{REG} AND T FOLLICULAR REGULATORY CELLS AND VIRAL-VECTOR VACCINATION 85
3.2.3. NK CELLS ARE ACTIVATED AND PRODUCE IFN-γ IN RESPONSE TO PEPTIDE STIMULATION AFTER VACCINATION 87
3.2.4. NK CELLS FROM VACCINATED MICE REQUIRE ACCESSORY CELLS TO PRODUCE IFN-γ AFTER VACCINATION 90
3.2.5. CHADOX1 VACCINATION DOES NOT ALTER NK CELL MATURITY OR EXPRESSION OF ACTIVATING RECEPTORS 92
3.2.6. MVA VACCINATION ALTERS PHENOTYPE AND MATURATION OF NK CELLS 95
3.2.7. RECEPTOR EXPRESSION AND ACTIVATION OF NK CELL MATURATION SUBSETS IS ALTERED BY VIRAL VECTOR VACCINATION 97
3.2.8. HETEROLOGOUS AND HOMOLOGOUS PRIME-BOOST VIRAL VECTOR VACCINATION EMPHASISE THE MVA-DRIVEN NK CELL PHENOTYPE. 101
3.2.9. INACTIVATED VIRION VACCINATION AND THE NK CELL PHENOTYPE 105
3.2.10. VIRAL VECTOR VACCINATION INDUCES DIFFERENT CELL DEATH PATHWAYS 107
3.2.11. NK CELL DEPLETION IN A MOUSE VIRAL VECTOR VACCINATION MODEL 109
3.3. DISCUSSION **115**
3.3.1. T CELL ACTIVATION AND REGULATORY T CELL POPULATIONS AFTER VACCINATION 115
3.3.2. NK CELL MEMORY AND CYTOKINE RESPONSE AFTER VACCINATION 116
3.3.3. MVA VACCINATION AND NK CELL PHENOTYPE 118

CHAPTER 4 : THE HUMAN NK CELL AND T CELL RESPONSE TO VIRAL-VECTORED VACCINES 124

4.1. INTRODUCTION AND AIMS **124**
4.2. RESULTS **126**
4.2.1. HEALTHY ADULTS AGED 18-55 VACCINATED WITH CHADOX1 NCOV-19 DEMONSTRATE SIGNIFICANT ACTIVATION AND PROLIFERATION OF CELL SUB-POPULATIONS UP TO 28 DAYS POST-VACCINATION 126
4.2.1.1. NK cells are activated, proliferate, and produce cytokines in response to vaccination 128
4.2.1.2. T cells are activated, proliferate, and produce cytokines in response to vaccination 130
4.2.1.3. B cells 134
4.2.2. COMPARISON OF SINGLE DOSE AND HETEROLOGOUS PRIME-BOOST VACCINATION WITH CHADOX1 AND MVA EXPRESSING INFLUENZA ANTIGENS NP AND M1 IN HEALTHY ADULTS. 134
4.2.2.1. tSNE analysis following ChAdOx1-prime, MVA-boost vaccination 135

4.2.2.2. NK cell activation and functionality after single dose and heterologous prime-boost vaccination 137
4.2.2.3. T cell responses to prime-boost vaccination 140
4.2.2.4. B cell responses to prime-boost vaccination 142
4.2.3. ALTERED NK CELL RESPONSE TO VACCINATION CORRELATES WITH CMV INFECTION IN AN EBOLAVIRUS VACCINE TRIAL. 142
4.2.3.1. NK cell IFN-γ reduction in CMV$^+$ individuals after prime-boost vaccination 143
4.3. DISCUSSION 147
4.3.1. SINGLE-DOSE CHADOX1 ACTIVATES AN IMMUNE RESPONSE IN MULTIPLE CELLULAR COMPARTMENTS 147
4.3.2. HETEROLOGOUS CHADOX1-MVA VACCINATION BOOSTS IMMUNE RESPONSE IN MULTIPLE CELLULAR COMPARTMENTS 149

CHAPTER 5 : ACUTE AND CHRONIC CMV INFECTION ON ACTIVATION OF INNATE AND ADAPTIVE IMMUNE CELLS IN A MOUSE MODEL 154

5.1. INTRODUCTION AND AIMS 154
5.2. RESULTS 158
5.2.1. NK CELL MATURATION AND ACTIVATION DURING ACUTE MCMV INFECTION 158
5.2.1.1. NK cell activation occurs during acute MCMV infection 158
5.2.2. TISSUE-RESIDENT NK CELLS ARE ENRICHED IN THE LIVER 160
5.2.2.1. Frequency dynamics of circulating and tissue resident NK cells in MCMV infection 161
5.2.2.2. Changes in frequency of CD49a$^+$ and CXCR6$^+$ DX5$^+$NK1.1$^+$ cNK cells during acute infection 163
5.2.2.3. Activation and polyfunctionality of DX5$^+$NK1.1$^+$ cNK cells during acute infection 165
5.2.2.4. Changes in frequency of CD49a$^+$ and CXCR6$^+$ DX5$^-$NK1.1$^+$ trNK cells during acute and chronic infection 168
5.2.2.5. Activation, cytokine expression and polyfunctionality of DX5$^-$NK1.1$^+$ NK cells 170
5.2.2.6. Enhanced cytokine secretion and degranulation of trNK cells during MCMV infection 174
5.2.3. T CELL PHENOTYPE AND ACTIVATION DURING ACUTE AND CHRONIC MCMV INFECTION 176
5.2.3.1. The frequencies of regulatory T cell populations during acute and chronic MCMV infection 176
5.2.3.2. T cell activation during acute and chronic MCMV infection 178
5.2.4. MAIT CELL AND T CELL ACTIVATION BY MCMV INFECTION 180
5.2.4.1. MAIT cell activation in chronic MCMV infection 180
5.2.4.2. T cell and MAIT cell activation during acute MCMV infection 182
5.2.5. PHENOTYPE OF NK CELLS AND RESPONSE TO VACCINATION IN MR1$^{-/-}$ MICE 186
5.2.5.1. The NK cell response in vaccinated MR1$^{-/-}$ mice compared to C57BL/6 mice 187
5.2.6. DEVELOPMENT OF A MOUSE MODEL OF MCMV INFECTION AND VIRAL VECTOR VACCINATION 187
5.3. DISCUSSION 190
5.3.1. NK CELL RESPONSES TO MCMV INFECTION 190
5.3.2. T CELL RESPONSES TO MCMV INFECTION 195
5.3.3. MAIT CELL RESPONSES TO MCMV INFECTION 196

CHAPTER 6 : CMV INFECTION AND THE IMMUNE RESPONSE TO VIRAL VECTOR VACCINATION IN CLINICAL TRIALS 199

6.1. INTRODUCTION AND AIMS 199
6.2. RESULTS 203

6.2.1. CMV SEROTYPING OF YOUNGER ADULTS AGED 18-55 VACCINATED WITH A SINGLE DOSE, HOMOLOGOUS, OR HETEROLOGOUS PRIME-BOOST CHADOX1 AND MVA REGIMEN 203
6.2.2. BACKGROUND IMMUNITY AND CMV SEROSTATUS IN 18–55-YEAR-OLD TRIAL PARTICIPANTS 205
6.2.3. STRATIFICATION OF THE CELLULAR IMMUNE RESPONSE BY CMV SEROSTATUS IN SINGLE-DOSE, HOMOLOGOUS, AND HETEROLOGOUS CHADOX1 AND MVA VACCINATION REGIMENS. 207
6.2.4. T CELL DIFFERENTIATION AND MEMORY POPULATIONS WITH CMV SEROSTATUS 210
6.2.5. T CELL ACTIVATION AND FUNCTIONALITY WITH CMV SEROSTATUS 213
6.2.6. TOTAL IGG ANTIBODY RESPONSES TO SINGLE-DOSE, HOMOLOGOUS AND HETEROLOGOUS PRIME-BOOST VACCINATION STRATIFIED BY CMV SEROSTATUS 216
6.2.7. B CELL MEMORY WITH CMV SEROSTATUS 219
6.2.8. NK CELL PHENOTYPE AND CMV SEROSTATUS 219
6.2.9. NK CELL RESPONSE TO VACCINATION REGIMENS AND CMV SEROSTATUS 221
6.2.10. CMV SEROTYPE AND VACCINE RESPONSE IN OLDER AGE ADULTS 225
6.2.10.1. CMV serotyping COV002 and FLU005 older adults. 225
6.2.11. PRE-EXISTING IMMUNITY IN THE OLDER ADULT COHORTS 226
6.2.12. OLDER ADULT IFN-γ ELISPOT RESPONSES WITH CMV SEROSTATUS 227
6.2.13. HUMORAL RESPONSES TO SINGLE DOSE, HOMOLOGOUS AND HETEROLOGOUS PRIME BOOST VACCINATION IN OLDER ADULTS STRATIFIED BY CMV SEROSTATUS 229
6.3. DISCUSSION 232
6.3.1. NK CELL PHENOTYPE AND FUNCTIONALITY 232
6.3.2. T CELL PHENOTYPE AND FUNCTIONALITY WITH CMV SEROSTATUS 235

CHAPTER 7 : THE COVID-19 PANDEMIC AND SARS-COV-2 VACCINE TRIALS 240

7.1. INTRODUCTION 240
7.2. WORK CONDUCTED DURING THE PANDEMIC 241
7.2.1. PRE-CLINICAL SAMPLE PROCESSING 241
7.2.2. CLINICAL TRIALS SAMPLE PROCESSING 241
7.2.3. THE IMPACT OF SEVERE INFLUENZA A AND COVID-19 ON THE IMMUNE SYSTEM 242
7.2.3.1. Cohort and study description 242
7.2.3.2. T cell activation and senescence 243
7.2.3.3. T cell memory profile 245
7.2.3.4. T cell cytokine production 247
7.2.3.5. NK cells activation and cytokine secretion during influenza A and SARS-CoV-2 infection 249
7.2.3.6. NK cell and T cell polyfunctionality in COVID-19 and IAV donors. 253
7.2.3.7. B cell phenotype in IAV and COVID-19 infection. 255
7.3. DISCUSSION 257
7.3.1. SARS-COV-2 INFECTION AND INFLUENZA A INFECTION ELICIT AN ABERRANT IMMUNE PROFILE 257
7.4. PAPERS PUBLISHED FROM PRE-CLINICAL AND CLINICAL TRIAL WORK OUTLINED IN THIS CHAPTER 260

CHAPTER 8 : CONCLUSIONS AND FUTURE DIRECTIONS 268

8.1. OVERVIEW 268
8.2. SUMMARY, LIMITATIONS AND FUTURE DIRECTIONS 269
8.2.1. VACCINATION WITH SINGLE DOSE, HOMOLOGOUS, OR HETEROLOGOUS VIRAL VECTOR VACCINES ALTER THE ACTIVATION AND SENESCENCE PROFILE OF NK CELLS IN A MOUSE MODEL 269
8.2.2. SINGLE DOSE AND HETEROLOGOUS BOOST VIRAL VECTOR VACCINATIONS ACTIVATE NK CELLS AND T CELLS 271
8.2.3. MCMV ACTIVATES TISSUE RESIDENT NK CELLS AND NON-CLASSICAL T CELLS 271

8.2.4. CMV SEROPOSITIVITY INDUCES A TERMINALLY DIFFERENTIATED IMMUNE PHENOTYPE AND REDUCES HETEROLOGOUS VACCINE IMMUNOGENICITY 273
8.3. FINAL REMARKS **274**

REFERENCES **275**

APPENDIX **307**

List of Figures

Figure 1.1. Human innate and adaptive immune cells 3
Figure 1.2 Maturational axes of NK cells in mice and humans 8
Figure 1.3. Intracellular expression of encoded antigen and immune activation by ChAdOx1 vaccination 26
Figure 1.4. Phylogenetic tree of human herpesviruses 36
Figure 3.1 Activation of T cells after vaccination with viral vector or split virion vaccines 84
Figure 3.2. Changes in frequency of regulatory T cell populations after vaccination 86
Figure 3.3. NK cell activation and IFN-gamma production post-vaccination 89
Figure 3.4. IFN-gamma production by whole splenocytes and isolated murine NK cells post-vaccination 91
Figure 3.5. ChAdOx1 vaccination and NK cell phenotype 94
Figure 3.6. MVA vaccination and NK cell phenotype 96
Figure 3.7. ChAdOx1 and MVA vaccination alters the phenotype of NK cells within maturational subsets 99
Figure 3.8. Homologous and heterologous ChAdOx1 and MVA vaccination alters the phenotype of NK cells within maturational sub-populations 104
Figure 3.9 CD11b^{+} and Ly49H^{+} NK cells after ChAdOx1-MVA or inactivated virion vaccination 106
Figure 3.10. Apoptosis and necroptosis of cells following vaccination 108
Figure 3.11. NK cell depletion in C57BL/6JOlaHsd mice 110
Figure 3.12. Changes in activation status of T cells following NK cell depletion and vaccination 111
Figure 3.13. Changes in T cell memory populations following NK cell depletion and vaccination 112
Figure 3.14 Changes in cytokine production and cytotoxicity of T cells following NK cell depletion and vaccination 114
Figure 4.1. t-SNE analysis of live unstimulated lymphocytes from 26 ChAdOx1 nCoV-19 vaccinated donors 127
Figure 4.2. NK cell activation post ChAdOx1 nCoV-19 vaccination 129
Figure 4.3. T cell activation and cytokine production post ChAdOx1 nCoV-19 vaccination 131
Figure 4.4. Correlation of T cell IL-2 secretion and NK cell activation 133
Figure 4.5. t-SNE analysis of live unstimulated lymphocytes from 10 ChAdOx1 NP+M1 prime, MVA NP+M1 boost vaccinated donors 136
Figure 4.6. NK cell activation and cytokine production following ChAdOx1 and MVA prime- and prime-boost vaccination 138
Figure 4.7. T cell activation and cytokine production following single dose and heterologous ChAdOx1 and MVA vaccination. 141
Figure 4.8. Expansion of CMV-specific NK cell populations 144
Figure 4.9. Production of inflammatory mediators by NK cells post-vaccination stratified by CMV serostatus 146
Figure 5.1. Frequencies of surface markers on NK cells in mice with acute and chronic MCMV infection. 159
Figure 5.2. NK cell phenotypes in the spleen and liver 160
Figure 5.3. The frequencies of circulating and tissue-resident NK cells in the spleen and liver during acute and chronic MCMV infection. 162
Figure 5.4. The frequency of CXCR6+ and CD49a+ DX5+NK1.1+ NK cells during acute and chronic MCMV infection 164
Figure 5.5. Cytokine production and polyfunctionality of DX5+NK1.1+ cNK cells 166
Figure 5.6. The frequency of CXCR6^{+} and CD49a^{+} DX5^{-}NK1.1^{+} trNK cells during acute and chronic MCMV infection. 169
Figure 5.7. Cytokine production and polyfunctionality of DX5^{-}NK1.1^{+} trNK cells 172
Figure 5.8. The frequency of NK cells expressing at least one cytokine post-MCMV infection 175
Figure 5.9. Frequencies of CD4^{+} regulatory T cell populations in MCMV-infected mice 177
Figure 5.10. Frequencies of surface markers on the T cells of MCMV-infected mice 179
Figure 5.11. 50-day and 7-day MCMV infection and the frequency of CD25^{+} and CD69^{+} MAIT cells in the inguinal LN and lungs. 181
Figure 5.12. 1-day, 4-day, and 7-day MCMV infection transiently activates CD4^{+} and CD8^{+} T cells 183
Figure 5.13. Activation of MAIT cells after 1-day, 4-day, and 7-day MCMV infection 185
Figure 5.14. The phenotype of NK cells in C57BL/6J and MR1$^{-/-}$ mice 186
Figure 5.15. The functionality of NK cells in C57BL/6J and MR1$^{-/-}$ mice 187
Figure 5.16. The T cell response in viral vector vaccinated mice with or without MCMV infection 189
Figure 6.1. Pre-existing immunogenicity to SARS-CoV-2 and Influenza A antigens in younger adults. 206

FIGURE 6.2. CELL IFN-GAMMA ELISPOT RESPONSE FOLLOWING SINGLE DOSE, HOMOLOGOUS AND HETEROLOGOUS BOOSTING STRATIFIED BY CMV SEROSTATUS. 209
FIGURE 6.3. T CELL TERMINAL DIFFERENTIATION AND MEMORY POPULATIONS WITH CMV INFECTION 212
FIGURE 6.4. T CELL ACTIVATION AND CYTOKINE PRODUCTION WITH CMV SEROSTATUS 214
FIGURE 6.5. ANTIBODY ELISA RESPONSE TO SINGLE DOSE, HOMOLOGOUS AND HETEROLOGOUS VACCINATION STRATIFIED BY CMV SEROSTATUS. 218
FIGURE 6.6. NK CELL PHENOTYPE WITH CMV SEROSTATUS 220
FIGURE 6.7. ACTIVATION AND CYTOTOXIC RESPONSE OF NK CELLS TO VACCINE PEPTIDES WHEN STRATIFIED BY CMV SEROSTATUS. 223
FIGURE 6.8. PRE-EXISTING IMMUNE RESPONSES TO SARS-COV-2 AND INFLUENZA A IN OLDER ADULTS 227
FIGURE 6.9. ELISPOT T CELL IFN-GAMMA IN COV002 TRIAL GROUP 7B AND GROUP 8B AND FLU005 GROUPS 5 AND 6 STRATIFIED BY CMV SEROSTATUS. 228
FIGURE 6.10. ELISPOT T CELL IFN-GAMMA AND TIGG ELISA RESPONSES IN COV002 TRIAL GROUP 7B AND GROUP 8B AND FLU005 GROUPS 5 AND 6 231
FIGURE 7.1. THE ACTIVATION AND DIFFERENTIATION PROFILE OF T CELLS IN IAV AND COVID-19 244
FIGURE 7.2. $CD4^+$ AND $CD8^+$ T CELL MEMORY POPULATIONS 246
FIGURE 7.3. THE CYTOKINE AND INFLAMMATORY MARKER PROFILE OF STIMULATED T CELLS FROM IAV AND COVID-19 PATIENTS 248
FIGURE 7.4. NK CELL PHENOTYPE AND ACTIVATION IN PATIENTS WITH SEVERE COVID-19 AND INFLUENZA A 250
FIGURE 7.5. THE NK CELL CYTOKINE AND INFLAMMATORY MEDIATOR RESPONSE TO SEVERE COVID-19 AND INFLUENZA A 252
FIGURE 7.6. THE CYTOKINE AND INFLAMMATORY MARKER PROFILE OF STIMULATED T CELLS FROM IAV AND COVID-19 PATIENTS 252
FIGURE 7.7. POLYFUNCTIONALITY OF NK CELLS, $CD4^+$ AND $CD8^+$ T CELLS FOLLOWING STIMULATION WITH COVID-19 OR IAV PEPTIDES 254
FIGURE 7.8. B CELL ACTIVATION AND MEMORY POPULATIONS 256

List of Tables

TABLE 1.1. NK CELL RECEPTORS IN MICE AND HUMANS 4
TABLE 1.2. VACCINE TYPES AND EXAMPLES 22
TABLE 1.3. VIRAL-VECTORED VACCINES IN PUBLISHED CLINICAL TRIALS AND LICENSED AROUND THE WORLD 24
TABLE 1.4. CLINICAL TRIALS FOR CHADOX1 AND MVA-VECTORED VACCINES 27
TABLE 1.5. HCMV GENES THAT ALTER ACTIVATION OF NK CELLS 38
TABLE 1.6. HCMV GENES INVOLVED IN T CELL INHIBITION 41
TABLE 2.1. REAGENTS AND MATERIALS USED IN THIS THESIS 49
BLE 2.2. HUMAN-TARGET ANTIBODIES USED IN THIS THESIS ON THE BD BIOSCIENCES FORTESSA CYTOMETER 50
TABLE 2.3. HUMAN-TARGET ANTIBODIES USED IN THIS THESIS ON THE CYTEK AURORA SPECTRAL CYTOMETER 51
TABLE 2.4. MOUSE-TARGET ANTIBODIES AND TETRAMERS USED IN THIS THESIS 53
TABLE 2.5. MOUSE DEPLETION ANTIBODIES USED IN THIS THESIS 53
TABLE 2.6. VACCINES FOR MURINE VACCINATION 56
TABLE 2.7. MOUSE NK CELL PANEL 1: MATURATION AND ACTIVATION 62
TABLE 2.8. MOUSE NK CELL PANEL 2: NK CELL MEMORY 62
TABLE 2.9. MOUSE T_{REG} PANEL 63
TABLE 2.10. MOUSE MAIT CELL PANEL 63
TABLE 2.11. MOUSE T CELL ACTIVATION PANEL 64
TABLE 2.12. MOUSE APOPTOSIS AND NECROPTOSIS PANEL 64
TABLE 2.13. VACCINES USED IN CLINICAL TRIALS STUDIED IN THIS THESIS 67
TABLE 2.14. HUMAN NK CELL PANEL 68
TABLE 2.15. HUMAN T_{REG}/T_{FR} PANEL 69
TABLE 2.16. AURORA CYTOMETER PANEL 71
TABLE 3.1. T CELL MARKERS OF ACTIVATION, MEMORY AND EXHAUSTION 82
TABLE 3.2. POPULATIONS AND DEFINING MARKERS OF REGULATORY T CELLS, FOLLICULAR HELPER T CELLS, AND FOLLICULAR REGULATORY T CELLS 85
TABLE 3.3. MATURATION, ACTIVATING AND INHIBITORY RECEPTORS ON MURINE NK CELLS 93
TABLE 3.4. CELL DEATH PATHWAYS 107
TABLE 4.1. THE FLU005 TRIAL GROUPS, PRIME VACCINE, BOOST VACCINE, AND DATE OF BOOST VACCINE 135
TABLE 5.1. MARKERS OF ACTIVATION, SENESCENCE AND MIGRATION ON T CELLS 178
TABLE 6.1. DETAILS OF COV001 GROUPS 1 AND 3, COV002 GROUP 5D, AND FLU005 GROUPS 1-4 VACCINATION REGIMENS 204
TABLE 6.2. COV002 GROUPS 7B AND 8B AND FLU005 GROUPS 5 AND 6 226

List of abbreviations

ACE-2	Angiotensin-converting enzyme 2
Ad	Adenovirus
ADCC	Antibody-dependent cellular cytotoxicity
AIDS	Acquired immunodeficiency syndrome
APC	antigen presenting cell
BCG	Bacille Calmette Guérin
BCR	B cell receptor
ChAdOx1	Chimpanzee adenovirus Ox1
cHCW	convalescent healthcare worker
CMV	Cytomegalovirus
cNK	circulating NK cells
CoV	Coronavirus
CTLA-4	Cytotoxic T lymphocyte-associated protein 4
DC	Dendritic cells
EAU	ELISA arbitrary units
EBOV	Ebolavirus
EBV	Epstein-Barr virus
ELISA	Enzyme linked immunosorbent assay
ELISpot	Enzyme-linked immunospot assay
EVD	Ebolavirus disease
Fab	Fragment antigen binding
Fc	Fragment crystallizable
FOXP3	Forkhead box P3
GC	Germinal centre
GP	Glycoprotein
HA	Haemagglutinin
hAd	human adenovirus
HBV	Hepatitis B virus
HC	Healthy control
HCMV	Human cytomegalovirus
HCV	Hepatitis C virus

HSV-1/2	Herpes simplex virus 1 or 2
IAV	Influenza A virus
ICS	Intracellular cytokine staining
IFN-γ	Interferon gamma
IL	Interleukin
iLN	Inguinal lymph node
ILC	Innate lymphoid cells
Ig	Immunoglobulin
i.m.	Intramuscular
i.u.	Infectious units
KLRG1	Killer lectin-like receptor G1
LA	Live attenuated
LMIC	Lower-middle income country
M1	Matrix 1
MAIT	Mucosal associated invariant T
MARV	Marburg virus
MCMV	Murine cytomegalovirus
MHC	Major histocompatibility complex
MLKL	Mixed lineage kinase-like protein
MVA	Modified Vaccinia Ankara
NA	Neuraminidase
NCR	Natural cytotoxicity receptors
NHP	Non-human primate
NK	Natural killer
NOD	Nucleotide-binding oligomerization domain
NP	Nucleoprotein
OVA	Ovalbumin
PAMPs	Pathogen associated molecular patterns
PBMC	Peripheral blood mononuclear cells
PD-1	Programmed cell death protein 1
PFU	Plaque-forming units
PMN	Polymorphonucleocytes

PRR	Pattern recognition receptors
RIG-I	Retinoic acid-inducible gene I
RIPK3	Receptor interacting protein kinase 3
RT	Room temperaturex
SARS	Severe acute respiratory syndrome
SFU	Spot forming units
SLO	Secondary lymphoid organ
SPF	Specific pathogen free
SUDV	Sudan virus
TCR	T cell receptor
T_{CM}	Central memory T cell
T_{EFF}	Effector T cell
T_{EM}	Effector memory T cell
T_{EMRA}	Effector memory T cell expressing CD45RA
T_{FH}	T follicular helper
T_{FR}	T follicular regulatory cell
T_{reg}	T regulatory cell
TLR	Toll-like receptor
TNF	Tumor necrosis factor
trNK	Tissue-resident NK cell
VSV	Vesicular stomatitis virus
VZV	Varicella Zoster virus
WHO	World Health Organisation
WT	Wildtype

Statement of Authorship

This thesis has been written by Hannah Sharpe, and all experiments presented have been conducted by Hannah Sharpe, unless otherwise described. Mouse experiments were assisted by Dr Claire Hutchings and Marta Ulaszewska, and mouse sample processing was assisted in part by Ciaran Gilbride, Jyothi Purushotham, Cameron Bissett and Dr Sandra Belij-Rammerstorfer. Clinical trial sample processing, and ELISpot and ELISA data collection was conducted by the COVID-19 vaccine trial group, or the FLU005 or EBL04 trial scientists. COV001 and AspiFlu PBMC staining and Aurora cytometry was assisted by Dr Nicholas Provine, and EBL04 NK cell staining was assisted by Dr Georgina Bowyer. All other analysis was conducted by Hannah Sharpe.

Chapter 1
Introduction

Chapter 1 Introduction

1.1. The immune system

The immune system acts as the protective barrier between an organism and infectious pathogens (Figure 1.1). Comprising a fast-responding innate arm, and an adaptive arm which forms long-lasting memory, the immune system is able to detect, neutralise, and protect against future pathogenic encounters.

1.2. The innate immune system

The innate immune system is the first line of defence against pathogens. Descending from the common myeloid progenitor cells in the bone marrow, the innate immunocytes consists of monocytes, macrophages, dendritic cells, NK cells and polymorphonucleocytes (PMN; basophils, eosinophils, mast cells and neutrophils). Another population of cells, the innate lymphoid cells (ILCs) also contribute towards the innate immune response and have a phenotype reflective of adaptive $CD4^+$ T cells (Figure 1.1)(1). Innate immune cells encode germline pattern recognition receptors (PRRs) that recognise pathogen-associated molecular patterns (PAMPs). PRRs are non-recombining receptors including Toll-like receptors (TLR), nucleotide-binding oligomerisation domain-like (NOD-like) receptors, and retinoic acid-inducible gene I (RIG-I) receptors, which between them recognise PAMPs including DNA, RNA, lipids and proteins from pathogens that are not expressed by human cells. Activation of PRRs induces a fast, non-specific cytotoxic response that primarily acts to eliminate pathogens, but can also activate other populations of immune cells. This occurs either indirectly through release of cytokines, or directly through antigen presentation on major histocompatibility (MHC) molecules to adaptive lymphocytes (2).

The acellular complement system facilitates pathogen removal by interacting with complement-binding antibodies to opsonise cells and activate inflammation (3).

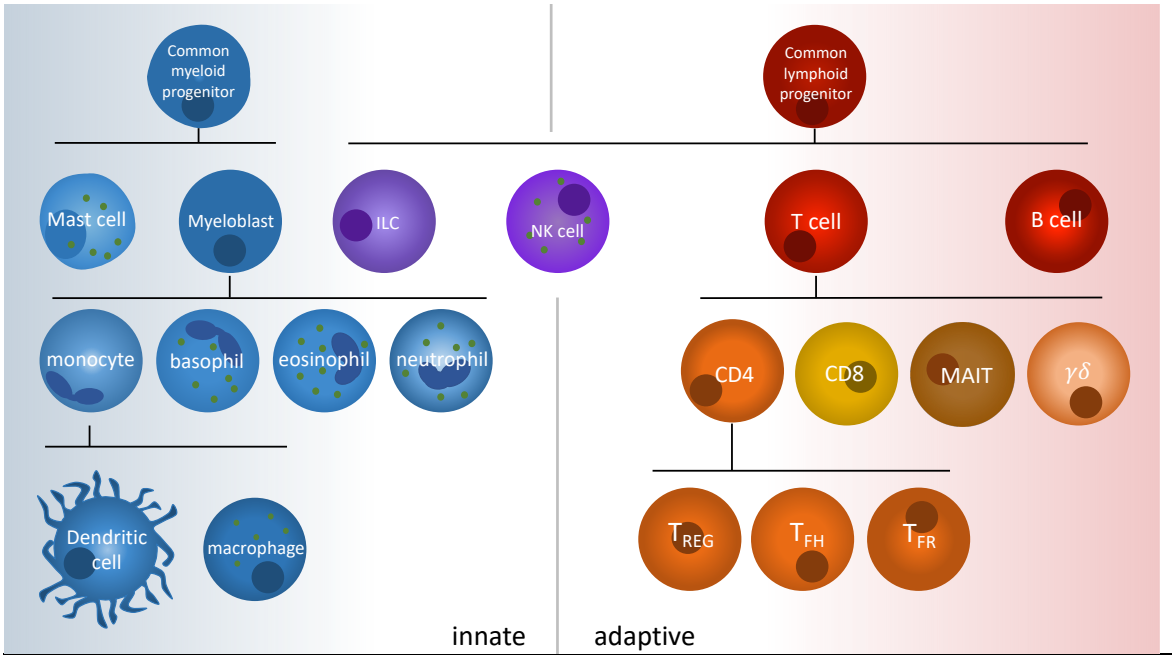


Figure 1.1. Human innate and adaptive immune cells

1.2.1. Natural Killer cells

Natural killer (NK) cells are lymphoid progenitor-derived innate immune cells that transcend the division between the innate and adaptive immune system. They constitute approximately 10% of lymphocytes in the peripheral blood (4) and are highly cytotoxic, facilitating a rapid innate response towards pathogen-infected cells and tumours (5). NK cells and T cells share the same lymphoid progenitor, express many common cell surface markers, and respond in a similar way to stimulus by production of inflammatory cytokines including interferon gamma (IFN-γ) and tumour necrosis factor (TNF), and direct cellular cytotoxicity through the release of granules with perforin and granzyme (6). NK cells also have a regulatory function on the T cell response during pathogen infection, which controls inflammation and prevents immunopathology to organs (7, 8).

1.2.1.1. Mechanisms of NK cell activation

NK cells have a heterogeneous cell surface profile and express numerous families of activating and inhibitory cell-surface receptors (table 1.1) (9). These receptors are germline-encoded and do not undergo somatic rearrangement (4, 6).

Receptor group	Species	Inhibitory receptors	Activating receptors
NKG2	Mouse and human	NKG2A	NKG2C NKG2E NKG2D
Natural cytotoxicity	Mouse and human	N/A	nKp46 nKp30 (human) nKp44 (human) nKp80 (human)
Ly49	Mouse	Ly49E Ly49I Ly49C Ly49F Ly49G	Ly49H Ly49D
KIR	Human	KIR2DL1 KIR2DL2 KIR2DL3 KLR2DL4 KLR2DL5 KIR3DL1 KIR3DL2 KIR3DL3	KIR2DS1 KIR2DS2 KIR2DS3 KIR2DS4 KIR2DS5 KIR3DS1

Table 1.1. NK cell receptors in mice and humans. Adapted from (10)

The NKG2 receptors are part of the C-type lectin-like family, which dimerise with CD94 and are present in mice and humans. They encode the inhibitory receptor NKG2A, and the activating receptors NKG2C/E/D (10), and recognise self and viral antigens presented by MHC-E on the cell surface (11). The natural cytotoxicity receptors (NCR) are up-regulated on activated NK cells, and include nKp30, nKp44, and nKp46 in humans, and nKp46 in mice (10). The Ly49 receptors are murine-specific type II transmembrane glycoproteins which

recognise MHC class I molecules in mice (12). The analogous receptors in human are encoded by human killer-cell Ig-like (KIR) receptors (10), which recognise HLA class I molecules and can act as inhibitory and activating receptors and mediate 'missing self' activation (13), for example, the inhibitory KIRs KIR2DL1 and KIR2DL3 recognise HLA-C, and KIR3DL2 recognises HLA-A expressed on healthy cells (14). The activating KIR KIR2DS1 can also recognise HLA-C, albeit with a lower affinity than KIR2DL1 (13). $Ly49^+$ and KIR^+ NK cells that do not express inhibitory receptors for self-HLA class I are 'non-educated' and lack cytotoxicity (15); cytotoxic function is gained through 'licensing' of immature NK cells by expression of receptors that recognise self-MHC class I alleles, which enhances effector function upon future activation and promotes self-tolerance (10, 16). NK cells expressing KIR can also recognise pathogen infected cells, for example the activating KIR KIR2DS2 can recognise conserved helicase peptides within flaviviruses including HCV, Dengue virus and Zika virus presented by the HLA-C*0102 allele (17). NK cells can also be activated by recognition of antibodies via the FcγRIII (CD16) receptor and exert antibody-dependent cellular cytotoxicity on infected cells (4). Other immune cells can also induce NK cell activation; type I interferon and interleukin (IL)-15 signalling from dendritic cells (DCs) induces NK cell cytotoxicity and proliferation (18, 19), whereas DC-mediated exposure to IL-12 and IL-18 leads to IFN-γ secretion (18, 20, 21). Furthermore, IL-2 from antigen-specific $CD4^+$ T cells can activate NK cells via IL-2R (CD25) and enhance NK cell functionality (22). NK cells respond to activation by cytokine secretion and direct cellular cytotoxicity through degranulation and perforin production, which initiate a robust antiviral response during early infection (23) and can also activate other lymphocyte populations and induce $CD4^+$ T cell maturation towards an inflammatory Th1 profile (24). NK cells also express TNF-related apoptosis-inducing ligand (TRAIL), which interacts with TRAIL receptor-expressing cells and

mediates apoptosis (25). Multiple pathogens and vaccinations have been demonstrated *in vivo* and *in vitro* to activate NK cells, including hantavirus, cytomegalovirus, chikungunya virus, Epstein-Barr virus, and HIV (15) and BCG, ad26 and yellow fever virus 17D vaccine, respectively (15, 26).

1.2.1.2. NK cell maturation and functional changes

NK cell maturity, tissue residency, and memory capacity are intersectional and define the properties and functionality of an NK cell. CD27 can define mouse and human NK cell maturity along an axis (9, 27); $CD27^-$ populations are more mature than $CD27^+$ NK cells and undergo sequential maturation involving CD11b expression (28). In mice, the $CD11b^-CD27^+$ phenotype represents the least mature population of NK cells that express the highest frequency of NKG2 receptors and respond to activation with cytokine secretion (9, 23). Mature $CD11b^+CD27^+$ exert greater cellular cytotoxicity by degranulation, and are activated most robustly by cytokine exposure (9, 23). The most mature $CD11b^+CD27^-$ NK cells express a higher frequency of KLRG1 and Ly49 receptors and lower levels of NKG2 receptors and are the most cytotoxic subset (figure 1.2A)(9, 23), As demonstrated by Hayakawa *et al*, and also within this thesis, tissue distribution varies with NK cell maturational stage (23, 29), with the most mature NK cells predominantly in the peripheral blood and spleen, and least mature NK cells in the lymph nodes, bone marrow, and liver (9, 28). Murine NK cells can also be defined along an NK1.1/CD49b (DX5) axis (Figure 1.2B). $NK1.1^+DX5^+$ cells are mature NK cells found in the periphery and spleen, within which the CD11b/CD27 axis of maturation occurs, whereas $DX5^-NK1.1^+$ are immature NK cells with a tissue resident phenotype that are enriched in the liver (30, 31). These $DX5^-NK1.1^+$ NK cells

express high levels of CXCR6 and CD49a and have memory-like properties (see section 1.2.1.4) (30, 31)

Within humans, the CD27 axis corresponds to CD56 expression; $CD56^{++}$ cells are less mature, have a reduced cytotoxic capacity, but can response after activation with robust cytokine production in response to vaccination and infection (32-35). They comprise about 10% of the NK cell population and are found predominantly in the primary and secondary lymphoid organs (36), whereas $CD56^{+}CD16^{+}$ cells are more cytotoxic and are found predominantly in the peripheral blood (figure 1.2C)(32, 37). The most mature, terminally differentiated NK cells express CD57 and are less responsive to activation by accessory cytokines (35, 38).

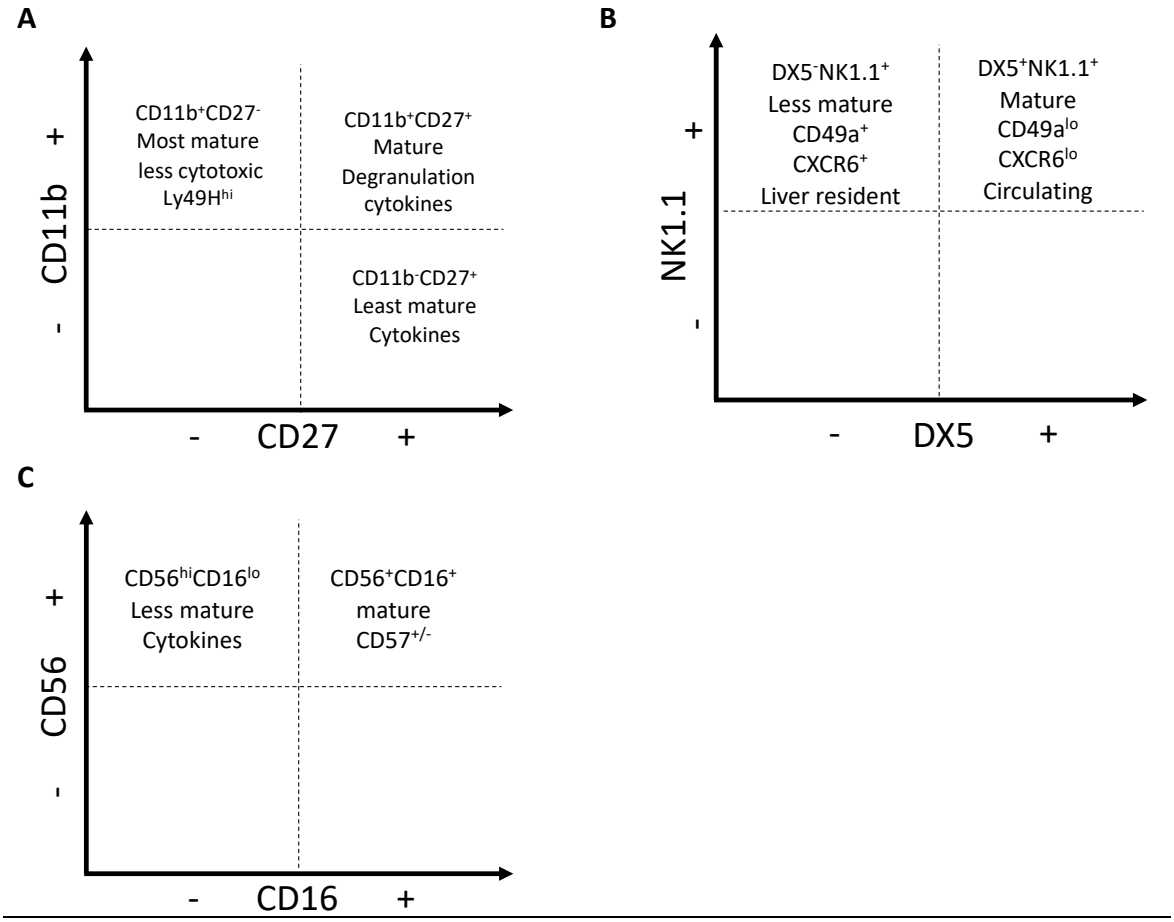


Figure 1.2. Maturational axes of NK cells in mice and humans

In mice: **A)** NK cell maturation can be defined along a CD11b/CD27 axis. $CD11b^{-}CD27^{+}$ NK cells are the least mature, and $CD11b^{+}CD27^{-}$ are the most mature. **B)** NK cell maturity can be separated along a DX5/NK1.1 axis. $DX5^{-}NK1.1^{+}$ NK cells are less mature, tissue resident and more cytotoxic than mature circulating $DX5^{+}NK1.1^{+}$ NK cells.

In humans: **C)** $CD56^{++}$ NK cells are less mature and have a highly cytotoxic profile. $CD56^{+}CD16^{+}$ NK cells are more mature, can express CD57, and constitute 90% NK cells in the periphery.

1.2.1.3. NK cell tissue residency in the liver

NK cell phenotype and function are dependent on tissue residency and cell maturity. Conventional circulating NK cells (cNK) are the predominant population in the spleen and peripheral blood and constitute approximately 10% of the lymphocyte population (30). In mice and humans, cNK cells have a $Tbet^{+}$ $Eomes^{+}$ transcription factor profile, analogous to

IFN-γ producing cytotoxic effector T cells (39, 40). These NK cells are phenotypically mature and respond to activation with cytokine secretion and cytotoxic degranulation (9)

Tissue resident NK cells (trNK) are a unique population found in the mouse and human liver, skin and uterus (41). This thesis focuses on trNK cells in the liver. Unlike the spleen and lymph nodes, the liver is not a secondary lymphoid organ and perpetuates a immunotolerant environment (10). In mice, trNK have an immature $DX5^{-}NK1.1^{+}$ phenotype and express high levels of the liver homing and residency markers CD49a and CXCR6 (27, 30, 31). Murine trNK cells are $Tbet^{+}Eomes^{-}$ and have a more inhibitory receptor profile, including increases expression of NKG2A and absence of Ly49H (10, 39). However, trNK cells are able to respond with robust IFN-γ secretion following viral and bacterial infection (41, 42). They also have a gene expression profile that is more similar to NKT cells than cNK cells (28). Peng *et al* demonstrated that adoptive transfer of $DX5^{-}NK1.1^{+}$ hepatic trNK cells did not induce maturation into circulating mature $DX5^{+}NK1.1^{+}$ NK cells, thus suggesting they are a distinct lineage and not an intermediate maturational stage (31). To further support this, research by Daussy *et al* shows that trNK cells develop in the foetal liver, and not in the bone marrow like conventional cNK cells (28). It has been proposed that $CXCR6^{+}$ and $CD49a^{+}$ murine trNK cells have memory-like capacity, and can respond to antigens in a T cell-independent manner (see section 1.2.1.4) (43).

In the human liver, tissue resident NK cells are phenotypically immature with high CD56 expression (40, 44). There is some discrepancy between transcription factor expression, which may ultimately reflect on undefined subset functionality; some studies report human trNK cells have a $Tbet^{+}Eomes^{-}$ transcription factor profile similar to mice (30, 40), however others report a $Tbet^{-}Eomes^{+}$ profile (45-48). Similar to mice, human liver trNK cells also express CXCR6, however only a small population are $CD49a^{+}$ and many are $CD49e^{-}$

, suggesting that CD49e defines tissue residency in humans in an analogous fashion to $DX5^-$ NK cells in mice (47). They are also $CD69^+$; in this instance, CD69 is also a marker of tissue residence as well as activation (37, 49). Overall, human liver trNK cells are less well defined than in mice and their function is still undefined (8). In the human lung, trNK cells are also immature $CD56^{++}CD16^-$ cells with co-expression of CD69, CD49a and the lung residency marker CD103 (50).

1.2.1.4. NK cell memory

NK cells do not undergo somatic hypermutation of their antigen receptors, therefore do not form canonical memory comparable to T and B lymphocytes. However, NK cells retain the ability to recognise antigens and respond robustly following activation; this has been postulated as a form of adaptive-like antigen memory. Three forms of NK cell memory have been identified thus so far (4):

- Cytokine-induced memory-like NK cells
- Memory to CMV antigens
- Antigen specific memory of liver trNKs to hapten challenge

Cytokine-induced memory-like NK cells are not activated directly by antigens but are primed following exposure to inflammatory cytokines. Naïve NK cells stimulated *in vivo* with IL-12, IL-15 and IL-18 have a significantly stronger and faster IFN-γ response following re-stimulation (51, 52). After seasonal influenza vaccination, IL-15-primed NK cells also demonstrate heightened cytokine secretion and proliferation after vaccine restimulation in the presence or absence of IL-15 (53). The phenotype of these NK cells in humans includes activating receptors $CD94^{hi}NKG2A^+CD69^+NKp46^+$. In mice, cytokine-induced

memory-like NK cells are indistinguishable from unprimed NK cells and are maintained by homeostatic proliferation for at least 4 weeks in a mouse adoptive transfer model (6, 51, 54).

Infection with cytomegalovirus (CMV) also induces memory-like NK cell phenotypes. Specific receptors on NK cells can recognise CMV epitopes presented by class I MHC molecules. In murine cytomegalovirus (MCMV) infection, the m157 peptide is recognised by the NK cell Ly49H receptor (55). Similarly, in humans the HCMV UL40 peptide is recognised by the analogous CD94/NKG2C receptor when presented by HLA-E (56, 57). Ligand recognition stimulates clonal proliferation and expansion of NK cells expressing these receptors. In mice, the $Ly49H^+$ population contracts following establishment of a chronic infection, whereas in humans, the $NKG2C^+CD57^+$ NK cell population remains expanded in the periphery (5). Both murine and human NK cells are able to proliferate further upon re-infection, and have an increased cytotoxic profile (5), and MCMV-specific $Ly49H^+$ NK cells from the liver are able to protect against MCMV infection by adoptive transfer in neonatal mice in an IL-12 dependent manner (6). No other known herpesvirus elicits a response in $CD57^+NKG2C^+$ NK cells, although a population of $CD56^{++}NKG2A^+$ NK cells accumulates in the tonsils and secretes IFN-γ in response to EBV infection (5). Co-infection of EBV and CMV also induces a higher frequency of $CD57^+NKG2C^+$ NK cells in children compared to infection with CMV alone, which may be driven through IL-15 exposure and up-regulation of HLA-E on the surface of infected cells (58). Similar $NKG2C^+$ NK cells are expanded during hantavirus infection, and rely on IL-15 and HLA-E expression on infected cells (59).

The mechanism of antigen-specific hapten memory NK cells has not been fully elucidated. These NK cells reside in the liver and express an immature profile with $CXCR6^+$

and CD49a^{+} populations in mice (5, 56). In humans, adaptive-like CD56^{++}NKG2C^{+}CD49a^{+} NK cells have been identified in the liver, lung and peripheral blood, and are hyperresponsive to target cells (60). Previous research demonstrates that hepatic Thy1^{+}CXCR6^{+} NK cells generated memory upon exposure to 2,4-dinitro-1-fluorobenzene and oxazolone in Rag$^{-/-}$ mice. These NK cells did not proliferate but were able to mediate long-lasting contact hypersensitivity following secondary exposure to the haptens (61), which was independent of T and B cells (56). Potential NK cell memory is also generated by influenza A, herpes simplex virus, and vaccinia virus infection in mice (62). NK cell memory to vaccination has been demonstrated in non-human primates (NHP) after vaccination with an adenovirus-26 vectored vaccine expressing HIV-1 env which elicited NKG2-dependent NK cell memory lasting over 5 years in a rhesus macaque model (63). Simian Immunodeficiency Virus also potentially generates NK cell memory in NHP (63, 64). There are some examples of human antigen-specific NK cell memory; in vaccinated humanised mice, hepatic NK cells could elicit a recall response upon vaccination with antigen-loaded dendritic cells. Furthermore NK cells expressing tissue-residency markers and expressing inflammatory cytokines can be detected in humans in response to childhood varicella Zoster virus (VZV) infection after intra-dermal injection of VZV antigens (56). Influenza A haemagglutinin is also recognised directly by the NK cell NKp46 activating receptor and triggers cytokine secretion and lysis of infected cells (65), although this does not cause detectable NK cell memory expansion (6).

1.3. The adaptive immune system

The adaptive immune system, which consists of T cells and B cells, can establish memory populations after encountering non-self-pathogens. Adaptive lymphocytes express

polymorphic receptors that can recognise multiple different epitopes and antigens from self and non-self-pathogens.

1.3.1. An overview of T cells

T cells develop in the thymus from the common lymphoid progenitor and are defined as adaptive lymphocytes expressing a T cell receptor (TCR) with co-expression of the CD3 activating protein complex (66). The TCR is constructed from two highly polyclonal proteins which recognise intracellular antigens when presented on MHC molecules by antigen presenting cells (APCs) (67). The TCR undergoes somatic hypermutation and recombination of receptor subunits during T cell development to generates a diversity of ~10^{18} potential TCR sequences in an individual (68). T cells are broadly classified into two groups, based on their heterodimeric TCR protein expression: $\alpha\beta$ and $\gamma\delta$. $\alpha\beta$ constitute the majority (approximately 90%) of the circulating T cell population in humans (68), and are the population most frequently studied in vaccinology. $\gamma\delta$ T cells are more abundant in the mucosa and skin, and are able to recognise antigens without need for MHC-facilitated epitope presentation and thus can react in a more innate-like manner to pathogens (69). Within the $\alpha\beta$ group, T cells express either CD4 or CD8 co-receptor molecules, which determine the class of MHC that the T cell recognises (66). MHC class I comprises of one polypeptide chain co-expressed with ß2-microglobulin and presents peptides of 8-10 amino acids in the peptide binding groove to $CD8^+$ T cells. It is constitutively expressed on the surface of most nucleated cells, and commonly presents cytosolic viral epitopes. MHC class II consists of two polypeptide chains and presents antigens of 13-17 amino acids to $CD4^+$ T cells. MHC class II is expressed by antigen presenting cells including B cells, dendritic cells, and macrophages, and presents intra-vesicular antigens (70). The peptide binding

grooves of both MHC class I and II are broadly specific and can present multiple similar antigens to T cells. The MHC-encoding region of the human genome is also highly polymorphic and can express multiple alleles of MHC genes across a population (66).

Upon initial pathogen infection, inflammatory cytokines from innate immune cells activate DC and macrophages and initiate presentation of pathogen antigens on MHC class I or II molecules. Naïve T cells are activated upon contact with these antigen-presenting cells (APCs) presenting an MHC:epitope complex specific to the TCR (71). This contact occurs in the secondary lymphoid organs and initiates proliferation and expansion of a population of T cells expressing this TCR, facilitated via co-signalling from OX40L/OX40 and CD80/CD86/CD28 receptor activation (72).

1.3.1.1. $CD8^+$ T cells

The function of T cells is highly conserved between mice and humans. $CD8^+$ T cells are cytotoxic mediators that undergo proliferation and initiate an inflammatory effector response to stimulation. During an acute infection, an oligoclonal population of T cells specific for pathogenic antigens expand and may take up the majority of the circulating T cell repertoire (73). $CD8^+$ T cells produce a cytotoxic and inflammatory cytokine profile including secretion of IL-2, IFN-γ and perforin, and expression of migration molecules including CD62L and CCR7 (73). After the infection has resolved, the majority (>90%) antigen specific $CD8^+$ T cells undergo apoptosis, whereas the remainder differentiate into either effector memory T cells (T_{EM}) in the periphery, or central memory T cells (T_{CM}) in secondary lymphoid organs, and can rapidly re-activate upon subsequent infection (73, 74)

1.3.1.2. $CD4^+$ T cell subsets and functions

$CD4^+$ T cells are a heterogeneous population that can have a cytotoxic effector function and generate memory populations following infection, or assist with B cell memory formation (74). Naïve $CD4^+$ T cells can mature into five populations depending on cytokine environment and transcription factor expression.

Th1 cells develop from naïve $CD4^+$ T cells by exposure to IL-12, which induces expression of the transcription factor Tbet. Th1 cells have an cytotoxic function through production of cytokines including IL-2 and IFN-γ, which mediate inflammatory responses towards intracellular pathogens (75). Th2 cells suppress Th1 responses by production of anti-inflammatory cytokines including IL-4, IL-5 and IL-10, and also facilitate antibody production (76, 77). They differentiate through exposure to IL-4 and express GATA3 and are functional against extracellular pathogens and helminths (78, 79). Th17 cells express the transcription factor ROR-γt and differentiate from naïve $CD4^+$ T cells by exposure to IL-1ß, IL-23 and IL-6. They mediate protection from extracellular pathogens and fungi by expression of IL-17A and IL-22 (75).

T follicular helper cells (T_{FH}) are specialised $CD4^+$ T cells that provide help to B cells undergoing affinity maturation in the lymphoid germinal centre, and can also circulate in the periphery (79). They express the transcription factor Bcl6, which promotes expression of CXCR5, CD40L and PD1 and maintains their location within the B cell follicle in the germinal centre (79, 80). They differentiate from naïve CD4 T cells by exposure to a complex array of cytokines including IL-6, IL-21, IL-12, IL-23, TGF–ß and ICOS (79). In the germinal centre, dendritic cells present antigen to naïve B cells, and localised T_{FH} provide 'help' to the B cells with the highest antigen affinity. T_{FH} secrete IL-21 and IL-4 which facilitate multiple rounds of B cell survival and ensure their successful class switching and

maturation to plasma and memory B cells. Physical interaction by CD40L with CD40 on B cells also induces proliferation (80, 81). Loss of T_{FH} function can lead to autoimmune diseases including systemic lupus erythematosus (80).

$CD4^+$ T cells are regulatory T cells (T_{reg}). T_{regs} do not typically have a cytotoxic profile but regulate antigen-specific B cell development in the germinal centre of lymph nodes and CD4/CD8 T cell activation in the periphery. They are defined as $CD4^+FoxP3^+$ $CD25^+$ T cells, and constitute ~13% peripheral $CD4^+$ T cells (77). T_{regs} can either be 'natural' and develop in the thymus, or 'induced' from $CD4^+FoxP3^-$ T cells *in vivo* and *in vitro* by presence of TGF-ß and IL-2 (82). They are essential for regulating immune response and ensuring tolerance against self-antigens, and suppress both Th1 and Th2 activation through production of IL-10, TGFß and inhibition of IL-2 in a contact-dependent mechanism (77). Dendritic cells can also be inhibited by T_{regs} via contact by binding of CTLA-4 to CD80/CD86 and LAG-3, which prevents T cell stimulation, thus reducing their antiviral response (82). T_{regs} also control the activation of T cells during infection, including production of inhibitory IL-10 and TGF-ß, which prevents a hyperinflammatory response (83). In mice and humans without T_{regs}, severe autoimmunity will occur due to proliferation of auto-reactive T cell clones (84).

T follicular regulatory cells (T_{FR}) are a subset of T_{reg} cells and are defined as $CD4^+CXCR5^+PD1^+FoxP3^+Bcl6^+$ T cells. T_{FR} have both regulatory (T_{reg}) and helper (T_{FH}) properties and negatively regulate the function and size of T_{FH} populations in the germinal centres. They do not synthesise IL-21 so cannot induce B cell maturation alone (80). There is still little known about this population and how vaccines and infectious disease influence their function.

1.3.2. MAIT cells: function and pathways of activation

Mucosal-associated invariant T (MAIT) cells are a non-classical innate-like immune cell with both innate and adaptive features, and share limited divergence between mammalian species (85). In humans, MAIT cells are $CD8^+$ (approximately 80%) or double negative T cells identified through their semi-invariant Vα7.2-Jα12/20/33 T-cell receptor (86), effector memory phenotype, and high expression of CD161, which negatively controls the cytokine response upon activation (87, 88). They constitute approximately 5-10% circulating $CD3^+$ PBMCs and are enriched in the liver and lymph nodes (89, 90). $CD8^+$ MAIT cells can exert four functions: a Th17-like profile with intracellular RORγT expression and abundant IL-17 and IL-22 production, a Th1-like profile with expression of T-bet, eomes, inflammatory cytokines and cytotoxicity, an innate-like profile expressing CD56, IL-18R and PLZF, and a tissue homing profile with tissue tropism molecules including CXCR6 and CCR6 (91, 92). It is important to note that these four profiles are not mutually exclusive within the MAIT cell population, and that all MAIT cells express all receptors and transcription factors, but it is unknown how these effector functions are independently regulated. In mice, MAIT cells are defined in flow cytometry as $CD3^-$ TCR$ß^+$ and MR1 $tetramer^+$ with the 5-OP-RU peptide (93). In comparison to humans, murine MAIT cells only constitute 0.1-0.5% circulating PBMCs, but are more abundant in the lymph nodes, lungs, and liver (93).

MAIT cells across different mammalian species are universally restricted by MR1 (91), which is expressed ubiquitously across cells and is the most highly conserved MHC molecule with a 90% sequence similarity between mice and humans (85, 86, 94). Due to the highly conserved nature of MR1, it was traditionally believed that MAIT cells could only be activated by specific metabolites derived from riboflavin that bind the MR1 groove independently of classical MHC class I and II (91, 94) and are synthesised by a limited

number of organisms including *Klebsiella, Staphylococcus*, *Streptococcus,* and yeast (94). Upon recognition of a ligand:MR1 complex, MAIT cells proliferate and exert an inflammatory cytokine response including IFN-γ, TNFα and cytolytic function via granzyme B (95). This activation is controlled in part by complementary negative regulation by neutrophils (95).

MAIT cells can also be activated through alternative pathways that do not involve MR1-presented vitamin B metabolites, and act as innate-like lymphocytes in response to viral infection. Van Wilgenburg *et al* demonstrated that MAIT cells are activated by dengue virus, hepatitis C virus, and influenza virus *in vitro* and *in vivo* in mice by cytokine stimulation with IL-18 and IL-12, IL-15 or Interferon-α (89, 96). Furthermore, $MR1^{-/-}$ mice were protected from lethal influenza A infection by adoptive transfer of MAIT cells from wild-type mice (97). Others have also demonstrated activation of MAIT cells following HIV, Dengue Virus, Zika virus, Hantavirus and SARS-CoV-2 infection (98-103), of which aberrant activation during SARS-CoV-2 infection may contribute towards disease severity (104). Detrimental activation of MAIT cells may also contribute towards autoinflammatory disease such as arthritis via excessive production of IL-17 (105). Viral infections can deplete MAIT cells in the peripheral blood and other organs, including Hepatitis C virus (106), Hepatitis B virus (90), HIV(98, 107), HTLV1(108), SARS-CoV-2 (104), and influenza (89), which can lead to their exhaustion, functional impairment, and increased disease severity (90, 98, 101).

Some pre-clinical and clinical studies have also described MAIT cell activation by vaccines. The viral vector vaccine ChAdOx1, but not Ad5, can activate MAIT cells via plasmacytoid dendritic cell-derived IFN-a and monocyte-derived IL-18 and TNF (109). Stimulation of PBMCs after vaccination with the *Mycobacterium tuberculosis* vaccine

bacille Calmette-Guérin (BCG) also induced robust IFN-γ cytotoxicity by MAIT cells via MR1-independent IL-12 and IL-18 activation up to one-year post-vaccination (110).

1.3.3. B cell immunology and memory formation

B cells are adaptive immune cells that are antigen-specific via expression of B cell receptors (BCRs). The BCR is functionally similar to the TCR; each B cell expresses a BCR with somatic hypermutations in the variable loci, meaning each B cell can recognise a unique antigen (111). Their main function is secretion of immunoglobulins (Ig, antibodies), which are soluble BCR proteins that bind to pathogens and exert either neutralising function preventing infection (neutralising abs), or activate other immune populations (non-neutralising abs) (112). Structurally, antibodies are built from a heavy chain and a light chain that expresses the hypervariable regions (113). Antibodies consist of a fragment antigen binding (Fab) region which recognises antigenic structures, and a fragment crystallisable (Fc) region which determines the effector function of antibodies (113). Engagement of the Fc region with Fc receptors, such as CD16 (FCγRIII), activates other cell functions and mediates cellular immunity (114). The antibody repertoire within an individual is highly diverse and able to recognise more than $5x10^{13}$ different antigens (111).

Mature B cells can be defined by expression of CD19 and/or CD20, with memory compartments defined as $CD27^{+}IgD^{\pm}$ or $CD27^{-}IgD^{-}$ (115). Naïve B cells circulate through the bloodstream, frequently passing through secondary lymphoid organs (SLO). Upon recognition of a pathogen by the BCR, B cells are activated and form germinal centres (GC) in the SLO where they undergo affinity maturation, proliferation and potentially class switch recombination upon interaction with $CD4^{+}$ T helper cells (116). This enhances B cell affinity for antigen and prevents expansion of populations that are not functional towards

pathogen neutralisation (111). Different outcomes are possible for antigen-specific B cells following activation. Antigen-specific short-lived B cells secrete IgM as a fast response to a pathogen without undergoing germinal centre maturation (117). Alternatively, B cells remain in the GC and undertake class switching, to broaden the antibody secretion profile to include IgG, IgA and IgE isotypes (117). Formation of B cell memory is vital for rapid response upon pathogen re-infection. B cells can differentiate into long-lived plasma cells and memory B cells which form the B cell memory pool and can re-activate and proliferate upon antigen re-exposure (116). Plasma cells relocate to the bone marrow, where they secrete antibodies and remain in a quiescent state until re-activation (117). These antigen-specific memory B cells can survive for decades without antigen stimulation, as demonstrated in survivors of the 1918 influenza pandemic (111), and in response to infection with VZV, and vaccination against tetanus and diphtheria (118).

1.4. Overview of vaccines

Variolation, the practice of administering small quantities of Variola virus cutaneously, has been practiced in India and China for centuries (119). The first known example of vaccination in the modern world was developed by Edward Jenner, who inoculated a child against smallpox with viral particles obtained from cowpox patients. Since then, the field of vaccinology has developed multiple different technologies for antigen delivery and immune cell stimulation to develop robust memory against a pathogen before natural infection. Vaccination has become the second most effective method of reducing the burden of infectious disease, after clean water (120). Table 1.2 outlines approved vaccines for each major vaccine type.

1.4.1. First-generation vaccines

Prior to the development of novel vaccine platforms, the majority of vaccines were either whole cell (Live attenuated (LA) and inactivated) and acellular (protein subunit and toxoid). LA vaccines are developed by continuous passage of virus in a cell line until it becomes less pathogenic to humans. Inactivated vaccines are exposed to chemicals, e.g., formaldehyde, or heat, which prevents replication (121). LA vaccines generate a broad and robust immune response with both humoral and cellular components, due to recognition of multiple epitopes within the whole virus by the immune system (122); inactivated vaccines are broadly immunogenic but often require use of an adjuvant for full protection (123).

Acellular vaccines circumvent handling of live pathogen, and require knowledge of a target antigenic protein, often expressed on the surface of the pathogen, and the ability to produce proteins on a large scale *in vitro* (124). Protein subunit vaccines predominantly elicit a humoral response and are often administered with an adjuvant to stimulate an immune response and generate higher quality immune memory (124). Toxoid vaccines generate an immune response against the toxin produced by the pathogen, rather than the pathogen itself, and are used to prevent disease caused by *Clostridium tetani* and *Corynebacterium diphtheriae* (125, 126).

Category	Approved examples
Live attenuated	Smallpox, measles, rubella, mumps, yellow fever, influenza, varicella, polio, BCG
Inactivated	Polio (iPV), rabies, hepatitis A
Toxoid	Tetanus, Diphtheria
Protein subunit	Hepatitis B, pertussis, human papillomavirus, *Haemophilus influenza* B, meningococcal bacteria, pneumococcal bacteria
Nucleic acid	SARS-CoV-2 (mRNA)
Viral vector	Japanese encephalitis (IMOJEV, Australia), Dengue virus (DENGVAXIA, Mexico and Brazil), Japanese encephalitis and West Nile virus (ChimeriVax, USA), ebolavirus (ERVEBO, USA), SARS-CoV-2 (Vaxzevria and J&J)

Table 1.2. Vaccine types and examples. Adapted from Sharpe *et al* 2020 **(127)**

1.4.2. Next generation vaccine platform technology: nucleic acid vaccines

Nucleic acid vaccines are molecules of DNA or mRNA encoding the target antigen, sometimes administered within a capsule or lipid nanoparticle to prevent premature degradation (128, 129). Once within the cell nucleus, DNA vaccines are transcribed and translated into the target protein which is presented to the immune system on the surface of the cell. Although immunogenic in pre-clinical trials, DNA vaccines have not elicited high immunogenicity in human studies and often require electrophoresis to aide administration (123, 130). Similarly, mRNA vaccines are translated directly into proteins in the cytoplasm of a cell (127). Nucleic acid vaccines are also inherently self-adjuvanting and elicit an immune response through activation of Toll-like receptors (128). mRNA vaccines predominantly stimulate an antibody response, although can induce polyfunctional T cells (127).

1.4.3. Next generation vaccine platform technology: Recombinant viral vectored vaccines

Viral vectored vaccines are modified viruses encoding pathogenic antigens that are expressed as proteins in the host cells. Viral vectors can self-adjuvant the delivery of antigenic sequences by using the innate activating properties of the viral vector backbone itself (131). Viruses that have been made into viral vectors for vaccine antigen delivery including adenoviruses, poxviruses and vesicular stomatitis virus (132, 133). Many of these viral vectors have been designed to be replication-incompetent for an enhanced safety profile and have undergone numerous clinical trials (table 1.3) (132). Viral vectored vaccines induce a strong cellular and humoral response after one dose (134), which can be boosted with a homologous or heterologous vaccine encoding the same antigen by increasing the polyfunctionality and magnitude of T cells and the sustainability and durability of antibodies (135, 136). Cellular responses are generated due to intracellular processing of the vaccine itself, and presentation of the encoded antigen via MHC pathways to T cells (119). Similarly, the encoded antigen can be produced as a protein and presented on the surface of the cell for recognition by B cells (Figure 1.3). Viral vectored vaccines that express antigens against cancer are also in early-stage clinical trials (137).

Viral vector	Subtype	Clinical trials	Ref	Approved (company, name)	Countries approved	Ref
Adenovirus (human)	Ad26	Ebolavirus	(138)	J&J, Zabdeno	EU	(138)
		SARS-CoV-2	(139)	J&J, COVID-19 vaccine	77 emergency approvals	(140)
	Ad4	Influenza A	(141)			
	Ad5	Malaria	(142)			
		Ebolavirus	(143)	CanSino Biologics	China	(144)
		SARS-CoV-2	(145)	Gamelaya research institute, Sputnik V	74 emergency approvals	(140, 145)
	Ad6	Hepatitis C	(146)			
	Ad35	Malaria	(147)			
Adenovirus (chimpanzee)	ChAd3	Hepatitis C	(148)			
		Ebolavirus	(149, 150)			
	ChAd63	Malaria	(151)			
		HIV	(152)			
	PanAd3	RSV	(153)			
	ChAdOx2	Crohn's disease	(154)			
	ChAdOx1	**See table 1.4**				
Vesicular stomatitis virus	N/A	HIV	(155)			
	N/A	Ebolavirus	(156, 157)	Merck, Ervebo	Democratic Republic of the Congo, EU, USA	(158)
Poxvirus	MVA	**See table 1.4**				
Yellow Fever virus	N/A	Japanese encephalitis	(159)	Sanofi, Imojev	Australia, Thailand	(160)
	N/A	Dengue virus	(161)	Sanofi, Dengvaxia	16 countries	(162)

Table 1.3. Viral-vectored vaccines in published clinical trials and licensed around the world.

1.4.3.1. The viral vector platforms ChAdOx1 and MVA

This thesis focuses on the viral-vectored vaccines chimpanzee adenovirus Ox1 (ChAdOx1) and modified Vaccinia Ankara (MVA). In early viral-vector vaccine research, recombinant human adenoviruses (hAds, family *Adenoviridae,* genus *Mastadenoviridae*) were focused on for vector development (132). Adenoviruses are large, double-stranded DNA viruses that are easy to manipulate *in vitro* (132). However, hAds have a high circulating seroprevalence and detectable neutralising antibodies of up to 60% and 90% of individuals in the USA and Sub-Saharan Africa respectively, inducing anti-vector neutralisation and precluding immune response (136, 163, 164). Therefore, vectors have been developed from non-human adenoviruses such as chimpanzee adenovirus, which has a maximum detected seroprevalence of 4% in the USA (164). ChAdOx1 is a recombinant chimpanzee adenovirus strain Y25 with deletion of the E1-E3 genes to prevent replication and increase the antigen insert carriage size to 8kb (165). ChAd-vectored vaccines have broad tissue tropism using coxsackie adenovirus receptor, which is present on multiple tissues including brain, heart, epithelial and endothelial cells (163). Several chimpanzee adenovirus-vectored vaccines (e.g., ChAd3, ChAd63) have been tested in clinical trials against multiple pathogens (see table 1.3) (119, 148, 149, 166, 167). Specifically, ChAdOx1 has been tested in clinical trials for pathogens including malaria, rabies, and SARS-CoV-2 (see table 1.4). In clinical trials, a single dose of ChAdOx1 is able to induce broad humoral and cellular immune responses after one (168) or two (169) doses. Currently, ChAdOx1 nCoV-19 (Vaxzevria) is the only approved ChAdOx1 vectored vaccine.

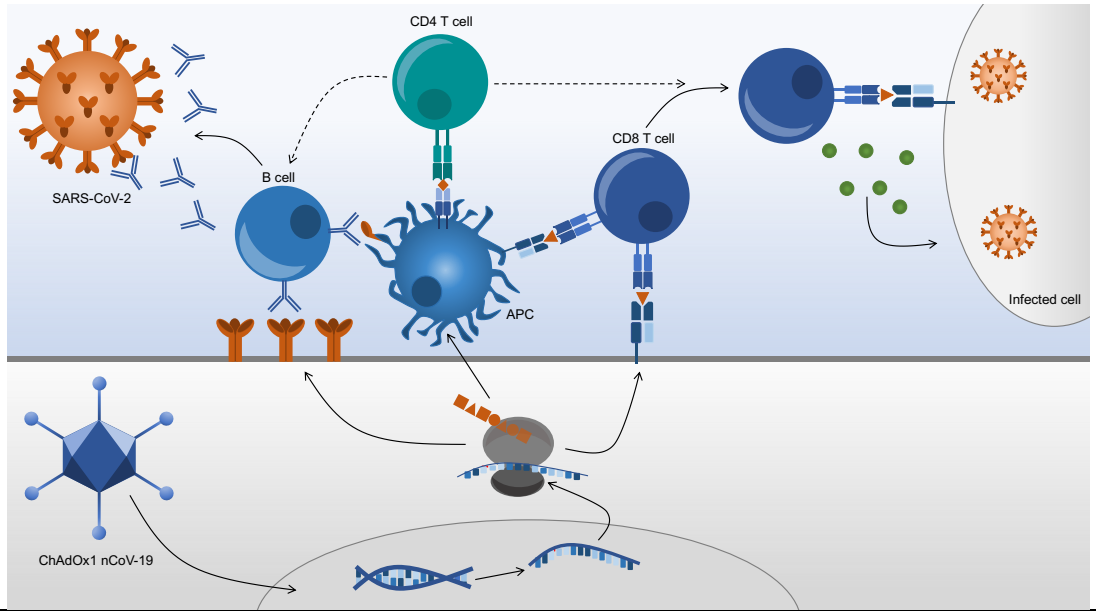


Figure 1.3. Intracellular expression of encoded antigen and immune activation by ChAdOx1 vaccination

Upon cellular entry, ChAdOx1 enters the nucleus and the encoded antigen is transcribed. The mRNA is translated in the cytosol. Spike proteins are expressed on the cell surface and in the extracellular matrix, where they initiate B cell memory. Spike peptides are presented on the cell surface by MHC molecules and activate T cells and APC which generate antigen-specific memory. Memory generation is facilitated by $CD4^+$ T cells. B cells can recognise spike protein and produce antibodies to neutralise SARS-CoV-2 virus. T cells can recognise antigen presented on the surface of infected cells and kill the cell via cytotoxic cytokine release.

MVA is a modified, non-replicative poxvirus viral vector descending from the Orthopoxvirus Chorioallantois Vaccinia virus Ankara, and was originally used as a smallpox vaccine in over 120,000 individuals (170). Since 2003, MVA has been used as a viral vector for vaccination (119) and has undergone several major genome deletions through serial passaging and can withhold an insert size up to 25kb, allowing for multiple antigen expression (171). Similar to other viral-vectored vaccines, MVA can elicit a humoral and cellular immune response and has been widely tested in clinical trials as a vaccine vector against emerging pathogens (171, 172)

Pathogen	Clinical status and pathogen antigen		Ref/CTN
	ChAdOx1	MVA	
Zaire and Sudan ebolavirus	Pre-clinical EBOV, SUDV and MARV glycoprotein	Authorised as MVABEA by the European Medicines Agency EBOV, SUDV, MARV and TAFV glycoprotein	(173-175)
Marburg Virus	Pre-clinical EBOV, SUDV and MARV glycoprotein	Authorised as MVABEA by the European Medicines Agency EBOV, SUDV, MARV and TAFV glycoprotein	(173-175)
Lassa virus	Pre-clinical LASV glycoprotein	Pre-clinical LASV nucleoprotein	(176, 177)
Influenza A	Phase I NP and M1	Phase I NP and M1	(178, 179)
Respiratory syncytial virus	N/A	Phase I Fusion, nucleocapsid and matrix proteins	(153, 180)
MERS-CoV	Phase I Spike protein	Phase I Spike glycoprotein	(181, 182)
SARS-CoV-2	Emergency approval by WHO and EU Spike glycoprotein	Pre-clinical Spike glycoprotein	(183-185)
Hepatitis C virus	Pre-clinical Conserved epitopes	Phase I Expressing NS_{mut}	(148, 186)
Hepatitis B virus	Phase I ongoing	Phase I HBV surface antigens	(187) NCT04297917
Rift valley fever virus	Phase I ongoing RVFV GnGc protein	Pre-clinical GnGc protein	(188) NCT04672824
Chikungunya virus	Phase I C, E3, E2, 6K, E1 proteins	Pre-clinical E3 and E2 proteins	(189, 190) NCT03590392
Yellow Fever	N/A	Phase I underway MVA-BN Yellow Fever	NCT02743455
Zika virus	Phase I ongoing	Pre-clinical E, prM, TM proteins	(191) NCT04015648
Human papilloma virus	Phase I ongoing	Phase II	NCT04607850 NCT04607850
HIV	Phase I ongoing HIVconsv	Phase I HIVconsv	(167) NCT04586673
Mycobacterium tuberculosis	Phase I 85A	Phase IIb 85A	(192-194)
Plasmodium falciparum	Phase I LS2	Phase I/IIa ME-TRAP / LS2	(195) NCT03203421

Table 1.4. Clinical trials for ChAdOx1 and MVA-vectored vaccines
The target pathogen, and details on ChAdOx1 and MVA-vectored vaccines, including the stage of clinical trial, the vaccine antigen, and relevant clinical trials reference numbers or publication references

1.4.4. Vaccine development for emerging pandemic pathogens

Next generation vaccine platforms are suitable for rapid vaccine development against emerging pathogens; they are quick to manufacture at a large scale, relatively cheap to produce, and have a favourable safety profile. Furthermore, vaccines made from mRNA or viral vectors can be stored short-term at 2-8°C, limiting the need for a cold chain of supply to remote locations (127, 136). These attributes favour quick development and distribution following the unforeseen outbreak of a new pathogen.

1.5. Epidemics and pandemics featured in this thesis

1.5.1. SARS-CoV-2

1.5.1.1. Epidemiology

The novel emerging pathogen Severe Acute Respiratory Syndrome Coronavirus 2 (SARS-CoV-2) was identified in December 2019 from a case of unknown pulmonary infection in Wuhan, China (196). SARS-CoV-2 is most closely related to SARS-CoV, the aetiological agent of an outbreak in 2004 that caused 8,422 cases with an 11% mortality rate (197, 198). The origin of SARS-CoV-2 is unknown, although shares a 96% genetic similarity to a bat coronavirus, indicating a likely zoonotic transmission to human hosts (199). On 11th March 2020 SARS-CoV-2 was declared a pandemic by the WHO (200). The resulting disease, named COVID-19, is likely to transmit through aerosol particles (201) and has a broad range of clinical symptoms typically identified as a cough, fever, and pneumonia (202), but can also feature disseminated pathology including cardiac damage and neuropathology (203). Approximately 19% diagnosed COVID-19 cases progress to severe or critical pathology, resulting in respiratory failure with an overall mortality of 2.3% (204). COVID-19 morbidity ranges from asymptomatic to severe; co-morbidities identified include older age, weight,

and male sex, and pre-existing conditions such as diabetes and coronary heart disease (205, 206).

1.5.1.2. SARS-CoV-2 virology

The spike glycoprotein is a highly glycosylated trimeric fusion protein and is exposed to the immune system on the virion surface (207). SARS-CoV-2 infects cells by spike protein binding to angiotensin-converting enzyme 2 (ACE-2), which is expressed in abundance in the respiratory tract, as well as other organs including the heart, kidneys, and intestines (208).

1.5.1.3. Immune response to SARS-CoV-2

The pathophysiology of SARS-CoV-2 is not fully understood, although infection often results in a highly pro-inflammatory response including IL-6, IL-1ß, TNF-α and IFN-γ, and conversely increased production of inhibitory cytokines including IL-2 and IL-10 (202, 209). One study suggests that serum levels of IL-6 and TNF are especially important predictors of survival following hospitalisation with SARS-CoV-2 infection (210). Severe COVID-19 disease progression is often driven by atypical inflammation causing lung damage also identified in other coronavirus infections (202). However, there is no singular immune phenotype that can predict disease severity, and multiple immune response profiles for mild to severe disease have been identified (211, 212). Identified profiles of moderate to severe infection are heterogeneous and include lymphocytopenia of $CD4^+$, $CD8^+$ and NK cells and exacerbated activation and functional exhaustion of $CD4^+$ and $CD8^+$ T cells (209, 213). Additionally, a lack of lymphocyte activation correlated with milder disease severity (211). Counterintuitively, some data suggest that a reduced IFN class I response or a hypo-

functional T cell profile correlates with a more severe disease outcome (214). MAIT cells also undergo heightened activation (213) and there is frequently an increased proportion of innate compartments including neutrophils and monocytes (211, 213, 214). Other research indicates that B cells and plasmablasts undergo a significant oligoclonal expansion, and robust anti-spike neutralising antibody response is crucial for survival of severe COVID-19 and a stronger anti-nucleocapsid response correlates with mortality (215, 216), although earlier seroconversion may correlate with hospitalisation (217).

Immune memory after COVID-19 may be long-lasting in humans; prior SARS-CoV-2 infection was demonstrated to have protective efficacy against re-infection in macaques (218). Conversely, immunity generated by seasonal coronavirus infection could cross-react to SARS-CoV-2 protein but did not offer any significant protection against infection (219). $CD4^+$ and $CD8^+$ T cells from convalescent individuals have a broad antigen recognition profile, and long-lived neutralising antibodies against Spike glycoprotein are present for at least 5 months post-infection (220)

1.5.1.4. Vaccines against SARS-CoV-2

The SARS-CoV-2 pandemic highlighted the need for rapid development and clinical trials for novel vaccine platforms. The frontrunner candidates at the end of 2020 included two mRNA vaccines from Moderna (USA) and Pfizer/BioNTech (USA, Germany), as well as two adenovirus-vectored vaccines from AstraZeneca/University of Oxford (ChAdOx1) and Janssen (Ad26). Pre-clinical ChAdOx1 nCoV-19 was demonstrated to be immunogenic and safe in a non-human primate model (221) and began phase I clinical trials on 23rd April 2020. Phase I/II data demonstrated the vaccine was safe and immunogenic (183), with equal immunogenicity in older adults aged 55+ (222) and initial efficacy of 70% against

infection (223). As of July 2021, ChAdOx1 nCoV-19 (now known as Vaxzevria and produced in partnership with AstraZeneca), has been approved for use in the UK, and by the European Medical Association and World Health Organisation, and by over 80 countries across the world (224, 225). Over one billion doses have now been distributed worldwide.

1.5.2. Influenza A

1.5.2.1. Epidemiology

Influenza A (IAV) is a highly contagious single-stranded RNA orthomyxovirus that infects the upper and lower respiratory tract. Influenza A circulates with annual epidemics and is associated with approximately 250,000-500,000 deaths per year (178). Influenza has higher mortality in older individuals, which contribute towards >90% of annual deaths from influenza (226).

1.5.2.2. Virology and immunology

Influenza A (IAV) undergoes error-prone viral replication, which can introduce new mutations especially at immune-facing external antigenic sites such as haemagglutinin (HA) and neuraminidase (NA) (227). Viral mutation is also mediated by subtype recombination, where genes from human, pig and bird influenza viruses can reassort and form new virulent strains (228). There are 18 different HA and 11 NA which can in theory recombine to make new subtype combinations. HA and NA also undergo substantial antigenic drift to evade neutralising antibodies (227). This makes long-lasting immunity to influenza A unlikely, and can also lead to development of pandemic strains which can have a more infective capacity (227).

Influenza A is susceptible to NK cell-mediated cytotoxicity in the lung, which accumulate and activate following infection. The cytotoxic response is primarily driven by

$CD56^{++}CD16^{-}$ NK cells (50), however, over-activation and over-production of IFN-γ and TNF from NK cells contributes towards lung tissue damage and mortality during later-stage disease (50). Both cellular and humoral immunity is necessary for protection against influenza infection in younger adults. Neutralising antibody responses are generated against the HA surface protein and prevent viral entry into respiratory epithelial cells (229). Non-neutralising antibodies, targeting the HA and NA stalk, are non-neutralising but activate immune responses via antibody-dependent cellular cytotoxicity (ADCC) (229). The antibody response to IAV infection can be limited by the antigenic drift of HA, or by generation of new strains through viral reassortment (229). $CD8^{+}$ T cells typically target the more conserved internal proteins including nucleoprotein and matrix (230). In studies of avian H7N9 influenza, the magnitude and early timing of the cross-reactive H7N9-activated $CD8^{+}$ T cell response correlated with control of viral titres and disease severity upon infection (230, 231). Lack of T cell activation is also a factor of IAV mortality (231). $CD8^{+}$ T cell memory and may elicit cross-protective immunity (230), whereas antibody responses do not offer cross-strain protection against the more variable HA and NA (230). Some studies suggest that the memory T cell population to IAV is long-lived (up to 12 years post-infection)(232), and can be life-long in mice when primed at 6 weeks (233), thus positing a role for a T cell-activating universal influenza vaccine.

1.5.2.3. Vaccines against influenza A

Current licensed seasonal influenza vaccines primarily generate neutralising antibodies against HA and NA surface proteins. The commonly-used trivalent inactivated vaccine contains HA/NA from an H1N1 strain, a H3N2 strain, and from influenza B virus (227). These vaccines can be 70-90% effective in young adults when they match the circulating strains,

but this is reduced to 30-50% in older adults through immune senescence and loss of low-frequency $CD8^+$ T cell clonotypes in the TCR repertoire (233-235), Seasonal influenza vaccines can be less than 50% effective as they cannot protect against other strains that might cause pandemics, and also can have reduced efficacy if new drift occurs (227). This is somewhat overcome with annual vaccination aimed especially at high-risk individuals. Live attenuated vaccines are administered as a nasal spray in children, and although they have limited replication in nasal epithelium, they are much more efficacious than inactivated vaccines in children between 2-7 years (227).

The vaccines included in this thesis are ChAdOx1 and MVA vectored vaccines expressing the internal nucleoprotein (NP) and matrix 1 (M1) antigens of influenza A H3N2 as a fusion protein. NP and M1 are much more highly conserved between influenza subtypes (178), and may provide heterosubtypic protection against multiple influenza strains. As previously discussed, viral-vectored vaccines also induce cytotoxic T cell responses, which can target internal proteins and may be effective in providing multi-subtype protection alongside neutralising antibodies. Most humans have been exposed to influenza and already have immune memory, demonstrated through the identification of cross-reactive $CD4^+$ and $CD8^+$ T cells to multiple subtypes (236). Therefore, viral vector vaccination may boost pre-existing T cell memory generated in young age, and improve recall responses upon re-infection (233). This is especially important in the instance of novel highly virulent influenza viruses making a zoonotic transfer from animal reservoirs to humans, for example avian influenza (H5N1), for which there would be no pre-existing humoral immunity (179, 236).

1.5.3. Ebolavirus

1.5.3.1. Epidemiology

Ebolavirus (EBOV), family Filoviridae, was discovered in 1976 and is closely related to Sudan virus and Marburg virus (237-239). EBOV is the aetiological agent of the 2013-2016 West African ebolavirus outbreak, the largest and most widespread epidemic of ebolaviruses to-date, which caused 11,310 documented deaths in Guinea, Liberia, and Sierra Leone, and 28,616 cases including in Nigeria, Senegal, Mali, Spain, and the USA (240). Ebolavirus disease (EVD) is spread by mucosal contact with infected bodily fluid and is the prototype viral haemorrhagic fever, with severe symptoms including petechiae, internal bleeding and multiple organ failure (241). Mortality following infection ranges from 50-90% upon symptom onset, dependent on species and strain of Ebolavirus.

1.5.3.2. Virology and immunology

Filoviruses are enveloped, non-segmented, negative-strand RNA viruses with a characteristic filamentous shape (242). Their proteome encodes seven genes, only one of which (glycoprotein, GP) is expressed as a trimer on the viral surface (241). Individuals with non-fatal or asymptomatic EVD have strong inflammatory immune responses during early infection, including secretion of cytokines and an association with nucleoprotein-specific IgG (243-245). The immune response associated with fatal EVD is dysregulated and delayed, with hypersecretion of inflammatory TNF, IL-8 and IL-6, higher levels of anti-inflammatory IL-10 and IL-1RA, and no detectable Ebola-specific IgG (243, 244, 246). Lymphopenia, especially of $CD8^+$ T cells and NK cells, is prominent following Ebolavirus infection in humans and NHP, and may prevent an appropriate antiviral immune response (247). The immune correlates of protection against EVD are currently uncertain, although

antibodies are necessary for EVD survival in pre-clinical studies (248), and $CD8^+$ T cells mediate strong responses post-vaccination and non-fatal EVD (243, 246, 249). The immune response to EVD is long-lasting, and survivors have detectable IgG over 11 years post infection (250, 251).

1.5.3.3. Vaccines against ebolavirus

The 2013-2016 EBOV epidemic highlighted the need for cheap and rapidly producible vaccine platforms for emerging pathogens. Phase I/II clinical trials of viral-vectored EBOV vaccines up to and during the epidemic included ChAd3-EBO-Z (252, 253) boosted with MVA-EBO-Z (149), rVSV-ZEBOV (254), Ad5-EBOV (255, 256), and Ad26-EBOV with MVA-EBOV (138). All vaccines in clinical trials targeted the surface GP of either EBOV alone, or bivalent EBOV and SUDV GP, and each vaccine candidate demonstrated safe and immunogenic humoral responses (257) and robust cellular immunogenicity (149, 257, 258). rVSV-EBOV was demonstrated to be effective in 9 out of 10 cynomolgus macaques in a pre-clinical trial (259), and interim efficacy of phase III rVSV-ZEBOV trials in Guinea indicated vaccine efficacy to be 70-100% when administered in ring vaccination (156, 157). Since 2016, rVSV-ZEBOV and hAd26.ZEBOV with MVA-BN-Filo boost have been approved for compassionate use in multiple countries (174).

1.6. Cytomegalovirus

1.6.1. Epidemiology

The herpesviruses are a globally distributed family of large, double-stranded DNA viruses, characterised by host species tropism and chronic infection with periods of reactivation (figure 1.4) (260). Herpesviruses are present throughout the animal kingdom and have

been found in multiple species, including mice, birds, fish and invertebrates (261), although have become highly species-tropic and co-evolved alongside their mammalian hosts over several million years (262).

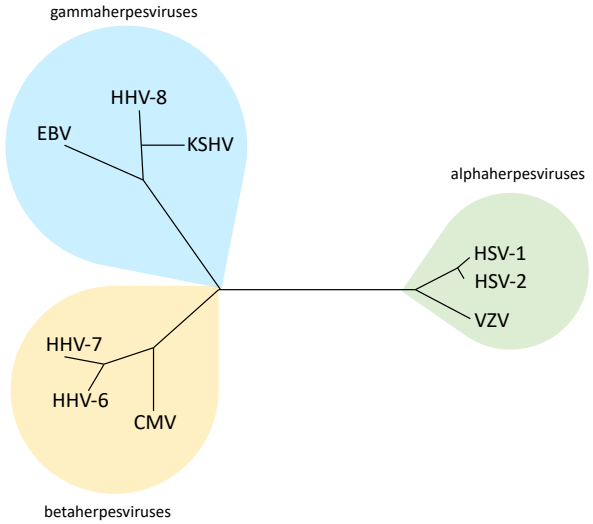


Figure 1.4. Phylogenetic tree of human herpesviruses. Adapted from Borie *et al* 2013 (263)

Cytomegalovirus (CMV) is a ß herpesvirus that establishes a latent infection in $CD34^{+}$ myeloid progenitor cells, monocytes, and macrophages in humans. Latency is interrupted sporadically with viral reactivation, and co-infection with multiple strains of cytomegalovirus is possible (260, 264, 265). Although infection is often sub-clinical in immunocompetent individuals, CMV can cause severe disease in the immunocompromised, such as organ transplant patients and people with AIDS. Infection during very early childhood can also have significant morbidity (260); neonatal CMV infection is the leading cause of non-genetic hearing loss and contributes to blindless and learning difficulties in 20% of infected neonatal children (4). Cytomegalovirus reactivation

can also occur after solid organ and haematologic cell transplant and is associated with increased mortality, organ rejection and increased opportunistic infections (266).

Although globally ubiquitous, the population burden of CMV infection is negatively correlated with socioeconomic status (260, 267). In the UK, CMV infection ranges from 40-60% of the adult population. By contrast, 85% of children in Sub-Saharan Africa are infected by the time they are 1 year old (264, 268). Globally, the occurrence of CMV seropositivity also increases with age (264). Other common herpesviruses (HSV1, HSV2, VZV, and Epstein-Barr virus, figure 1.3) also have high prevalence in Sub-Saharan Africa, ranging from 85-100% infected by adulthood (269). This high burden of chronic infections, as well as exposure to other endemic disease such as malaria, may contribute towards reduced vaccine efficacy in clinical trials conducted in Africa when compared to the UK (175, 270-272).

Murine cytomegalovirus (MCMV) is the homologous CMV virus that specifically infects mice and is frequently used as a model of human CMV (HCMV) infection (273). HCMV and MCMV share many similar lifecycle events, including replication in salivary glands and establish latency in similar organs, including spleen, lungs and bone marrow (265).

1.6.2. Immunology of Cytomegalovirus in mice and humans

1.6.2.1. NK cells

In both humans and mice, the relationship of NK cells and CMV is intricately intertwined. NK cells play a crucial role containing herpesviruses upon primary infection and can control CMV infection independent of T cells (274). Individuals with NK cell deficiencies such as

Severe Combined Immunodeficiency (SCID) are disproportionately prone to herpesvirus infections (275). As well as antiviral properties, NK cells have a protective function: IL-10 produced by murine NK cells regulates T cell cytotoxicity and prevents excessive liver damage during acute MCMV infection (276). Therefore, a large proportion of the CMV genome is dedicated to avoiding NK cell responses and down-regulating NK cell activation (table 1.5) (4).

HCMV gene	Function	Ref
US9	MIC*008 degradation in proteasome	(277)
US12/US13/US20	ULBP2 and MICB degradation	(277)
UL16	Prevents presentation of ligands to NKG2D	(278)
UL18/US20	Binds inhibitory receptor LILRB1, lysosome degradation of MICA	(279)
UL40	Stabilises cell surface HLA-E expression and promotes Interact with inhibitory NK receptor NKG2A	(280)
miR-UL112	Inhibition of MICB translation	(277)
UL141	Retention of CD155 and CD112 prevents NK cell activation	(281, 282)
UL142	Retains MICA and ULBP3 in Golgi	(277)
UL147A	Downregulation of MIC*008, prevention of NKG2D activation	(277)
UL148A	Lysosome degradation of MICA	(277)
pp65	Inhibition of NKp30 activating receptor	(283)

Table 1.5. HCMV genes that alter activation of NK cells

Immediately after CMV infection, NK cells proliferate indiscriminately and a memory-like NK cell population is generated (284). These memory-like NK cells have a terminally differentiated phenotype and express activating receptors that recognise specific CMV proteins. These cells also have substantial changes in DNA methylation and resemble $CD8^+$ T cells in their function and cell surface receptor expression (37). In mice, these NK cells are $KLRG1^+Ly6C^+DNAM\text{-}1^{lo}CD11b^+CD27^-$ (52) and express the activating receptor Ly49H, which although monoclonal recognises the glycoprotein m157 when expressed on the cell surface of infected cells (55, 285). Upon recognition of their CMV peptide ligands, memory-like NK cells proliferate, clonally expand and exert cytokine-mediated killing of infected cells (285). Once chronic infection has been established, memory NK cells contract during latency in a manner reminiscent of T cell memory and reside in lymphoid and non-lymphoid tissues (286). The remaining population can re-expand readily upon later recognition of MCMV and have enhanced effector function compared to other NK cells (52, 287). These NK cell populations rely on IL-18 and IL-12 from $CD8\alpha^+$ DC to ensure optimal activation and survival after MCMV infection (288). Adoptive transfer experiments of $Ly49H^+$ NK cells from MCMV-challenged mice demonstrated that these memory NK cells are sufficient to prevent chronic MCMV infection in naïve mice (289). Cytokine-induced memory-like NK cells, as described previously, are also activated during MCMV infection (52). In humans, CMV-specific NK cells are mature $CD57^+CD56^+$ and express the Ly49H-analogous activating receptor CD94/NKG2C. NKG2C can recognise the non-classical MHC molecule HLA-E, which is up-regulated and stabilised on the cell surface by the leader sequence of the HCMV peptide UL40 during cytomegalovirus infection (57, 290-294). Unlike murine NK cells, $CD57^+NKG2C^+$ NK cells in humans remained at an expanded proportion in the peripheral blood after viral latency is established (293, 295) and require signalling from $CD14^+$ derived

IL-15 and IL-2 for maintenance (285, 286, 296). Following CMV infection, there is also an expansion of NK cells expressing the activating KIRs KIR2DS2, KIR2DS4 and KIR3DS1 (297). Similarly, the activating KIR KIR2DS1 is able to recognise a HCMV ligand expressed on HLA-C2 that is not present on a healthy cell surface, and which induces NK cell activation (298).

1.6.2.2. T cells

From first infection to control of viral latency, CMV encodes multiple genes to diminish the T cell response, including disruption of MHC presentation (Table 1.6). The chronic stress of CMV infection and re-activation on the immune system contributes towards a distinctive T cell phenotype, characterised by a high frequency of circulating CMV-specific effector T cells, and an expansion of terminally differentiated T cell populations. $CD8^+$ T cells are crucial for controlling intracellular pathogens, and virus-specific T cells cannot eradicate CMV entirely but are important for controlling sporadic reactivation and replication of CMV. However, the adoptive transfer of CMV-specific T cells in mice is able to protect immunosuppressed hosts from CMV infection (299, 300), demonstrating their essential role in protection and potential for T cell-mediated vaccine induced protection.

HCMV gene	Function	Ref
US6	Blocks peptide translocation	(301)
UL111.5	Anti-inflammatory IL-10 analogue	(302)
US2, US11	Directs MHC class I for degradation in the proteasome	(303)
US3	Retains MHC class I in the endoplasmic reticulum	(303)
UL18	HLA class I homolog, prevents T cell activation	(303, 304)

Table 1.6. HCMV genes involved in T cell inhibition

1.6.2.3. Memory inflation

During the course of primary CMV infection, a sub-population of oligoclonal effector memory $CD8^+$ T cells to specific CMV epitopes undergo proliferation and substantial expansion and do not contract during viral latency (305, 306). Re-infection, reactivation, and constant exposure to CMV antigens contribute towards sustaining this population (307, 308). These T cells can sustain their effector function do not exhibit regular markers of exhaustion common in late-stage memory, including PD1 and KLRG1 (309). This process, known as memory inflation, accounts for over 10% of circulating memory T cells in the blood of CMV^+ individuals (267, 310, 311), and is self-regulated in a murine model by T cell-secreted IL-10 (300). Expanded CMV-specific T cells remain stable for the duration of the host's life and can amass up to 50% of memory $CD8^+$ T cells and 30% of memory $CD4^+$ T cells in elderly individuals (311, 312). The effector memory phenotype and magnitude of this response is governed by initial infectious dose (313). A compartment of classical memory T cells also expands and contracts following standard memory patterns during CMV infection (314). Similar memory inflation of T cells has been observed in mice

vaccinated with an adenovirus vectored vaccine expressing LacZ (315, 316), although it is not seen after infection with other chronic viruses and herpesviruses (305).

1.6.2.4. CMV and immunosenescence

Many parallels can be drawn between the CMV-derived immune phenotype and immunosenescence that occurs from biological aging, which has a profound impact on the effector response and memory plasticity of the immune system (311). The immune system of older individuals has a reduced proliferative and cytotoxic capacity and higher proportions of terminally differentiated T cells expressing CD57, and with a reduced T cell antigen receptor diversity (317-319).

In comparison, immune cells from CMV-seropositive younger adults closely share the phenotype of immune cells found in older adults regardless of their CMV serostatus (299). Chronic CMV infection induces a late-differentiated effector $CD4^+$ and $CD8^+$ T cell phenotype similar to that of immunosenescent T cells in elderly individuals, identified by an expanded population of $CD57^+KLRG1^+$ T cells and lower expression of CD27, CD28 and CD62L (311, 312, 320-323). There is also an expansion of CMV-specific T_{EMRA} $CD45RA^+CCR7^-$ effector memory T cells, which are less proliferative and less cytotoxic (324). This immune profile is unique to CMV infection, and not seen with other chronic herpesvirus infections including Epstein-Barr virus and HSV (311, 322).

1.6.2.5. Functionality of T cells with CMV infection

Clonally expanded, exhausted $CD8^+$ effector T cells in elderly individuals have a significant decline in functionality and cytokine production in response to stimulation (311, 317). Ouyang *et al* demonstrated that in elderly CMV^+ individuals, exhausted CMV antigen-

specific KLRG1$^+$CD8$^+$ T cells make up a large proportion of the circulating memory CD8$^+$ T cell population, produce less IFN-γ in response to CMV peptide, and more anti-inflammatory IL-10 than comparative CD8$^+$ T cells from CMV-seronegative individuals (320, 325). This effect, however, was not observed to the same extent in younger adults (311). Further studies demonstrate that older adults have reduced CD8$^+$ T cell granzyme B (226) and IFN-γ (311) production in response to vaccine peptides, and that the ability of memory T cells to produce cytokines inversely correlates with anti-CMV antibody titre in elderly individuals (326). Conversely, CMV may contribute towards chronic inflammation, through chronic production of granzyme B by resting CD8$^+$ T cells, which prevents the production of inducible granzyme B in response to vaccination or immunological challenge (327, 328). This loss of response to antigen stimulation and constant background inflammation may leave individuals at higher risk of being unable to control infection from other pathogens.

Superinfection of CMV$^+$ hosts with other pathogens often results in higher mortality due to immune exhaustion. Studies in mice have shown that MCMV co-infection reduces the CD8$^+$ T cell response to West Nile Virus and HHV-1, but improves innate immune responses to *Listeria monocytogenes and Yersinia pestis* (329, 330). Similar heightened morbidity was observed in individuals co-infected with HCMV and influenza virus, due to a reduction in GzB production and lower titres of pathogen-specific IgG (226). Conversely, studies in CMV seropositive humans infected with either West Nile Virus or Epstein-Barr virus did not observe any impact of CMV infection or aging upon immune response to infection (331). The inflammatory IFN-γ response from CMV-specific CD8$^+$ T cells is also associated with increased morbidity in infant *Mycobacterium tuberculosis* infection (332).

1.6.2.6. Cytomegalovirus and vaccine immunogenicity in clinical trials

The clonal expansion of anergic, terminally differentiated effector $CD8^+$ T cells may contribute to the reduction in functional response to pathogens and vaccines in CMV seropositive and elderly individuals. These T cells are resistant to apoptosis (333), and potentially remove immunological 'space' for new antigen memory development, which may prevent the expansion of memory populations towards new antigens and increases the likelihood of infection (320, 321, 334). However, in clinical trial data, the effect of CMV infection on vaccine efficacy is unclear and relatively few studies take burden of infectious disease into account when investigating immunogenicity.

Several studies define a correlation between CMV seropositivity, age, and vaccine immunogenicity in young and old adults vaccinated with seasonal influenza vaccines and in a ChAd3-MVA vaccine regimen against ebolavirus. These studies show an increase in T cells with an immunosenescent phenotype and reduced inflammatory cytokine secretion in older adults and younger CMV seropositive adults (226, 328, 335). CMV associated reduction in B cell function is less clear; some studies define a correlation between CMV seropositivity and reduced humoral response (336-339), but other studies do not identify the same correlation in younger and older vaccinees against vaccine antigens including influenza, measles and diphtheria (328, 338).

Other literature demonstrates that CMV infection may have either no effect (340-343), or a beneficial effect on immune response to vaccination (344-347). Reasoning for this discrepancy suggests that as CMV infection stimulates chronic low-level background inflammation, this could stimulate a stronger vaccine response in some individuals (348). These studies also do not take into account differences in population CMV burden, age of exposure, and number of potential repeat infections, which may contribute towards

altered responses to vaccination. These data may also indicate a biological advantage of CMV infection in younger adults towards vaccine immunogenicity, which negates the senescent immunophenotype in older age. It is clear that many confounding factors of CMV immunobiology, as well as context-specific differences including method of vaccination, any additional adjuvants, and size, age and demographics of the cohort analysed.

1.7. Thesis outline and aims

Successful vaccination elicits a broad and robust immune response that confers protection from disease to the individual. This thesis builds on data that I collected at the start of this PhD, which demonstrates an interplay between CMV infection the NK cell response to vaccination (Figure 4.9), and from this I investigate how viral vector vaccination and CMV infection affect NK cells and T cells in humans and in a mouse model. The first half of this thesis aims to delineate the immune response in mice and humans to single-dose and prime-boost viral vector vaccination in non-canonical populations including NK cells and in T cell populations. The second half addresses the impact of cytomegalovirus infection on NK cell and T cell immunogenicity in mice, and after vaccination in younger and older adults in viral vector vaccine regimens in the UK. Due to the coronavirus pandemic, I also undertook work processing vaccine trial samples as part of the Oxford COVID-19 vaccine trials team. Thus so, my thesis takes the following structure:

Viral vectored vaccination and the NK cell response

- Chapter three describes in-depth analysis of how viral vector vaccination affects the NK cell phenotype and cytotoxic response in mice, and how NK cell depletion alters vaccine immunogenicity.
- Chapter four utilizes multi-parameter spectral cytometry to investigate the NK cell and T cell response following a single-dose ChAdOx1 vaccination against SARS-CoV-2, and mixed single-dose and heterologous prime-boost ChAdOx1 and MVA vaccination against Influenza A. Finally, this chapter addresses the first data collected on cytomegalovirus infection and the NK cell response to vaccination.

Cytomegalovirus infection and the NK cell response

- Chapter five predominantly is an exploratory immunology chapter, and describes how murine cytomegalovirus activates innate and innate-like cell populations during acute and chronic infection.
- Chapter six investigates the effect of cytomegalovirus infection on vaccine immunogenicity in younger and older UK adults participating in viral vector vaccination clinical trials. This chapter also further details the immune response phenotype to infection with CMV, and the NK cell cytotoxic response following vaccination.

COVID-19 clinical trials

- Chapter seven summarises the work conducted during the COVID-19 pandemic whilst working as part of the Oxford COVID-19 vaccine trials team. I also present data on the immune response in severe COVID-19 and influenza A disease in ICU-admitted patients in comparison to convalescent and healthy donors collected as part of a clinical trial.

Chapter 2
Materials and Methods

Chapter 2 Materials and methods

2.1. Materials and reagents

2.1.1. General materials and reagents

Material/Reagent	Company	Catalogue no.
α-Modified Eagle's Medium	Sigma Aldrich, UK	M4526-500ML
0.5mL insulin syringe	BD BioSciences, UK	037-7614
12-well tissue culture plate	Corning	3737
15mL Falcon tube	Sarstedt	554502
20mL syringe	BD BioSciences, UK	300613
24-well tissue culture plate	Corning	3738
25G gauge BD Vacutainer butterfly needle	BD BioSciences, UK	367285
50mL Falcon tube	Sarstedt	547254
5mL polypropylene FACS tubes	BD Biosciences, UK	352063
5mL syringes	BD BioSciences, UK	309647
6-well tissue culture plate	Corning	3736
70μM cell strainer	Fisher Scientific UK	10788201
7mL Bijou tubes	Sigma Aldrich, UK	Z645338
96-well U-bottom plate	BD Biosciences, UK	353077
96-well V-bottom plate	BD Biosciences, UK	511V96
ACK lysis buffer	ThermoFisher Scientific UK	A1049201
Anti-CD28	eBioScience	16-0289-81
Anti-CD49d	eBioScience	16-0499-85
Anti-mouse compensation beads	BD Biosciences, UK	552843
Anti-rat compensation beads	BD Biosciences, UK	552845
Anti-REA compensation beads	Miltenyi	130-104-693
Apoptosis/Necrosis assay kit (blue, green, red)	Abcam	Ab176749
Apoptosis/Necrosis assay kit (blue, red, green)	Abcam	Ab176750
ArC Amine Reactive compensation beads	ThermoFisher Scientific UK	A10346
Benzonase	Millipore	70664
Bovine Serum Albumin	Sigma Aldrich, UK	A7906-100G
Brilliant Stain buffer	BD Biosciences, UK	563794
Carbonate-Bicarbonate tablets	Sigma Aldrich, UK	P2194
Casyton	OLS OMNI Life Science	5651808
Collagenase type XI	Sigma Aldrich, UK	C7657-25MG
Dimethyl Sulfoxide (DMSO)	Sigma Aldrich, UK	D2650
DNAse	Sigma Aldrich, UK	D5025
Dulbecco's Phosphate Buffered Saline	Sigma Aldrich, UK	D8537-500ML
FACS Lysing solution 10x concentration	BD Biosciences	349202
Foetal Calf Serum	Gibco	10500-064

Fixation/Permeabilization Solution kit	BD Biosciences, UK	554714
FoxP3 Fixation/Permeabilisation buffer set	Biolegend	421403
GentleMACS C tubes	Miltenyi Biotec, UK	130-096-334
GolgiPlug (with monensin)	BD Biosciences, UK	554724
GolgiStop (with Brefeldin A)	BD Biosciences, UK	555029
Human anti-cytomegalovirus IgG ELISA kit	Abcam	Ab108724
IsoFlo	Oxford Veterinary Sciences	N/A
L-Glutamine	Sigma Aldrich, UK	G7513-100ML
MAIP ELISpot plates	Millipore	MAIPS4510
Mouse IFN-γ ELISpot Kit (ALP)	Mabtech	3321-2A
MS columns	Miltenyi Biotec, UK	130-042-201
NK cell isolation kit, mouse	Miltenyi Biotec, UK	130-115-818
OneComp eBeads	ThermoFisher Scientific UK	01-1111-42
Paraformaldehyde	Alfa Aesar	43368
Pasteur pipette	Fisher Scientific UK	
Penicillin (100U)/Streptomycin (100µg)	Sigma Aldrich, UK	P-0781
Percoll	Sigma Aldrich, UK	P1644-500ML
Phosphate buffered saline tablets	Sigma Aldrich, UK	P4417-100TAB
PMA/ionomycin cell activation cocktail	BioLegend	423301
RPMI-1640 medium	Sigma Aldrich, UK	R0883-500ML
Staphylococcal enterotoxin B (SEB)	Sigma Aldrich, UK	S4881
Sodium Azide (NaN_3)	Sigma Aldrich, UK	S2002
Sterile H_2O	Sigma Aldrich, UK	W3500-500ML
Trypan Blue	Gibco	15250061

Table 2.1. Reagents and materials used in this thesis

2.1.2. Human antibodies and tetramers (BD BioSciences Fortessa cytometer)

Cell surface antibodies				
Antibody	**Clone**	**Fluorochrome**	**Supplier**	**Catalogue number**
Live/Dead stain	N/A	Aqua	ThermoFisher Scientific, UK	L34957
CD14	61D3	eF506	ThermoFisher Scientific, UK	69-0149-41
CD19	HIB19	eF506	ThermoFisher Scientific, UK	69-0199-41
CD3	UCHT1	eF506	ThermoFisher Scientific, UK	69-0038-42
CD3	UCHT1	AF700	eBioScience	56-0038-82
CD4	RPA-T4	APC eF780	eBioScience	47-0042-82
CD56	5.1H11	PE-Cy7	BioLegend	362509
CD56	HCD56	PerCP Cy5.5	BioLegend	362505
CD57	HCD57	PE	BioLegend	322312
CD16	3G8	BV711	BioLegend	302043
NKG2A	REA110	APC	Miltenyi	130-114-089
NKG2C	REA205	PE	Miltenyi	130-103-700
NKG2C	REA205	PE Vio770	Miltenyi	130-103-637
CD45RA	HI100	Pacific Blue	BioLegend	304118
CXCR5	MU5UBEE	PerCP eFluor710	eBioScience	46-9185-41
CXCR3	G025H7	APC	BioLegend	353707
CCR7	G043H7	FITC	BioLegend	353215
CTLA4	BNI3	PE-Cy7	BioLegend	369613
PD1	EH12.1	BV650	BD BioSciences	564104
Intracellular antibodies				
Granzyme B	QA16A02	AF700	BioLegend	372221
IFN-γ	4S.B3	FITC	BioLegend	502506
IFN-γ	4S.B3	PE	BioLegend	502508
IL10	JES3-9D7	PerCP-Cy5.5	BioLegend	501418
CD107α	H4A3	BV421	BioLegend	328626
IL21	eBio3A3-N2	PE	eBioScience	12-7219-42
FoxP3	206D	PE dazzle 594	BioLegend	320125

Table 2.2. Human-target antibodies used in this thesis on the BD BioSciences Fortessa cytometer

2.1.3. Human antibodies (Cytek Aurora spectral cytometer)

Cell surface antibodies				
Live/Dead	N/A	Zombie UV	BioLegend	423107
CD3	OKT3	BUV661	ThermoFisher Scientific, UK	38-0037-41
CD4	OKT4	AF700	BioLegend	317425
CD8	3B5	AF405	ThermoFisher Scientific, UK	MHCD0826
CD19	CD19.11	Spark NIR 685	BioLegend	302269
CD56	5.1H11	APC	BioLegend	362503
CD16	3G8	BUV496	BD BioSciences	564654
CD45RA	HI100	Superbright 702	ThermoFisher Scientific, UK	67-0458-41
CCR7	G043H7	PerCP Cy5.5	BioLegend	353219
PD1	EH12.2H7	PE Dazzle 594	BioLegend	329939
CD57	HNK-1	PE Cy7	BioLegend	359624
CD27	O323	PerCP eF710	ThermoFisher Scientific, UK	46-0279-41
KLRG1	2F1/KLRG1	VioBlue	Miltenyi	138421
CD138	MI25	BUV805	BD Biosciences	748350
NKG2C	REA205	PE	Miltenyi	130-103-700
NKG2A	131411	BV480	BD BioSciences	747923
CD71	L01.1	BUV563	BD Biosciences	748314
CD20	2H7	AF532	ThermoFisher Scientific, UK	58-0209-42
IgM	G20-127	BB515	BD BioSciences	564622
CD25	M-A251	BV737	BioLegend	356137
CD69	FN50	BV750	BD BioSciences	747522
IgG	G18-145	BV650	BD BioSciences	562581
Ki-67	SolA15	APC eF780	ThermoFisher Scientific, UK	47-5698-80
Intracellular antibodies				
IFN-γ	42.B3	BV650	BioLegend	502537
CD107α	H4A3	BV786	BioLegend	328643
TNFα	Mab11	BUV395	BD BioSciences	563996
IL2	MQ1-17H12	BV605	BioLegend	500331

Table 2.3. Human-target antibodies used in this thesis on the Cytek Aurora spectral cytometer

2.1.4. Mouse antibodies and tetramers

Mouse Tetramers			
Tetramer	**Tetramer target**	**Fluorochrome**	**Supplier**
M45	HGIRNASFI	PE	NIH tetramer core facility
M38	SSPPMFRV	APC	NIH tetramer core facility
MR1/5-OP-RU	5-OP-RU	PE	NIH tetramer core facility
MR1/nonspecific	6-FP	PE	NIH tetramer core facility

Surface antibodies				
Antibody	**Clone**	**Fluorochrome**	**Supplier**	**Catalogue number**
Live/Dead	N/A	Near IR	ThermoFisher Scientific, UK	L10119
Live/Dead	N/A	Aqua	ThermoFisher Scientific, UK	L34957
CD3	17A2	APC-Cy7	BioLegend	100222
CD8	PerCP Cy5.5	53-6.7	eBioScience	45-0081-82
CD4	RM4-5	APC-eF780	eBioScience	47-0042-82
CD4	RM4-5	APC-Cy7	BioLegend	100525
CXCR5	2G8	PE-Cy7	BD Biosciences	560617
CTLA4	UC10-4B9	PE Dazzle 594	BioLegend	106318
CX3CR1	SA011F11	Pacific Blue	BioLegend	149022
CD62L	MEL-14	AF700	BioLegend	102012
CD62L	MEL-14	PE-Cy7	BioLegend	104418
CD127	A7R34	PE	BioLegend	135010
PD1	RMP1-30	FITC	eBioScience	11-9981-82
PD1	29F.1A12	BV605	BioLegend	135220
NK1.1	PK136	BV650	BioLegend	108736
NKG2A	16A11	PE	BioLegend	142804
NKG2C	FAB1382N	AF700	R&D BioTechne	FAB1382N-100UG
CD11b	M1/70	APC	eBioScience	17-0112-82
CD27	LG.3A10	PerCP Cy5.5	BioLegend	124214
CD27	LG.3A10	PE	eBioScience	MA5-17905
KLRG1	2F1/KLRG1	PE Dazzle 594	BioLegend	138424
Ly49H	3D10	PE-Cy7	BioLegend	144714
CXCR6	SA051D1	BV711	BioLegend	151111
CD44	IM7	AF700	BioLegend	103025
CD49a	HMα1	PE	BioLegend	142604
CD49b	DX5	PE Cy7	BioLegend	108921
CD19	1D3	BV510	BD Biosciences	562956
F4/80	BM8	BV510	BioLegend	123135
TCR-ß	H57-597	BV650	BioLegend	109251
CD25	PC61	APC	BioLegend	102012
CD69	H1.2F3	PE-Cy7	BioLegend	104511
CD69	H1.2F3	PerCP	BioLegend	104520

CD69	H1.2F3	BV421	BioLegend	104527
Caspase-3	C92-605	PE	BD BioSciences	550821
RIP3K	B-2	FITC	SC BioTech	Sc-374639 FITC
Intracellular antibodies				
IL21	FFA21	APC	eBioScience	17-7211-82
FoxP3	FJK-16s	PE Cy5.5	eBioScience	35-5773-82
IFN-γ	XMG1.2	eF450	eBioScience	48-7311-82
IFN-γ	XMG1.2	PE	BioLegend	505808
CD107a	eBio1D4B	AF488	eBioScience	53-1071-82
TNFα	MP6-XT22	APC	BioLegend	506308
Granzyme B	QA16A02	PE Dazzle 594	BioLegend	372215

Table 2.4. Mouse-target antibodies and tetramers used in this thesis

2.1.5. Mouse depletion antibodies

Depletion antibodies				
Target	**Clone**	**Dose**	**Supplier**	**Catalogue number**
NK1.1	PK136	N/A	2B Scientific	BE0036-1MG
IgG Isotype control	PIP	N/A	2B Scientific	BE0260-5MG

Table 2.5. Mouse depletion antibodies used in this thesis**.**

2.2. Solutions

2.2.1. R0 media

500mL RPMI (Sigma Aldrich), 5mL 100U Penicillin + 100µg Streptomycin (Sigma Aldrich), 5mL 4mM L-glutamine (Sigma Aldrich).

2.2.2. Complete α-MEM/ R10 media

500mL α-MEM (Sigma Aldrich) OR 500mL RPMI (Sigma Aldrich), 5mL 100U Penicillin+100µg Streptomycin (Sigma Aldrich), 5mL 4mM L-Glutamine (Sigma Aldrich), 50mL heat-inactivated foetal bovine serum (Sigma Aldrich).

2.2.3. FACS buffer

500mL Dulbecco's Phosphate Buffered Saline (Sigma Aldrich), 0.1% Bovine Serum Albumin, 0.01% Sodium Azide.

2.2.4. Percoll gradient solution

For 15 livers: 50mL Percoll (Sigma Aldrich), 15mL 10x PBS (Sigma Aldrich), 85mL sterile H_2O (Sigma Aldrich).

2.2.5. NK cell isolation buffer

Sterile PBS (Sigma Aldrich), 0.5% Bovine Serum Albumin, 2mM EDTA.

2.3. Mouse Immunology

2.3.1. Animals

The mice used in these experiments were female C57BL/6J purchased at six weeks old from Charles River or C57BL/6JOlaHsd purchased from Envigo. $MR1^{-/-}$ mice on a BL/6 background were bred in-house at the Biomedical services building (BSB). All experiments were conducted following the guidelines of the Animals (Scientific Procedures) Act (1976) under the University of Oxford PHL and under either the PPL P9804B4F1 (Adrian Hill), or P874AC0F0 (Paul Klenerman). FELASA PIL A/B/C training was complete prior to

commencement of any animal work (PIL: I66CFDC49). Mice were housed in either the Wellcome Trust Centre for Human Genetics Functional Genomics Facility (FGF), or the BSB, in individually ventilated cages under specific pathogen free (SPF) conditions. Food and water were available *ad Libitum*. At the experimental end points, mice were humanely culled by a schedule 1 method. Training and assistance were provided by Dr Claire Hutchings and Dr Lian Ni Lee at the BSB, and Marta Ulaszewska at the FGF, as well as by the staff at each facility.

2.3.2. Infections

Mice were infected with $1x10^6$ plaque-forming units (PFU) of murine cytomegalovirus (MCMV, Smith Strain) in 100µL sterile PBS, administered via the tail vein (i.v.).

2.3.3. Anaesthesia

Prior to vaccination in the FGF, mice were anaesthetised using aerosolised IsoFlo™ isofluorane (2.5% Isofluorane in 2L/min oxygen).

2.3.4. Vaccinations

All vaccinations were administered as 50µL doses in sterile PBS, injected intramuscularly (i.m.) to the left leg. ChAdOx1-vectored vaccines were administered at a dose of $1x10^7$ to $1x10^8$ infectious units (i.u.), and MVA-vectored vaccines were administered at $1x10^6$ to $1x10^7$ PFU. Fluarix was administered at 0.2µg/dose (table 2.6).

Viral-vectored vaccines were manufactured at the Viral Vector Core Facility (VVCF, Jenner Institute, University of Oxford). Vaccinations were assisted by Dr Claire Hutchings in the BSB.

Name	Antigen	Dose	Route
MVA EBOV	Ebolavirus glycoprotein	$1x10^6$ PFU	i.m.
ChAdOx1 EBOV	Ebolavirus glycoprotein	$1x10^8$ i.u.	i.m.
ChAdOx1 OVA	Ovalbumin (OVA)	$1x10^7$ i.u.	i.m.
MVA-GFP2-tPA OVA	Ovalbumin (OVA)	$1x10^7$ i.u.	i.m.
ChAdOx1-LPTOS-tPA-eSP TRIP	*Plasmodium falciparum* TRIP	$1x10^7$ i.u.	i.m.
MVA TRIP	*Plasmodium falciparum* TRIP	$1x10^7$ PFU	i.m.
Fluarix	H1N1 A/California/07/2009, H3N2 A/Perth/16/2009, B/Brisbane/60/2008	0.2µg HA	i.m.

Table 2.6. Vaccines for murine vaccination

2.3.5. NK cell depletion

Mice were injected via the intraperitoneal route with 500µg α-NK1.1 PK136 (2B Scientific) in 200µL sterile PBS at -2 days before vaccination. NK cell depletion was assisted by Marta Ulaszewska in the FGF.

2.3.6. Peptides

Custom peptides were ordered from Mimotopes and reconstituted according to manufacturer's instructions in DMSO and stored at -20°C. Peptides were diluted to a working stock concentration of 1mg/mL in PBS. In intracellular staining assays, OVA peptides were used at a final concentration of 1µg/mL, TRIP peptides were used at a final concentration of 2µg/mL, EBOV GP peptides were used at a final concentration of 5µg/mL, and HA peptides were used at a final concentration of 10µg/mL. Peptide concentrations were optimised prior to the start of this research.

2.3.7. Tail vein bleed PBMC preparation

50-150µL peripheral blood was collected from the tail vein of mice into 1mL FACS buffer in an Eppendorf tube, and kept on ice prior to processing. Samples were centrifuged for 5 minutes at 1350rpm, and supernatant was discarded. The cells were then incubated in 500µL FACS lysis buffer for 3 minutes, and the reaction was stopped by addition of 1mL FACS buffer. The cells were centrifuged and re-suspended in 150µL FACS buffer for antibody staining.

2.3.8. Splenocyte preparation

Spleens were harvested into Eppendorf tubes containing 1mL complete α-MEM. Spleens were mashed with the flat end of a 5mL syringe in a 6-well plate and transferred with sterile PBS to a 50mL Falcon tube through a 70µM cell strainer. Cells were centrifuged at 1350rpm for 5 minutes, supernatant discarded, and re-suspended in 5mL ACK lysis buffer (0.15M NH_4Cl, 1mM KCO_3, 0.1mM Na_3EDTA) for 5 minutes. The lysis reaction was stopped by addition of 25mL PBS, and cells were then centrifuged again, supernatant discarded, and re-suspended in 5mL complete α-MEM. Splenocytes were counted at a dilution of 1:2000 in CasyTon on a CasyCounter, and volumes were re-adjusted to $1x10^7$ cells/mL for ELISpot analysis.

2.3.9. Inguinal lymph node preparation

Inguinal lymph nodes (iLN) were harvested and transferred into Eppendorf tubes containing 1mL α-MEM. iLN were mashed with the flat end of a 5mL syringe through a 70µM cell strainer into a 6-well plate, and then transferred with sterile PBS into a 15mL Falcon tube. The cell suspension was then centrifuged at 1350rpm for 5 minutes, the

supernatant discarded, and cells re-suspended in 500µL α-MEM. The cells were counted at a dilution of 1:2000 in CasyTon on a CasyCounter.

2.3.10. Liver preparation

During harvesting, ~5mL sterile PBS was perfused through the liver via cannulation of the hepatic portal vein with a butterfly needle connected to a 20mL syringe. The liver was subsequently collected into 7mL Bijou tubes containing 4mL complete α-MEM. Care was taken to ensure the gall bladder was removed before harvesting. Livers were crushed with the flat end of a 5mL syringe in a petri dish and transferred with sterile PBS into a 15mL Falcon tube through a 70µM cell strainer. Hepatocytes were centrifuged (700xg, 5 minutes), and supernatant discarded. The cells were then re-suspended in 10mL 33% Percoll solution and centrifuged for 12 minutes at 697xg without the brake. The hepatocytes and supernatant were removed using a Pasteur pipette. Remaining cells were re-suspended in 1mL ACK lysis buffer and incubated for 5 minutes. The reaction was stopped with 10mL PBS. Cells were centrifuged at 700xg for 5 minutes and re-suspended in 500µL complete α-MEM. The cells were counted at a dilution of 1:2000 in CasyTon on a CasyCounter.

2.3.11. Lung preparation

Lungs were collected into 1mL serum-free α-MEM, and transferred into GentleMACS tubes with 4mL RPMI (0% FCS) 45µL Collagenase C7657 and 30µL DNAse. Lungs were homogenised using the gentleMACS dissociator and incubated for 1hr at 37°C in a shaking incubator. 400µL FCS added and the contents of the tube mashed through a 70µm sieve into a 6 well plate. The sieve was washed with RPMI (with 10% FCS) and the contents of

the well transferred to a 15mL falcon tube. Cells were centrifuged at 1350 RPM for 5 minutes and re-suspended in 3mL ACK lysis buffer for up to 2 minutes. 10mL 10% RPMI was added to the samples, cells centrifuged and resuspended in 1000µL 10% RPMI. The cells were counted at a dilution of 1:1000 in CasyTon on a CasyCounter.

2.3.12. NK cell isolation

NK cell isolation was performed following the protocol provided with the NK cell isolation kit and MACS MS columns (Miltenyi) Briefly, Whole splenocytes or liver cells were centrifuged at 300xg for 10 minutes. The supernatant was removed, and cells re-suspended in 40µL NK cell isolation buffer per $1x10^7$ cells. 10µL biotin antibody cocktail (Miltenyi) was added per $1x10^7$ cells and incubated in the fridge for 5 minutes. 2mL buffer was added and cells were centrifuged. The supernatant was removed, and cells re-suspended in 80µL buffer per $1x10^7$ cells. 20µL anti-biotin microbeads were added per $1x10^7$ cells and incubated for 10 minutes in the fridge. MACS MS columns were placed in an OctoMACS magnetic separator and washed once with 500µL buffer. The cell suspension was adjusted to 500µL with buffer and passed through columns. Flow-through was collected, and the columns were washed once with 500µL buffer, which was also collected.

2.3.13. Murine IFN-γ ELISpot

Murine splenocyte ELISpots were conducted following Jenner Protocol J050v6. Briefly, MAIP Millipore plates were coated with 5µg/mL anti-mouse IFN-γ antibody in coating buffer (carbonate-bicarbonate tablets (Sigma) in PBS) and incubated at 4°C overnight. 1 hour before use, the antibody was removed, and plates were blocked with 100µL complete α-MEM and incubated at room temperature (RT) for 1 hour. Between $5x10^5$ cells and

$1.25x10^5$ cells were added per well to the plate in 50µL media. 50µL peptide at a final concentration of 2µg/mL or media for unstimulated wells were added to each well, and plates were incubated for 18 hours at 37°C. To develop, the plates were washed with PBS and incubated with 1µg/mL biotinylated rat anti-mouse IFN-γ diluted in PBS, for 2 hours at RT in the dark. The plates were washed again and incubated with 1µg/mL Streptavidin Alkaline Phosphatase polymer in PBS for 1 hour at RT. The plates were developed using the BioRad AP Conjugate development kit and read on an AID plate reader. Values were calculated from subtracting unstimulated well values from stimulated well values. IFN-γ was expressed as spot forming cells per million splenocytes (SFU/10^6 splenocytes).

2.3.14. Cell stimulation

$1x10^6$ to $2x10^6$ cells were plated per well in 100µL media. Peptides (concentrations in section 2.3.6.) were added to stimulated wells in 100µL media, and incubated for 2 hours at 37°C. For NK cell and T cell activation, 0.2µL/well a-CD107a was added alongside the peptide stimulation. 100µL media was used for unstimulated wells. After 2 hours, 0.2µL/well GolgiPlug was added per well, and cells were incubated for a total of 6 hours total at 37°C.

2.3.15. Tetramer staining

Cells were centrifuged at 1350rpm for 5 minutes, and the supernatant was discarded. Cells were washed twice in FACS buffer, and then incubated in 50µL FACS buffer containing a 1:500 dilution of tetramer. For the MCMV epitope tetramer staining, cells were incubated for 40 minutes at RT in the dark. For the MAIT cell tetramer staining, cells were incubated

for 30 minutes at 37°C. 150µL FACS buffer was added, and cells washed twice. Surface and intracellular cytokine staining was then conducted on the cells.

2.3.16. Murine cellular surface staining

Panels used for surface and intracellular staining of mouse PBMCs can be found in tables 2.8-2.12. Cells centrifuged 1350rpm for 5 minutes, and supernatant discarded. Cells were washed 2x in FACS buffer, re-suspended in 100µL surface antibody stain (tables 2.7-2.12), and incubated at 4°C in the dark for 30 minutes. 100µL FACS buffer was added to each well, and cells centrifuged and supernatant discarded.

2.3.17. Murine intracellular cytokine staining

Cells washed again in FACS buffer and incubated for 25 minutes on ice in 100µL Fix/Perm solution (BD Biosciences) or FoxP3 Fix/Perm solution (BioLegend). 100µL Perm/Wash buffer was added, cells were centrifuged and supernatant discarded. Cells were then re-suspended in 100µL intracellular antibody stain (tables 2.7-2.12) and incubated at 4°C in the dark for 30 minutes. Cells were then washed in 200µL Perm/Wash, 200µL FACS buffer, and then re-suspended in 100-120µL FACS buffer for acquisition on a BD Fortessa (BD BioSciences) using FACSDiva v9.0 (BD BioSciences). A minimum of 200,000 live events were collected for each sample. Single-fluorochrome compensation was calculated from single-stained beads (BD BioSciences) or cells.

Antibody	Stage	Fluorochrome	Dilution
Live/Dead	Surface	Aqua	1:1000
CD3	Surface	APC Cy7	1:100
NK1.1	Surface	BV650	1:100
CD11b	Surface	APC	1:100
CD27	Surface	PE or PerCP Cy5.5	1:100 or 1:50
Ly49H	Surface	PE Cy7	1:100
NKG2A	Surface	PE	1:100
NKG2C	Surface	AF700	1:25
KLRG1	Surface	PE Dazzle 594	1:100
CXCR6	Surface	BV711	1:100
CD107a	Stimulation	AF488	1:500
IFN-γ	Intracellular	eF450	1:100

Table 2.7. Mouse NK cell panel 1: Maturation and activation

Antibody	Stage	Fluorochrome	Dilution
Live/Dead	Surface	Aqua	1:1000
CD3	Surface	APC Cy7	1:100
NK1.1	Surface	BV650	1:100
DX5	Surface	PE Cy7	1:100
CD49a	Surface	PE	1:100
CD69	Surface	PerCP or PerCP Cy5.5	1:50
CXCR6	Surface	BV711	1:100
TNFα	Intracellular	APC	1:100
GzB	Intracellular	PE Dazzle 594	1:50
CD107a	Stimulation	AF488	1:500
IFN-γ	Intracellular	eF450	1:100

Table 2.8. Mouse NK cell panel 2: NK cell memory

Antibody	Stage	Fluorochrome	Dilution
Live/Dead	Surface	Aqua	1:1000
CD8	Surface	PerCP Cy5.5	1:100
CD4	Surface	APC Cy7	1:100
CXCR5	Surface	PE Cy7	1:100
CX3CR1	Surface	Pacific Blue	1:100
CD62L	Surface	AF700	1:50
CTLA4	Surface	PE Dazzle 594	1:100
PD1	Surface	FITC	1:50
CD25	Surface	APC	1:100
FoxP3	Intracellular	PE Cy5.5	1:50
IFN-γ	Intracellular	PE	1:100

Table 2.9. Mouse T_{reg} panel

Antibody	Stage	Fluorochrome	Dilution
Live/Dead	Surface	Aqua	1:1000
CD8	Surface	PerCP Cy5.5	1:100
CD4	Surface	eF450	1:100
CD3	Surface	APC Cy7	1:100
Tetramer	Surface	PE	1:1000
TCRß	Surface	BV650	1:100
CD25	Surface	APC	1:100
CD69	Surface	PE Cy7	1:100
CD19	Surface	BV510	1:100
F4/80	Surface	BV510	1:100

Table 2.10. Mouse MAIT cell panel

Antibody	Stage	Fluorochrome	Dilution
Live/Dead	Surface	Aqua	1:1000
CD8	Surface	PerCP Cy5.5	1:100
CD4	Surface	Qdot 605	1:100
CD62L	Surface	PE Cy7	1:100
CD44	Surface	AF700	1:100
CD69	Surface	BV421 or BV711	1:100
NK1.1	Surface	BV650	1:100
CD25	Surface	APC	1:100
CD127	Surface	PE	1:100
CXCR6	Surface	BV711	1:100
KLRG1	Surface	PE Dazzle 594	1:100
CD107a	Stimulation	AF488	1:1000
IFNg	Intracellular	eF450	1:100

Table 2.11. Mouse T cell activation panel

Antibody	Stage	Fluorochrome	Dilution
Live/Dead	Surface	Aqua	1:1000
CD3	Surface	APC Cy7	1:100
NK1.1	Surface	BV650	1:100
Caspase 3	Intracellular	PE	1:100
RIPK3	Intracellular	FITC	1:100

Table 2.12. Mouse apoptosis and necroptosis panel

2.4. Human immunology

2.4.1. Clinical trials studied during this PhD

All trials were conducted through the Jenner Institute and Centre for Clinical Vaccinology and Tropical Medicine at the University of Oxford. All participants provided written informed consent. All studies were conducted according to the Declaration of Helsinki (2008) and following Good Clinical Practice (GCP) guidelines. All vaccines in clinical trials were manufactured to good manufacturing practice (GMP) standards. PBMCs and serum from these trials are used in these studies. Table 2.13 outlines the vaccines administered during the clinical trials.

2.4.1.1. EBL04

The EBL04 clinical trial (NCT02485912) was a phase Ia trial conducted in Oxford, UK, in healthy adults aged 18-50 years old. This trial used the replication-deficient chimpanzee adenovirus serotype 3 (ChAd3) encoding the glycoprotein from Zaire ebolavirus strain Mayinga (EBO-Z) administered at a dose of $1x10^8$PFU, and the replication deficient MVA expressing glycoprotein of ebolavirus, Sudan virus, Marburg virus, and the nucleoprotein of Taï Forest virus at a dose of $1.5x10^8$ PFU. This thesis uses PBMCs from group 2 of this trial (n=16).

2.4.1.2. FLU005

The FLU005 clinical trial (NCT01818362) was a phase 1 trial conducted in Oxford, UK, in healthy adults aged 18-50 (groups 1-4 n=46), and aged 50+ (groups 5 and 6 n=23). This trial used replication-deficient ChAdOx1 encoding the nucleoprotein (NP) and matrix 1 protein (M1) as a fused protein from influenza A H3N2/A/Panama/2007/99 at a dose $2.5x10^{10}$ viral

particles (v.p.), and MVA encoding NP+M1 at a dose of $1.5x10^8$ PFU. This thesis uses PBMCs from groups 1-4 of this trial, and ELISpot and ELISA data collected prior to the start of this thesis.

2.4.1.3. COV001/COV002

The COV001 clinical trial was conducted in Oxford, UK, in healthy adult volunteers aged 18-55 (group 1, n=88). 44 volunteers were vaccinated with one dose of ChAdOx1 encoding the spike glycoprotein from SARS-CoV-2 (nCoV-19) at a dose of $5x10^{10}$ viral particles. The remaining participants received a placebo vaccine (MenACWY). Serum from all group 1 volunteers and PBMCs from 30 group 1 volunteers (n=26 receiving ChAdOx1 nCoV-19) were used during this thesis. COV001 group 3 (n=10) all received the same dose of ChAdOx1 nCoV-19 followed by a homologous booster dose after 28 days.

The COV002 clinical trial was conducted in the UK in healthy adult volunteers. This thesis used serum samples from UK volunteers aged 18-55 (Group 5d, n=49 received ChAdOx1 nCoV-19), 55-70 (Group 7b, n=30 received ChAdOx1 nCoV-19), and 70+ (group 8b, n=50 received ChAdOx1 nCoV-19). The vaccine regimen and doses used were the same as in COV001.

2.4.1.4. AspiFlu

The COVID-19 and Influenza A participants were enrolled as part of the AspiFlu study (https://www.isrctn.com/ISRCTN51287266) at St George's Hospital, London. Convalescent healthcare worker samples were collected under the ethics outlined in "Gastrointestinal Illness in Oxford: prospective cohort for outcomes, treatment, predictors and biobanking" (REF:11/YH/0020)

Vaccine	Antigen	Made by	Dose	Route	Clinical Trial	Ref
ChAd3 EBO-Z	Ebolavirus glycoprotein	Advent (GSK)	$3.6x10^{10}$ v.p.	i.m.	EBL04	(175)
MVA EBO-Z	Ebolavirus, Sudan virus and Marburg virus glycoprotein, Tai Forest virus nucleoprotein	Emergent BioSolutions, Gaithersburg, MD, USA	$1x10^{8}$ PFU	i.m.	EBL04	(175)
ChAdOx1 NP+M1	Influenza H3N2 Nucleoprotein and M1 protein	CCMP (Oxford, UK)	$2.5x10^{10}$ PFU	i.m.	FLU005	(179)
MVA NP+M1	Influenza H3N2 Nucleoprotein and M1 protein	Impfstoffwerk (Germany)	$1.5x10^{8}$ v.p.	i.m	FLU005	(179)
ChAdOx1 nCoV19	SARS-CoV-2 spike glycoprotein	CCMP/ Advent Srl (Italy)/ Astra Zeneca	$5.0x10^{10}$ v.p.	i.m.	COV001/ COV002	(183)

Table 2.13. Vaccines used in clinical trials studied in this thesis

2.4.2. PBMC defrosting

1mL vials of PBMCs from vaccine trial donors were selected from -180°C or liquid nitrogen storage. Cells were kept on dry ice until defrosting. Vials were defrosted in a 37°C water bath and transferred into 9mL pre-warmed complete R10 media with 2U/mL benzonase. Cells were then centrifuged at 1440rpm for 5 minutes, and re-suspended in 10mL fresh R10. Cells were counted using trypan blue and re-suspended at a concentration of $2x10^{7}$ cells/mL. Vials were frozen at approximately $1x10^{7}$ cells/mL for each trial. For COV001 samples, between $1.31x10^{6}$ and $11.4x10^{6}$ cells were recovered from vials, with an average viability of 78.8%. For FLU005 samples, between $2x10^{6}$ and $14x10^{6}$ cells were recovered

per sample, with an average viability of 70.4%. EBL04 samples had between $6.4x10^6$ and $11.1x10^6$ cells recovered and an average viability of 55.1%.

2.4.3. PBMC stimulation

$2x10^6$ PBMCs per well were plated in a 96 well plate and stimulated with a final concentration of 1-2μg/mL peptides. 100μL media was used as a negative control, and 0.1μL/well PMA-ionomycin (BioLegend) used as a positive control. For T cell analysis, PBMCs were co-stimulated in the presence of 1μg/mL anti-CD28 and anti-CD49d (Life Technologies Ltd). For T cell and NK cell analysis, cells were also incubated with anti-CD107a (tables 2.13 and 2.15). Cells were incubated for 2 hours at 37°C, and then incubated for a further 16 hours following the addition of 1μg/mL Brefeldin A and 1μl/mL Monensin (BioLegend).

2.4.4. BD Fortessa and LSR-II antibody panels

Antibody	Stage	Fluorochrome	Titration
CD14	Surface	eF506	1:100
CD19	Surface	eF506	1:100
CD3	Surface	eF506	1:100
Live/dead	Surface	Aqua	1:1000
CD56	Surface	PE or PerCP Cy5.5	1:100 or 1:33
CD16	Surface	BV711	1:100
CD57	Surface	PE	1:50
NKG2A	Surface	APC	1:50
NKG2C	Surface	PE or PEvio770	1:33
IFN-γ	Intracellular	FITC	1:200
GzB	Intracellular	AF700	1:50
CD107a	Stimulation	BV421	1:500

Table 2.14. Human NK cell panel

Antibody	Stage	Fluorochrome	Titration
CD14	Surface	eF506	1:100
CD19	Surface	eF506	1:100
Live/dead	Surface	Aqua	1:1000
CD3	Surface	AF700	1:75
CD4	Surface	eF780	1:100
CD45RA	Surface	Pacific Blue	1:50
CXCR5	Surface	PerCP eF710	1:33
CXCR3	Surface	APC	1:33
CCR7	Surface	FITC	1:50
CTLA4	Surface	PE Cy7	1:33
PD1	Surface	BV650	1:200
IL-21	Intracellular	PE	1:50
FoxP3	Intracellular	PE Dazzle 594	1:33

Table 2.15. Human T_{reg}/T_{FR} panel

2.4.5. Cytek® Aurora panel design

Flow cytometry on the Aurora spectral cytometer can accommodate a larger range of fluorochromes than on the BD Fortessa cytometer. Spectral cytometry measures the complete emission spectrum of a fluorochrome, rather than a set range at the peak of emission. This can identify fluorochromes that share a peak emission frequency, but have differing emission spectra, in a way that is not possible with traditional cytometry. This allows for a larger range of fluorochromes on each panel.

Marker	Fluorochrome	Cells	Function	Titration	Reference
CCR7	PerCP Cy5.5	T cells	Memory and lymph node migration marker	1:50	(349)
CD107a	BV785	T cells, NK cells	Degranulation	1:100	
CD138	BUV805	B cells	Marker of plasma memory B cells	1:100	(350)
CD16	BUV496	NK cells	FCγRIII, NK cell marker and IgSF activating receptor	1:200	(351)
CD19	Spark NIR 685	B cells	B cell lineage	1:200	(111)
CD20	AF532	B cells	B cell lineage and development marker	1:50	(111)
CD25	BUV737	T cells, NK cells	IL-2Rα, activation	1:100	(352)
CD27	PerCP eF710	B cells, T cells, NK cells	TNF receptor family molecule. Co-stimulatory molecule on T cells and regulates function, binds to CD70 and regulates B cell activation and memory. Marker of maturation on NK cells	1:200	(353)
CD3	BUV661	T cells	T cell lineage	1:400	(352)
CD4	AF700	T cells	$CD4^+$ T cells	1:400	(352)
CD45RA	SuperBright 702	T cells	Memory T cells, expressed on T_{EMRA} and naïve cells	1:100	(354)
CD56	APC	NK cells	NCAM-1, NK cell lineage	1:400	(355)
CD57	PE Cy7	T cells, NK cells	Terminal differentiation and reduced proliferation	1:100	(293)
CD69	BV750	T cells, NK cells	Activation	1:100	(352)

CD71	BUV563	B cells	B cell activation and proliferation	1:100	(356)
CD8	AF405	T cells	$CD8^+$ T cells	1:100	(352)
IFN-γ	BV650	T cells, NK cells	Cytotoxic cytokine	1:100	(352)
IgG	BV421	B cells	Class-switched antibody produced by and expressed on switched memory B cells	1:100	(111)
IgM	BB525	B cells	First antibody produced in response to infections; expressed on unswitched memory B cells	1:100	(357)
IL-2	BV605	T cells, NK cells	Cytotoxic cytokine	1:100	(34)
Ki67	APC eF780	B cells, T cells, NK cells	Proliferation	1:100	
KLRG1	VioBlue	T cells, NK cells	Inhibitory receptor, terminal differentiation	1:100	(320)
Live/Dead	Zombie UV	All	Live cell gating	1:250	
NKG2A	BV480	NK cells	Inhibitory receptor on NK cells	1:100	(358)
NKG2C	PE	NK cells	Activating receptor on NK cells, expanded populations during CMV infection	1:200	(292)
PD1	PE Dazzle 594	T cells	Inhibitory receptor, prevents T cell activation	1:100	(359)
TNF	BUV395	T cells, NK cells	Cytotoxic cytokine	1:100	(352)

Table 2.16 Panel markers, cell expression and function of lymphocyte cell surface and intracellular markers used in the Aurora spectral cytometry assays.

2.4.6. Human cellular surface staining

Panels for human surface and intracellular staining can be found in tables 2.14-2.16. PBMCs were centrifuged 1440rpm for 3 minutes, supernatant was discarded, and cells were re-suspended and washed in 200µL FACS buffer. After removal of supernatant, cells were re-suspended in 100µL surface cocktail antibody stain (tables 2.14-2.16) and incubated in the dark for 30 minutes at 4°C. 100µL FACS buffer was added, and cells washed twice by centrifugation and discarding supernatant.

2.4.7. Intracellular cytokine staining

PBMCs were incubated in CytoFix/CytoPerm solution (BD BioSciences) for 30 minutes in the dark at 4°C. Cells were washed twice in 100-200µL Perm/Wash buffer (BD BioSciences) and incubated for 30 minutes in the dark at 4°C in 100µL intracellular antibody cocktail (tables 2.14-2.16). Cells were then washed twice in Perm/Wash and once in FACS buffer, and re-suspended in 100µL-200µL FACS buffer for acquisition on the BD Fortessa (BD BioSciences) or Aurora (Cytek BioSciences). A minimum of 300,000 live lymphocytes were collected per sample. Single-fluorochrome compensation was calculated from single-stained beads or human PBMCs.

2.4.8. Anti-CMV IgG ELISA

Anti-CMV IgG ELISA kits were used following manufacturer's instructions (Abcam). Briefly, serum was diluted 1:100 in dilution buffer and 100µL was plated in duplicate on ELISA plates coated with cytomegalovirus antigens. Positive, negative, and cut-off controls were also included. Plates were incubated at 37°C for 1 hour in the dark, and then washed 3x with 300µL wash buffer. Wells were then incubated in the dark at room temperature with 100µL cytomegalovirus anti-IgG HRP conjugate for 30 minutes. Plates were developed with 100µL TMB substrate solution for 15 minutes in the dark. The reaction was stopped with addition of 100µL stop solution. Plates were read at 405nm within half an hour of development. Standardised ELISA units were calculated as:

$$\frac{OD\ value\ \times\ 10}{Cut\ off\ value}$$

Values within ±10% of cut off value were assigned 'indeterminate' status and repeated.

2.5. Data analysis

2.5.1. Flow cytometry analysis

Analysis of raw flow cytometry data was conducted on FlowJo (v10.6.2, BD BioSciences) using a hierarchical gating strategy (Supplementary Figures 1-6). Cytokine response was calculated by subtracting the unstimulated background value from the peptide stimulated value. Combinatorial cytokine and activation marker responses were calculated using Boolean gating, firstly by creating 'OR' gates on positive populations, followed by 'Combination' gates.

2.5.2. tSNE plots

t-distributed stochastic neighbour embedding (tSNE) plot analysis was conducted in FlowJo v.10.7.1. Down-sampling was achieved by random selection of '*n*' cells per sample, and concatenation of all chosen samples into one file. tSNE parameter generation included all selected fluorochromes, time points, and keywords with 100,000 iterations and a perplexity of 30, using Barnes-Hut gradient algorithm.

2.5.3. Statistical analysis

Statistical analysis was performed on GraphPad Prism version 8. Grouped data points are shown as Standard Error of the Mean (SEM) unless otherwise stated. Normality of data distribution was tested using the Shapiro-Wilk normality test or the D'Agostino and Pearson test. For groups of data with less than 10 points, non-normal distribution was assumed. For non-normal distributed data, statistical significance of data was determined through Mann-Whitney U Test when comparing n=2 groups or Kruskal-Wallis test with

Dunn's multiple comparisons when comparing n>2 groups. Normally distributed data was tested using a paired t-test for n=2 groups or ANOVA analysis for n>2 groups. Grouped data sets across multiple time points were analysed using mixed-effects analysis with Sidak multiple comparisons. Graphs and heatmap data representations were created in GraphPad Prism v8. Statistical significance was defined as * $p<0.05$, ** $p<0.01$, *** $p<0.005$, **** $p<0.0001$.

2.6. COVID-19 pre-clinical and clinical trial sample processing and assay set up.

2.6.1. Rhesus macaque and ferret PBMC separation

Blood samples were received at the Jenner laboratory in lithium heparin tubes. Blood samples were layered over lymphoprep (density 1.077g) in 15mL Falcon tubes and centrifuged for 30 minutes at 1000xg. PBMCs formed a visible layer, which was removed by transfer pipette and transferred to a clean 15mL falcon tube. PBMCs were washed with Hanks Balanced Salt Solution (HBSS) and centrifuged for 5 minutes at 1440rpm. The supernatant was discarded and PBMCs were re-suspended in 2mL RPMI media.

2.6.2. Clinical trial PBMC separation

2.6.2.1. COV001/COV002

4 lithium heparin tubes of blood per volunteer were received by the Jenner laboratory and processed in the microbiological safety cabinet. Blood from the lithium heparin tubes was poured into leucosep tubes (2 lithium heparin tubes per leucosep tube, 2 leucosep tubes per volunteer), and tubes centrifuged for 13 minutes at 1000xg without brake. The top layer of blood separated by the leucosep tube contains plasma. 4mL plasma was removed from the leucosep tube by transfer pipette and transferred into 2 labelled cryovial tubes. The remainder of each leucosep tube was poured into a 50mL falcon and topped up to 40mL with R0 media (2 falcon tubes per volunteer). Falcon tubes were centrifuged for 5

minutes at 1800rpm and supernatant discarded. PBMCs from the same donor were pooled into one falcon tube in 30mL R0 media. Falcon tubes were centrifuged again for 5 minutes at 1800rpm and supernatant discarded. PBMCs were re-suspended in 10mL R10 media. 10µL PBMC suspension was transferred into 10mL CASYTON and inverted to mix. Cells were counted on a CASY counter using programme 1 (cell diameter: 5.75µM-15µM, 400µL sample volume, 150µM capillary). Cells were resuspended to volume calculated by the lab record form.

2.6.2.2. COV006

1 lithium heparin tube of blood per volunteer was received by the Jenner laboratory and processed in the microbiological safety cabinet. Tubes were centrifuged at 2000rpm for 10 minutes with the brake on. The top layer of separated blood contained the plasma. As much plasma as possible was collected by transfer pipette and transferred into a labelled cryovial. The remainder of the lithium heparin tube was topped up to 10mL with R0 media and gently inverted to mix. The blood was then transferred equally between two 12mL leucosep tubes and centrifuged for 13 minutes at 1000xg with the brake off. The top layer separated by the leucosep tube contains a layer of PBMCs. The PBMC layer from the leucosep tube was collected by transfer pipette and transferred to a 50mL falcon tube. If more than one leucosep tube per donor was centrifuged, the PBMCs were pooled into a single falcon tube for each donor. PBMCs were topped up with 20mL R0 and centrifuged at 1800rpm for 5 minutes. The supernatant was then removed and the cell pellet was resuspended in 10mL R0 media. Cells were centrifuged again at 1800rpm for 5 minutes, supernatant discarded, and resuspended in 2mL R10 media. PBMCs were counted as

following the COV001/COV002 counting protocol, except using 5mL PBMC suspension in 10mL CASYTON.

2.6.3. Clinical trial ELISpot set up

2.6.3.1. General protocol for COV001/COV002 and COV006

Prior to ELISpot set up, MAIP plates were coated with 10µg/mL antibody in 50mL coating solution and incubated at RT for 3-8 hours. On the day of ELISpot set up, coating solution was flicked off the plates and wells washed 2-3x with 100µL sterile PBS. Plates were then blocked with 100µL/well R10 and incubated at RT for 1-8 hours. Stimulating peptides and unstimulated controls were pre-prepared in 96 well plates at a concentration of 2µg/mL. The blocking R10 was then flicked off the plate and 50µL per well of peptide/control were added to the wells in the outlined layout. 50µL PBMCs at a concentration of $1x10^6$ were added to relevant wells and ELISpot plates were incubated for 18-20h at 37°C in 5% CO_2. ELISpot plates were then developed and read by another member of the vaccine clinical trials team.

2.6.4. COV001/COV002 Clinical trial intracellular cytokine staining (ICS) set up

ICS conducted in 5mL polypropylene tubes in a microbiological safety cabinet. Four tubes per donor were set up prior to addition of PBMCs: 1x unstimulated, 1x positive control (10µl SEB at 1µg/mL), 1x S1 peptide pool (10µL at 2µg/mL), 1x S2 peptide pool (10µL at 2µg/mL). Each tube had 400µL supplemental R10 added (containing 1µg/mL a-CD28, 1µg/mL a-CD49d and 1µl/mL a-CD107a PE-Cy5). 600µL ($3x10^6$) PBMCs were added to each tube and vortexed. FACs tubes incubated at 37°C in 5% CO_2. After 2 hours, 10µg/mL Brefeldin A and 1µl/mL monensin was added to each tube, tubes were vortexed. FACS

tubes were then incubated for a further 16-20 hours at 37°C in 5% CO_2 for staining and analysis by flow cytometry.

2.6.5. PBMC sample freeze down

During PBMC counting, the number of PBMC vials to be frozen was calculated on the lab record form. PBMC vials were frozen at a concentration of 7-10 million cells/mL. PBMCs were centrifuged at 1800rpm for 5 minutes, and resuspended in chilled FCS at half the final required volume. PBMCs were incubated at 4°C for 20 minutes. Freeze mix (FCS+20% DMSO) was added to make up the total volume needed for freezing. Cells were transferred to cryovials (1mL per vial) and stored at -80°C overnight in a Cool Cell. Cryovials were transferred to -150°C the following day.

Chapter 3

Viral vector vaccination and the murine NK cell response

Chapter 3 : Viral vector vaccination and the murine NK cell response

3.1. Introduction and Aims

Viral vector vaccination regimens of ChAdOx1-prime and MVA-boost induces a robust humoral, T cell and B cell response in pre-clinical and clinical trials (179, 192, 360) However, the effect of viral vector vaccination on other immune populations is less well understood. NK cells are among the first immune cells activated in response to viral infections, including cytomegalovirus, influenza, Epstein-Barr virus and hantaviruses (15, 21, 361), and elicit a cytotoxic response. Some vaccines, for example BCG, seasonal influenza and ad26.EBO-Z, also induce NK cell activation, proliferation, and subsequent cytotoxicity upon restimulation with vaccine antigen in humans and non-human primates (53, 362-364). It has been proposed that vaccines and pathogens may also generate long-lived NK cell memory populations that can recognise specific antigens (5, 55). NK cell antigen-specific memory has been demonstrated in VZV infection in humans (56) and upon ad26-vectored vaccination in macaques (63), potentially facilitated by liver-resident NK cells expressing CXCR6 (43, 65, 365).

It is currently unknown whether ChAdOx1 vaccination elicits a cytotoxic NK cell response or facilitates NK cell memory formation. The effect of either ChAdOx1 and MVA vaccination on the phenotype and maturation of NK cells has also not been previously described. In mice, NK cell maturation is correlated with functional capacity, and can be defined along an axis of CD11b and CD27 expression (29). As outlined in the introduction (Section 1.2.1.2), the least mature $CD11b^{-}CD27^{+}$ NK cells are less cytotoxic but can respond to activation with robust cytokine production. $CD11b^{+}CD27^{+}$ are more mature and respond to stimulation with cytotoxic granule formation and cytokine production. The most mature $CD11b^{+}CD27^{-}$ NK cells do not respond to activation with strong cytokine production,

although still elicit a cytotoxic response. These NK cells are the most terminally differentiated, and have heightened expression of inhibitory markers including KLRG1 (9, 366). Alongside inflammatory functionality, NK cells can regulate $CD4^+$ and $CD8^+$ T cell function during chronic viral infection and upon vaccination, which prevents excessive immunopathology of infected tissues (7, 367-369). This is achieved through secretion of anti-inflammatory IL-10 (370), through PD1/PD-L1 interactions (8), by elimination of DCs to prevent antigen presentation (371), or by direct killing of activated T cells (7).

In this chapter, I investigate T cell and NK cell activation and functional response to viral vector vaccination. Firstly, I describe how populations of regulatory T cells respond to vaccination with ChAdOx1 and MVA in mice. I then outline how ChAdOx1 and MVA vaccination alter the NK cell phenotype in single-dose and prime-boost experiments. These responses are compared to vaccination with inactivated influenza virus. Finally, I investigate how NK cell depletion prior to heterologous ChAdOx1-MVA vaccination affects T cell activation, memory population formation, and antigen-specific cytotoxic response.

Aims of Chapter Three

- Establish the T cell and regulatory T cell phenotype following viral vector vaccination and compare to the response elicited from inactivated virus vaccination.
- Identify NK cell activation and functional response following vaccination with ChAdOx1- and MVA-vectored vaccines and ascertain whether a T cell-independent NK cell memory population is generated.
- Identify vaccine-specific NK cell phenotypes following ChAdOx1 and MVA vaccination, and establish a mechanism behind phenotypic modulation.
- Investigate the effect of NK cell depletion of heterologous ChAdOx1-MVA prime-boost vaccine regimens on T cell activation, memory formation and effector function.

3.2. Results

3.2.1. T cell activation and migration following viral vector and inactivated virus vaccination

Throughout this chapter, I use three different antigen-encoding ChAdOx1- and MVA-vectored vaccines to ensure that any changes to cell phenotype were caused by the vaccine vector and not the antigen insert (table 2.6). To characterise the T cell response to ChAdOx1-prime, MVA-boost vaccination, C57BL/6JOlaHsd mice (n=5 per group) were vaccinated intramuscularly (i.m.) in a prime-boost regimen with $1x10^8$ i.u. ChAdOx1 followed by $1x10^6$ PFU MVA at an interval of three weeks. A separate group of mice (n=5) were also vaccinated with two doses of 0.2μg Fluarix® at an interval of three weeks. Fluarix is an unadjuvanted split-virion vaccine that has robust immunogenicity in single dose and MVA-boost vaccine regimens (372). One-week post-boost, the animals were culled and T cell activation in the spleen and inguinal lymph nodes (iLN) was assessed (Table 3.1).

Marker	Function	Reference
CD25	IL-2Rα; T cell activation	(373)
CD62L	Cell adhesion, central memory	(374)
CTLA4	Inhibitory receptor, T cell tolerance	(375)
PD-1	Inhibitory receptor, T cell exhaustion	(376)

Table 3.1. T cell markers of activation, memory and exhaustion.

Both ChAdOx1-MVA (Ad-M) and Fluarix (Flu) vaccinated mice had activated ($CD25^+$) $CD4^+$ T cells in the iLN and spleen ($p<0.04$). There was also significantly more $CD25^+$ splenic $CD8^+$ T cells from Flu vaccinated mice, and a similar trend in Ad-M vaccinated mice ($p=0.039$, Figure 3.1A). Ad-M vaccinated mice had a higher frequency of $CD62L^+CD4^+$ T cells in the

spleen but a trend towards fewer $CD62L^+CD8^+$ T cells in the iLN (p=0.0089 spleen, p=0.059 iLN, Figure 3.1B). This potential increase in central memory T cells following adenovirus vaccination has been previously demonstrated following Ad26 and Ad48 vaccination (374, 377). CTLA4 expression did not change on $CD4^+$ T cells in vaccinated mice, although there were significantly fewer splenic $CTLA4^+CD8^+$ T cells from Flu vaccinated mice in comparison to unvaccinated mice (p=0.032, Figure 3.1C). Finally, Ad-M vaccination increased frequency of $PD1^+CD4^+$ T cells in the iLN when compared to unvaccinated mice, and splenic $PD1^+CD8^+$ T cells when compared to Flu vaccinated mice (p<0.048, Figure 3.1D).

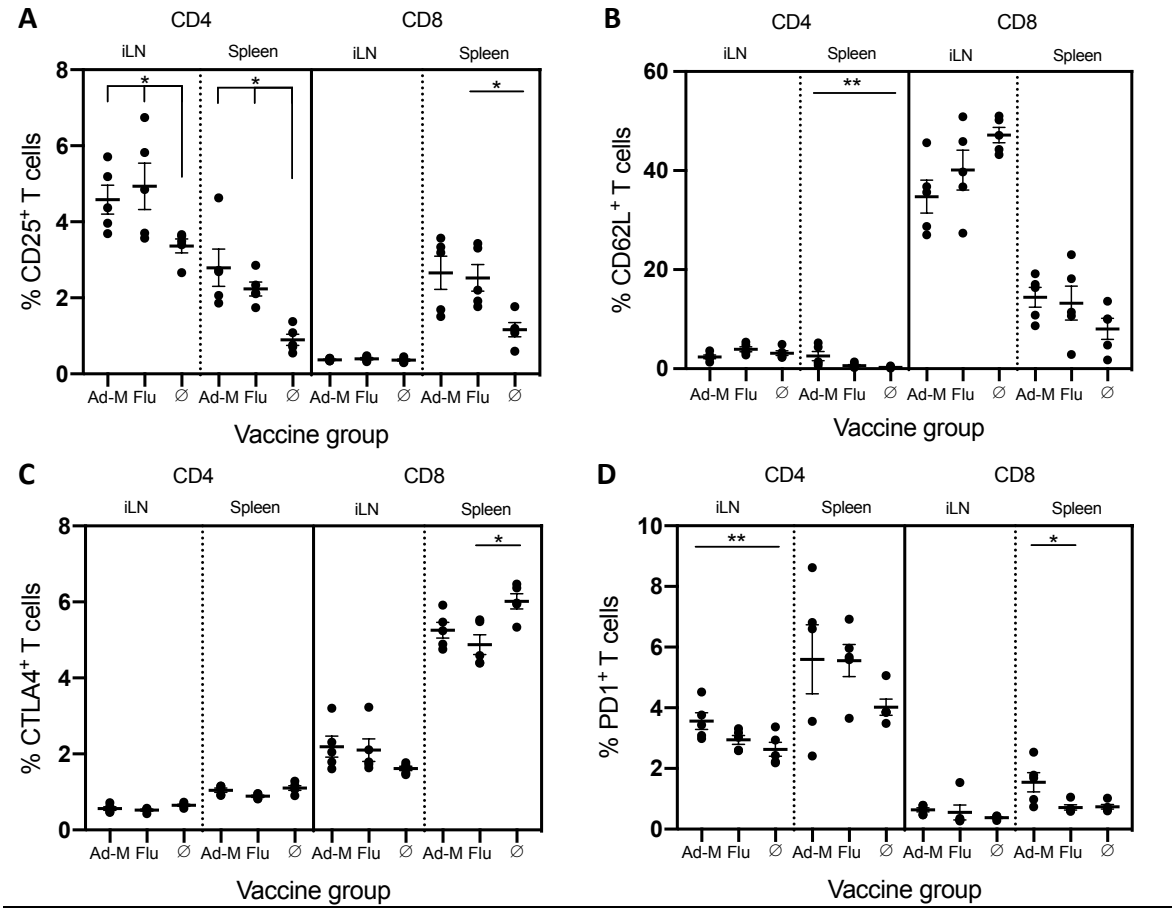


Figure 3.1. Activation of T cells after vaccination with viral vector or split virion vaccines.

C57BL/6J mice (n=5 per group) were left unvaccinated (∅) or were vaccinated intramuscularly with $1x10^8$ i.u. ChAdOx1 and $1x10^6$ PFU MVA (Ad-M), or with two doses 0.2µg Fluarix (Flu) at a three-week interval and culled at one-week post-boost. Frequency of T cells expressing **A)** CD25, **B)** CD62L, **C)** CTLA4, **D)** PD1.

Statistical analysis conducted using Kruskal-Wallis test with Dunn's multiple comparisons. Error bars shown as mean± SEM. *p<0.05, **p<0.01.

3.2.2. T_{reg} and T follicular regulatory cells and viral-vector vaccination

Alongside the activation and phenotype of T cells, I also analysed the effect of viral vector and inactivated virion vaccination on subsets of regulatory T cell populations. Mice were vaccinated as previously described in section 3.2.1. with either an Ad-M or Flu regimen. After one-week post-boost, the animals were culled and iLN, spleens and livers harvested. The frequency of regulatory T cell populations (Table 3.2) were measured via flow cytometry following the gating strategy outlined in supplementary figure 4.

Population	**Markers**
Activated T_{reg}	$CD4^+FoxP3^+CD25^+$
T follicular helper (T_{FH})	$CD4^+CXCR5^+PD1^+$
T follicular regulatory (T_{FR})	$CD4^+FoxP3^+CD25^+$ $CXCR5^+PD1^+$

Table 3.2. Populations and defining markers of regulatory T cells, follicular helper T cells, and follicular regulatory T cells.

Overall, the proportions of regulatory T cells did not change with ChAd-MVA or inactivated vaccination. $FoxP3^+$ T_{regs} from vaccinated mice expressed slightly more CD25 in the spleen and iLN, as also demonstrated in figure 3.1 ($p=0.053$, Figure 3.2A). There were no significant changes in the frequency of T follicular helper cells in any organ (Figure 3.2B), or T follicular regulatory cells in the iLN or spleen (Figure 3.2C). Overall, T_{FR} cells as a proportion of total $CD4^+$ T cells was very low across all experiments.

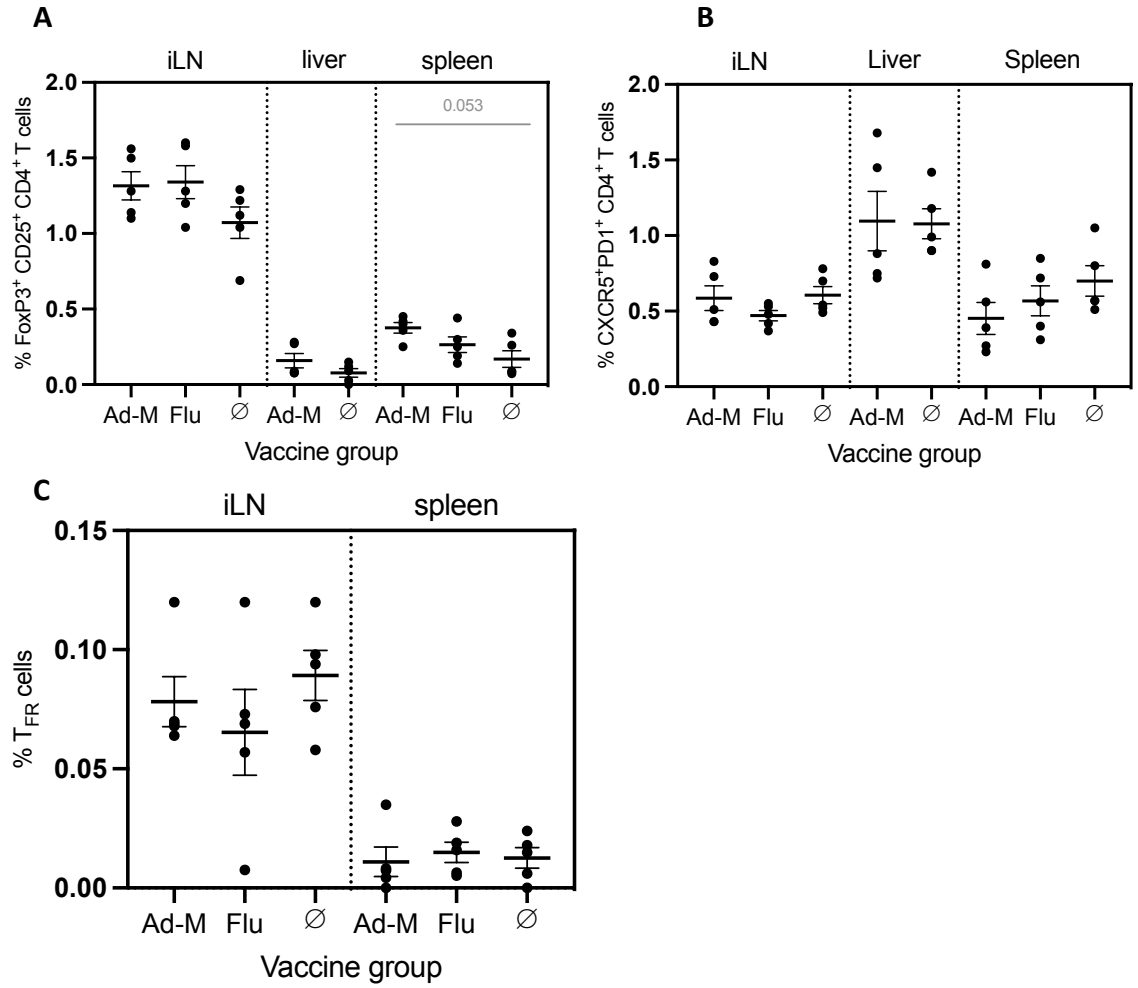


Figure 3.2. Changes in frequency of regulatory T cell populations after vaccination.

C57BL/6J mice (n=5 per group) were left unvaccinated (∅) or were vaccinated intramuscularly with $1x10^8$ i.u. ChAdOx1 and $1x10^6$ PFU MVA (Ad-M), or with two doses 0.2µg Fluarix (Flu) at a three-week interval. These data show the frequency of **A)** T_{reg}, **B)** T_{FH}, and **C)** T_{FR} cells.

Statistical analysis conducted using Kruskal-Wallis test with Dunn's multiple comparisons. **p*<0.05, ***p*<0.01, ****p*<0.005, *****p*<0.0001. Error bars shown as mean± SEM.

3.2.3. NK cells are activated and produce IFN-γ in response to peptide stimulation after vaccination

It is currently unknown whether NK cells are activated following ChAdOx1 vaccination, and whether they can secrete cytokines upon re-stimulation with vaccine antigen. To explore this further, I first assessed whether a single dose of ChAdOx1 or MVA elicited a cytotoxic response from NK cells. C57BL/6JOlaHsd mice (n=5 per group) were vaccinated with $1x10^7$ i.u. ChAdOx1 or $1x10^7$ PFU MVA, or left unvaccinated as a control. After one week, spleens, livers and iLN were harvested and stimulated with overlapping pools of respective vaccine antigen peptides, and activation was measured by intracellular cytokine staining and flow cytometry following the gating strategy in supplementary figure 2.

The side-scatter of NK cells (SSC-A) can be used to determine NK cell activation and also blastogenesis following stimulation with IL-2 and IL-12 (378). NK cells had a significantly higher SSC-A after vaccination with single-dose ChAdOx1 than unvaccinated or MVA-vaccinated mice (Fig 3.3A). NK cells also produced a modest yet non-significant amount of IFN-γ in single-dose ChAdOx1 vaccinated mice. In the iLN, the least mature and most cytotoxic $CD11b^-CD27^+$ NK cell subset from ChAdOx1-vaccinated mice produced more IFN-γ than MVA-vaccinated or unvaccinated mice (0.558% NK cells from ChAdOx1 vaccinated mice vs 0% from unvaccinated mice, p=0.06. Figure 3.3B).

A second cohort of mice were vaccinated with a prime-boost regimen consisting of homologous ChAdOx1-ChAdOx1 (Ad-Ad) or MVA-MVA (M-M), or heterologous ChAdOx1-MVA (Ad-M) at an interval of one week, and were subsequently culled one-week post-boost. All vaccines were administered i.m. and at the same dose as previously stated. NK cells in the iLN and spleen of mice vaccinated with all regimens responded to peptide stimulation. In splenic NK cells from Ad-M and M-M vaccinated mice, there was a

significant increase in the proportion of $CD107a^{+}IFN\text{-}\gamma^{+}$ NK cells in the spleen after peptide stimulation when compared to unvaccinated mice (Ad-M p=0.01, M-M p=0.017. Figure 3.3C). Together, this data represents activation of NK cells in the iLN and spleen post-viral vectored vaccination, and NK-derived IFN-γ in response to peptide stimulation.

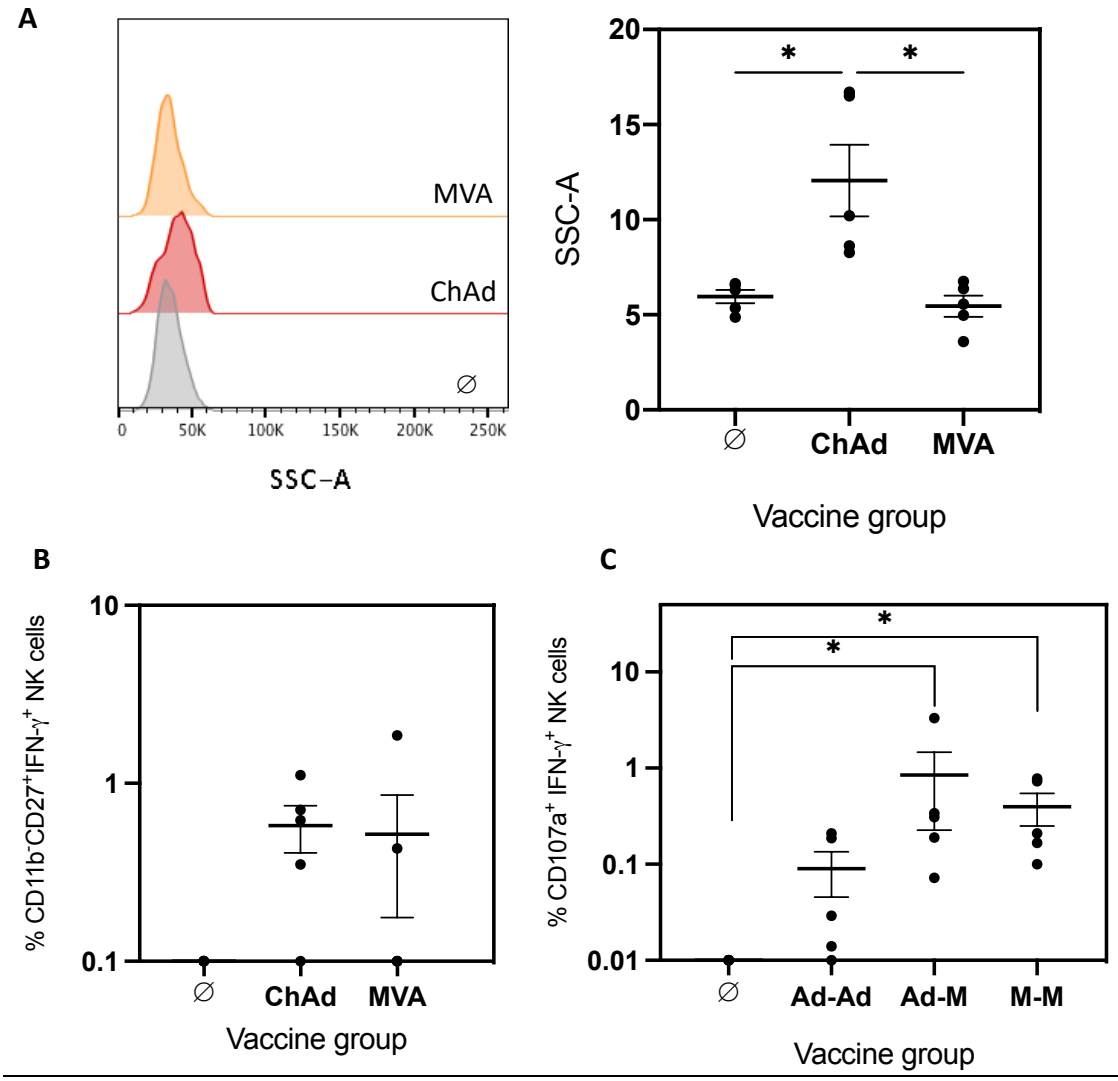


Figure 3.3. NK cell activation and IFN-γ production post-vaccination.

Mice (n=5 per group) were left unvaccinated (∅) or were vaccinated intramuscularly with $1x10^7$ i.u. ChAdOx1 (ChAd) or MVA (MVA). IFN-γ production was measured through flow cytometry in the liver, iLN and spleen. **A)** The SSC-A of NK cells in the spleen in ChAdOx1-vaccinated mice. **B)** IFN-γ production by $CD11b^-CD27^+$ NK cells in the iLN.

Mice were vaccinated with a homologous regimen of $1x10^8$ i.u. ChAdOx1-ChAdOx1 (Ad-Ad) or $1x10^6$ PFU. MVA-MVA (M-M), or heterologous ChAdOx1-MVA (Ad-M) at an interval of one week. **C)** Frequency of $CD107a^+IFN\text{-}\gamma^+$ NK cells in the spleen following peptide stimulation.

Statistical analysis conducted using Kruskal-Wallis Test with Dunn's multiple comparisons ns= no significance, *p<0.05. Error bars shown as mean± SEM.

3.2.4. NK cells from vaccinated mice require accessory cells to produce IFN-γ after vaccination

NK cells can be activated by cytokines, including IL-2, IL-15, and IL-18, produced by constitutively activated T cells and leukocytes in response to antigen stimulation (19, 286, 362, 379, 380). However, it is unknown if NK cells can form T cell-independent antigen-specific memory after ChAdOx1 vaccination, or if the NK cell activation described in figure 3.3 is dependent on lymphocyte-derived cytokines.

NK cells were isolated from the livers or spleens of C57BL/6JOlaHsd mice (n=5 per group) culled seven days after vaccination with a prime-boost regimen of $1x10^8$ i.u. ChAdOx1 and $1x10^6$ PFU MVA at a 1-week interval. The isolated NK cells were pooled from each group of 5 mice, and divided into three wells to obtain at least 100,000 NK cells per well for this experiment. Within the purified NK cell samples, there was an average of 81.7% $NK1.1^+$ cells. IFN-γ production from isolated NK cells was measured by ELISpot assay following overnight peptide stimulation, and a whole-splenocyte ELISpot assay was set up as a comparison for T cell IFN-γ production. Significantly more IFN-γ was produced by ChAd-MVA vaccinated mice than unvaccinated mice in the whole splenocyte ELISpot (p=0.0079. Figure 3.4A). Comparatively, there was no significant difference in IFN-γ production by purified NK cells from the liver or spleen in vaccinated mice and unvaccinated controls (Figure 3.4B). This indicates that isolated NK cells from the spleen or liver of vaccinated mice do not respond to produce IFN-γ directly in response to incubation with vaccine antigen peptides. These NK cells were isolated through magnetic column separation, and future experiments could be improved by using cell sorting to ensure a higher NK cell yield and purity, which may reduce the variation in the NK cell response between groups.

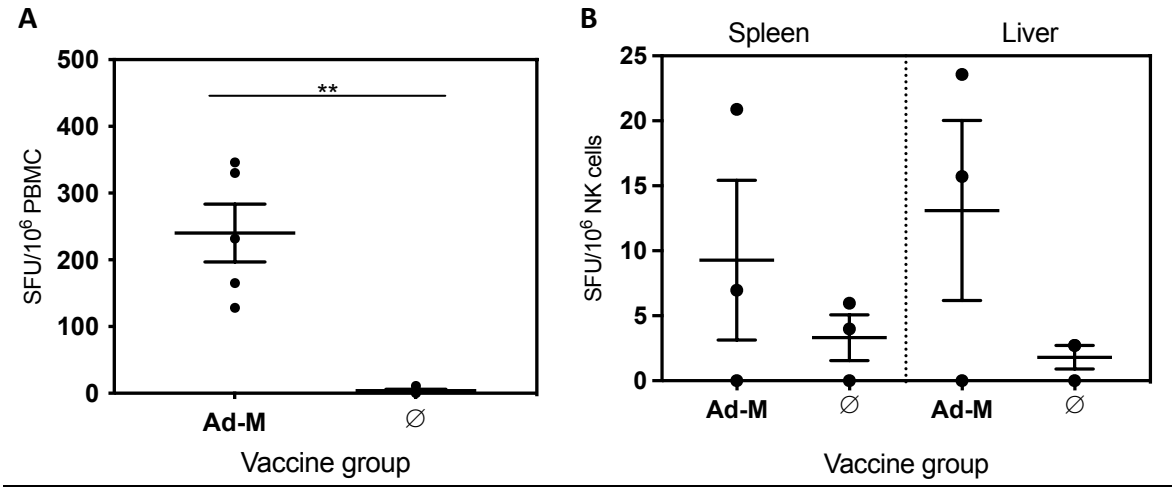


Figure 3.4. IFN-γ production by whole splenocytes and isolated murine NK cells post-vaccination.

Mice (n=5 per group) were left unvaccinated (∅) or were vaccinated intramuscularly with $1x10^8$ i.u. ChAdOx1 (Ad) followed by $1.x10^6$ PFU MVA (M) 7 days later. Spleens and livers were harvested 7 days post-boost and IFN-γ production was measured by IFN-γ ELISpot analysis in **A)** whole splenocytes, or **B)** pools of isolated NK cells from the spleen or liver. Isolated NK cells from the spleens and livers were pooled and re-distributed into n=3 wells per group, with at least 127,200 cells per well. Values were calculated by subtracting unstimulated values from stimulated values. SFU = spot-forming units per 10^6 cells. Statistical analysis conducted using Mann-Whitney U test, $^{**}p<0.01$.

3.2.5. ChAdOx1 vaccination does not alter NK cell maturity or expression of activating receptors

As demonstrated in figure 3.3, NK cells can produce a cytotoxic IFN-γ response upon vaccination with single dose or multiple doses of ChAdOx1 and MVA. In order to further define the NK cell response to viral vector vaccination, mice were vaccinated i.m. with a single dose of $1x10^7$ i.u. ChAdOx1 or $1x10^7$ PFU MVA, and the changes in the NK cell phenotype were assessed at day 7 post-vaccination in two secondary lymphoid organs; the inguinal lymph nodes (iLN) and spleen, and also in the liver. Specifically, the expression of maturation, activation, and migration markers (table 3.3) were assessed.

Marker	Function	Reference
CD11b	CD11b and CD27 form an NK cell maturation gradient. $CD11b^{+}CD27^{-}$ are the most mature NK cells, followed by $CD11b^{+}CD27^{+}$, then $CD11b^{-}CD27^{+}$ as the least mature NK cells	(9)
CD27		
KLRG1	Inhibitory receptor and marker of senescence on NK cells	(366)
Ly49H	Activating receptor	(381)
NKG2A	Inhibitory receptor	(382)
NKG2C	Theoretical activating receptor: NKG2C is an activating receptor on human NK cells	(383)
CXCR6	Migration marker; facilitates NK cell migration to the liver. Associated with NK cell memory-like function.	(43)

Table 3.3. Maturation, activating and inhibitory receptors on murine NK cells.

One-week post-ChAdOx1 vaccination, there was no significant change in most measured NK cell marker of maturation, or activation or inhibitory receptors across the total NK cell population in the iLN, spleen, or liver (Figure 3.5). However, there was a significantly increased frequency of $NKG2C^{+}$ NK cells in the spleen of vaccinated mice (p=0.039. Figure 3.5F).

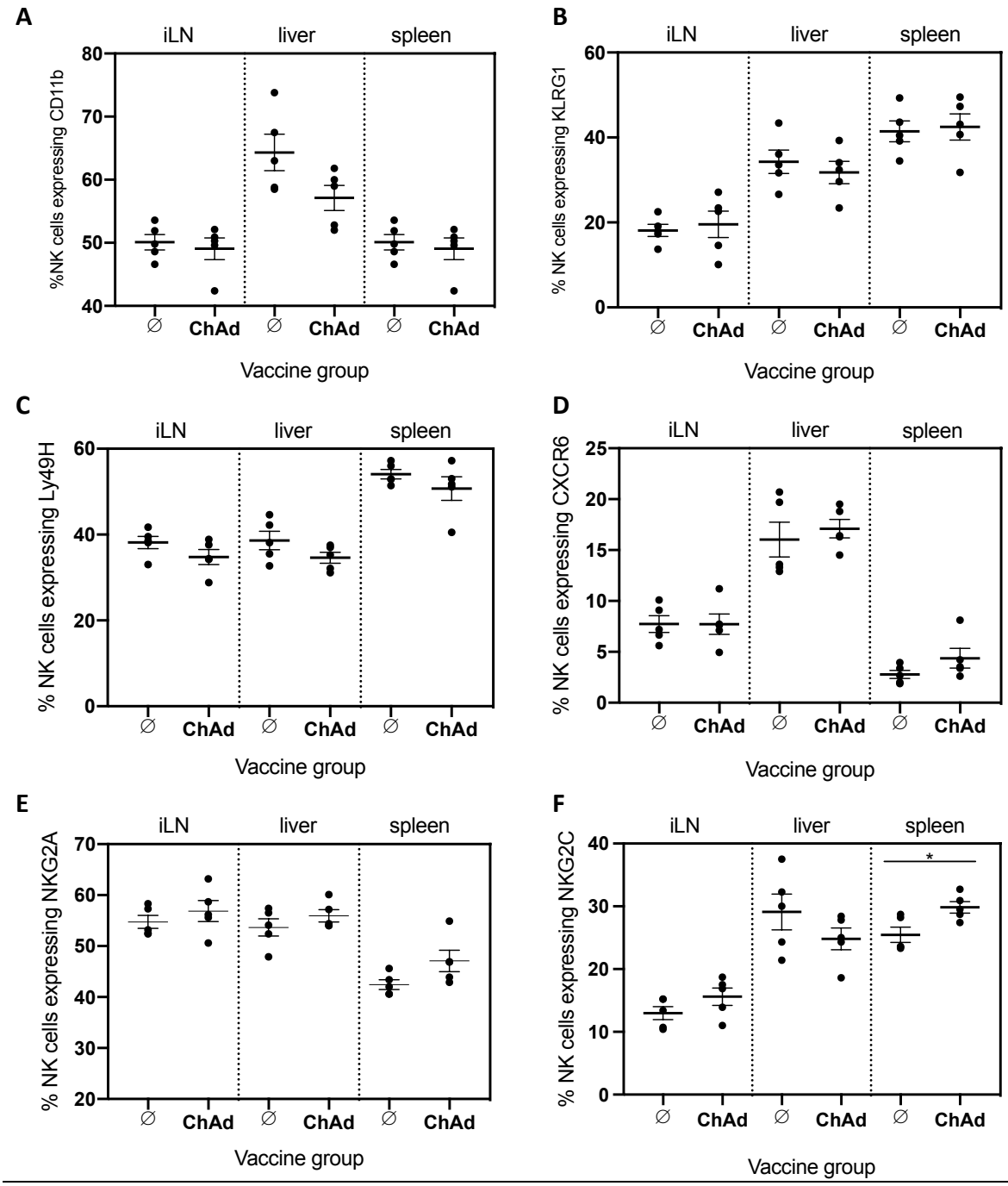


Figure 3.5. ChAdOx1 vaccination and NK cell phenotype

Mice (n=5 per group) were left unvaccinated (∅) or were vaccinated intramuscularly with $1x10^7$ i.u. ChAdOx1 (ChAd). Cell surface expression of inhibitory and activation receptors and markers of differentiation were analysed by flow cytometry in the inguinal lymph nodes (iLN), liver, and spleen; **A)** CD11b, **B)** KLRG1**, C)** Ly49H, **D)** CXCR6**, E)** NKG2A, **F)** NKG2C Statistical analysis conducted using Mann-Whitney U test, *p<0.05.

3.2.6. MVA vaccination alters phenotype and maturation of NK cells

Comparatively to ChAdOx1 vaccination, the maturation and activation phenotype of NK cells across all three organs was significantly altered one-week post-vaccination with MVA. Most clearly, the frequency of $CD11b^+$ NK cells in the iLN, liver, and spleen was reduced, suggesting a potential systemic reduction in the frequency of mature $CD11b^+$ NK cells (*p<0.03, Figure 3.6A). There was also a reduction of $Ly49H^+$ NK cells across all organs (iLN p=0.055, liver p=0.032, spleen p=0.016 figure 3.6C). CXCR6 frequency was also significantly higher in the spleen of vaccinated mice (p=0.0079, figure 3.6D).

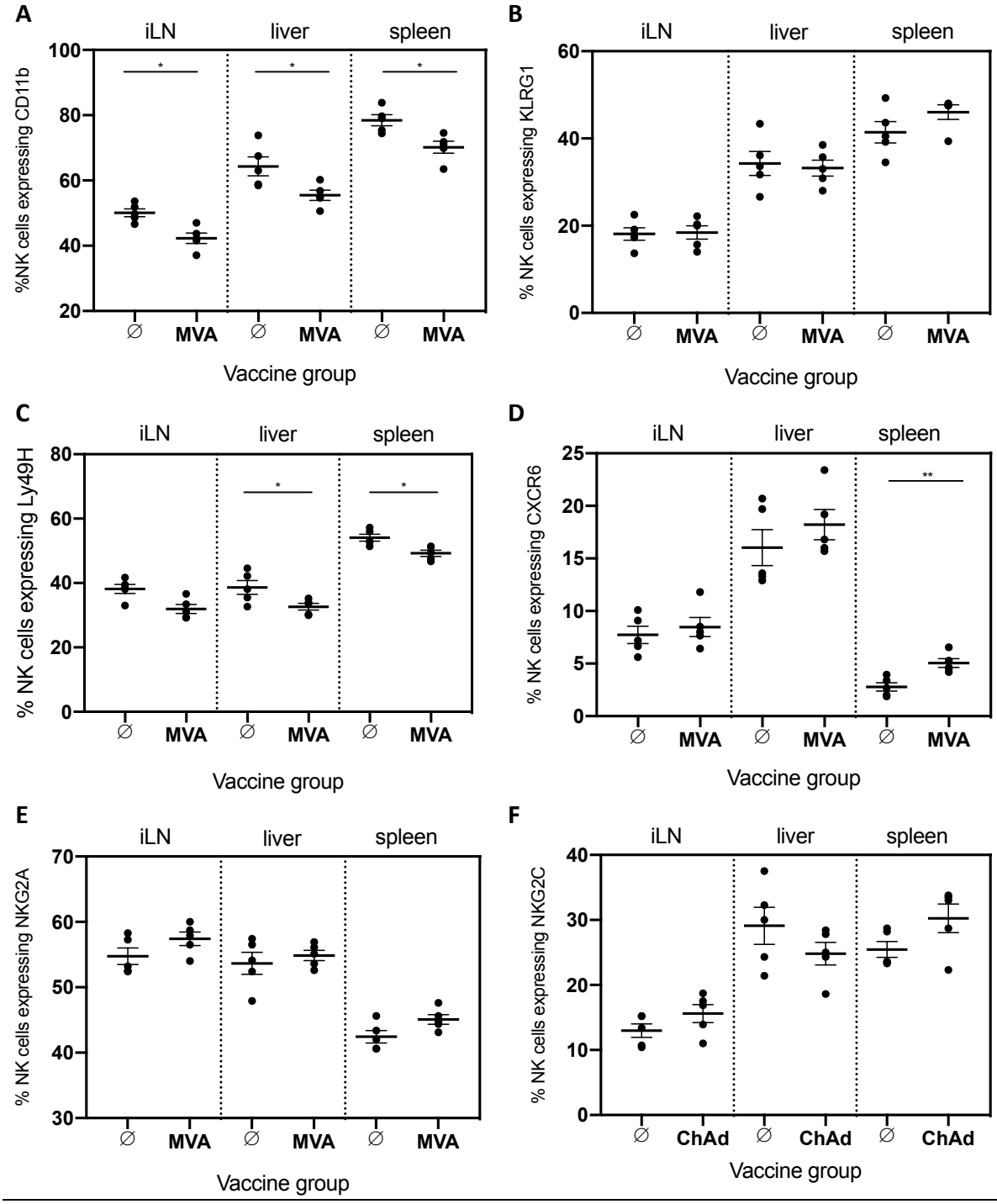


Figure 3.6. MVA vaccination and NK cell phenotype

Mice (n=5 per group) were left unvaccinated (∅) or were vaccinated intramuscularly with $1x10^7$ i.u. MVA (MVA). In the iLN, liver and spleen, NK cells were analysed for frequency of NK cells expressing **A)** CD11b, **B)** KLRG1, **C)** Ly49H **D)** CXCR6, **E)** NKG2A, **F)** NKG2C.

Statistical analysis conducted using Mann-Whitney U test. *p<0.05, **p<0.01. Error bars shown as mean± SEM.

3.2.7. Receptor expression and activation of NK cell maturation subsets is altered by viral vector vaccination

These data demonstrate that vaccination with MVA decreases the frequency of $CD11b^+$ NK cells across all measured organs. This implies a systemic reduction in the mature NK cell populations, which would have an effect on the overall function of the NK cell response to vaccination in mice. To investigate this further, the NK cell populations in the iLN, spleen, and liver were gated into the defined maturational axis ($CD11b^+CD27^-$ most mature; $CD11b^+CD27^+$ mature; $CD11b^-CD27^+$ least mature) and the expression of cell surface receptors was analysed. Stratification of NK cells along these three main subsets of NK cell maturation unveiled distinct changes in receptor expression by organ, maturation status, and vaccine administered (Figure 3.7A). As previously demonstrated, the liver had higher proportions of $CXCR6^+$ NK cells with an immature phenotype (43). KLRG1, NKG2C and Ly49H were preferentially expressed on the two more mature NK cell populations, whereas NKG2A was expressed on the least mature NK cell population (Figure 3.7A, (15)).

The most mature ($CD11b^+CD27^-$) NK cell subpopulation expressed the highest levels of the terminal differentiation marker KLRG1 across all organs. KLRG1 had a strong trend towards an increase in mice vaccinated with MVA (p=0.053, Figure 3.7B). These NK cells also expressed significantly more NKG2C in the spleen of ChAdOx1 vaccinated, but not MVA vaccinated mice (p=0.0483, Figure 3.7C)

Mature NK cells ($CD11b^+CD27^+$) demonstrated a trend towards a decrease in the activating receptor Ly49H and an increase in the inhibitory receptor NKG2A across all organs after vaccination (Figure 3.7D and E). There was also a significant increase in splenic $NKG2C^+$ NK cells with MVA (p=0.0175, figure 3.7F). MVA-vaccinated mice also had significantly increased populations of NK cells expressing CXCR6; a liver-homing and

memory-like marker usually expressed on the least mature NK cell subset (p=0.0039, Figure 3.7G). This implies potential activation of memory-like NK cell populations after vaccination.

The least mature ($CD11b^{-}CD27^{+}$) NK cell population did not demonstrate significant changes in phenotype between vaccination regimens. Overall, these data suggest that the most mature functional NK cell populations are phenotypically changed the most by MVA vaccination.

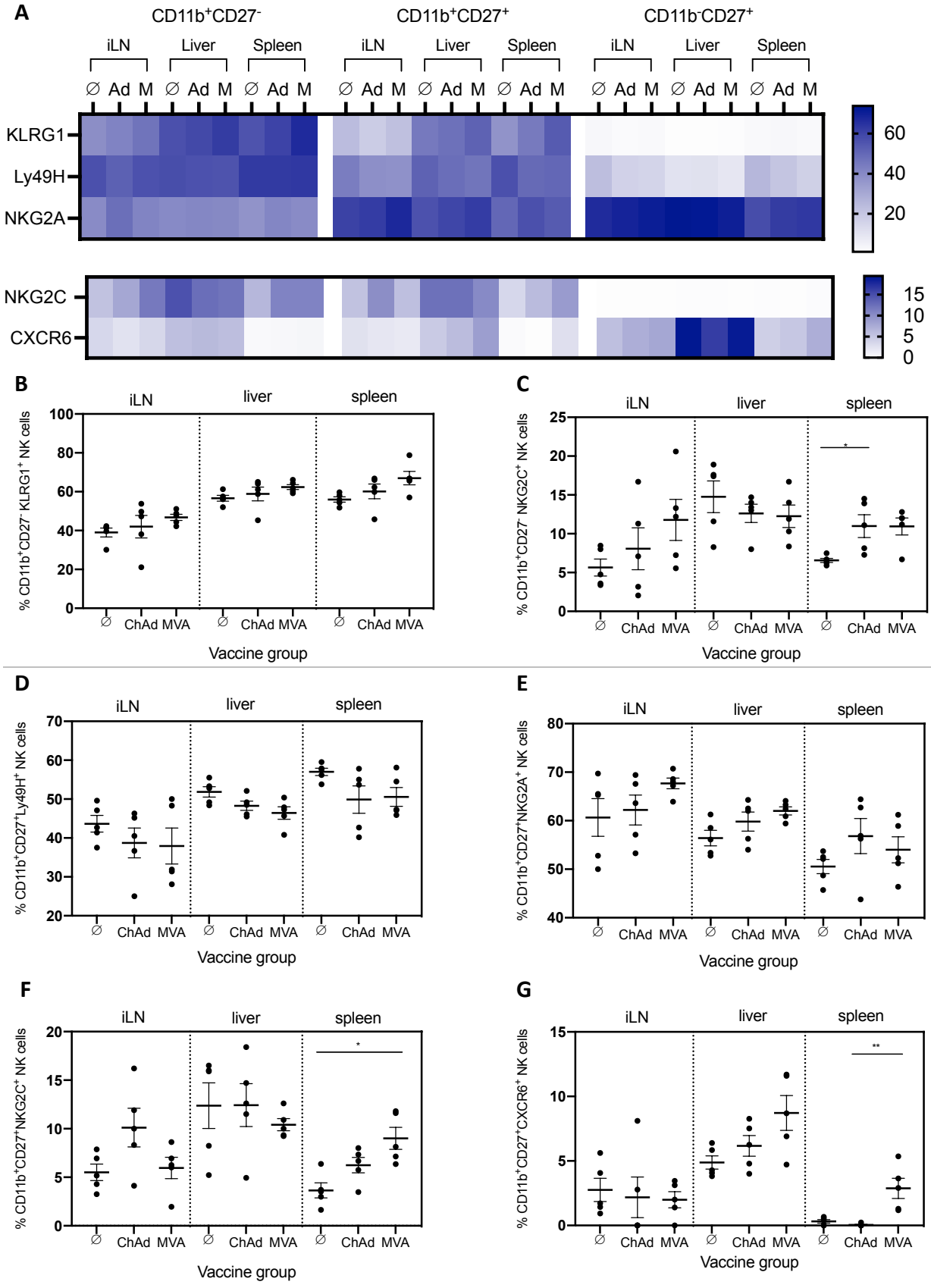

A
CD11b+CD27-
CD11b+CD27+
CD11b-CD27+
iLN
Liver
Spleen
∅ Ad M
KLRG1
Ly49H
NKG2A
NKG2C
CXCR6
60
40
20
15
10
5
0
B
C
D
E
F
G
iLN
liver
spleen
% CD11b+CD27- KLRG1+ NK cells
% CD11b+CD27- NKG2C+ NK cells
% CD11b+CD27+Ly49H+ NK cells
% CD11b+CD27+NKG2A+ NK cells
% CD11b+CD27+NKG2C+ NK cells
% CD11b+CD27+CXCR6+ NK cells
∅ ChAd MVA
Vaccine group

Figure 3.7. ChAdOx1 and MVA vaccination alters the phenotype of NK cells within maturational subsets.

Mice (n=5 per group) were left unvaccinated (∅), were vaccinated intramuscularly with $1x10^7$ i.u. ChAdOx1 (ChAd), or with $1x10^7$ PFU MVA (MVA). NK cell maturation and cell surface markers were measured in the spleen, iLN and liver 7 days post-boost on **A)** Overall heatmap of NK cell maturation and cell surface marker expression. Individual frequency of NK cells expressing **B)** $CD11b^+CD27^-$ KLRG1. **C)** $CD11b^+CD27^-$ Ly49H, **D)** $CD11b^+CD27^+$ Ly49H, **E)** $CD11b^+CD27^+$ NKG2A, **F)** $CD11b^+CD27^+$ NKG2C **G)** $CD11b^+CD27^+$ CXCR6

Statistical analysis conducted using Kruskal-Wallis test with Dunn's multiple comparisons. *p<0.05, **p<0.01,. Error bars shown as mean± SEM.

3.2.8. Heterologous and homologous prime-boost viral vector vaccination emphasise the MVA-driven NK cell phenotype.

Next, I aimed to identify whether homologous boosting with either ChAdOx1 or MVA, or a heterologous ChAdOx1-MVA vaccination regimen, would further exacerbate the MVA-driven phenotype of NK cells. Mice were vaccinated i.m. with a homologous or heterologous vaccine regimen with previously-described doses at an interval of two weeks, and the iLN and spleen were harvested one-week post-boost. Vaccination with heterologous and homologous regimens altered the surface expression and maturation of NK cells across the iLN and spleen (Figure 3.8A). Mice vaccinated with either ChAdOx1-MVA (Ad-M) or MVA-MVA (M-M), but not two doses of ChAdOx1 (Ad-Ad) had a significant decrease in their frequency of mature $CD11b^{+}CD27^{+}$ NK cells in the iLN and spleen compared to unvaccinated mice ($p<0.03$) and a reciprocal significant increase in the less mature $CD11b^{-}CD27^{+}$ NK cells ($p<0.026$, figure 3.8B and C). Furthermore, there was a significant decrease in Ly49H expression in M-M vaccinated mice, and a trend within the Ad-M vaccine group, across both organs ($p<0.0088$, Figure 3.8D). This response was observed within the $CD11b^{+}CD27^{-}$ and $CD11b^{+}CD27^{+}$ NK cell populations, which express the highest levels of Ly49H. The most mature NK cells in the spleen exhibited a higher $KLRG1^{+}$ frequency after heterologous ChAdOx1-MVA vaccinated mice ($p=0.0249$, figure 3.8E). As previously demonstrated, mature NK cells from homologous MVA vaccinated mice had more splenic $NKG2C^{+}$ NK cells ($p=0.0436$, figure 3.8F) and higher CXCR6 expression in the iLN of Ad-M vaccinated mice ($p=0.0197$, Figure 3.8G).

Overall, these data suggest that heterologous and homologous vaccination with MVA enhances the previously observed phenotype in single-dose MVA vaccinated mice,

and push the NK cell population towards a less mature and more inhibitory phenotype that potentially has higher migratory properties through enhanced CXCR6 expression.

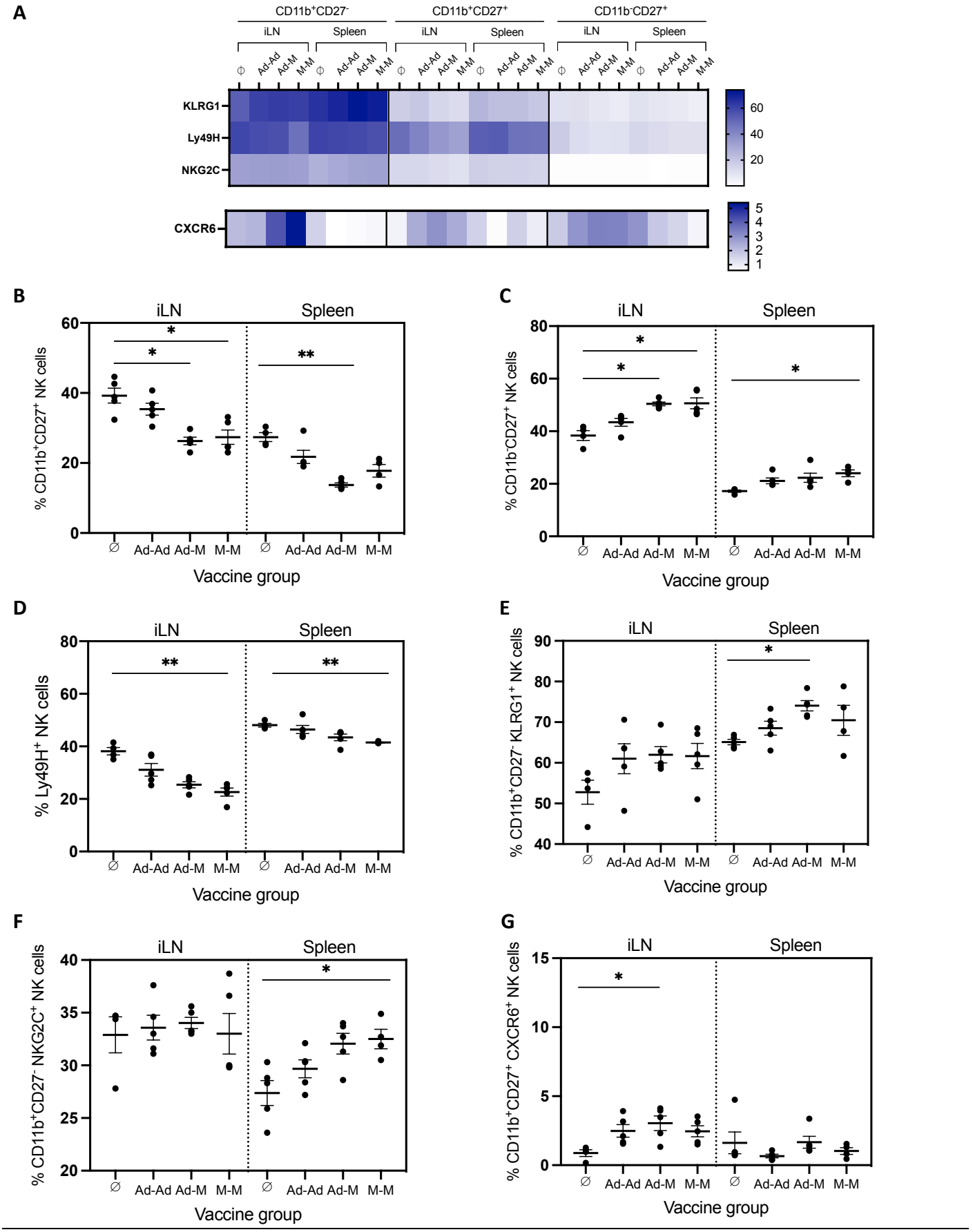

A
CD11b+CD27-
CD11b+CD27+
CD11b-CD27+
iLN
Spleen
ϕ
Ad-Ad
Ad-M
M-M
KLRG1
Ly49H
NKG2C
CXCR6
60
40
20
5
4
3
2
1
B
% CD11b+CD27+ NK cells
C
% CD11b-CD27+ NK cells
D
% Ly49H+ NK cells
E
% CD11b+CD27-KLRG1+ NK cells
F
% CD11b+CD27-NKG2C+ NK cells
G
% CD11b+CD27+ CXCR6+ NK cells
Vaccine group

Figure 3.8. Homologous and heterologous ChAdOx1 and MVA vaccination alters the phenotype of NK cells within maturational sub-populations

Mice were left unvaccinated (∅), or were vaccinated intramuscularly with $1x10^7$ i.u. ChAdOx1 followed by $1x10^7$ PFU MVA (Ad-M), or two doses of ChAdOx1 (Ad-Ad), or two doses of MVA (M-M). Boost vaccinations occurred at an interval of one week. 7 days post-boost, iLN and spleens were harvested and analysed by flow cytometry. **A)** heatmap of NK cell maturation subsets and analysed markers in the iLN and spleen. Frequencies of **B)** $CD11b^+CD27^+$ NK cells, **C)** $CD11b^-CD27^+$ NK cells, **D)** $Ly49H^+$ NK cells**, E)** $CD11b^+CD27^-$ $KLRG1^+$ NK cells, **F)** $CD11b^+CD27^-$ $NKG2C^+$ NK cells**, G)** $CD11b^+CD27^+$ $CXCR6^+$ NK cells.

Statistical analysis conducted using Kruskal-Wallis test with Dunn's multiple comparisons. **p*<0.05, ***p*<0.01. Error bars shown as mean± SEM.

3.2.9. Inactivated virion vaccination and the NK cell phenotype

To explore whether the modification of NK cell phenotype was unique to MVA vaccination, I conducted a comparative analysis between inactivated virion vaccination and viral vector vaccination. Mice (n=5) were vaccinated i.m. with $1x10^8$ i.u. ChAdOx1 followed with a booster dose of $1x10^6$ PFU MVA 21 days later. A further 5 mice were vaccinated with 0.2µg HA unadjuvanted Fluarix at days 0 and 21, as described previously (372). At day 28, organs were harvested and the effect of prime-boost inactivated virion vaccination was contrasted to a similar viral-vectored vaccine regimen. In the viral-vectored vaccine group, there was a significant decrease in the frequency of $CD11b^+$ NK cells in the iLN ($p<0.05$) and liver ($p<0.058$), and a similar trend in the spleen, in comparison to unvaccinated and Fluarix-vaccinated mice (Figure 3.9A). There was also a lower frequency of $Ly49H^+$ NK cells (liver $p<0.05$, Figure 3.9B). Overall, the phenotype of NK cells from Fluarix vaccinated mice was comparable to ChAdOx1 vaccinated mice, and did not differ substantially from unvaccinated mice.

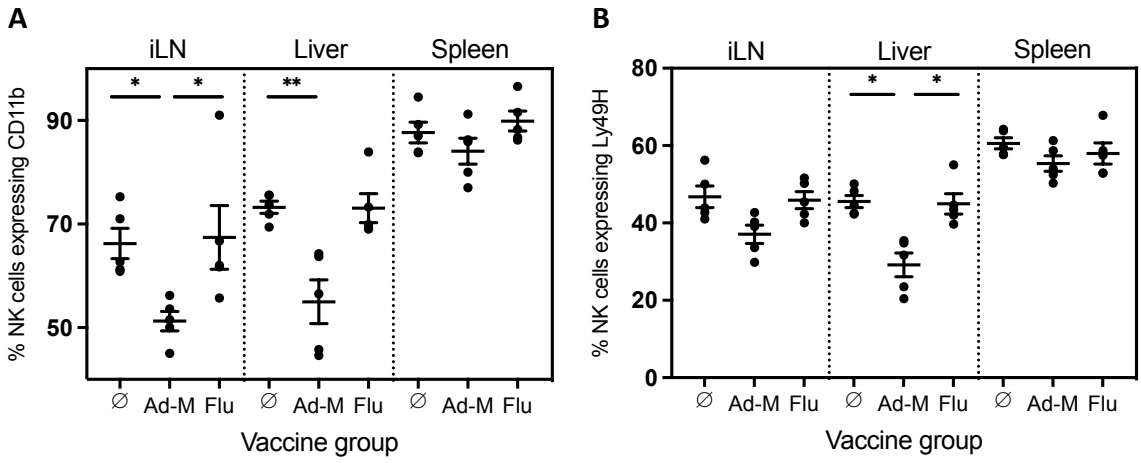


Figure 3.9. CD11b$^+$ and Ly49H$^+$ NK cells after ChAdOx1-MVA or inactivated virion vaccination

C57BL/6J mice (n=5 per group) were left unvaccinated (∅) or were vaccinated intramuscularly with 1x10^8 i.u. ChAdOx1 and 1x10^6 PFU MVA (Ad-M), or with two doses 0.2µg Fluarix (Flu) at a three-week interval. At one-week post-boost, NK cell maturation and surface expression of markers were analysed by flow cytometry. Frequency of **A)** CD11b$^+$ NK cells **B)** Ly49H$^+$ NK cells.

Statistical analysis conducted using Kruskal-Wallis test with Dunn's multiple comparisons. *p<0.05, **p<0.01. Error bars shown as mean± SEM.

3.2.10. Viral vector vaccination induces different cell death pathways

Next, I investigated whether the loss of mature NK cells could be affected by changes to cell death pathways following vaccination. Mice (n=5 per group) were prime vaccinated with $1x10^7$ i.u. ChAdOx1 or $1x10^7$PFU MVA, and followed with a homologous boost vaccination 3 days later. Mice were sacrificed 1-day post-boost vaccination and splenocytes were stained for markers of apoptosis and necrosis (table 3.4) and measured by flow cytometry following the gating strategy in supplementary figure 3.

Cell death pathway	**Markers**
Classic apoptosis	$Caspase3^+RIPK3^-$ (live/dead)
RIP1-dependent apoptosis	$Caspase3^+RIPK3^+$
Necrosis	$Caspase3^-$Dead
Necroptosis	$Caspase3^-RIPK3^+$

Table 3.4. Cell death pathways defined by caspase 3, RIPK3 and viability markers. Outlined in Vossenkamper *et al* 2018 (384)

Within the homologous ChAdOx1 (Ad-Ad) vaccine group, both $CD3^+$ cells and NK cells demonstrated an increase in classic apoptosis (p<0.048, Figure 3.10A). Similarly, there was a trend towards more necroptotic NK cells in M-M vaccinated mice (p=0.07. Figure 3.10B).

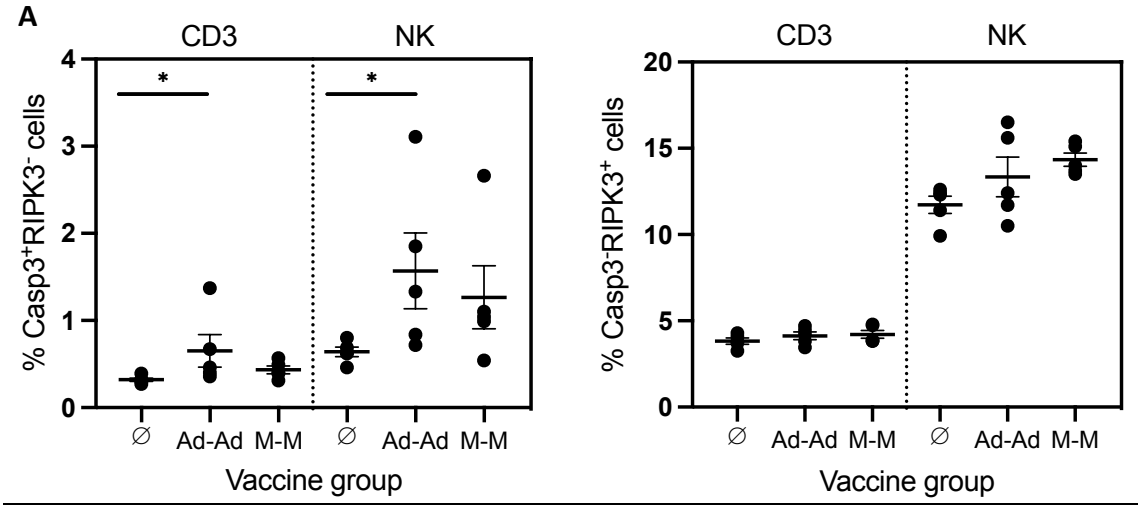


Figure 3.10. Apoptosis and necroptosis of cells following vaccination.

C57BL/6J mice (n=5 per group) were left unvaccinated (∅) or were vaccinated intramuscularly with a homologous regimen of $1x10^7$ i.u. ChAdOx1 (Ad-Ad) or $1x10^7$ PFU MVA (M-M) at an interval of three days. One day post-vaccination, splenocytes were stained for cell death markers. **A)** the frequency of apoptotic $Casp3^+RIPK3^-$ cells, **B)** the frequency of necroptotic $Casp3^-RIPK3^+$ cells.

Statistical analysis conducted using Kruskal-Wallis test with Dunn's multiple comparisons. *p<0.05. Error bars shown as mean± SEM.

3.2.11. NK cell depletion in a mouse viral vector vaccination model

The role of NK cells in vaccine immunogenicity has not been fully elucidated. In order to determine whether NK cells are significantly involved in the overall immune response to viral-vectored vaccination, C57BL/6JOlaHsd mice were either depleted of NK cells using 500µg α-NK1.1 functional grade antibody 2 days prior to vaccination or left as wildtype (WT) (n=6-7 mice per group). Mice were vaccinated with $1x10^7$ i.u. ChAdOx1, followed by a boost of $1x10^7$ PFU MVA after 7-14 days. 9-14 days post-boost, mice were culled and spleens and iLN harvested for analysis. NK cell depletion was confirmed after 23 days, and NK-depleted mice had approximately 5.5-fold fewer NK cells than WT mice (NK-depleted: 0.49% live lymphocytes, WT: 2.72% live lymphocytes. Figure 3.11). Although α-NK1.1 is widely used for NK cell depletion in C57Bl/6J mice, it can also induce the depletion of other cell populations including $NK1.1^+$ T cells and ILC1 cells (385, 386), which may contribute to the overall vaccine response. No significant differences were found between NK-depleted and WT unvaccinated mice, and the unvaccinated group consists of n=2 NK-depleted and n=3 WT mice.

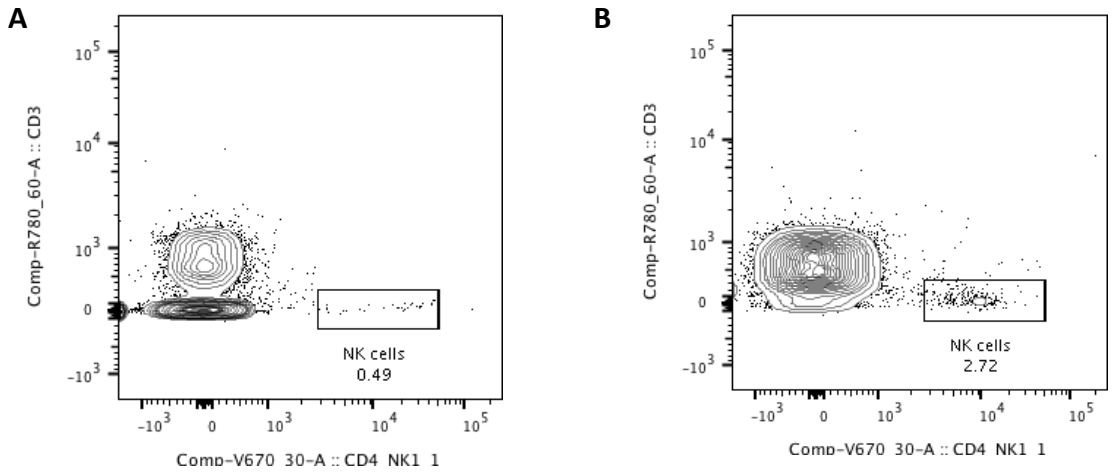


Figure 3.11. NK cell depletion in C57BL/6JOlaHsd mice

C57BL/6JOlaHsd mice were injected i.p. with 500µg α-NK1.1 prior to vaccination. 9 days post-boost vaccination, mice were culled and splenocytes stained with live/dead, α-CD3 and α-NK1.1 from **A)** an NK cell-depleted mouse, **B)** a control mouse.

Splenocytes and iLN were stained for T cell activation, memory, and cytokine production following stimulation with vaccine antigen peptides. Interestingly, NK-depleted mice had significantly fewer activated $CD25^{+}CD44^{+}$ $CD4^{+}$ T cells (p=0.0017, figure 3.12A), but a significantly higher frequency of activated $CD44^{+}$ $CD8^{+}$ T cells in the spleen (p<0.015, figure 3.12B)

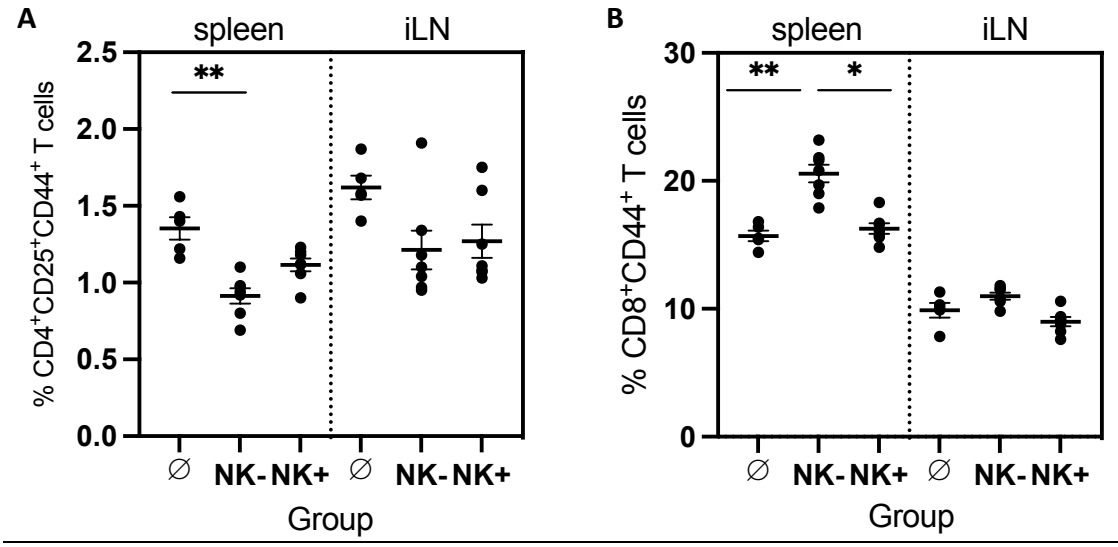


Figure 3.12. Changes in activation status of T cells following NK cell depletion and vaccination

C57BL/6JOlaHsd mice (n=7 per group) were depleted of NK cells prior to vaccination. 9 days post-boost vaccination, mice were culled and splenocytes and inguinal lymph nodes (iLN) stained for T cells and activation **A)** The frequency of activated $CD4^+CD25^+CD44^+$ T cells in the spleen and iLN, **B)** The frequency of activated $CD8^+$ $CD44^+$ T cells in the spleen and iLN.

Statistical analysis conducted using Kruskal-Wallis test with Dunn's multiple comparisons. *p<0.05, **p<0.01. Error bars shown as mean± SEM.

The memory profile of CD4 and CD8 T cells in the spleen were analysed using CD127 and CD62L as markers of effector and tissue-resident phenotype. NK-depleted mice had significantly more $CD127^-CD62L^-$ $CD8^+$ effector T cells (T_{eff}) than unvaccinated mice, however WT mice did not have significantly more (p=0.007, Figure 3.13A). WT mice had significantly more $CD127^+CD62L^-$ $CD8^+$ T_{EM} cells than NK-depleted mice (p=0.035, figure 3.13B), and significantly fewer $CD127^+CD62L^+$ $CD8^+$ T_{CM} than unvaccinated mice (p=0.038, figure 3.13C). Overall, these data support previous research demonstrating that NK-depletion may enhance $CD8^+$ T cell effector function following vaccination, however may impair the generation of $CD127^+CD62L^-$ effector memory populations.

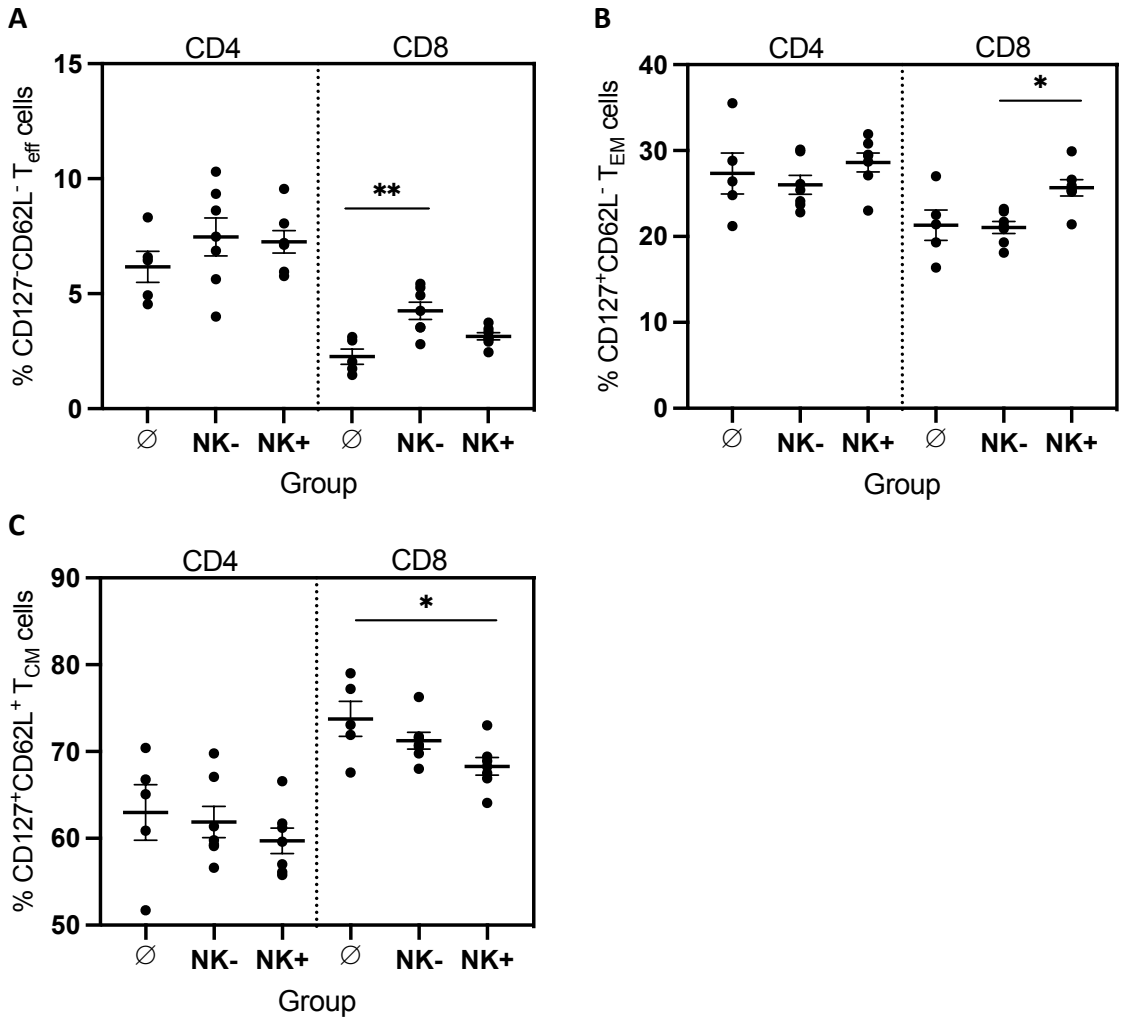


Figure 3.13. Changes in T cell memory populations following NK cell depletion and vaccination

C57BL/6JOlaHsd mice (n=7) were depleted of NK cells prior to vaccination. 9 days post-boost vaccination, mice were culled and splenocytes stained for T cell memory formation. **A)** The frequency of $CD127^{-}CD62L^{-}$ effector T cells, **B)** the frequency of $CD127^{+}CD62L^{-}$ effector memory T cells, **C)** The frequency of $CD127^{+}CD62L^{+}$ central memory T cells.

Statistical analysis conducted using Kruskal-Wallis test with Dunn's multiple comparisons. *p<0.05, **p<0.01. Error bars shown as mean± SEM.

Splenocytes were stimulated for six hours with peptides from the antigen encoded in the vaccine, and stained for T cell IFN-γ and CD107a expression. Across the total $CD8^+$ T cell population, there was a significant increase in the expression of IFN-γ between unvaccinated and NK-depleted mice (p=0.0019) and CD107a between both groups (unvaccinated, p=0.06, WT p=0.0031, figure 3.14A). Furthermore, this pattern of expression was replicated within the T_{EM} and T_{CM} populations, including in the $CD4^+$ T_{CM} population (Figures 3.14B and C). These data demonstrate that NK-depleted mice establish a more robust cytokine and cytotoxic response in their T_{EM} and T_{CM} following ChAdOx1-MVA vaccination than WT mice with functional NK cells.

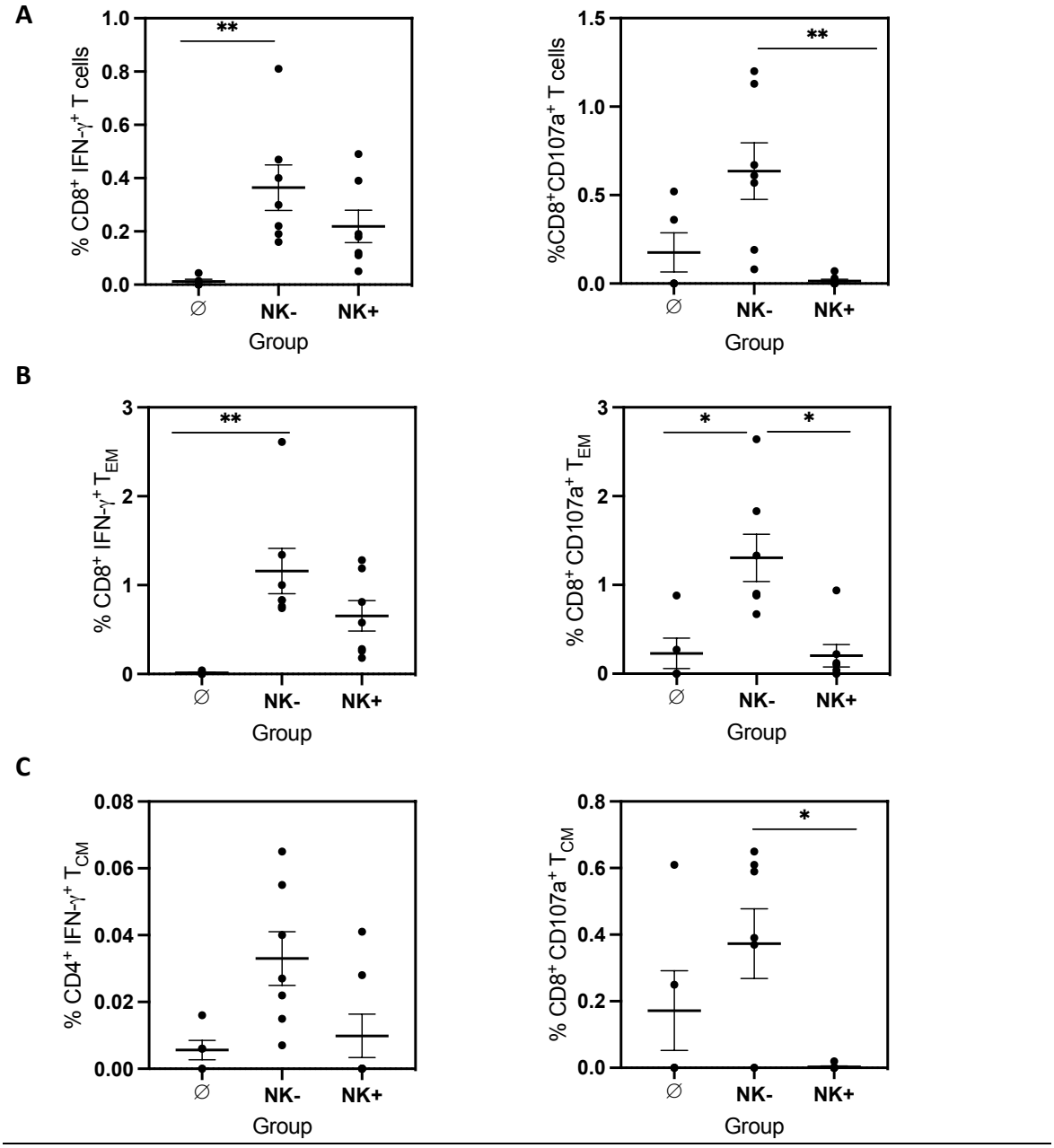


Figure 3.14. Changes in cytokine production and cytotoxicity of T cells following NK cell depletion and vaccination

C57BL/6JOlaHsd mice (n=7) were depleted of NK cells prior to vaccination. 9 days post-boost vaccination, mice were culled, splenocytes stimulated and stained for T cell IFN-γ and CD107a expression. **A)** Total T cell IFN-γ and CD107a expression. **B)** T_{EM} cells IFN-γ and CD107a expression **C)** $CD4^+$ T_{CM} cells IFN-γ and $CD8^+$ T_{CM} CD107a expression. Statistical analysis conducted using Kruskal-Wallis test with Dunn's multiple comparisons. **p*<0.05, ***p*<0.01. Error bars shown as mean± SEM.

3.3. Discussion

In this chapter, I demonstrate that:

- After viral vector vaccination, T cells are activated in a similar manner to inactivated virion vaccination, however T_{regs} and other regulatory T cells are not altered in frequency by either viral vector vaccination or inactivated virion vaccination.
- NK cells are activated upon vaccination with ChAdOx1 and express IFN-γ and CD107a following stimulation with antigenic peptides. This response is boosted after either homologous or heterologous vaccination with MVA.
- MVA vaccination, but not ChAdOx1 or Fluarix® vaccination, alters NK cell phenotype and contributes towards a more inactivated receptor expression profile with reduced expression of maturity markers.
- NK cell depletion enhances the $CD8^+$ T cell IFN-γ and CD107a response to vaccination, but reduces the frequency of effector memory $CD8^+$ T cells.

3.3.1. T cell activation and regulatory T cell populations after vaccination

During the experiments within this chapter, I used three antigens inserts (Ebolavirus glycoprotein, *Plasmodium falciparum* TRIP, and ovalbumin (OVA)) to ensure that the antigen itself was not influencing NK cell function. I compared the effect of heterologous ChAdOx1-MVA vaccination to vaccination with split virion influenza virus (Fluarix®) to establish similarities in T cell activation, memory formation, and populations of regulatory T cells. Both vaccines activated T cells to a similar extent through measurement of CD25, however ChAdOx1-MVA vaccination had increased expression of the inhibitory marker PD1

in both the iLN and spleen. PD1 is expressed on T cells and negatively regulates activation following overstimulation with the T cell antigen after pathogen infection (387, 388). PD1 is also a marker of exhaustion on effector T cells after chronic antigen stimulation and viral persistence (376, 389). An increase in $PD1^+$ cells following vaccination may indicate that ChAdOx1 vaccination induces robust T cell activation, and therefore a reciprocal up-regulation of PD1 acts in balance to control the cytotoxic response. This up-regulation of PD1 and 'partial exhaustion' of T cells has previously been demonstrated following Ad5 vaccination in mice and rhesus macaques (374, 377, 390). Conversely, I did not identify a significant increase in the frequency of $CTLA4^+$ ChAdOx1-vaccinated T cells, indicating that 'exhaustion' might not be a permanent phenotype on T cells following ChAdOx1 vaccination (376).

Previous research by others demonstrates expansion of regulatory T cell populations in mice and sheep following sub-optimal dose vaccination with unadjuvanted influenza A peptides, which impeded the T cell antigen-specific and antibody response (391, 392), and was associated with an increase in IL-10 (392). Aside from a slight increase in T_{reg} cells in the spleen following Ad-M vaccination, there were no observed changes in the frequency of regulatory T cell populations following either Ad-M or Fluarix vaccination. Given the robust immune response of Ad-M vaccination regimens, it is unlikely this increase has a significant effect on vaccine T cell and humoral immunogenicity.

3.3.2. NK cell memory and cytokine response after vaccination

In this chapter, I demonstrate that NK cells from the iLN of mice vaccinated with ChAdOx1 are activated and can produce IFN-γ in response to peptide stimulation. This is in agreement with previously published work showing NK cell activation and cytokine

production following adenovirus vaccination and infection (393-395), VSV-vector vaccination (395) and seasonal influenza vaccination (53, 362, 396, 397). Homologous MVA and heterologous ChAdOx1-MVA prime-boost vaccination also induced significant expression of double positive $CD107a^{+}IFN\text{-}\gamma^{+}$ NK cells following peptide stimulation in the spleen. Previous work by Gillard *et al* describes how Vaccinia virus, but less so MVA, can induce Thy-1^{+} hepatic NK cells that are activated upon re-challenge and can protect immunodeficient hosts upon adoptive transfer (62). This may explain why heterologous and homologous boosting with MVA induces a stronger MVA-driven response than vaccination with single-dose MVA. This is also in concordance with Palgen *et al*, who show that MVA activates NK cells and induces cytokine production after prime-boost vaccination in NHPs (364). Contrastingly, Milo *et al* demonstrate robust activation and proliferation of NK cells in the bone marrow and spleen of mice after MVA vaccination, which we did not demonstrate here above background levels (398).

Although NK cells from vaccinated mice demonstrated activation following stimulation with vaccine antigen peptides, this is unlikely to be T cell-independent antigen-specific NK cell memory, as similar IFN-γ production was not elicited when NK cells were isolated from the spleen and liver and stimulated with vaccine peptides in comparison to whole splenocyte stimulation. The liver was selected for these experiments as there is a population of immature, tissue-resident NK cells expressing memory markers CXCR6 and CD49a, which have memory-like properties following vaccination and infection. These NK cells have previously been shown to elicit a T cell-independent response upon hapten re-challenge in humans, non-human primates, and mice (31, 43, 56, 62, 63, 399). Although CXCR6 expression was significantly increased on NK cells after MVA vaccination, this does not definitively demonstrate antigen-specific memory, as the exact role of these receptors

in the memory recall response is currently unknown. Possibly in these experiments, NK cells are activated after vaccination by T cell-mediated cytokine production or by antibody-dependent cellular cytotoxicity (ADCC). Antigen specific IL-2 secreted by $CD4^+$ T cells activates NK cells in conjunction with antibody-dependent activation (361, 400), and accessory cytokines including IL-12, IL-15 and IL-18 from monocytes and macrophages (19, 401). As viral vectors elicit a robust T cell response and encode antigens within the vector that activate the innate immune system (132, 402), it is likely that the majority of the observed NK cell response is stimulated by these two routes.

3.3.3. MVA vaccination and NK cell phenotype

Vaccination with ChAdOx1 and inactivated influenza virions did not significantly alter NK cell surface expression of activating or inhibitory receptors, nor was cell maturity affected. However, vaccination with MVA did alter NK cell phenotype; I observed a significant reduction in the expression of CD11b and Ly49H up to three weeks post-vaccination in single-dose, homologous prime-boost, and heterologous ChAdOx1-MVA prime-boost. Neither MVA nor ChAdOx1 efficiently infect NK cells or T cells, so this effect is unlikely to be directly from viral infection itself (403-405). Previous studies have demonstrated that infection of C57BL/6J mice with Vaccinia virus, the original virus from which MVA is derived, also induces an immature ($CD11b^-CD27^+$) NK cell phenotype (406). In this paper, Hatfield *et al* outline how Vaccinia virus infection also reduces expression of Ly49H, CD69 and cytotoxins including perforin and granzyme B. We observed this same depletion of mature $CD11b^+$ NK cells and NK cells expressing Ly49H with MVA vaccination, resulting in an overall more immature and inactivated phenotype. Furthermore, the authors observed an increase in expression of the inhibitory receptor NKG2A; a trend which was also

somewhat replicated in these studies. This phenotype may be induced by low levels of IFN type I secretion following either Vaccinia virus or MVA infection, which is associated with an increase in inhibitory receptors including NKG2A, and an inverse correlation with NK cell activation and degranulation (406, 407). In both ChAdOx1 and MVA vaccinated mice, we also see an increase in NKG2C expression. The function of NKG2C in mice is not well defined (383). In humans it is a heterodimeric activating receptor that recognises the non-classical MHC class Ib molecule HLA-E that presents antigen-specific peptides encoded by cytomegalovirus (293, 408), however, the analogous function of CMV antigen recognition in mice is fulfilled by Ly49H on NK cells (381). These data suggest that, in mice, NKG2C is a redundant activating receptor similar in function to Ly49H that is up-regulated during viral vector vaccination and may contribute towards an activated NK cell phenotype.

Hatfield *et al* did not explore further the mechanism behind the depletion of mature NK cells and resulting inhibitory phenotype. In this thesis, I have begun to answer whether vaccination with MVA induces more cell death than other vaccination regimens. Infection-induced cell death by apoptosis and necroptosis activates an innate inflammatory response, and thus promotes viral clearance across multiple different viral infections (409, 410). The genes encoded in the E1b-E3 gene cassette of wildtype human adenovirus suppress intrinsic and extrinsic apoptosis during infection (411). However, these genes are deleted during generation of replication incompetent adenovirus vectors including ChAdOx1 (165). Large DNA viruses, such as vaccinia virus and cytomegalovirus, have evolved to encode inhibitors of the apoptosis-inducing protein caspase 8 (412, 413). Inhibition of apoptosis by vaccinia virus sensitises the cell death pathway towards necroptosis, which is a caspase-independent inflammatory cell death pathway mediated by receptor interacting protein kinase (RIPK) 3 and RIPK1, which phosphorylate mixed

lineage kinase-like protein (MLKL) and activate necroptosis via membrane pore formation (413, 414). It is hypothesised that the necroptosis cell death pathway arose to control pathogens that evolved to inhibit caspase 8-mediated apoptosis (415). Mice that are deficient in RIPK3 are unable to control vaccinia virus or reovirus infection (410, 412), however herpesviruses including MCMV and HSV-1 has evolved further mechanisms to prevent necroptosis (412, 416). In this chapter, I measured the frequency of cells undergoing apoptosis through levels of caspase 3 expression, and the frequency of necroptotic cells by RIPK3 expression. $CD3^+$ and NK cells from ChAdOx1 vaccinated mice had higher levels of the apoptosis-related protein caspase 3, which is consistent with removal of the adenovirus E1-E3 cassette that inhibits apoptosis (411). MVA-vaccinated mice had higher frequencies of NK cells undergoing necroptosis than ChAdOx1-vaccinated cells, indicating that although MVA is an attenuated viral vector, it still activates the necroptotic pathway of cell death upon infection. This may account for the loss of mature NK cells following vaccination which ultimately shifts the NK cell phenotype towards a less mature cell surface expression. Less mature NK cells are sensitive to antigen stimulation and respond with robust cytokine secretion (9), potentially explaining the strong cytotoxic response observed following homologous and heterologous MVA vaccination.

Finally, I investigated how depletion of NK cells affects the immune response to heterologous ChAdOx1 MVA vaccination. NK cells regulate T cells either directly through killing of activated $CD4^+$ and $CD8^+$ T cells, or indirectly through inhibition of antigen presentation by APCs (7, 417). In murine LCMV infection, NK-mediated regulation establishes chronic infection yet exacerbates liver pathology. Without NK cells, $CD8^+$ T cells are able to fully remove the virus (7, 371). This is believed to maintain a balance between chronic viral infection and T cell-mediated immunopathology (418, 419). Similarly, NK cells

deplete exhausted $CD8^+$ T cells during murine *Toxoplasma gondii*, and secrete IL-10 which has an inhibitory effect on T cells (420, 421). Conversely in mouse models of RSV, *Chlamydia muridarum, Bordetella pertussis* and *Ehrlichia muris* infection, NK cell depletion worsened disease pathology or facilitated less IFN-γ secretion by memory T cells and a Th2-skewed T cell response (422-424). Some studies identify that NK cell depletion prior to vaccination or infection increases the frequency of total and $CD44^+CCR7^+CD62L^+$ central memory T cells (368, 418) and resident-memory T cells (386), however facilitates a reduction in the population size of effector memory T cells (368).

Following heterologous ChAdOx1-MVA vaccination, there was a significant increase in $CD8^+$ T_{eff} frequency, but fewer $CD8^+$ T_{EM} and T_{CM} compared to WT mice. Overall, NK depleted mice had significantly more expression of antigen-specific CD107a and IFN-γ in all $CD8^+$ T cell subsets following vaccination compared to WT mice. These data are in confirmation with some previous reports regarding increased T cell activation yet reduction in T_{EM} population frequency, however there was not an increase in T_{CM} frequency in the spleen or iLN as previously suggested (368, 418). Furthermore, other reports do not identify a difference in T cell cytokine secretion following NK cell depletion (386, 418). The increase in $CD8^+$ T cell cytokine secretion following vaccination in NK-depleted mice may be due to a loss of NK cell-mediated killing of CD4+ or CD8+ T cells, potentially mediated via perforin (7, 419). The lack of T_{EM} population formation following vaccination in NK depleted mice may indicate a role for NK cell cytokine secretion in the lymph nodes, which has been demonstrated to induce Th1-skewed $CD4^+$ T cell responses and may facilitate memory cell generation (24). However, others demonstrate that NK cell depletion enhances T cell memory formation following infection (425). Further research could establish the role of NK cells and T cell memory formation; some literature demonstrates

an increase in CD127 expression on T cells of NK-depleted mice, which enhances the generation of memory populations (386). Also, it is unclear whether this mechanism of negative regulation occurs by perforin-induced T cell killing, or by other demonstrated methods of NK cell-mediated regulation including IL-10 secretion (370) or interaction with T cell inhibitory receptors (8).

To summarise, in this chapter I demonstrate that T cells and NK cells are activated by ChAdOx1 and MVA vector vaccination, and can elicit a substantial effector response upon prime-boost vaccination. I also show that MVA vaccination alters the NK cell phenotype, and drives a stronger inactivated and immature profile than ChAdOx1 vaccination. Furthermore, upon depletion of NK cells and heterologous ChAdOx1-MVA vaccination, I demonstrate that $CD8^+$ T cells are more cytotoxic and secrete higher levels of IFN-γ, however do not establish robust T_{EM} populations in comparison to wildtype mice.

Chapter 4

The human NK cell and T cell response to viral-vectored vaccines

Chapter 4 : The human NK cell and T cell response to viral-vectored vaccines

4.1. Introduction and Aims

Previous research has demonstrated that viral vector vaccination elicits a robust humoral and cellular immune response after one dose in pre-clinical and clinical trials (168, 183, 195, 256, 426). Vaccination with a second, heterologous dose will boost the immune response and improve memory cell duration, cytokine response, and polyfunctionality (138, 147-149, 166, 179). Viral vector vaccination can induce comparable immune responses to natural infection (168, 181) and recently approved vaccines against ebolavirus and SARS-CoV-2 have demonstrated high efficacy against severe disease (157, 223, 427).

Adenoviruses have strong self-adjuvanting immunogenicity (132), however seroprevalence and pre-existing immunity against human adenoviruses can prevent optimal immune responses against the encoded antigen (163). Therefore, chimpanzee adenoviruses have been modified to make viral vectors which do not have significant seroprevalence across all tested populations. The ChAdOx1 vaccine was developed from chimpanzee adenovirus strain Y25 (165), and as demonstrated in Chapter 3 is immunogenic in a mouse model. Modified Vaccinia Ankara (MVA) is a poxvirus vector derived from Vaccinia virus, which has been tested in clinical trials and can be used in heterologous prime-boost vaccination regimens, commonly with adenovirus vaccines (119, 171). These platform technologies have been used to develop vaccines against a number of infectious disease pathogens. In this chapter, I will focus on two studies using clinical trial data from two emerging and outbreak pathogens, SARS-CoV-2 and influenza.

The development of a safe and immunogenic vaccine against COVID-19 was critical for establishing population-wide immunity to control viral spread and severity of disease. It was also vital that a vaccine was developed that could be easily transported and readily

administered across the globe, thus making viral-vectors an ideal platform to develop. The University of Oxford developed a ChAdOx1-vectored vaccine (ChAdOx1 nCoV-19) expressing the spike glycoprotein of SARS-CoV-2. This vaccine was tested in phase I/II/III clinical trials and found to be safe, immunogenic and efficacious (183). Detailed immunophenotyping of the response to ChAdOx1 nCoV-19 vaccination will be presented in this chapter.

Due to the high antigenic shift and drift of influenza, it is difficult to make a vaccine that targets the surface antigens haemagglutinin (HA) and neuraminidase (NA) and that will have productive cross-reactivity between strains (179). The internally expressed proteins nucleoprotein (NP) and matrix 1 (M1) have less genetic variation between strains of influenza than HA and NA and make promising targets for a seasonal universal influenza vaccine.

In this chapter, I describe the NK cell, T cell and B cell response to vaccination with two ChAdOx1 viral-vectored vaccines, ChAdOx1 nCoV-19 and ChAdOx1 NP+M1, and the effect of heterologous boosting on ChAdOx1 NP+M1 and MVA NP+M1 vaccination. As outlined in chapter 3, the NK cell response to viral vector vaccination in humans and animals is not fully understood and a careful dissection of this population after vaccination is described in this chapter.

Aims of Chapter Four

- Analyse NK cell and T cell activation and cytokine response to single dose ChAdOx1 nCoV-19 vaccination using multi-parameter spectral cytometry.
- Analyse how prime-boost vaccine regimens with ChAdOx1 and MVA encoding influenza A NP+M1 affect NK cell and T cell activation and cytotoxic response.

4.2. Results

4.2.1. Healthy adults aged 18-55 vaccinated with ChAdOx1 nCoV-19 demonstrate significant activation and proliferation of cell sub-populations up to 28 days post-vaccination

The COV001/002 vaccine trial assessed the safety and immunogenicity of the ChAdOx1 nCoV-19 vaccine against COVID-19. COV001 Group 1 consisted of 88 individuals who received either ChAdOx1 nCoV-19 at a dose of $5x10^{10}$ i.u. or a licensed MenACWY vaccine at a ratio of 1:1. 26 ChAdOx1 nCoV-19-vaccinated participants were randomly selected for mapping of their immune response to vaccination by multi-colour flow cytometry (table 2.16). PBMCs from day 0, 7, 14, and 28 post-vaccination were analysed, individual parameters were assessed for changes in cell population phenotypes and cytokine production, and the overall phenotype of the immune system was characterised by t-stochastic neighbour embedding (tSNE) analysis (Figure 4.1). tSNE plots separated by time point identified areas of Ki-67 up-regulation in NK cells at day 7, and $CD27^{+}IgG^{+}$ (switched memory) B cells and $CD4^{+}$ T cells at day 14 (Figure 4.1. Numbers 1-3 on figure).

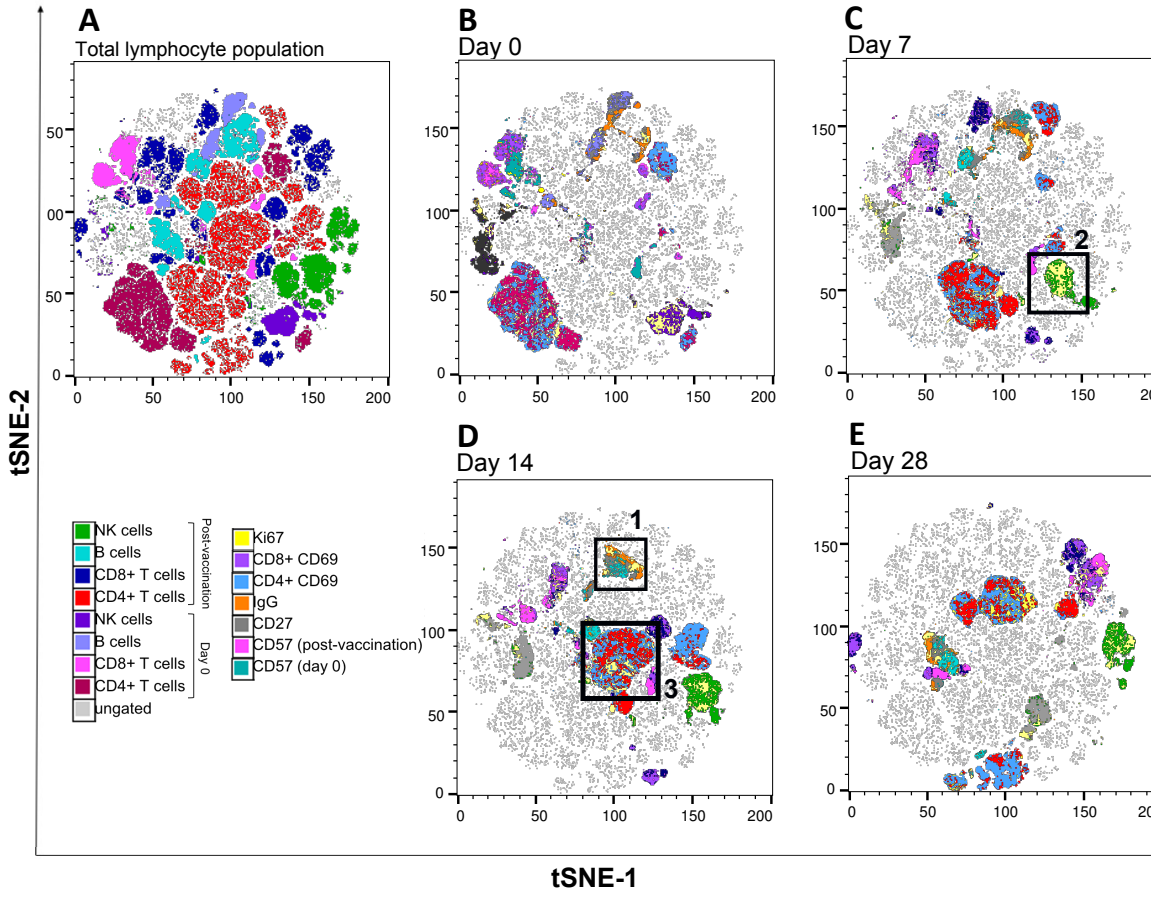


Figure 4.1. tSNE analysis of live unstimulated lymphocytes from 26 ChAdOx1 nCoV-19 vaccinated donors.

Analysis conducted on 9,600,000 live unstimulated lymphocytes from 26 vaccine trial participants across four time points (Day 0 *n* = 24, Day 7 *n* = 23, Day 14 *n* = 25 and Day 28 *n* = 24). The tSNE plot was generated by concatenation 100,000 randomly selected live lymphocytes from each sample**. A)** Global clustering of immune cells across all samples. Further tSNE population analysis at **B)** day 0, **C)** day 7, **D)** day 14, and **E)** day 28. Areas of Ki-67^{+} activity (yellow) cluster in IgG^{+}CD27^{+} switched memory B cells (1), NK cells (2) and CD4^{+} T cells (3) after vaccination.

Figure published in Ewer et al 2020 (168)

4.2.1.1. NK cells are activated, proliferate, and produce cytokines in response to vaccination

NK cells were analysed by flow cytometry for parameters including activation, terminal differentiation, and cytokine production following the gating strategy in supplementary figure 5. There was a slight yet non-significant increase in NK cell frequency at day 7 and day 14 post-vaccination (Figure 4.2A), which was accompanied by a similar increase in the frequency of $CD56^{++}$ NK cells (Figure 4.2B). Similarly, NK cell proliferation measured by Ki-67 expression increased towards day 28 post vaccination (Figure 4.2C).

Next, the production of inflammatory mediators by NK cells after peptide stimulation was measured. PBMCs were stimulated for 18 hours with two peptide pools (S1 and S2) encompassing the spike glycoprotein antigen encoded in the vaccine. The range of responses was very broad between individuals. Within the total NK cell population, there was an up-regulation of CD107a (p=0.051) at 28 days post-vaccination, and a similar trend in TNF, but not IFN-γ secretion (Figure 4.2D). In the $CD56^{++}$ NK cell population, there was a significant increase in CD107a expression at day 28 post-vaccination than at all other time points (p<0.0001). However, there were no significant changes in the secretion of TNF or IFN-γ (Figure 4.2E).

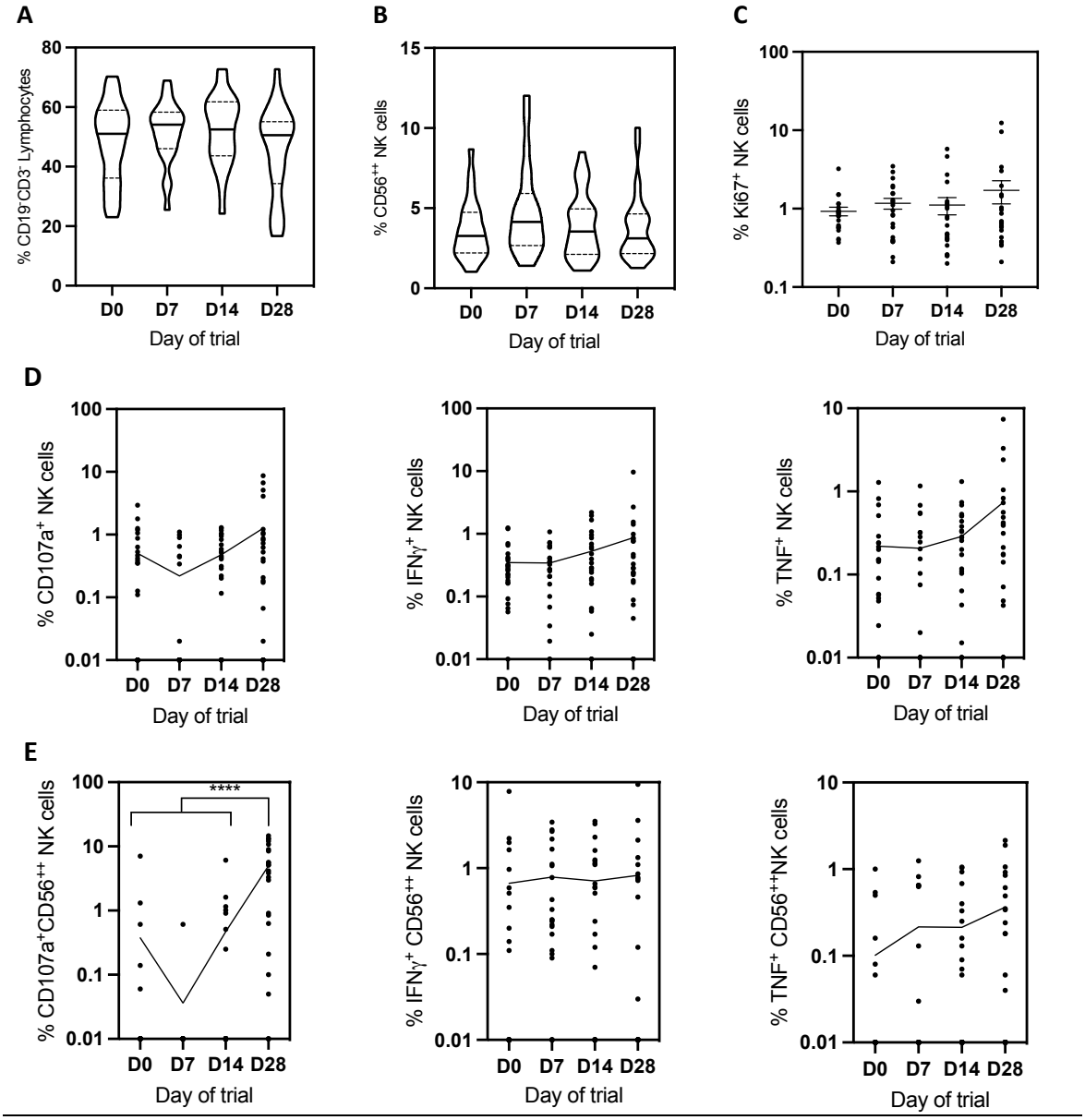


Figure 4.2. NK cell activation post ChAdOx1 nCoV-19 vaccination.

PBMCs from 26 donors vaccinated with ChAdOx1 nCoV-19 were analysed by multi-parameter flow cytometry. **A**) NK cells frequency, **B)** $CD56^{++}$ NK cell frequency **C)** Ki-67+ NK cells, all at 0-, 7-, 14-, and 28-days post-vaccination. Analysis conducted on unstimulated PBMCs.

PBMCs were stimulated for 18 hours with peptides encoding the spike glycoprotein antigen and the production of inflammatory mediators was measured at 0, 7-, 14-, and 28-days post-vaccination. Background activation was removed by subtracting unstimulated values.

D) CD107a expression, IFN-γ secretion and TNF secretion in the total NK cell population. **E)** CD107a expression, IFN-γ secretion and TNF secretion in the $CD56^{++}$ NK cell population.

Statistics conducted using Kruskal-Wallis test with Dunn's multiple comparisons. ****p<0.0001. Error bars shown as mean± SEM.

4.2.1.2. T cells are activated, proliferate, and produce cytokines in response to vaccination

$CD4^+$ and $CD8^+$ T cells from unstimulated PBMC samples were analysed for markers of activation and terminal senescence. $CD4^+$ T cells were substantially activated after vaccination, with increases in Ki-67 expression at days 7 and 14, and an increase in CD69 expression to day 28. By comparison, $CD8^+$ T cells did not express the same activation, although a trend towards increased Ki-67 was observed at day 28 (Figure 4.3A and B). There were no changes in the expression of terminal differentiation and senescence markers KLRG1, CD57 or PD1 (data not shown). There were also no significant changes to any T cell memory population frequency post-vaccination (data not shown), Cytokine production was measured by stimulation of PBMCs following the same method as above. $CD4^+$ T cells produced more IL2, TNF, and IFN-γ after stimulation at day 14 post-vaccination (Figure 4.3C). By comparison, $CD8^+$ T cells had a similar trend towards higher cytokine expression at day 28 (Figure 4.3D). Overall, this represents a Th1-skewed inflammatory phenotype.

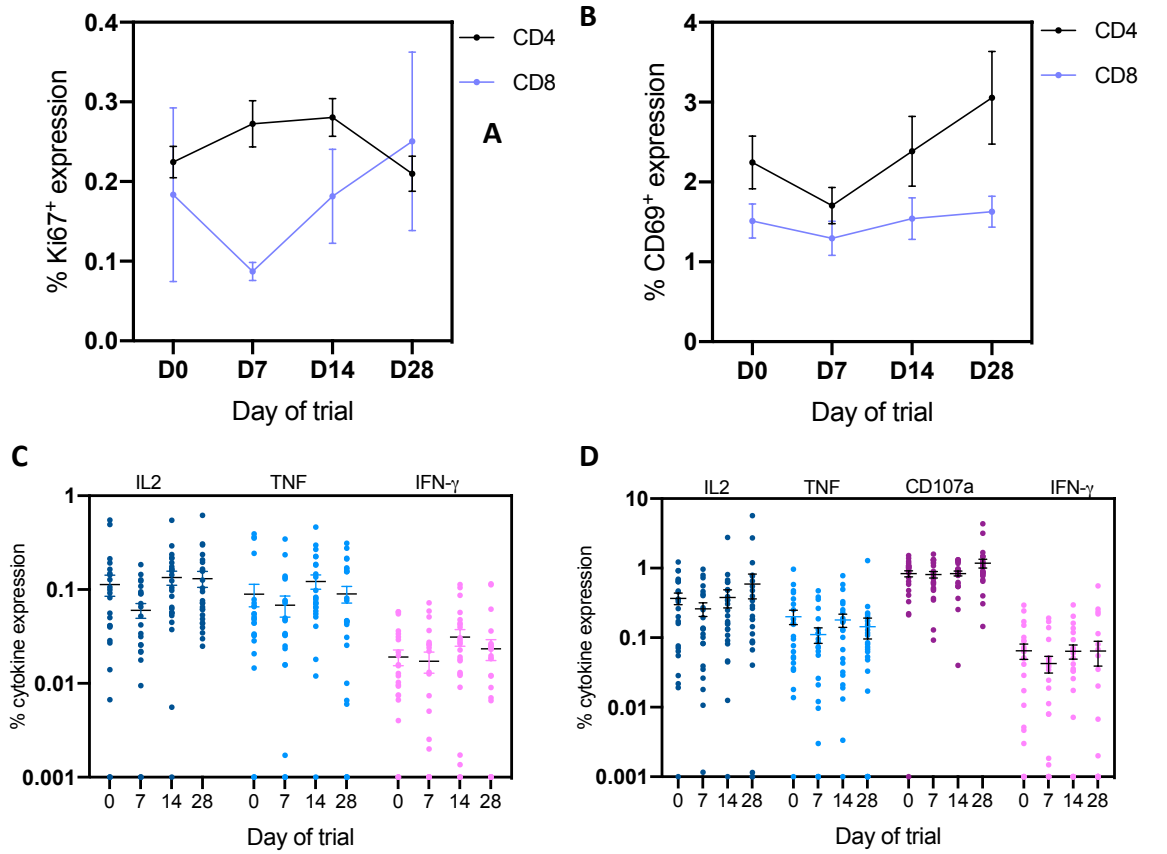


Figure 4.3. T cell activation and cytokine production post ChAdOx1 nCoV-19 vaccination.

PBMCs from 26 donors vaccinated with ChAdOx1 nCoV-19 were analysed by multi-parameter flow cytometry. T cells were analysed for changes in frequency, activation, and memory phenotype, including expression of **A)** Ki-67, and **B)** CD69 and **C)** Cytokine production from $CD4^+$ T cells, **D)** Cytokine production from $CD8^+$ T cells. Background activation was removed by subtracting unstimulated values. Purple = CD107a, dark blue = IL2, pink = IFN-γ, light blue = TNF. Statistics conducted using Kruskal-Wallis test with Dunn's multiple comparisons. Error bars shown as mean± SEM.

It is currently unknown whether NK cells have an antigen-specific memory response to vaccine antigen following vaccination with ChAdOx1. If the NK cell response is T cell dependent, NK cells would be activated by the vaccine indirectly through production of inflammatory cytokines by T cells including IL-2. I investigated the correlation between T cell IL-2 production and NK cell activation. At day 28 post-vaccination, there was a moderate correlation between antigen-specific IL-2 from $CD4^+$ T cells, and the proliferation of NK cells measured by Ki-67 (p=0.0003, r^2=0.43), and the activation of NK cells measured by CD25 (p=0.0003, r^2=0.42. Figure 4.4).

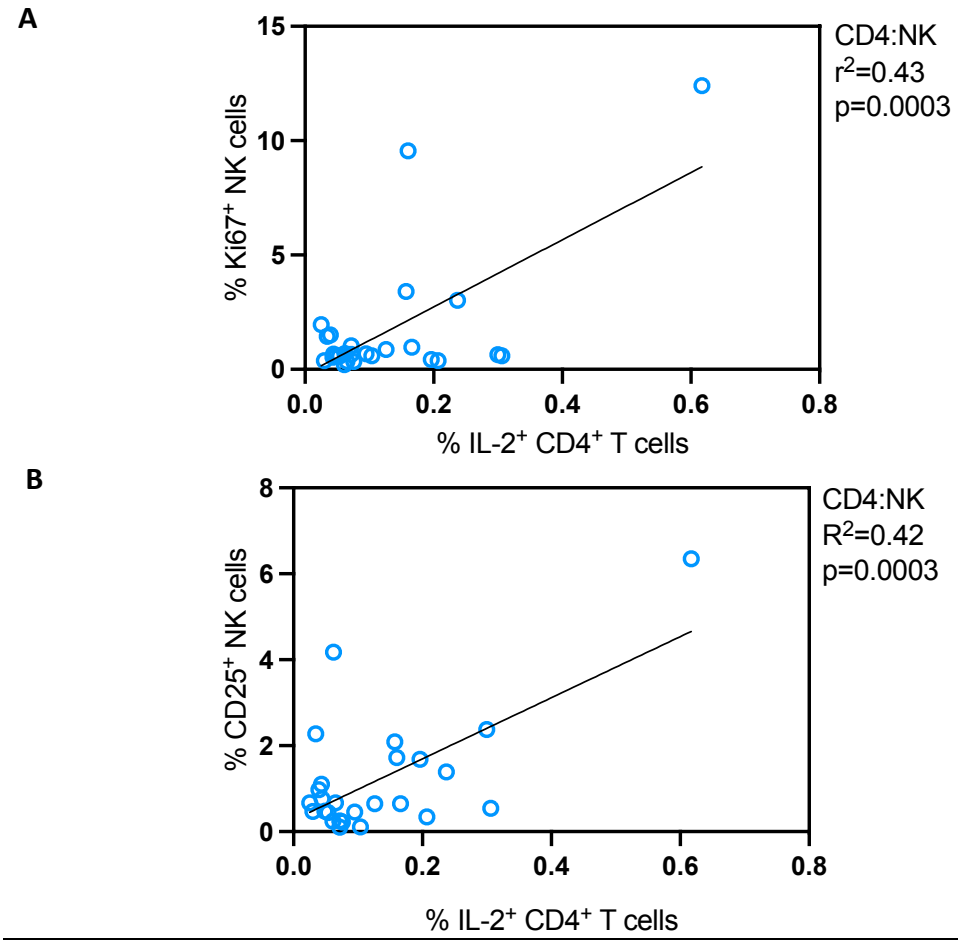


Figure 4.4. Correlation of T cell IL-2 secretion and NK cell activation

PBMCs from 26 donors were analysed for the correlation between $CD4^+$ T cell IL-2 or $CD8^+$ T cell IL-2 and NK cell activation. Correlations were found for **A)** Ki-67 and **B)** CD25 at day 28 post-vaccination. The Goodness of fit r^2 value (r^2) and significance of slope (p) were calculated between $CD4^+$ T cell IL-2 production when correlated with NK Ki67 or CD25 expression. Statistical analysis conducted using linear regression.

4.2.1.3. B cells

B cell populations showed no significant changes following ChAdOx1 vaccination (Supplementary Figure 7).

4.2.2. Comparison of single dose and heterologous prime-boost vaccination with ChAdOx1 and MVA expressing influenza antigens NP and M1 in healthy adults.

The FLU005 clinical trial was conducted in 2013-2014 (clinical trial reg: NCT01818362) to investigate the safety and immunogenicity of ChAdOx1- and MVA- vectored vaccines encoding the influenza A proteins Nucleoprotein (NP) and Matrix 1 (M1). Groups 1-4 of the FLU005 clinical trial each enrolled n=12 healthy adults aged 18-50 (Table 4.1). There was a distinct skew towards younger (average age= 25), and female (28/43) volunteers (Supplementary Figure 8). Flow cytometric analysis was conducted on day 0 (day of prime), day 14 post-prime, week 10 (groups 1 and 3, 2 weeks post-boost) and 6 months post-prime (figure 4.5B).

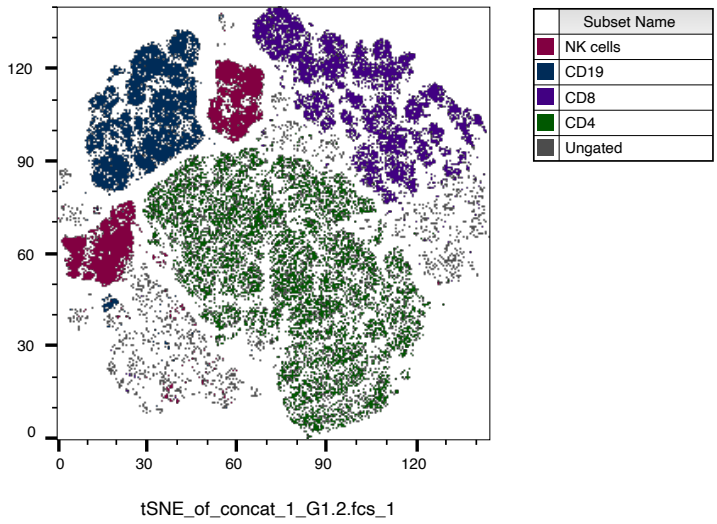
Group	N	Prime	Prime dose	Boost	Boost dose	Boost date
1	12	ChAdOx1 NP+M1	$2.5x10^{10}$ v.p.	MVA NP+M1	$1.5x10^{8}$ PFU	8 weeks
2	12	ChAdOx1 NP+M1	$2.5x10^{10}$ v.p.	MVA NP+M1	$1.5x10^{8}$ PFU	52 weeks
3	12	MVA NP+M1	$1.5x10^{8}$ PFU	ChAdOx1 NP+M1	$2.5x10^{10}$ v.p.	8 weeks
4	12	MVA NP+M1	$1.5x10^{8}$ PFU	ChAdOx1 NP+M1	$2.5x10^{10}$ v.p.	52 weeks

Table 4.1. The FLU005 trial groups, prime vaccine, boost vaccine, and date of boost vaccination.

4.2.2.1. tSNE analysis following ChAdOx1-prime, MVA-boost vaccination

tSNE analysis was conducted on live unstimulated lymphocytes from group 1 participants of the FLU005 vaccine trial at time points D14 (2 weeks post ChAdOx1 prime) and W10 (2 weeks post MVA boost) (Figure 4.5). At day 14, there is a distinct up-regulation of Ki-67 proliferation in $IgG^{+}CD27^{+}$ switched memory B cells. $CD4^{+}$ and $CD8^{+}$ T cells also express Ki-67, CD69 and T_{EM} markers ($CD45RA^{-}CCR7^{-}$). At week 10, there is a reduction in Ki-67 expression but an overall increase in T cell CD69 and T_{EM} frequency.

A



B: 14 days post-ChAdOx1 **C: 14 days post-MVA boost**

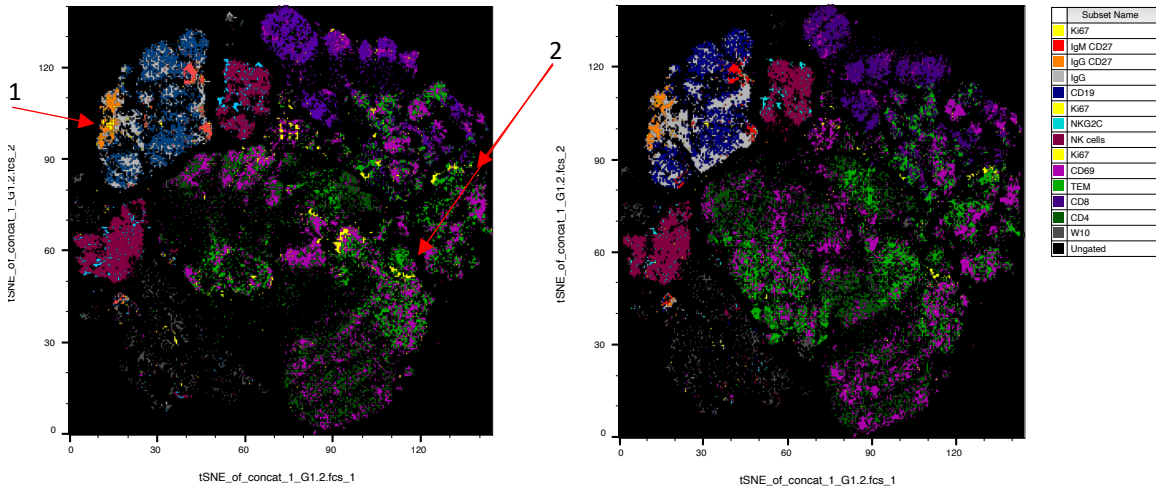


Figure 4.5. t-SNE analysis of live unstimulated lymphocytes from 10 ChAdOx1 NP+M1 prime, MVA NP+M1 boost vaccinated donors

Analysis conducted on 80,000 live unstimulated lymphocytes from 10 vaccine trial participants across two time points (Day 14 post-prime, day 14 post-boost (week 10)). The tSNE plot was generated by concatenation of 20,000 randomly selected live lymphocytes from each sample**. A)** Global clustering of immune cells across all samples. Further tSNE population analysis at **B)** day 14, **C)** week 10.

At day 14, areas of proliferating Ki-67^{+} activity (yellow) cluster in IgG^{+}CD27^{+} switched memory B cells (1), and CD4^{+} and CD8^{+} CD69^{+} T_{EM} (2). At week 10, there is a reduction in Ki-67 expression but an increase in overall CD4 and CD8 CD69 expression and T_{EM} frequency.

4.2.2.2. NK cell activation and functionality after single dose and heterologous prime-boost vaccination

PBMCs from FLU005 participants were analysed using the Aurora panel described in table 2.16. Donor samples were either stimulated with pooled NP and M1 overlapping peptides or left unstimulated as a control, and NK cells were measured for parameters of activation, terminal differentiation, and proliferation by spectral flow cytometry following the gating strategy in supplementary figure 5. There was no significant change in the frequency of NK cells across the experimental time course, although a slight decrease post-prime and post-boost vaccination could be accounted for by an expansion of antigen-specific T and B cells (Figure 4.6A). There was no significant expression of Ki-67 post-ChAdOx1 or MVA prime, however a significant increase in cellular proliferation was observed 2 weeks post- MVA boost in group 1 (ChAdOx1-MVA, p=0.034. Figure 4.6B). Similarly, there was enhanced expression of activation markers CD25 and CD69 at 2 weeks post-boost in groups 1 and 3, with a more pronounced increase following ChAdOx1-MVA heterologous vaccination (Figure 4.6C and D).

NK cell degranulation and cytokine secretion was measured across available time points. In participants receiving ChAdOx1-MVA, there was no significant impact of MVA boosting on the secretion of inflammatory cytokines when compared to single dose ChAdOx1 NP+M1. Conversely, a mild boosting effect in group 3 after MVA-ChAdOx1 vaccination could be seen on the expression of CD107a, TNF, and IL-2 (figure 4.6E-H). However, the response of NK cells to vaccination was very broad and no significant effect of vaccination or boosting was observed.

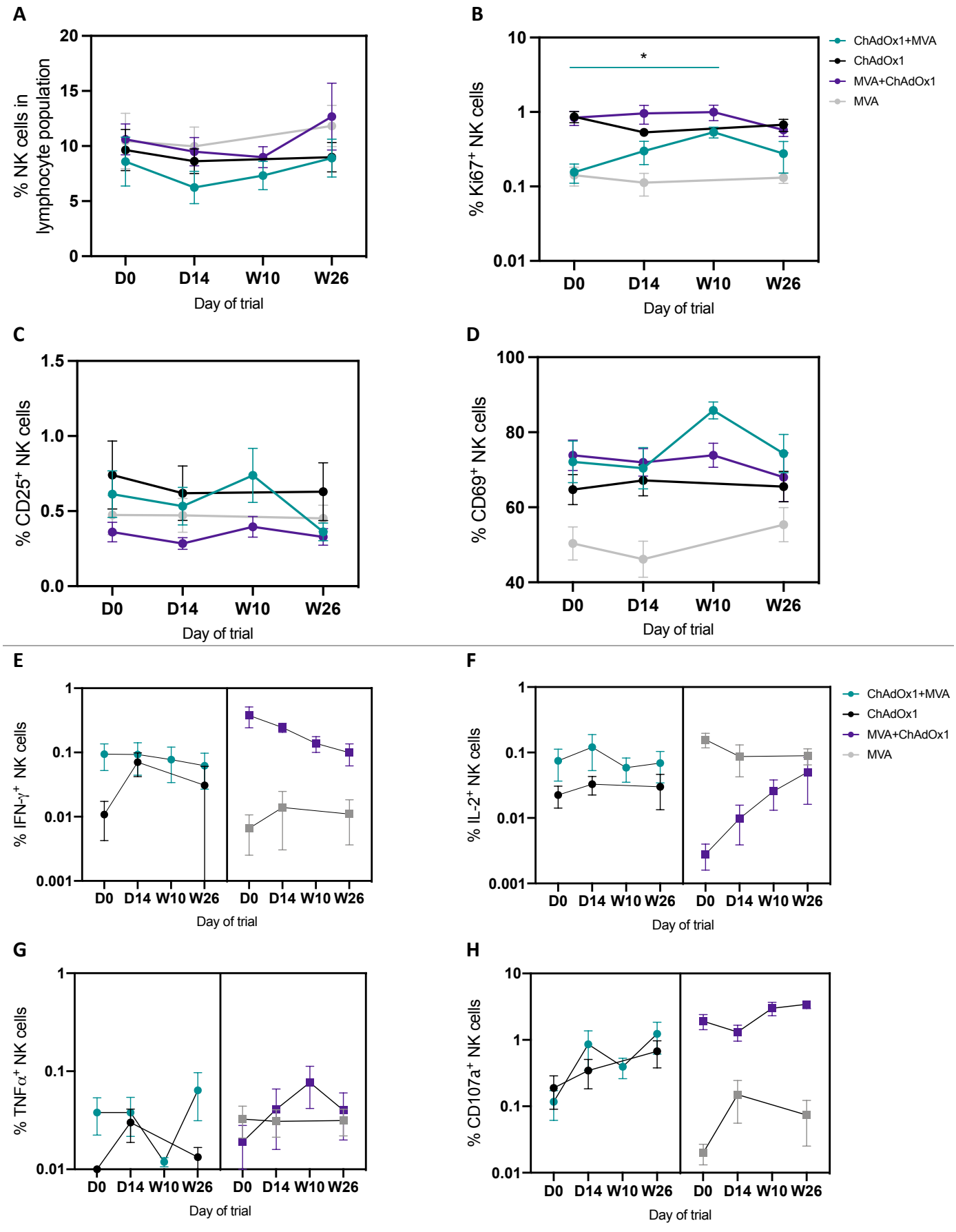

A
% NK cells in lymphocyte population
20
15
10
5
0
D0
D14
W10
W26
Day of trial
B
% Ki67+ NK cells
10
1
0.1
0.01
*
ChAdOx1+MVA
ChAdOx1
MVA+ChAdOx1
MVA
C
% CD25+ NK cells
1.5
1.0
0.5
0.0
D
% CD69+ NK cells
100
80
60
40
E
% IFN-γ+ NK cells
1
0.1
0.01
0.001
F
% IL-2+ NK cells
G
% TNFα+ NK cells
H
% CD107a+ NK cells

Figure 4.6. NK cell activation and cytokine production following ChAdOx1 and MVA prime- and prime-boost vaccination.

PBMCs from individuals vaccinated as part of the FLU005 vaccine trial were analysed by multi-parameter flow cytometry (Groups 1, 3, 4 n=10, group 2 n=9). NK cells were analysed for changes in frequency expression and activation phenotype, including frequency of **A)** NK cells as a percentage of the total lymphocyte population, **B)** Ki-67, **C)** CD25, and **D)** CD69 expression at days 0 and 14, and weeks 10 (groups 1 and 3) and 26 post-vaccination. Analysis conducted on unstimulated PBMCs.

PBMCs were stimulated for 18 hours with peptides encoding the NP and M1 protein antigen and the production of inflammatory mediators was measured at days 0 and 14, and weeks 10 (groups 1 and 3) and 26 post-vaccination. **E)** IFN-γ production**, F)** IL-2 production, **G)** TNF production, **H)** CD107a expression. Background activation was removed by subtracting unstimulated values.

Statistics conducted using Kruskal-Wallis test with Dunn's multiple comparisons, or Friedman test with multiple comparisons. *p<0.05. Error bars shown as mean± SEM.

4.2.2.3. T cell responses to prime-boost vaccination

As above, T cells were also analysed for markers of activation, proliferation, and cytokine production by multiparameter flow cytometry. In prime-boost groups (groups 1 and 3), there was a significant increase in Ki-67 proliferation at week 10, which was not observed in prime-only groups (ChAdOx1-MVA p=0.013, MVA-ChAdOx1 p=0.034. Figure 4.7A). ChAdOx1-MVA vaccination significantly increased expression of CD107a in $CD8^+$ T cells at week 10 (ChAdOx1-MVA p=0.027). This was significant at day 14 after single-dose MVA vaccination (p=0.081), and was near-significance at week 10 after MVA-ChAdOx1 vaccination (p=0.017. Figure 4.7B). Similarly, both groups receiving ChAdOx1-MVA and MVA-ChAdOx1 regimens had significant increases of IFN-γ expression at week 10 post-vaccination (ChAdOx1-MVA p=0.0062, MVA-ChAdOx1 p=0.049. Figure 4.7C). TNF secretion was also significantly increased in both prime-boost groups, this time at week 26 when compared to day 0 (ChAdOx1-MVA p=0.037, MVA-ChAdOx1 p=0.019. Figure 4.7D).

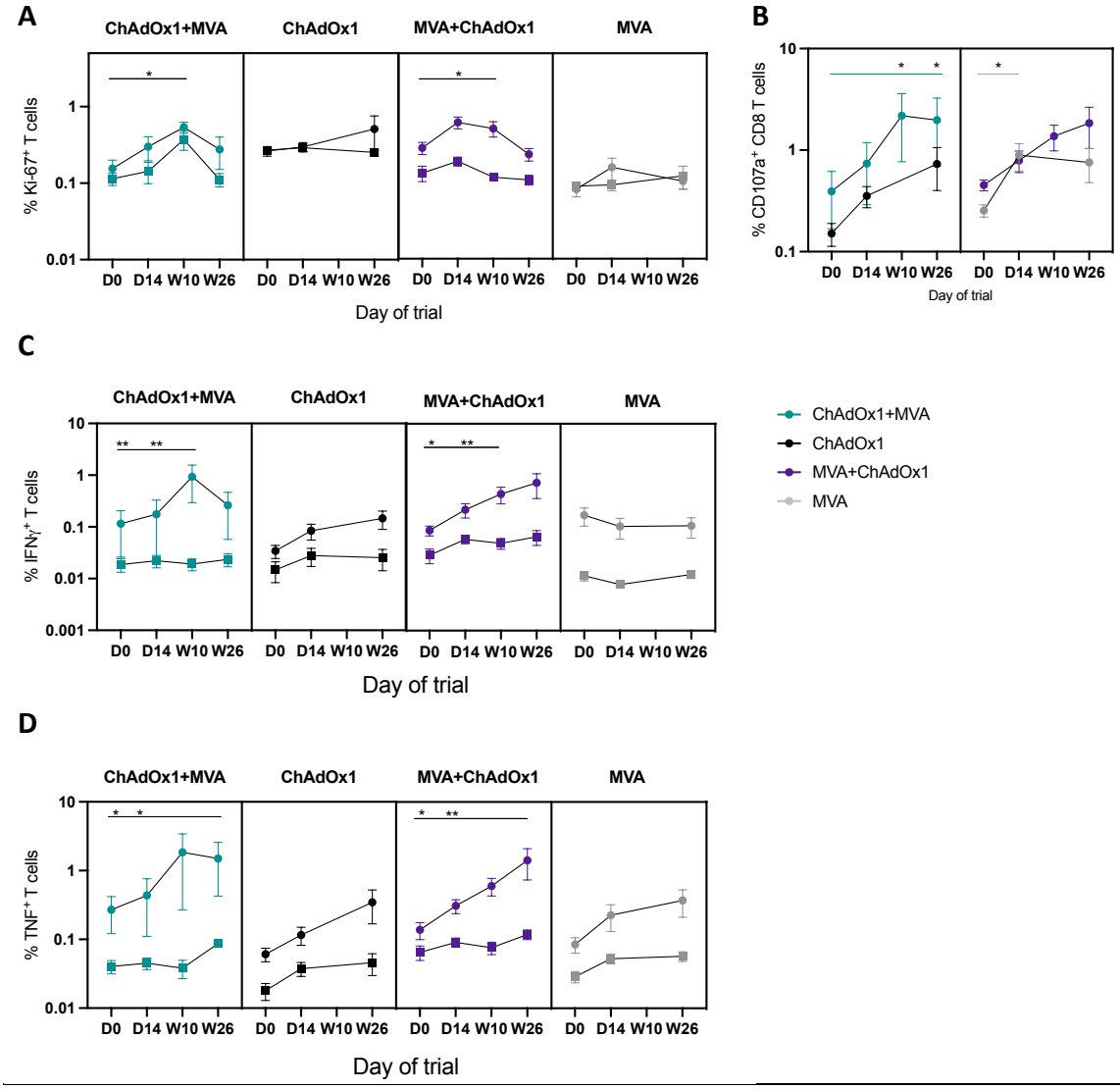


Figure 4.7. T cell activation and cytokine production following single dose and heterologous ChAdOx1 and MVA vaccination.

PBMCs from individuals vaccinated as part of the FLU005 vaccine trial were analysed by multi-parameter flow cytometry (Groups 1, 3, 4 n=10, group 2 n=9). **A)** T cells were analysed for expression Ki-67. Circles = $CD8^+$ T cells, squares = $CD4^+$ T cells.

PBMCs were stimulated for 18 hours with peptides encoding the NP and M1 protein antigen and the production of inflammatory mediators was measured at days 0 and 14, and weeks 10 (groups 1 and 3) and 26 post-vaccination. **B)** $CD8^+$ CD107a expression **C)** IFN-γ production, **D)** TNF production. Background activation was removed by subtracting unstimulated values.

Statistics conducted using Kruskal-Wallis test with Dunn's multiple comparisons *p<0.05, **p<0.01. Error bars shown as mean± SEM.

4.2.2.4. B cell responses to prime-boost vaccination

As with single dose ChAdOx1 vaccination, there was no significant difference to the frequency or phenotype of B cell populations following prime- and prime-boost regimens with ChAdOx1 and MVA (Supplementary Figure 9).

4.2.3. Altered NK cell response to vaccination correlates with CMV infection in an ebolavirus vaccine trial.

The EBL04 vaccine trial was conducted in 2015 At sites in Oxford and London, UK, and Dakar, Senegal. This trial investigated the immunogenicity of a prime-boost regimen of $3.6x10^{10}$ v.p. ChAdOx1 EBOV-GP expressing the glycoprotein from Zaire ebolavirus (Mayinga strain) and $1.x10^{8}$ PFU MVA EBOV-GP expressing ebolavirus, Sudan Virus and Marburg virus glycoproteins, and Tai Forest virus nucleoprotein (175). Analysis was conducted on PBMCs from volunteers who were boost-vaccinated with MVA EBOV-GP 7 days post-prime.

It has been shown that volunteers from Senegal had significantly lower antigen-specific IFN-γ ELISpot and IgG antibody responses than participants from the UK (339). Donors were screened for a wide array of pathogens, and it was found that infection with cytomegalovirus (CMV) correlated with a reduction in immune response to vaccination. Further cellular analysis highlighted a T cell phenotype with an expanded population of $CD8^{+}CD57^{+}KLRG1^{+}$ T cells, which are demonstrative of CMV infection and the presence of which correlate with reduced T cell IFN-γ and B cell IgG production.

To further investigate the impact of CMV infection on the immune system response of this cohort of EBL04 volunteers, the NK cell phenotype and T cell regulatory and memory phenotypes was analysed in participants from a cohort of individuals in the trial. PBMCs

were stimulated with peptides encoding either EBOV-GP, CMV pp65, SEB as a positive control, or left unstimulated, and stained with relevant panels for flow cytometry analysis.

4.2.3.1. NK cell IFN-γ reduction in CMV^+ individuals after prime-boost vaccination

The population frequencies of T_{reg} and NK cells were measured at day 7 post vaccination. Between day 0 and day 14, there was no significant increase in the total NK cell population in either CMV^- or CMV^+ participants (Figure 4.8A). There was however the expected significant increase in expression of CD57 and NKG2C on NK cells from CMV-seropositive participants (NKG2C p=0.0003, CD57 p=0.014, $NKG2C^+CD57^+$ p=0.0006. Figure 4.8B and C). There was no significant difference in the frequency of T_{reg}, T_{FH} or T_{FR} cells with CMV serostatus, however there was a previously-described increase in $CD45RA^+$ T_{EMRA} T cells (Supplementary Figure 10).

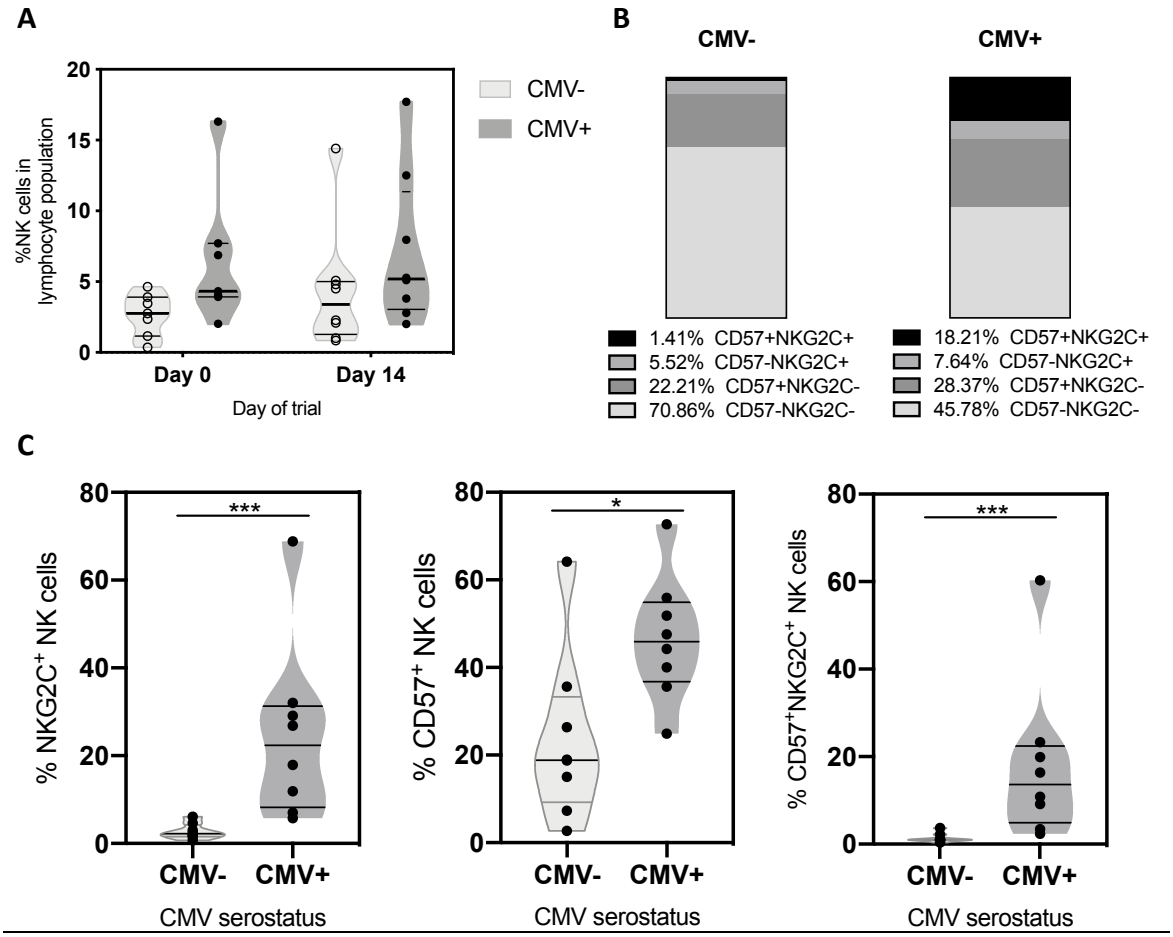


Figure 4.8. Expansion of CMV-specific NK cell populations

PBMCs from group 2 participants of the EBL04 clinical trial (n=16) were stained for NK cell markers of terminal senescence and maturation. **A)** The frequency of $CD56^{+}CD16^{+}$ NK cells as a proportion of total $CD15^{-}CD19^{-}CD3^{-}$ lymphocytes, **B-C)** The frequency of NK cells expressing CD57, NKG2C, and CD57 NKG2C double-positive NK cells stratified by CMV serostatus.

Statistics conducted using Mixed effect analysis with Holm-Sidak multiple comparisons, and Mann-Whitney U test. *p<0.05, **p<0.01, ***p<0.005. Error bars shown as mean± SEM.

Within the total NK cell population and expanded NKG2C^{+} population, we assessed the participants' ability to generate a cytotoxic and cytolytic response following peptide stimulation. There was no difference in the production of IFN-γ, GzB, or CD107a between CMV serotypes in the overall NK cell population (Figure 4.9A). Surprisingly, NKG2C^{+} NK cells expressed significantly less IFN-γ, and a trend towards less GzB, in CMV^{+} individuals 1-week post-boost vaccination (IFN-γ p=0.015, GzB p=0.12. Figure 4.9B). Contrastingly, these NK cells up-regulated significantly more CD107a (p=0.004, Figure 4.9B). This suggests the function of NK cells is altered after vaccination in CMV infection and skews this NK cell subset away from a cytotoxic response towards a cytolytic response.

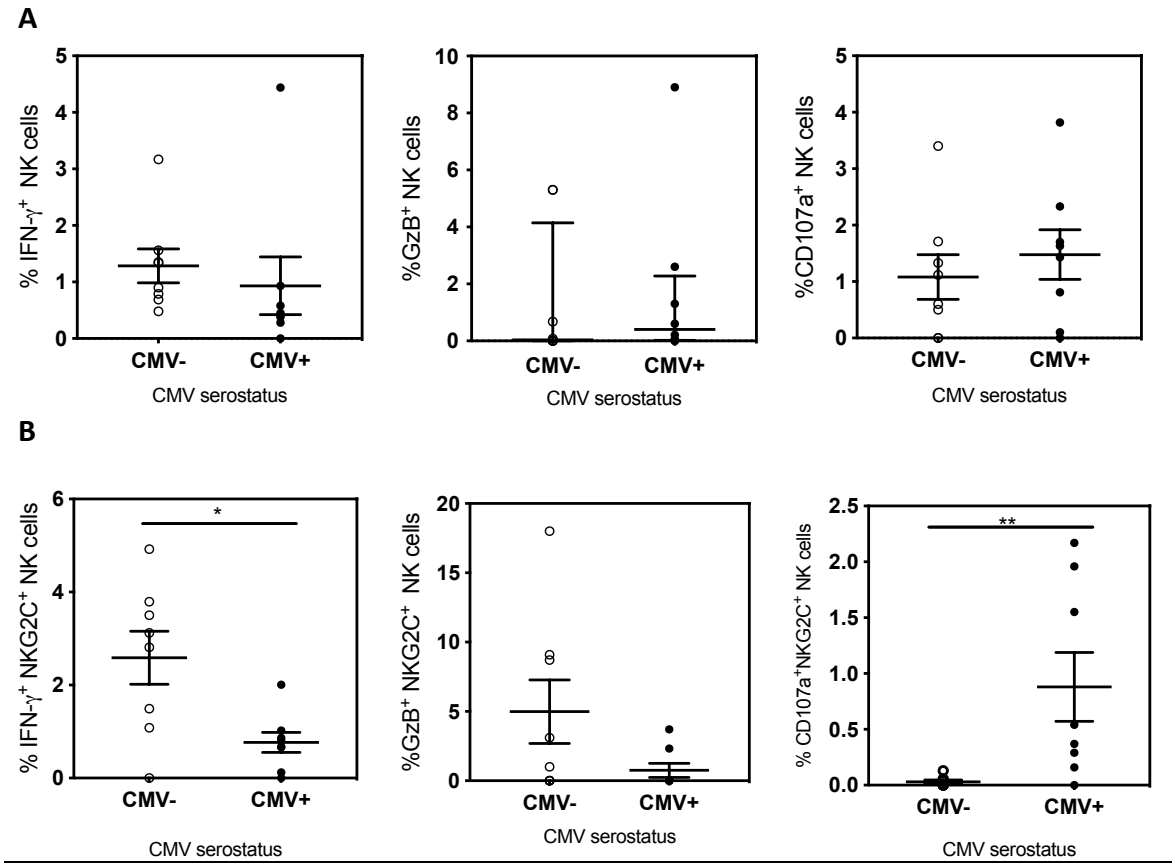


Figure 4.9. Production of inflammatory mediators by NK cells post-vaccination stratified by CMV serostatus

PBMCs from group 1b participants of the EBL04 clinical trial (n=16) were stimulated with overlapping EBOV-GP peptides and stained for NK cell markers of activation. Donors were stratified according to CMV serostatus. **A)** IFN-γ production, GzB production, and CD107a expression by the total $CD56^{+}CD16^{+}$ NK cell population. **B)** IFN-γ production, GzB production, and CD107a expression by $NKG2C^{+}$ NK cells.

Statistics conducted using Mann-Whitney U test, *p<0.05, **p<0.01. Error bars shown as mean± SEM.

4.3. Discussion

In this chapter, I demonstrate that:

- One dose of ChAdOx1 nCoV-19 activates NK cells and T cells and induces cytokine secretion
- Heterologous ChAdOx1 and MVA vaccination boost T cell and NK cell activation and proliferation
- CMV seropositivity in UK adults changes NK cell response following heterologous prime-boost vaccination.

The effect of CMV infection on the murine T_{reg} and NK cell response will be discussed in further detail in chapter 5, and chapter 6 outlines how CMV infection further alters NK cell and T cell immunogenicity in prime and prime-boost viral vector vaccination regimens.

4.3.1. Single-dose ChAdOx1 activates an immune response in multiple cellular compartments

This chapter demonstrates that a single dose of ChAdOx1 nCoV-19 activates the human immune system within adaptive and innate compartments, and generates a cytotoxic and humoral response that is readily detectable from 14 days post-vaccination. This is in keeping with previously described pre-clinical and clinical data on the T cell IFN-γ response and B cell antibody response after ChAdOx1 vaccination across multiple antigens (178, 428, 429).

Vaccine development for SARS-CoV-1 demonstrated that morbidity of Infection could be enhanced through generation of $CD4^+$ Th2 cell responses, by secretion of IL-10 and IL-14 which are immunosuppressive towards cytotoxic $CD8^+$ T cells (430). Although

neutralising antibody titres were generated, the Th2 skew facilitated immunopathology in the lung via eosinophil infiltration in a mouse model. It is therefore important that vaccines generate a Th1 inflammatory cytokine profile, with heightened expression of IFN-γ and TNF. This was achieved with the ChAdOx1 nCoV-19 vaccine and demonstrated in this chapter and by others, alongside neutralising antibody titres equivalent to those generated following natural infection (168, 183).

The immune profile of the NK cell compartment has not been previously detailed to this extent following ChAdOx1 vaccination. NK cells proliferated and were activated, but did not demonstrate any senescence or increase in quiescent populations as demonstrated with MVA vaccination in chapter 3. Activation of the NK cell compartment was observed in previous research with Ad26 and seasonal influenza vaccination, corresponding with up-regulation of CD25, CD69 and Ki-67 as corroborated in this chapter (33, 431). Interestingly, NK cells in vaccinated individuals demonstrated an increase in cytokine production following peptide stimulation, which reached a peak at 28 days post-vaccination. Although the response was very broad across participants, these data indicate NK cell response and potential memory population generation, which may contribute towards vaccine immunogenicity. Several studies have demonstrated that cytotoxic NK cells express IL-2Rα (34) and $CD4^+$ T cell IL-2 secretion is necessary for NK cell activation and proliferation after BCG, rabies virus, and influenza vaccination (26, 400), malaria infection (400) and influenza infection (361). To determine if there was a relationship between NK and T cells, I tested for a correlation between T cell IL-2 and NK cell activation markers. A moderate correlation between NK cell Ki-67 and CD25 expression with $CD4^+$ IL-2 secretion was measured at day 28, when the NK cell vaccine response was strongest. This association suggests the NK cell vaccine response may be partially mediated by antigen-specific $CD4^+$ T cell IL-2 and that T

cells may have an NK cell activating function as well as a cytotoxic function following ChAdOx1 vaccination.

4.3.2. Heterologous ChAdOx1-MVA vaccination boosts immune response in multiple cellular compartments

This chapter presents data on the immune response to heterologous ChAd-MVA vaccination across two clinical trials; FLU005 and EBL04. Phenotyping analysis of the T cell response in the EBL04 cohort has been conducted previously (339).

I analysed the immune response to a single dose or heterologous regimen of ChAdOx1 and MVA vaccines encoding the influenza A internal proteins NP and M1. Both T cell and antibody responses have been identified as being protective against influenza infection, therefore an efficacious vaccine will need to elicit a durable response in both compartments (432). Universal influenza vaccination will likely require targeted immunity towards conserved epitopes present in the majority of circulating strains. This has previously been achieved in mice, ferrets and NHP with prime-boost Ad5-vectored vaccines expressing HA epitopes conserved across multiple strains of Influenza A, followed by seasonal influenza vaccination with matching HA. This regimen generated broadly neutralising antibodies targeted towards conserved epitopes in the HA stem, rather than the more variable head region (433). T cell memory against conserved internal proteins, such as nucleoprotein and matrix 1, is also induced following vaccination and is cross-reactive against multiple strains of influenza A in mice (434, 435).

The general dynamics of activation and cytokine production have been described albeit in less detail than here (148, 179, 436). I show T cells proliferate, degranulate, and secrete IL-2, IFN-γ and TNF following a boost of either ChAdOx1 or MVA. These data are not directly

comparable to the single dose ChAdOx1 nCoV-19 results, given the difference in antigens and time points analysed, however demonstrates that a heterologous dose of covid vaccine may be beneficial for establishing stronger T cell responses.

Following a heterologous boost dose of either ChAdOx1 or MVA, NK cells expressed more Ki-67, CD25 and CD69, suggesting increased activation. This has also been observed on NK cells for up to 180 days following prime-boost of Ad.26-ZEBOV and MVA-BN-Filo (363). In this thesis, ChAdOx1-MVA vaccination did not elicit increased cytokine secretion at week 10, although a moderate boosting effect was seen in TNF and CD107a expression from NK cells following MVA-ChAdOx1 vaccination. The explanation for this difference is supported in part by data from Palgen *et al*, who demonstrate that a single dose of MVA induces NK cell proliferation and activation following subcutaneous vaccination in cynomolgus macaques, and that increased NK cell CD107a, CD69 and granzyme B were observed following a second booster dose of MVA (364). However, it is unusual that ChAdOx1-MVA vaccination did not elicit a boost response in NK cell cytotoxicity, given that other studies show that Ad.26-MVA vaccination induces NK cell secretion of IFN-γ and CD107a at two weeks post-MVA boost, and also after homologous BCG vaccination (26, 363, 437). NK cell boosting by BCG vaccination is facilitated by $CD4^+$ T cell IL-2 secretion (26), similarly to single-dose ChAdOx1 vaccination in this chapter, however I did not observe any significant correlation with IL-2 and NK cell activation in these prime-boost analyses. One explanation for this lack of boosted NK cell response is that individuals within groups showed a considerable variation in pre-existing immunity to influenza at day 0, as most adults will be exposed annual to circulating influenza virus. As suggested by Jost *et al*, prior exposure to influenza antigens may prime NK cells so that further vaccination induces anergy and lack of cytotoxic response via down-regulation of activating NK cell

receptors (33), which may not be the case with antigens that have only been seen by the volunteers through the prime vaccination. Interestingly, NK cells following prime-boost vaccination with MVA-ChAdOx1 showed some increase in IL-2 expression, which is previously unreported. These data could potentially be explained by up-regulation of the IL-2R complex during activation and capture of IL-2 from other immune cells (438).

NK cells from the EBL04 vaccine trial were analysed following stratification for CMV. NK cells from CMV seropositive donors displayed the hallmark $CD57^{+}NKG2C^{+}$ phenotype, and had altered response to vaccine antigen, with reduced IFN-γ secretion but increased CD107a expression within the expanded $NKG2C^{+}$ subset. Lower cytotoxicity and reciprocal increase in degranulation (albeit measured by perforin expression) was demonstrated in part by Lee *et al* to correspond with increased IL-10 secretion and an immunoregulatory function on $CD8^{+}$ T cells during MCMV infection in mice (439). However, I did not observe any increase in NK cell IL-10 secretion in this study (data not shown), but from the data presented we cannot rule out a less inflammatory and more regulatory profile of NK cells with CMV seropositivity following vaccination. In these experiments, I did not investigate whether antibody dependent cellular cytotoxicity (ADCC) via CD16 signalling also induced NK cell activation, as seen in NK cells in response to EBOV-specific antibodies post-vaccination (363).

This chapter demonstrates how single dose vaccination can activate and produce a functional response in NK cells and T cells, and how heterologous boosting can increase these responses. Furthermore, this chapter begins to discuss how CMV seropositivity can alter the NK cell response to vaccination, which will be explored further in chapters 5 and 6.

Papers published using data from this chapter

- Ewer, K.J.*, Barrett, J.R.*, Belij-Rammerstorfer, S.*, **Sharpe, H**., Makinson, R., Morter, R., Flaxman, A., Wright, D., Bellamy, D., Bittaye, M., Dold, C., Provine, N.M., Aboagye, J., Fowler, J., Silk, S.E., Alderson, J., Aley, P.K., Angus, B., Berrie, E., Bibi, S., Cicconi, P., Clutterbuck, E.A., Cheysheva, I., Folegatti, P.M., Fuskova, M., Green, C.M., Jenkin, D., Kerridge, S., Lawrie, A., Minassian, A.M., Moore, M., Mujadidi, Y., Plested, E., Poulton, I., Ramesamy, M.N., Robinson, H., Song, R., Snape, M.D., Tarrant, R., Voysey, M., Watson, M.E.E., Douglas, A.D., Hill, A.V.S.^, Gilbert, S.C.^, Pollard, A.J.^, Lambe, T.^ and the OCVT Group. T cell and antibody responses induced by a single dose of ChAdOx1 nCoV-19 (AZD1222) vaccine in a phase I/II clinical trial. Nature Medicine. 2021 Feb; 27(2): 270-278.
- Bowyer, G., **Sharpe, H.,** Venkatraman, N., Ndiaye, P.B., Wade, D., Brenner, N., Mentzer, A., Mair, C., Waterboer, T., Lambe, T., Dieye, T., Mboup, S., Hill, A.V.S., Ewer, K.J. Reduced Ebola vaccine responses in CMV+ young adults is associated with expansion of CD57+KLRG1+ T cells: J Exp Med. 2020. Jul 6;217(7).

Chapter 5

Acute and chronic CMV infection on activation of innate and adaptive immune cells in a mouse model

Chapter 5 : Acute and chronic CMV infection on activation of innate and adaptive immune cells in a mouse model

5.1. Introduction and aims

Murine cytomegalovirus (MCMV) establishes a chronic, latent infection in C57BL/6 mice, and is used widely as a model for human cytomegalovirus (HCMV) infection (273). Using MCMV to model HCMV allows investigation into the early dynamics of the immune response to the virus and exploration into multiple tissues, which is not easily possible in human populations. Most knowledge about human cytomegalovirus infection is from the immune response in the peripheral blood and little is known about the phenotype of immune cells in other organs, or tissue resident cells, and their response to infection. In this chapter, I aim to describe the phenotype and functionality of innate and innate-like immune cells during acute and chronic MCMV infection in mice, and develop a model of MCMV infection and viral vector vaccination that can mimic the clinical trial response described in section 4.2.3.

NK cells are essential for early control of MCMV infection and establish cellular memory for enhanced activation during subsequent infections (292, 440). The activating NK cell receptor Ly49H is peptide-specific for MCMV m157, which is expressed as an MHC class I-like molecule on the surface of infected cells (289, 441). Upon receptor activation, a clonal population of $Ly49H^+$ NK cells proliferate and activate to control viral spread. After latency has occurred, the population contracts, although is able to re-expand rapidly upon re-infection or reactivation (289). Balb/c mice, which do not express Ly49H, are unable to control MCMV infection and do not establish a latent infection (442). The receptor NKG2C in humans is analogous in function to Ly49H and recognises the HCMV UL40 peptide

presented by HLA-E (443). Unlike Ly49H$^+$ NK cells, in humans the NKG2C$^+$ NK cells remain expanded following CMV latency, and have a more terminally differentiated phenotype through expression of CD57 (293).

Tissue-resident NK cells (trNK) in the liver form a separate lineage to conventional circulating NK cells (cNK), and are retained in the hepatic sinusoids (44). trNK cells have been more defined in mice, with an immature DX5$^-$NK1.1$^+$ phenotype and a Tbet$^+$Eomes$^-$ transcription factor profile (28, 31). They express the liver residency markers CD49a and CXCR6 (43, 444). CD49a is the α1 subunit of $\alpha1\beta1$ integrin, which binds to collagen IV and laminin in the liver and facilitates cell retention (445). CXCR6 is the sole receptor for CXCL16, which is expressed on sinusoidal endothelial cells in the liver and promotes tissue residency (49). Zhou *et al* demonstrated that trNK cells can have a negative immunoregulatory function on CD4$^+$ and CD8$^+$ T cells during viral infection through PD1 signalling. This is in contrast to cNK-mediated antiviral activation, and acts to regulate the tolerogenic environment of the liver (8). However, other evidence suggests that trNK cells in mice can also have a robust cytotoxic function during early acute infection, and can produce IFN-γ in response to MCMV, *Francisella tularensis* and Vaccinia virus (42, 446).

T cells facilitate control of latent MCMV and prevent viral re-activation (308). They establish classical memory populations, which follow canonical expansion and contraction after infection resolution, and 'inflationary' populations which remain at high frequency following viral latency yet are highly functional and do not express markers of senescence or terminal differentiation (314). Mucosal-associated invariant T (MAIT) cells are innate-like T cells, which share limited differences between mice and humans and express a semi-invariant TCR repertoire restricted by the MHC class-I related molecule MR1 (87, 94). MR1 can only present conserved riboflavin-derived ligands synthesised by bacteria and yeast,

leading to the original belief that MAIT cells could only respond to specific infections (94). However, more recent research demonstrates that MAIT cells can also be activated by viral infection, including influenza A and HCV infection, in a MR1-independent manner through IL-12, IL-15, IL-18 and IFN-α produced by monocyte-derived dendritic cells and macrophages (89, 102, 103, 109). The response of MAIT cells to MCMV infection is not yet known, although McSharry *et al* demonstrated a reduction in MAIT cell activation to HSV-1 infection mediated by a suppression of MR1 (447).

In this chapter, I outline how MCMV infection affects immune activation across multiple organs in a mouse model. I investigate how chronic and acute MCMV infection affects the activation response of two non-classical immune cell populations; trNK cells and MAIT cells, in comparison to canonical NK cells and T cells. Finally, I establish a model of MCMV infection and viral vector vaccination, with an aim to replicate the loss of vaccine immunogenicity observed in human clinical trial samples in chapter 4.

Aims of chapter 5

- Investigate the response of cNK and trNK cells in the liver and spleen to acute and chronic MCMV infection.
- Describe the activation phenotype of T cells, T regulatory cells and MAIT cells in response to acute and chronic MCMV infection.
- Explore the use of MCMV as a model for human CMV infection and vaccine immunogenicity.

5.2. Results

5.2.1. NK cell maturation and activation during acute MCMV infection

5.2.1.1. NK cell activation occurs during acute MCMV infection

C57Bl/6J mice were infected i.v. with $1x10^6$ i.u. MCMV for the previously-established duration of 50 days (chronic infection), 7 days (acute infection), or left uninfected (⊗) to investigate whether MCMV infection alters the activation and maturation profile of NK cells in the liver and spleen in a similar way to viral vector vaccination. Analysis by flow cytometry (supplementary figure 2) indicated that there was a higher frequency of $KLRG1^+$ NK cells during acute infection, which returned to pre-infection frequency by 50 days post-infection (liver p=0.0027, spleen p<0.026. Figure 5.1A). Interestingly, this up-regulation was observed on the least mature $CD11b^-CD27^+$ NK cells, which typically express a very low frequency of KLRG1 in a naïve mouse ((448) liver p=0.04, spleen p=0.01. Figure 5.1B). The most mature $CD11b^+CD27^-$ NK cells were reduced in frequency during acute 7-day infection, and were restored by day 50 (liver p=0.03. Figure 5.1C). Within this $CD11b^+CD27^-$ subset, there was an increase in the liver-migration marker and potential NK cell memory marker CXCR6 at acute infection in the liver, but not the spleen (p=0.02. Figure 5.1D) This was unexpected, as CXCR6 expression is usually confined to the least mature $CD11b^-CD27^+$ NK cells (365), however there was no observable change in CXCR6 expression on this population (Data not shown). At day 7 post-infection, there was a higher frequency of $Ly49H^+$ mature $CD11b^+CD27^+$ NK cells, which has previously been demonstrated to be up-regulated during acute MCMV infection (381) (liver p=0.009, spleen p=0.008. Figure 5.1E). These data support previous literature on the transient activation of NK cells during acute MCMV infection, which unlike during HCMV infection, return to pre-infection phenotypes by day 50.

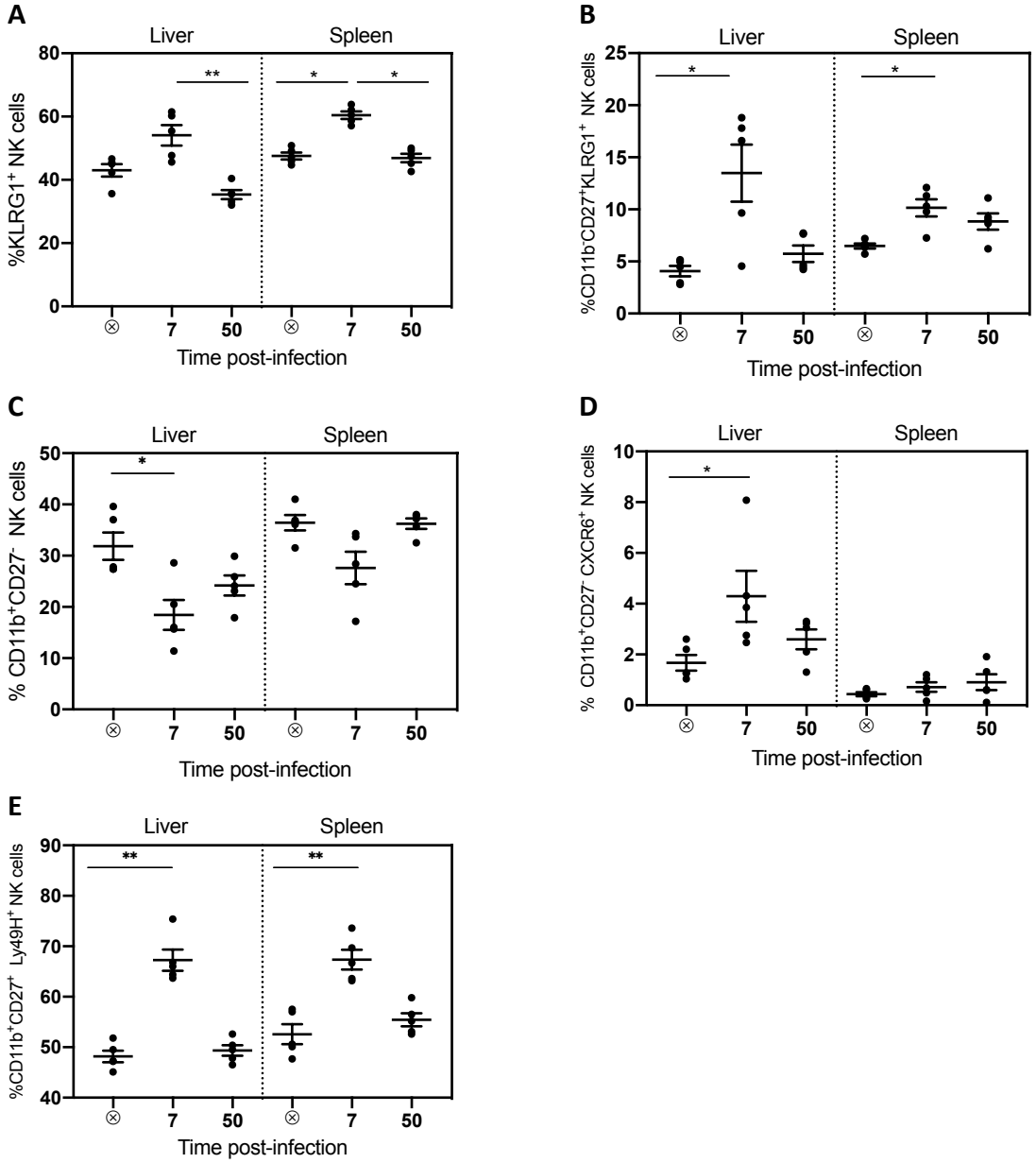


Figure 5.1. Frequencies of surface markers on NK cells in mice with acute and chronic MCMV infection.

Mice (n=5 per group) were infected via the tail vein with $1x10^6$ i.u. MCMV for a chronic (50 days) or acute (7 days) duration or left uninfected (⊗). Spleens and livers were harvested, and NK cells were stained for markers of maturity and activation; **A)** Overall expression of KLRG1 on $CD3^-NK1.1^+$ NK cells**, B)** Frequency of $KLRG1^+$ $CD11b^-CD27^+$ NK cells. **C)** Frequency of $CD11b^+CD27^-$ NK cells, **D)** Frequency of $CXCR6^+$ $CD11b^+CD27^-$ NK cells, **E)** Frequency of $Ly49H^+$ $CD11b^+CD27^+$ NK cells.

Statistics conducted using Kruskal-Wallis test with Dunn's multiple comparisons. *p<0.05, **p<0.01. Error bars shown as mean± SEM.

5.2.2. Tissue-resident NK cells are enriched in the liver

NK cell maturation can be defined along an NK1.1/DX5 axis (figure 5.2). Double positive DX5^{+}NK1.1^{+} NK cells are the most abundant sub-population in the spleen (Figure 5.2A) and can be defined as 'canonical' circulating NK cells (cNK). The liver also supports a sub-population of tissue-resident DX5^{-}NK1.1^{+} NK cells (trNK, figure 5.2B)

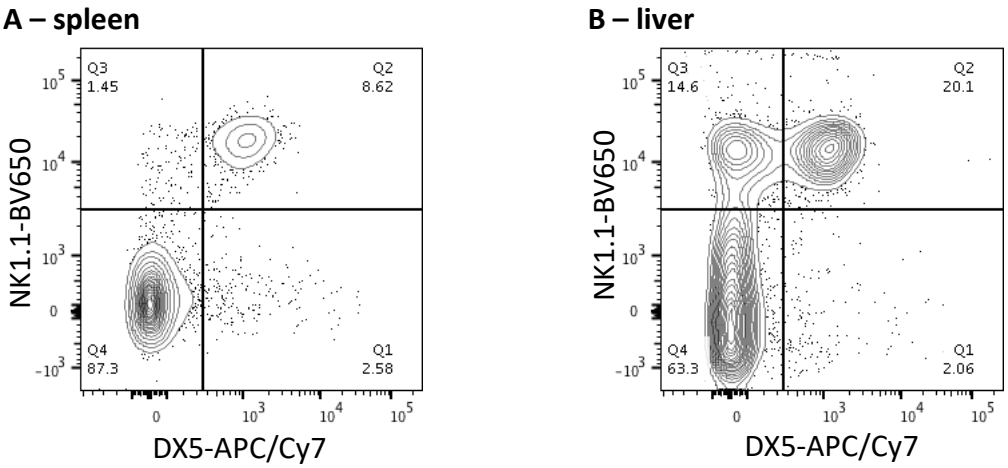


Figure 5.2. NK cell phenotypes in the spleen and liver

NK cell phenotype staining from the spleen and liver of one representative C57BL/6J mice. Gating conducted on live CD3^{-} cells. **A)** the spleen has predominantly mature DX5^{+}NK1.1^{+} NK cells and a low frequency of DX5^{-}NK1.1^{+} NK cells, **B)** The liver is enriched for DX5^{+}NK1.1^{+} NK cells, and has an expanded population of DX5^{-}NK1.1^{+} NK cells

5.2.2.1. Frequency dynamics of circulating and tissue resident NK cells in MCMV infection

As demonstrated in section 5.2.1, NK cells are activated during acute MCMV infection and exhibit increased terminal differentiation and expression of liver migration markers. To determine differences in the frequencies of cNK and trNK cells during acute MCMV infection, mice were infected as previously established for 7 days, 4 days, 1 day, or 0 days (uninfected). A separate group of mice were also infected with MCMV for the established time points for chronic and acute infection (50 days and 7 days, respectively). Spleens and livers were harvested from these cohorts, and the frequencies and phenotype of cNK and trNK cells in these organs were analysed by flow cytometry following the gating strategy in supplementary figure 1.

In the spleen, there was a slight decline in the frequency of $DX5^{+}NK1.1^{+}$ cNK cells over the 7-day course of infection, potentially due to an influx of other lymphocytes into the spleen (p=0.016, figure 5.3A). The NK cell population in the liver is enriched for $DX5^{+}NK1.1^{+}$ NK cells, and this proportion was significantly increased at day 4 post-infection (p<0.0326, figure 5.11A). These data are supported by the total count of cNK cells in each organ (data not shown). As expected, the frequency of the $DX5^{-}NK1.1^{+}$ trNK cell sub-population in the spleen remained very low (day 0 frequency = 0.5% of lymphocytes). Although trNK cells are enriched in the liver, they decreased in frequency throughout the duration of the acute infection (p<0.27, Figure 5.3B). Between uninfected, acute, and chronically infected mice, there was no significant difference in the frequencies of either sub-population of NK cells, although there was a trend towards a decrease in frequency of trNK cells in the liver (Figure 5.3C and D).

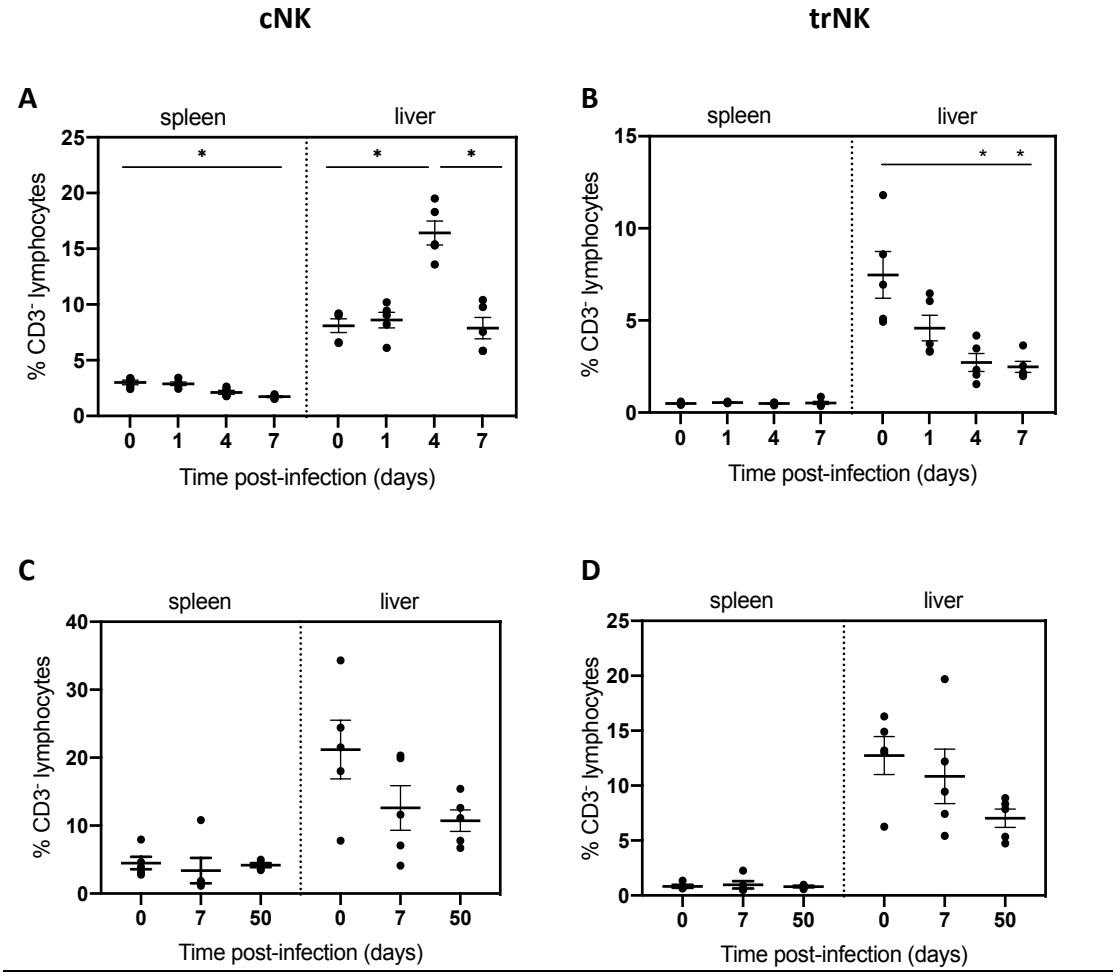


Figure 5.3. The frequencies of circulating and tissue-resident NK cells in the spleen and liver during acute and chronic MCMV infection.

C57BL/6J mice (n=5 per group) were infected with $1x10^6$ i.u. MCMV for 7, 4, or 1 days, or uninfected (0 days). The frequency of **A)** $DX5^+NK1.1^+$ (circulating) and **B)** $DX5^-NK1.1^+$ (tissue-resident) NK cells were measured as a proportion of the $CD3^-$ lymphocyte population in the spleen and liver.

MCMV infections were established in mice for 50 days (chronic), or 7 days (acute) or left uninfected. The frequency of **C)** $DX5^+NK1.1^+$ and **D)** $DX5^-NK1.1^+$ NK cells were measured as a proportion of the $CD3^-$ lymphocyte population in the spleen and liver.

Statistics conducted using Kruskal-Wallis test with Dunn's multiple comparisons. *p<0.05. Error bars shown as mean± SEM.

5.2.2.2. Changes in frequency of CD49a$^+$ and CXCR6$^+$ DX5$^+$NK1.1$^+$ cNK cells during acute infection

CXCR6 and CD49a both promote migration to and retention in the murine liver, and are required for NK cell adaptive-like features and antigen-specific memory (365). They are primarily expressed on trNK cells, however can be induced on cNK cells following inflammatory cytokine stimulation (365). Firstly, I analysed the phenotype of DX5$^+$NK1.1$^+$ cNK cells during acute and chronic infection, beginning with the frequency of CXCR6$^+$ and CD49a$^+$ splenic and hepatic cNK cells. During acute infection, CXCR6$^+$ cNK cells significantly increased in frequency at day 4 post-infection in the spleen (p=0.0009, Figure 5.4A and C). There were more CD49a$^+$ cNK cells in both organs, with a significant increase to day 7 in the spleen (p=0.008, figure 5.4B). This trend was also seen when comparing acute and chronic infection; there was minimal change in CXCR6 expression across acute and chronic time points (Figure 5.12C), however there was a significant increase in CD49a$^+$ NK cell frequency at day 7 post-infection, which returned to pre-infection levels at day 50 (p<0.032, figure 5.4D). These data suggest that, on cNK cells, CD49a expression may facilitate migration of cNK cells to the liver during acute infection.

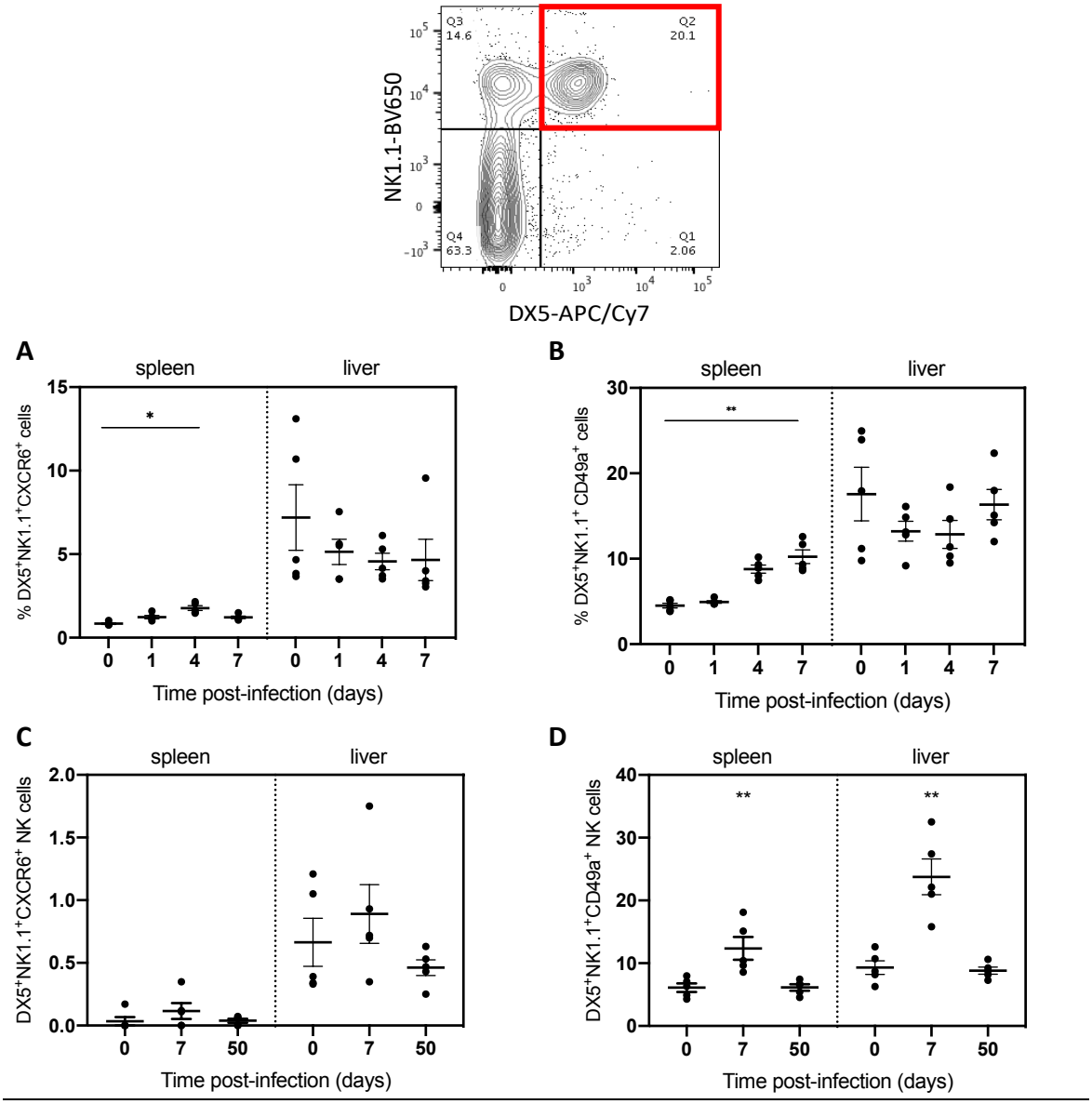


Figure 5.4. The frequency of CXCR6$^+$ and CD49a$^+$ DX5$^+$NK1.1$^+$ NK cells during acute and chronic MCMV infection

C57BL/6J mice (n=5 per group) were infected with 1x10^6 i.u. MCMV for 7, 4, or 1 days, or left uninfected. Spleens and livers were harvested, and the frequency of **A)** CXCR6, and **B)** CD49a, were measured on cNK cells at each time point. MCMV infections were established in mice for 50 days, 7 days, or left uninfected as a control. The frequency of **C)** CXCR6$^+$ and **D)** CD49a$^+$ NK cells were measured as a proportion of the cNK cell population in the spleen and liver. Statistics conducted using Kruskal-Wallis test with Dunn's multiple comparisons. *p<0.05, **p<0.01. Error bars shown as mean± SEM.

5.2.2.3. Activation and polyfunctionality of $DX5^+NK1.1^+$ cNK cells during acute infection

Next, I measured the cytokine production and degranulation of circulating NK cells during the course of acute MCMV infection. The activation of cNK cells were measured by increase in SSC-A shift. cNK cells in the spleen at day 4 post-infection had a larger SSC-A area than cNK cells from uninfected mice, suggesting increased activation and granule production (p=0.0006). A similar yet non-significant trend was seen in the liver cNK cells (Figure 5.5A).

I then assessed the polyfunctional ability of cNK cells in both organs using Boolean gating. Polyfunctionality, the ability of cNK cells to produce or up-regulate more than one marker, of splenic cNK cells peaked at day 4 post-infection, with a geometric mean of 0.016% NK cells producing all 4 inflammatory mediators (Figure 5.5B). However, cNK cells in the liver were not as polyfunctional during acute infection. We could not detect all 4 inflammatory mediators at any time point, although at 4 days post-infection there was a geometric mean of 0.113% NK cells expressing 3 inflammatory mediators (Figure 5.5C).

To determine the most highly secreted cytokines by cNK cells during acute infection, individual proportions of each inflammatory mediator were calculated. In the spleen, IFN-γ^+ and $CD107a^+$ cNK cells significantly increased in frequency until day 7 post-infection (p=0.0017 and p=0.019 respectively. Figure 5.5D). GzB production also peaked at day 4 post-infection when compared to pre-infection responses (p=0.0005. Figure 5.5D). Contrastingly in the liver, the only significant change in post-infection time points was a peak in GzB secretion at day 4 (p=0.0046. Figure 5.5D). These describe a different functional capacity of a sub-population of cNK cells in the spleen and liver during acute MCMV infection; splenic cNK cells are more responsive to acute MCMV infection than cNK cells in the liver.

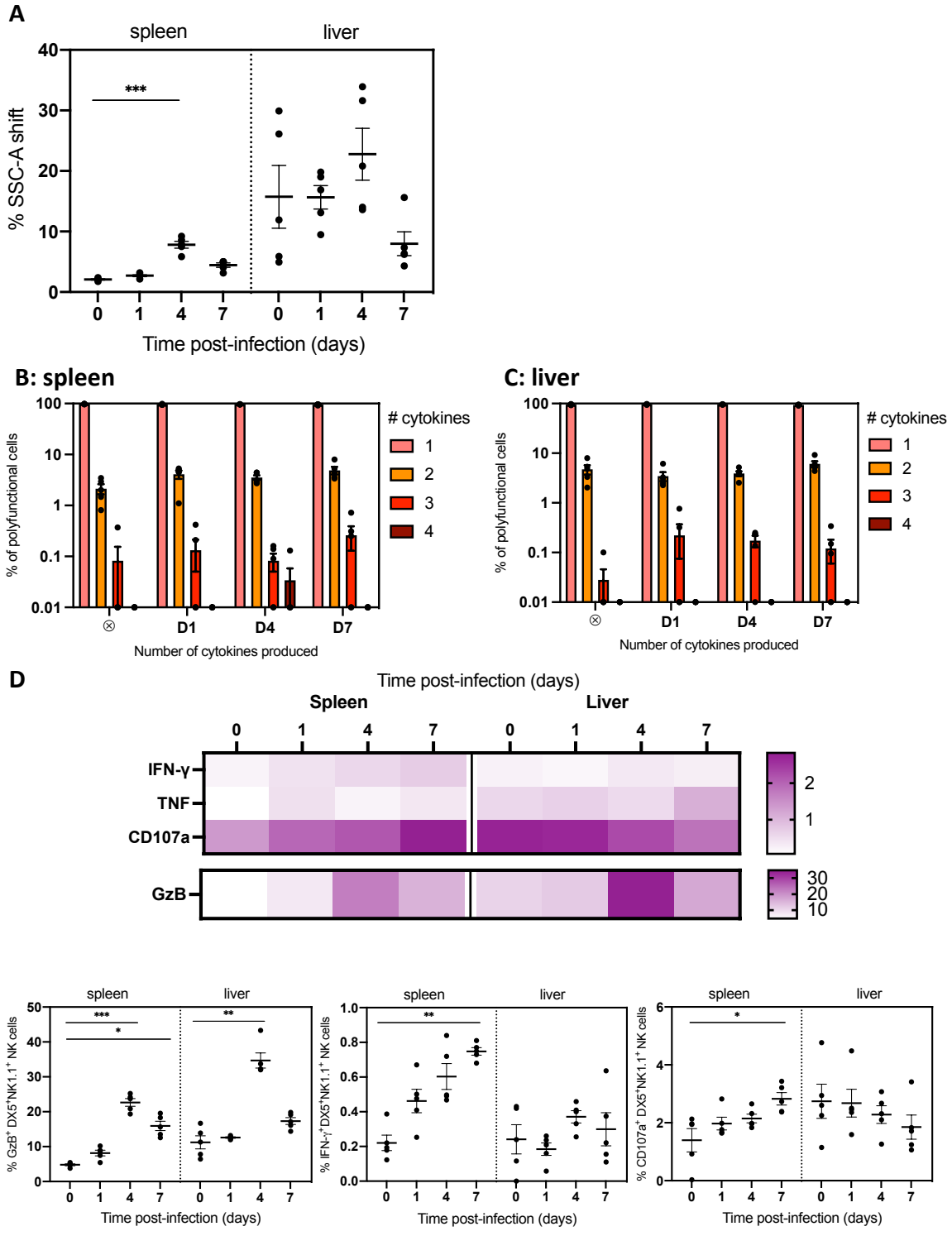

A
spleen
liver
% SSC-A shift
***
Time post-infection (days)
B: spleen
C: liver
% of polyfunctional cells
# cytokines
1
2
3
4
D1
D4
D7
Number of cytokines produced
D
Time post-infection (days)
Spleen
Liver
IFN-γ
TNF
CD107a
GzB
% GzB+ DX5+NK1.1+ NK cells
% IFN-γ+DX5+NK1.1+ NK cells
% CD107a+ DX5+NK1.1+ NK cells

Figure 5.5. Cytokine production and polyfunctionality of $DX5^+NK1.1^+$ cNK cells

C57BL/6J mice (n=5 per group) were infected with $1x10^6$ i.u. MCMV for 7, 4, or 1 days, or left uninfected (day 0). Spleens and livers were harvested post take-down and PBMCs incubated for 2 hours at 37°C in the presence of Brefeldin A and monensin. PBMCs were then stained for $DX5^+NK1.1^+$ cNK cells and CD107a, TNF-α, GzB, and IFN-γ.

This figure shows **A)** The SSC-A of cNK cells in the spleen and the liver during acute infection, **B)** The polyfunctional response of cNK cells in the spleen, and **C)** the polyfunctional response in the liver, measured for all 4 inflammatory mediators ((IFN-γ, TNF, CD107a, GzB) at all time points. **D)** The production of GzB, IFN-γ, TNF and CD107a at day 0, 1, 3 and 7 post-infection. Statistics conducted using Kruskal-Wallis test with Dunn's multiple comparisons or Two-way ANOVA with Tukey's multiple comparisons. *p<0.05, **p<0.01, ***p<0.005. Error bars shown as mean± SEM.

5.2.2.4. Changes in frequency of CD49a$^+$ and CXCR6$^+$ DX5$^-$NK1.1$^+$ trNK cells during acute and chronic infection

The frequency and functionality of trNK cells during acute and chronic MCMV infection was analysed next. Tissue resident DX5$^-$NK1.1$^+$ trNK cells are found predominantly in the liver and are a subset of NK cells with an immature phenotype (448). They express more CXCR6 and CD49a than conventional DX5$^+$NK1.1$^+$ NK cells, and have a capacity for adaptive memory-like responses (365, 397). The frequency of CXCR6$^+$ trNK cells in the spleen was much higher than CXCR6$^+$cNK cells. CXCR6$^+$ frequency decreased by day 7 post-infection in the spleen (p=0.0025), however increased significantly at day 4 in the liver (p=0.038. Figure 5.6A). The frequency of CD49a$^+$ trNK cells increases significantly at day 4 in the spleen (p=0.0327) however decreases by day 7 in the liver (p=0.0017, figure 5.6B). During chronic MCMV infection, the frequency of splenic CXCR6$^+$ trNK cells continues to decrease in comparison to uninfected cells (Figure 5.6C). However, there was no significant change in CD49a$^+$ trNK frequency between acute and chronic infection in either organ (Figure 5.6D). This is in contrast to the frequency of CD49a$^+$DX5$^+$NK1.1$^+$ cNK cells, which was substantially increased in expression at day 7 post-infection in the liver and spleen (Figure 5.4D).

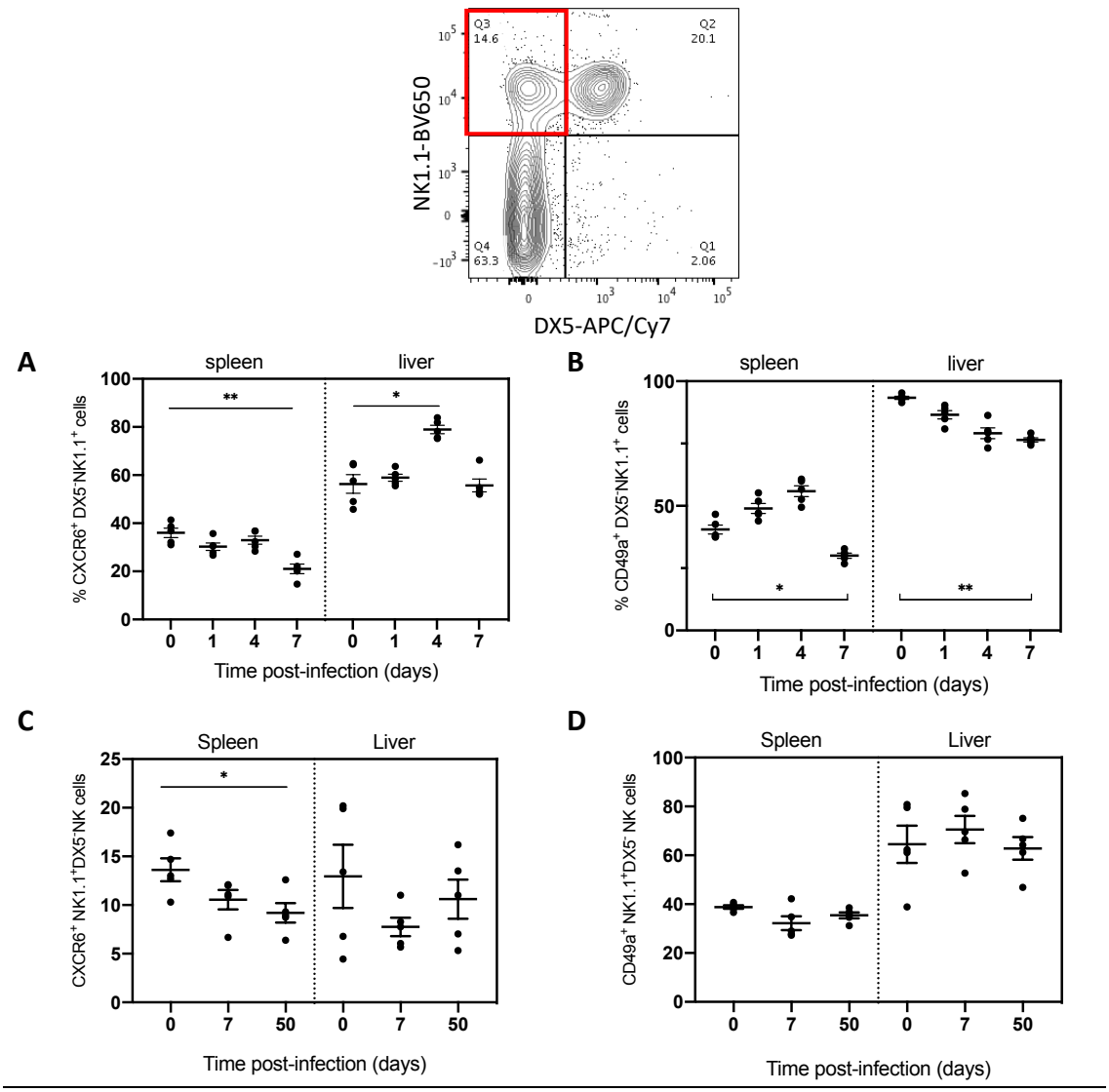


Figure 5.6. The frequency of CXCR6$^+$ and CD49a$^+$ DX5$^-$NK1.1$^+$ trNK cells during acute and chronic MCMV infection.

C57BL/6J mice (n=5 per group) were infected with 1x10^6 i.u. MCMV for 7, 4, or 1 days, or left uninfected. Spleens and livers were harvested, and the frequency of **A)** CXCR6$^+$, and **B)** CD49a$^+$ DX5$^-$NK1.1$^+$ trNK cells was measured at each time point. MCMV infections were established in mice for 50 days (chronic), or 7 days (acute) or left uninfected as a control. The frequency of **C)** CXCR6$^+$ and **D)** CD49a$^+$ NK cells were measured as a proportion of the trNK cell population in the spleen and liver.

Statistics conducted using Kruskal-Wallis test with Dunn's multiple comparisons. *p<0.05, **p<0.01, ***p<0.005, ****p<0.0001. Error bars shown as mean± SEM.

5.2.2.5. Activation, cytokine expression and polyfunctionality of $DX5^{-}NK1.1^{+}$ NK cells

The cytokine production and degranulation ability of trNK cells was measured during the course of acute MCMV infection for comparison to cNK cells across the same time course. Similarly to cNK cells, the SSC-A shift activation measurement of tissue-resident NK cells significantly peaked at day 4 in both the spleen and the liver, before returning to pre-infection levels by day 7 (p=0.0011 and p=0.0031 respectively, figure 5.7A)

Similar polyfunctionality analysis was conducted on trNK cells to assess the expression of the inflammatory mediators CD107a, TNF, IFN-γ and GzB. Splenic $DX5^{-}NK1.1^{+}$ trNK cells are a very small population, and did not follow any significant trend with regards to polyfunctionality responses post-infection (Figure 5.7B). However, all post-infection time points in the liver had a small proportion of tissue-resident NK cells that express all 4 inflammatory mediators, representing a geometric mean of 0.026% trNK cells at day 7 (Figure 5.7C). This demonstrates that $DX5^{-}NK1.1^{+}$ trNK cells in the liver have a more inflammatory profile after MCMV infection in comparison to circulating NK cells and NK cells found in the spleen, which only expressed up to 3 inflammatory mediators post-infection.

To further analyse the inflammatory mediators produced by trNK cells, the production of individual cytokines was measured after infection. trNK cells have differential frequency of cytokine positive cells in the liver and the spleen and also differ in their cytokine production compared to cNK cells (Figure 5.7D). Although they are a small population, splenic trNK cells produced significantly more CD107a at day 4 compared to uninfected mice (p=0.0011), and this peak of expression was also seen in liver trNK cells (p=0.012). Liver trNK cell IFN-γ production significantly increased by day 4 post-infection

(*p*=0.0037), although this did not occur in splenic trNK cells. GzB production in the liver was high at day 0, and decreased significantly from day 0 to day 7 (*p*=0.008, Figure 5.7D). The cytokine response was also assessed in the potential NK cell memory sub-populations (liver-resident CXCR6$^+$ and CD49a$^+$ DX5$^-$NK1.1$^+$ cells). The CXCR6$^+$ population was more responsive to MCMV infection than the CD49a$^+$ population. CD49a$^+$ DX5$^-$NK1.1$^+$ NK cell demonstrated a significant increase in CD107a expression at day 4 post-infection (*p*=0.019), but no other significant changes in cytokine production (data not shown). The CXCR6$^+$ population had a significant increase in TNF secretion (*p*=0.038), IFN-γ secretion (*p*=0.0021), and CD107a expression (*p*=0.013) at day 4 post-infection (Figure 5.7E). Neither population demonstrated an enhanced Granzyme B response. This data implies that MCMV elicits a robust IFN-γ and cytolytic response from trNK cells, which does not involve GzB secretion, during acute infection in the liver.

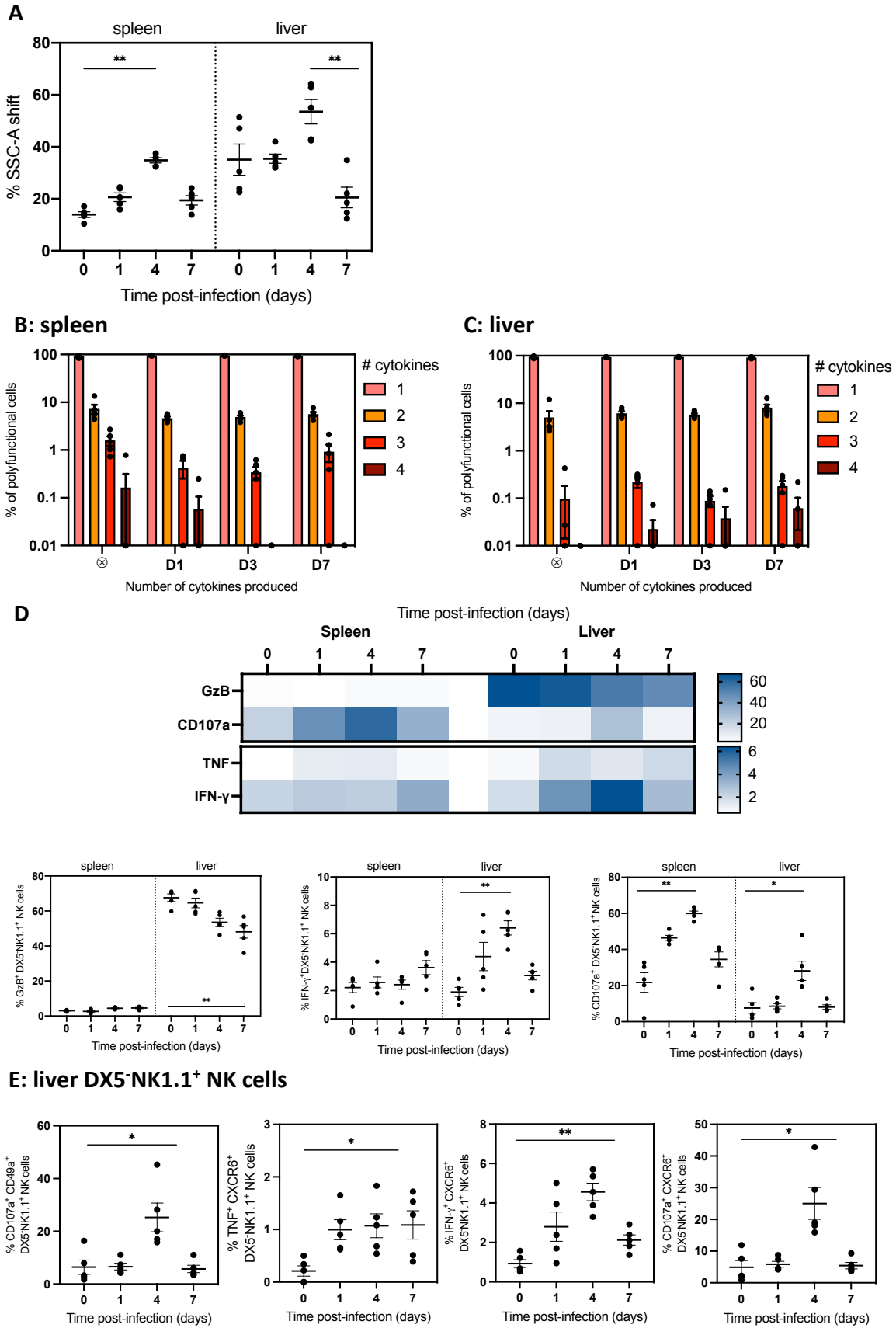

A
spleen
liver
% SSC-A shift
Time post-infection (days)
B: spleen
C: liver
% of polyfunctional cells
# cytokines
Number of cytokines produced
D
Time post-infection (days)
Spleen
Liver
GzB
CD107a
TNF
IFN-γ
E: liver DX5⁻NK1.1⁺ NK cells

Figure 5.7. Cytokine production and polyfunctionality of DX5$^-$NK1.1$^+$ trNK cells

C57BL/6J mice (n=5 per group) were infected with 1x10^6 i.u. MCMV for 7, 4, or 1 days, or left uninfected. Spleens and livers were harvested post take-down and stained for DX5$^+$NK1.1$^+$ cNK cells and CD107a, TNF-α, GzB, and IFN-γ.

This figure shows **A)** The SSC-A of trNK cells in the spleen and the liver during acute infection, **B)** The polyfunctional response of trNK cells in the spleen, and **C)** the liver, measured for all 4 inflammatory mediators at all time points. **D)** The production of cytokines and markers of degranulation (GzB, IFN-γ, CD107a) days 1, 3 and 7 post infection. **E)** Cytokine production and degranulation by hepatic DX5$^-$NK1.1$^+$ NK cells. Left to right: CD49a$^+$ CD107a expression, CXCR6$^+$ TNF expression, CXCR6$^+$ IFN-γ expression, CXCR6$^+$ CD107a expression.

Statistics conducted using Kruskal-Wallis test with Dunn's multiple comparisons. *p<0.05, **p<0.01. Error bars shown as mean± SEM.

5.2.2.6. Enhanced cytokine secretion and degranulation of trNK cells during MCMV infection

The enhanced cytokine secretion and degranulation of tissue resident NK cells was further demonstrated by analysis of the proportion expressing at least one cytokine during acute infection (Figure 5.8). A higher proportion of trNK cells produced at least one inflammatory mediator compared to circulating NK cells at all time points in the spleen and the liver. All NK cell subsets demonstrated peak activation at day 4 post-infection, and a reduction in cytokine secretion or degranulation at day 7 post-infection (Figure 5.8). A three-way ANOVA with Tukey's multiple comparisons demonstrated a very significant difference in cytokine production between NK cell type (****$p<0.0001$).

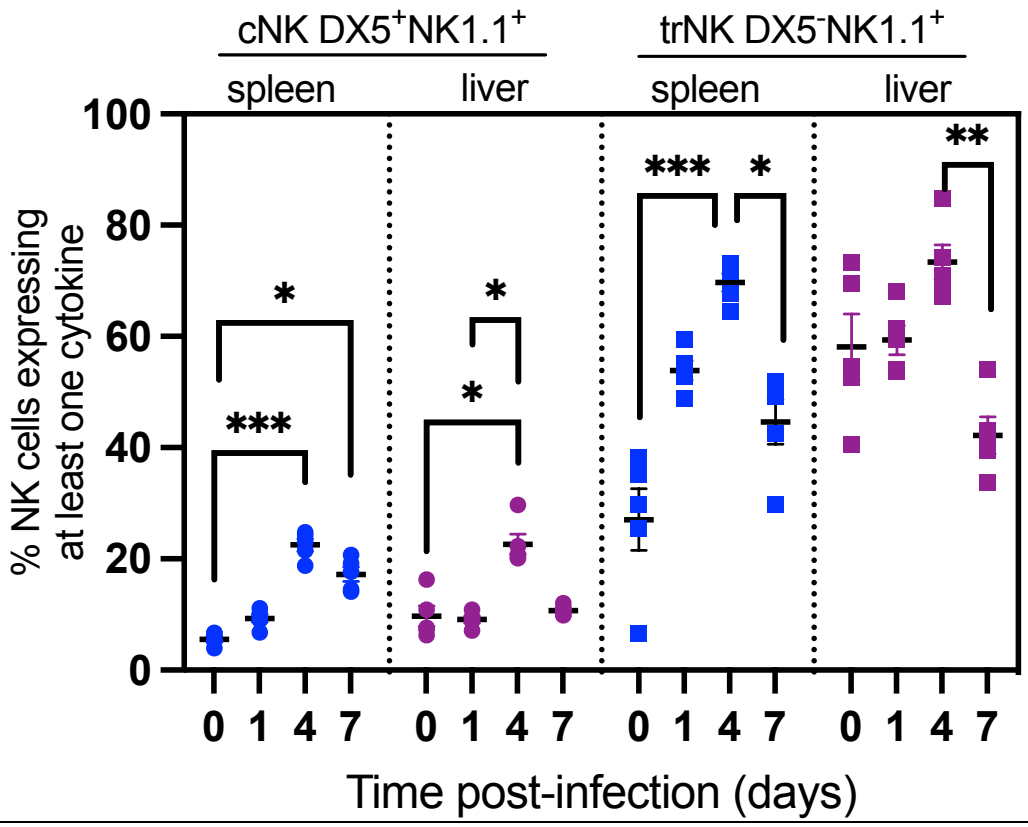


Figure 5.8. The frequency of NK cells expressing at least one cytokine post-MCMV infection.

C57BL/6J mice (n=5 per group) were infected with $1x10^6$ i.u. MCMV for 7, 4, or 1 days, or left uninfected. Spleens and livers were harvested post take-down and stained for $DX5^+NK1.1^+$ cNK cells and CD107a, TNF-α, GzB, and IFN-γ. This graph shows the percentage of cNK and trNK in the spleen and liver expressing at least one inflammatory mediator at each time point post infection.

Statistics conducted using three-way ANOVA test with Tukey's multiple comparisons (overall comparison) and Kruskal-Wallis test with Dunn's multiple comparisons (individual groups). *p<0.05, **p<0.01, ***p<0.005. Error bars shown as mean± SEM.

5.2.3. T cell phenotype and activation during acute and chronic MCMV infection

5.2.3.1. The frequencies of regulatory T cell populations during acute and chronic MCMV infection

Next, I established the phenotypes of T cell populations following infection with MCMV. The dynamics of murine canonical and inflationary T cells during acute and chronic MCMV infection are fairly well characterised (299). However, less is known about changes to regulatory T cell populations during the MCMV infection cycle. To explore this, I infected C57BL/6J mice with $1x10^6$ i.u. MCMV for 50 days (chronic infection), 7 days (acute infection), or left uninfected (⊗). T cell populations were measured by flow cytometry following the gating strategy in supplementary figure 4.

Overall, acute and chronic MCMV infection did not have any outstanding changes to T_{reg} frequency. Similar to other literature (265), there was a slight reduction in the frequency of T_{regs} between days 0 and 7, followed by a significant increase in frequency between days 7 and 50 post-infection in the iLN (p=0.0027), and a similar trend in the spleen (Figure 5.9A). Minor changes in the frequency of T_{FH} cells were observed, with a small but significant increase in frequency between uninfected and chronically infected mice in the iLN (p=0.0218) and a slight decrease in frequency at post-infection time points in the spleen (Figure 5.9B). Similarly, there was an increase in the frequency of T_{FR} cells in the iLN between acute and chronic infection (p=0.0321, Figure 5.9C). The liver is not a secondary lymphoid organ so the frequency of T_{FH} and T_{FR} were very low.

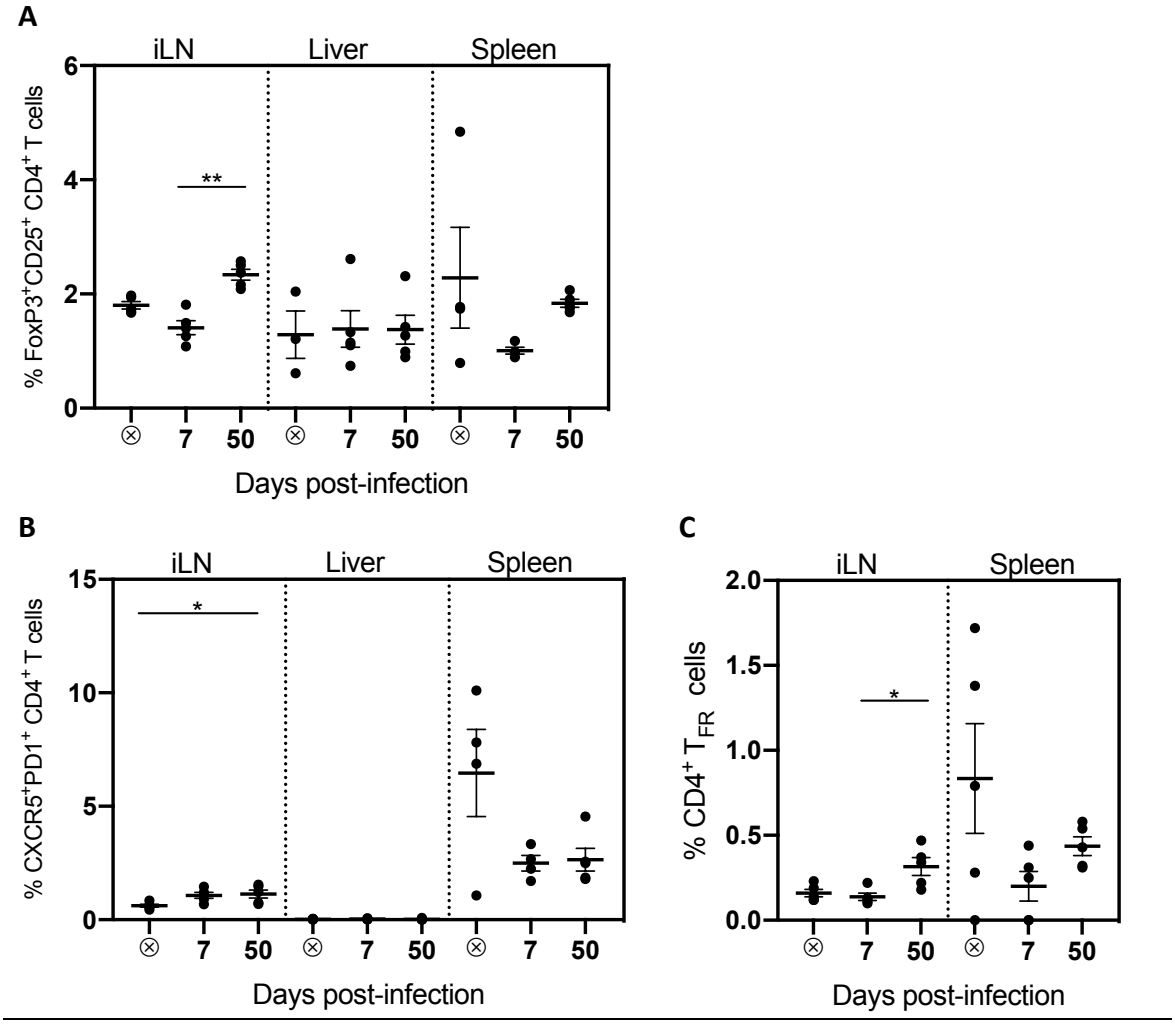


Figure 5.9. Frequencies of CD4$^+$ regulatory T cell populations in MCMV-infected mice

Mice (n=5 per group) were infected with 1x10^6 i.u. MCMV for a chronic (50 days) or acute (7 days) duration, or left uninfected (⊗). Inguinal lymph nodes (iLN), spleens and livers were harvested, and CD4 T cells were stained for markers of migration and T-regulatory populations. **A)** Frequency of T_{reg} (FoxP3$^+$CD25$^+$CD4$^+$) T cells, **B)** T_{FH} (CXCR5$^+$PD1$^+$ CD4$^+$) T cell frequencies, **C)** T_{FR} (CD4$^+$FoxP3$^+$ CD25$^+$CXCR5$^+$PD1$^+$) T cells as a proportion of total CD4$^+$ T cells.

Statistics conducted using Kruskal-Wallis test with Dunn's multiple comparisons. *p<0.05, **p<0.01. Error bars shown as mean± SEM.

5.2.3.2. T cell activation during acute and chronic MCMV infection

T cell marker	Function	Reference
PD1	Immunosuppressive receptor	(388)
KLRG1	Terminal maturation	(366)
CX3CR1	Expressed on peripheral blood/ lymph node effector memory T cells	(449, 450)
NKG2A	Inhibitory receptor on T cells (and NK cells)	(451)
CXCR6	Marker of migration expressed on liver and lung tissue-resident T cells (and NK cells). Expression is also increased during inflammation	(452, 453)

Table 5.1. Markers of activation, senescence and migration on T cells modulated by MCMV infection

Next, the dynamics of acute and chronic MCMV infection on T cell activation and migration were assessed using the markers in table 5.1. As previously, C57BL/6J mice were infected with $1x10^6$ i.u. MCMV for 50 days, 7 days, or left uninfected as a control group, and T cells in the iLN, liver and spleen were analysed for activation and migration. At day 7 of infection, $CD3^+$ T cells had an up-regulation of KLRG1 (p=0.0012), CXCR6 (liver p=0.04, spleen p=0.005), and NKG2A (liver and spleen p=0.0027), which returned to uninfected control levels by day 50 (Figure 5.10A). The subset of lymph node-resident cytotoxic effector $CD62L^+CX3CR1^+CD8^+$ T cells also expanded at day 7 post-infection before contracting by day 50, as observed previously in mice with LCMV and MCMV infection (454, 455) (p=0.0089. Figure 5.10B). Furthermore, in both the iLN and liver there was an increased frequency of $PD1^+CD4^+$ and $CD8^+$ T cells at day 7 post-infection compared to day 0 (iLN CD4 p=0.043, liver CD4 p=0.047, liver CD8 p=0.006. Figure 5.10C). This data demonstrates a transient, regulated activation of T cells during acute MCMV infection. Unlike HCMV

infection, there is no expansion of KLRG1$^+$ T cells with a terminally differentiated phenotype.

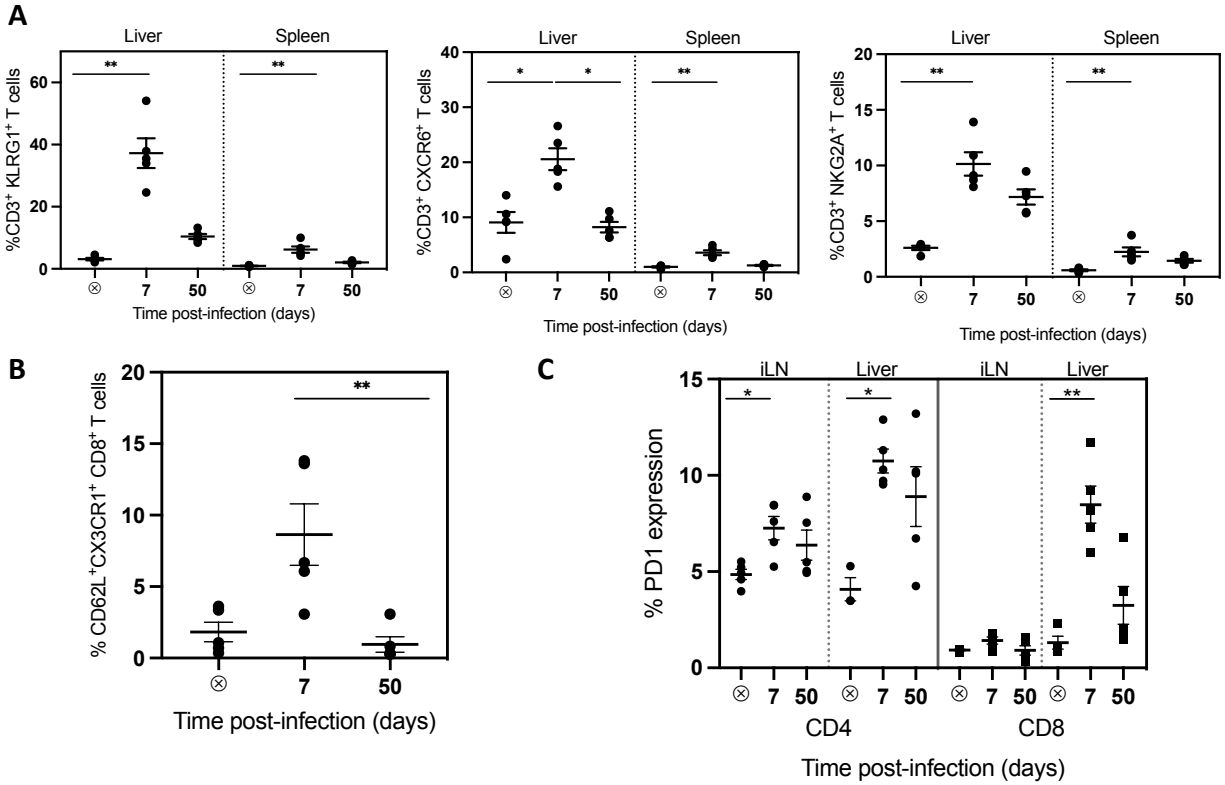


Figure 5.10. Frequencies of surface markers on the T cells of MCMV-infected mice

Mice (n=5 per group) were infected with 1x10^6 i.u. MCMV via the tail vein for a chronic (50 days) or acute (7 days) duration or left uninfected (⊗). Inguinal lymph nodes (iLN), spleens, and livers were harvested. **A)** Frequency of KLRG1$^+$, CXCR6$^+$, and NKG2A$^+$ CD3$^+$ T cells. **B)** Frequency of CX3CR1$^+$CD62L$^+$ CD8$^+$ effector T cells in the iLN, **C)** CD4$^+$ and CD8$^+$ T cell PD1 expression in the iLN and liver.

Statistics conducted using Kruskal-Wallis test with Dunn's multiple comparisons, *p<0.05, **p<0.01. Error bars shown as mean± SEM.

5.2.4. MAIT cell and T cell activation by MCMV infection

Next, the activation of MAIT cells during chronic MCMV infection was investigated to see whether they contributed towards dysregulated inflammation and immune senescence. MAIT cells were identified by flow cytometry in the lung and iLN as $CD3^-$ lymphocytes positive for TCRß and the MAIT cell tetramer 5-OP-RU, which is a canonical MAIT cell receptor ligand (456) (gating strategy in supplementary figure 6). I also analysed the activation of $CD4^+$ and $CD8^+$ T cells in the lungs and iLN as a comparison.

5.2.4.1. MAIT cell activation in chronic MCMV infection

There were overall no outstanding changes in the frequency of activated $CD4^+$ and $CD8^+$ T cells day 50 post-infection, aside from a slight increase in the frequency of lung $CD4^+$ T cells expressing CD25 (Supplementary Figure 11). The frequency of MAIT cells in the iLN decreased significantly (p=0.008) after 50 days of infection. Conversely, there was no significant difference in the frequency of lung MAIT cells at any time point, although there was a trend towards a lower frequency at day 7 (Figure 5.11A). There was no significant change in the expression of CD69 on MAIT cells in the iLN, however there was a significant decrease in the frequency of $CD69^+$ MAIT cells between day 7 and day 50 on the MAIT cells in the lungs (p=0.026, Figure 5.11B). Similarly, there was no change in CD25 expression on MAIT cells at either 50 days or 7 days post-infection (Figure 5.11C). These data suggest that MAIT cells are not activated during chronic MCMV infection.

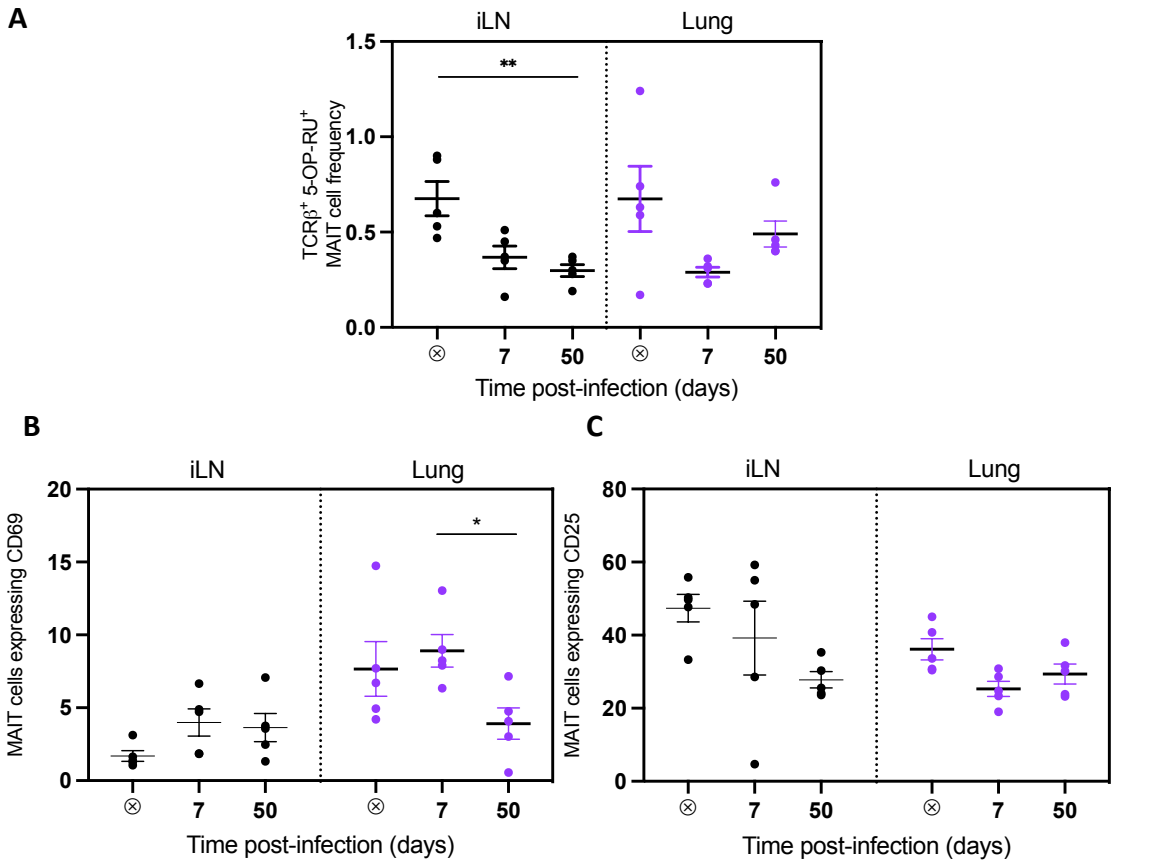


Figure 5.11. 50-day and 7-day MCMV infection and the frequency of CD25$^+$ and CD69$^+$ MAIT cells in the inguinal LN and lungs.

Mice (n=5 per group) were infected with 1x10^6 i.u. MCMV for a chronic (50 days) and acute (7 days) duration. Inguinal lymph nodes (iLN) and lungs were harvested, and MAIT cell activation was measured. These graphs show **A)** the frequency of MAIT cells in each organ, and the percentage of MAIT cells expressing **B)** CD69 in inguinal LN and lungs, and **C)** CD25 in the inguinal LN and lungs, at 0-, 7-, and 50-days post-infection.

Statistics conducted using Kruskal-Wallis test with Dunn's multiple comparisons, *p<0.05, **p<0.01. Error bars shown as mean± SEM.

5.2.4.2. T cell and MAIT cell activation during acute MCMV infection

I next compared the activation of MAIT cells and T cells during acute MCMV infection. Mice were infected with $1x10^6$ i.u. MCMV at 7 days, 4 days, and 1 day prior to take-down or left as an uninfected control (day 0). In the iLN and liver, the frequency of $CD25^+CD4^+$ T cells peaked at day 4 post-infection, in comparison to uninfected mice (iLN p=0.008, liver p=0.0073. Figure 5.12A). Similarly, the frequency of $CD69^+CD4^+$ T cells peaked at day 4 post-infection in the iLN and liver (iLN p=0.0017, liver p=0.083) and at day 7 in the lungs (p=0.0067. Figure 5.12B). $CD8^+$ T cells followed a similar activation profile; the frequency of $CD25^+CD8^+$ T cells peaked at day 4 across all organs (Figure 5.12C). Similarly, the highest proportion of $CD69^+$ $CD8^+$ T cells in the iLN and liver was at day 4, and at day 7 in the lungs (Figure 5.12D). These data demonstrate that MCMV can activate T cells systemically, with peak activation occurring day 4 post-infection.

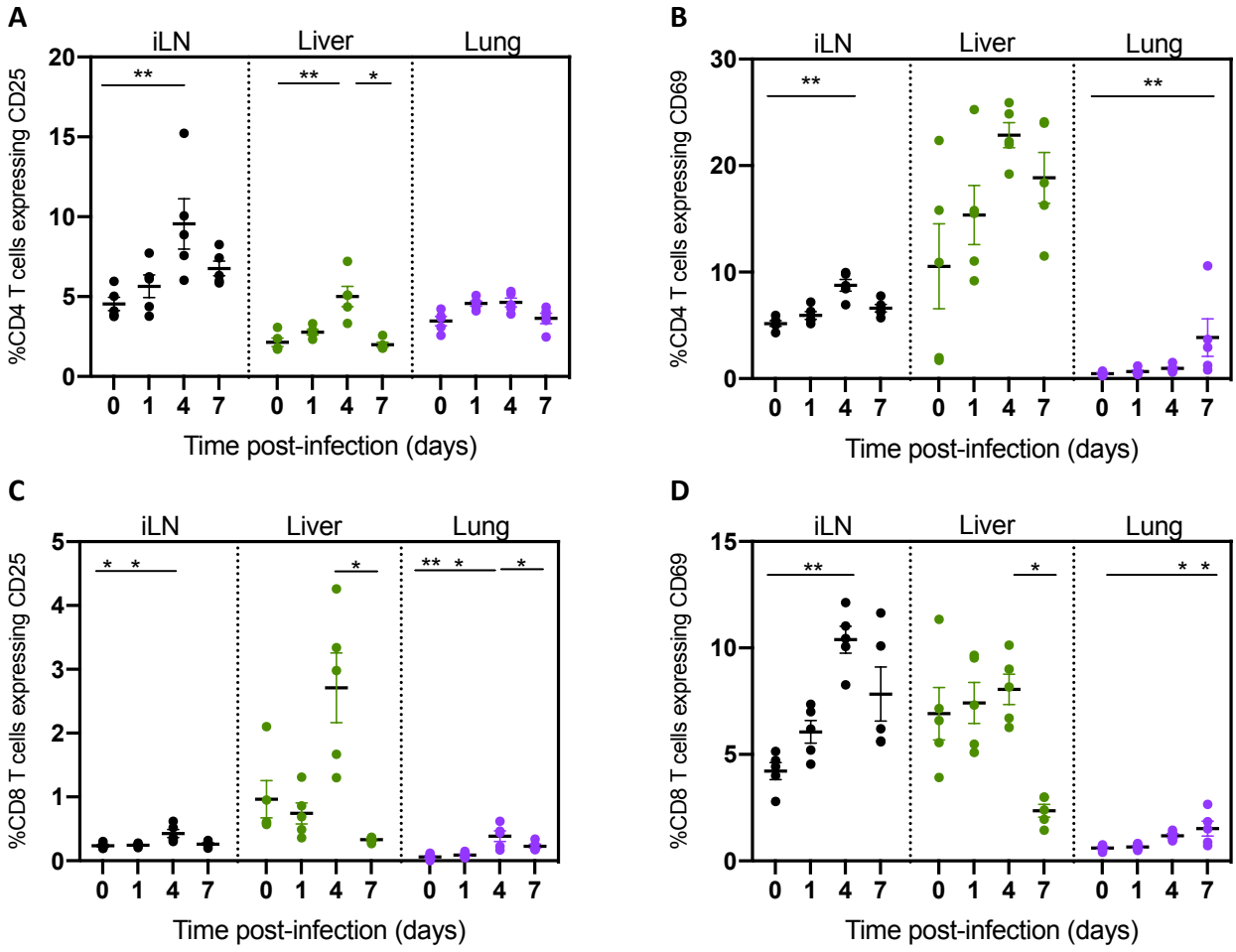


Figure 5.12. 1-day, 4-day, and 7-day MCMV infection transiently activates CD4⁺ and CD8⁺ T cells

C57BL/6J mice (n=5 per group) were infected with $1x10^6$ i.u. MCMV for either 7 days, 4 days, or 1 day, or left uninfected (day 0). Inguinal lymph nodes (iLN), livers, and lungs were harvested, and $CD4^+$ and $CD8^+$ T cell CD25 and CD69 expression was measured. These graphs show the percentage of **A)** $CD25^+$ $CD4^+$ T cells and **B)** $CD69^+$ $CD4^+$ T cells **C)** $CD8^+$ T cells expressing CD25, and **D)** $CD8^+$ T cells expressing CD69 in the inguinal LN, liver, and lungs, at 0-, 1-, 4-, and 7-days post-infection. Statistics conducted using Kruskal-Wallis test with Dunn's multiple comparisons. *p<0.05, **p<0.01. Error bars shown as mean± SEM.

The frequency of MAIT cells did not significantly change in the iLN or lung across the 7-day infection course. There was a decrease in the frequency of liver MAIT cells at day 4 post-infection, with a similar trend visible in the lungs (p=0.027, Figure 5.13A). Across the liver and lungs, there was no significant increase in CD25 expression on MAIT cells at any time point post-infection. Interestingly, in the liver there was a significant decrease in the frequency of $CD25^+$ MAIT cells by day 7 of infection (p<0.007. Figure 5.13B). On day 4 post-infection, there was a significant peak in the frequency of $CD69^+$ MAIT cells in the iLN (p=0.038), lung (p=0.017), and liver (p=0.045), which declined by day 7 (Figure 5.13C). These data suggest a transient activation of MAIT cells in different tissues during acute MCMV infection through expression of CD69, but not CD25, which peaks at day 4 and returns to background levels by day 7. The lack of CD25 (IL-2Rα) up-regulation in comparison to T cells may suggest that MCMV is preventing CD25 expression, thus reducing responsiveness to inflammatory IL-2 and reducing MAIT cell cytotoxicity during early infection.

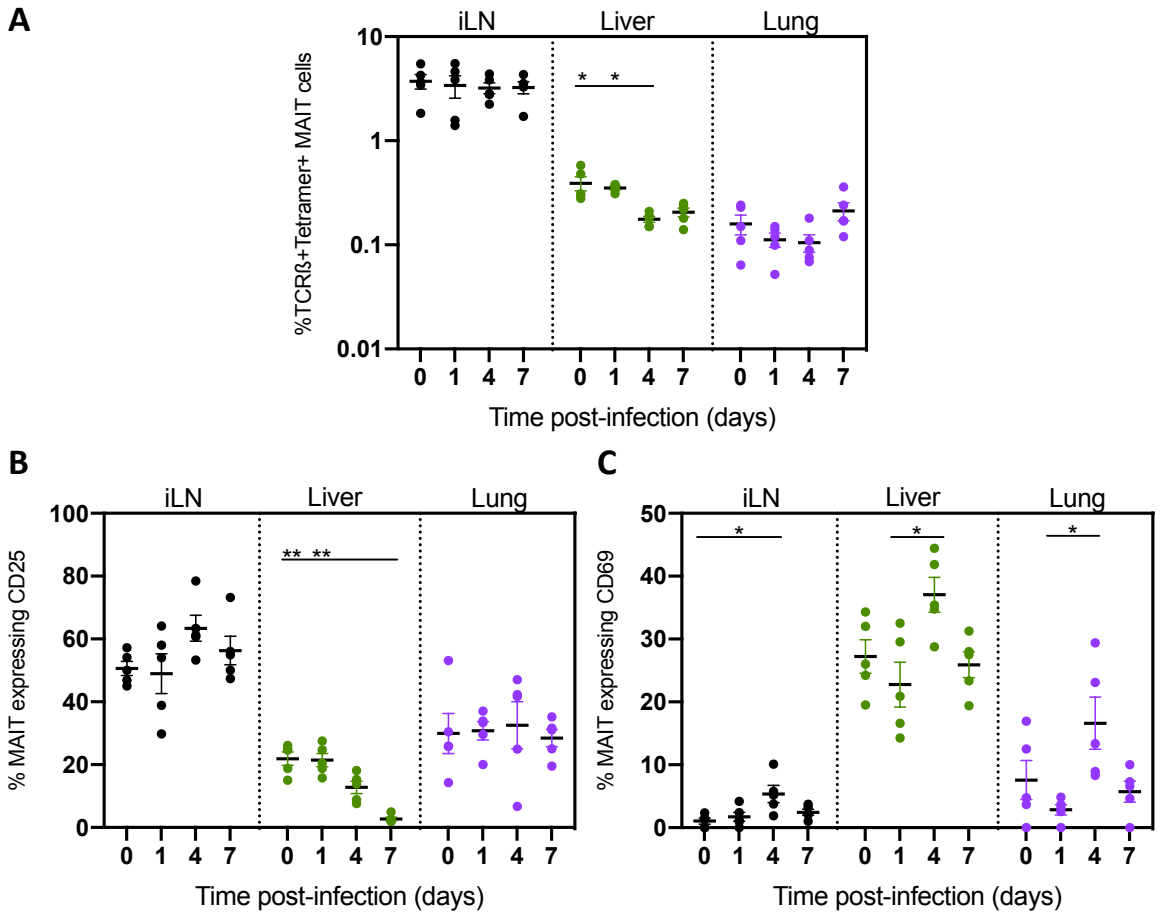


Figure 5.13. Activation of MAIT cells after 1-day, 4-day, and 7-day MCMV infection

C57BL/6J mice (n=5 per group) were infected with $1x10^6$ i.u. MCMV for either 7 days, 4 days, or 1 day, or left uninfected. Inguinal lymph nodes (iLN), livers, and lungs were harvested, and MAIT cell CD69 and CD25 expression was measured**. A)** The frequency of TCRß$^+$5-OP-RU$^+$ MAIT cells, **B)** The frequency of CD25$^+$ MAIT cells, **C)** The frequency of CD69$^+$ MAIT cells.

Statistics conducted using Kruskal-Wallis test with Dunn's multiple comparisons. *p<0.05, **p<0.01. Error bars shown as mean± SEM.

5.2.5. Phenotype of NK cells and response to vaccination in MR1$^{-/-}$ mice

This work was conducted during the COVID-19 pandemic

MR1 knockout (MR1$^{-/-}$) mice lack functional MAIT cells due to the role of MR1 restriction during MAIT cell development (457). The interactions between MAIT cells and NK cells are currently unknown in the context of MCMV infection and viral vector vaccination. We investigated whether MR1$^{-/-}$ mice have differences in the functionality or maturation of their NK cells following vaccination with 1x10^8 i.u. of the viral vector vaccine ChAdOx1 nCoV-19. There was no significant difference in the frequency of NK cells in the spleen. However, the total NK cell population and least-mature CD11b$^-$CD27$^+$ NK cells expressed more CD69 post-vaccination (*p*=0.03, Figure 5.14C).

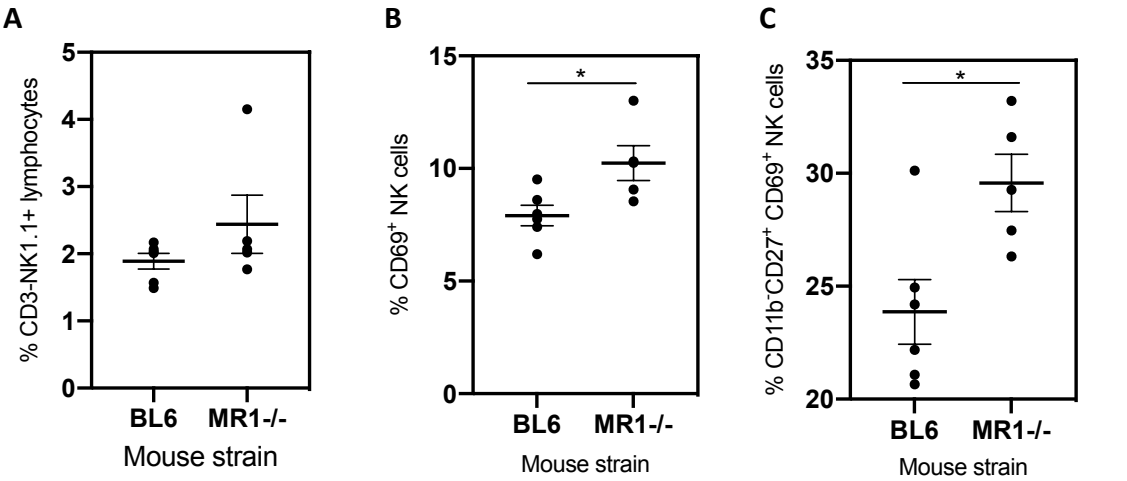


Figure 5.14. The phenotype of NK cells in C57BL/6J and MR1$^{-/-}$ mice

C57BL/6J mice (BL6, n=6) or MR1$^{-/-}$ mice (n=5) were vaccinated with 1x10^8 ChAdOx1 nCoV-19. The phenotype of NK cells was measured by flow cytometry, specifically **A)** total CD3$^-$NK1.1$^+$ NK cell proportion, **B)** frequency of NK cell CD69 expression, and **C)** CD69 expression within the CD11b$^-$CD27$^+$ NK cell subset. Statistics conducted using Mann-Whitney U test, *p<0.05. Error bars shown as mean± SEM.

5.2.5.1. The NK cell response in vaccinated MR1$^{-/-}$ mice compared to C57BL/6 mice

The functional response of NK cells to peptide stimulation was analysed between the vaccinated MR1$^{-/-}$ and C57BL/6 mice. There was no significant difference in the production of IFN-γ or CD107a in the whole NK cell population in response to peptide stimulation (Figure 5.15A and B). However, in the least mature CD11b^{-}CD27^{+} NK cell population, there was significantly higher frequency of CD107a^{+} cells (*p*=0.047, figure 5.15C).

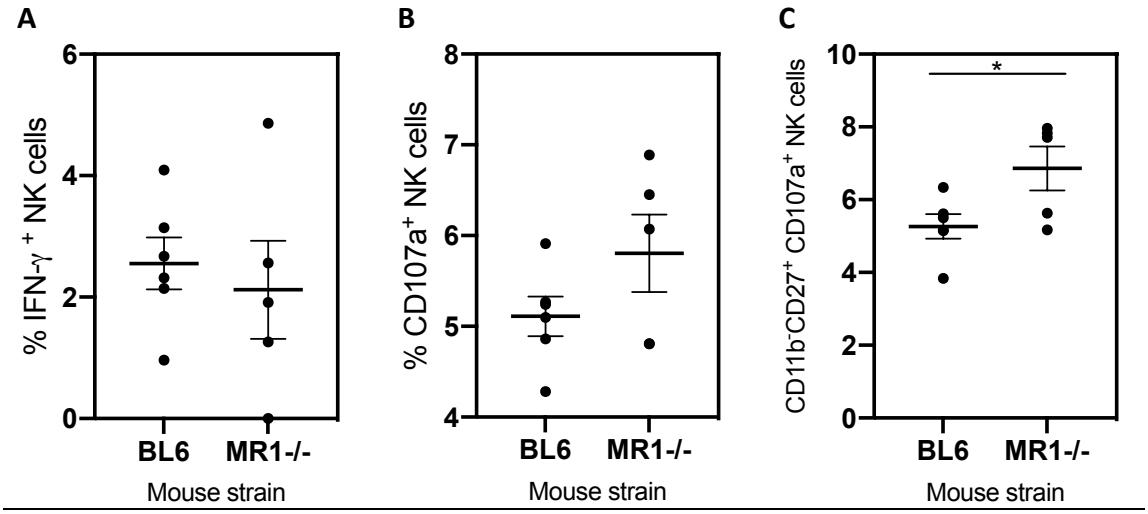


Figure 5.15. The functionality of NK cells in C57BL/6J and MR1$^{-/-}$ mice

C57BL/6J mice (BL6, n=6) or MR1$^{-/-}$ mice (n=5) were vaccinated with 1x10^{8} i.u. ChAdOx1 nCoV-19. The functional response of NK cells to SARS-CoV-2 spike peptide stimulation was measured by flow cytometry, specifically **A)** IFN-γ, **B)** CD107a, and **C)** CD107a within the CD11b^{-}CD27^{+} NK cell subset. Statistics conducted using Mann-Whitney U test, *p<0.05. Error bars presented as mean± SEM.

5.2.6. Development of a mouse model of MCMV infection and viral vector vaccination

CMV infection in humans has been shown previously to reduce vaccine efficacy through a negative correlation of CMV antibody titre and tIgG antibody titre and IFN-γ T cell ELISpot

response (339). As described above, MCMV and HCMV have comparable impact on their host immune system, although MCMV exerts a more transient profile than HCMV. To investigate whether infection with murine MCMV also reduces viral vector vaccine efficacy, C57BL/6J mice (n=5 per group) were infected with $1x10^6$ i.u. MCMV and left to establish a chronic infection. After at least 50 days, mice were vaccinated with $1x10^7$ to $1x10^8$ i.u. of a ChAdOx1-vectored vaccine, followed by $1x10^6$ to $1x10^7$ PFU of an MVA-vectored vaccine 7 days later. The antigen insert was changed each time to reduce the potential effect of the encoded protein on vaccine immunogenicity and cell phenotype. Spleens, iLN and livers were harvested at the experiment end point to assess vaccine immunogenicity. Two experiments ended one-week post-boost vaccination, however one experiment ended four months post-boost vaccination due to the University shut down but advantageously this allowed the study of long-term immune responses post-vaccination in the presence of CMV.

One-week post-boost, there was no change in IFN-γ production by T cells as measured by ELISpot in vaccinated mice, regardless of CMV serostatus (Figure 5.16A). At four months post-boost, there was a trend towards a reduction in splenic $CD8^+$ T cell IFN-γ production in CMV-seropositive mice (p=0.095) but no significant difference in $CD4^+$ T cell IFN-γ (Figure 5.16B). There was no significant difference in the expression of any other surface receptor measured, or of cytokine secretion by NK cells, between CMV serotype (data not shown).

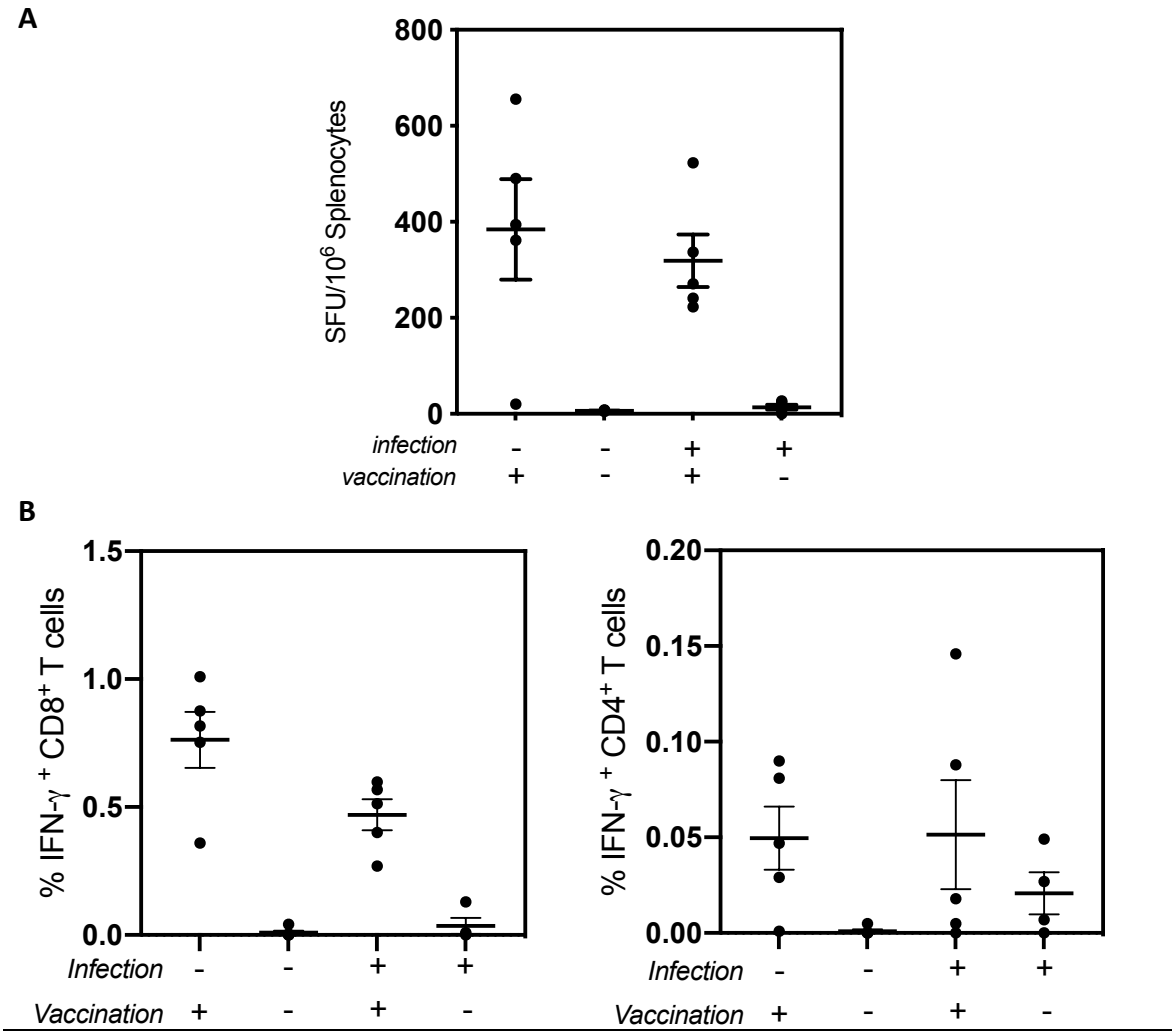


Figure 5.16. The T cell response in viral vector vaccinated mice with or without MCMV infection.

C57BL/6J mice (n=5 per group) were infected with $1x10^6$ i.u. MCMV (n=10), or left uninfected (n=10). After 50 days, mice (n=5 CMV+, n=5 CMV-) were vaccinated with a heterologous ChAOx1-MVA prime-boost regimen with a 7-day interval. **A)** T cell ELISpot response 1-week post-boost vaccine. **B)** Intracellular IFN-γ staining in $CD8^+$ (left) and $CD4^+$ (right) T cells at four months post-boost.

Statistics conducted using Kruskal-Wallis test with Dunn's multiple comparisons. Error bars shown as mean± SEM.

5.3. Discussion

In this chapter, I demonstrate that:

- Circulating and tissue-resident NK cells are differentially activated during acute MCMV infection
- MAIT cell activation is limited during acute and chronic MCMV infection
- Chronic MCMV infection and heterologous ChAdOx1-MVA vaccination does not reduce T cell IFN-γ secretion in a mouse model

5.3.1. NK cell responses to MCMV infection

The phenotype of canonical NK cells was established during acute and chronic MCMV infection to compare to the known literature. With similarity to murine T cells, NK cells expressed an increase of terminal differentiation markers (KLRG1) across all maturation phases, although this was not sustained in chronic infection as previously demonstrated (458). There was also a decrease in the most mature $CD11b^{+}CD27^{-}$ NK cells at 7 days post-infection. This may be analogous to the loss of $CD11b^{+}$ NK cells demonstrated following MVA infection in chapter 3. Ly49H, which recognises the MCMV epitope m157, was also up-regulated during acute infection (289).

The response of trNK and cNK cell populations to acute and chronic MCMV infection was also and analysed. Circulating NK cells are fully mature ($DX5^{+}NK1.1^{+}$), found in both the spleen and liver of mice, and do not express a high frequency of the liver residency markers CXCR6 and CD49a (31). Tissue-resident NK cells are found predominantly in the liver and at a lower frequency in the periphery, and have a more immature $DX5^{-}NK1.1^{+}$ phenotype (365), or are otherwise defined by their lower expression of the transcription factor Eomes (46, 459). They do not migrate from the liver (46), nor do they mature into

canonical $DX5^{+}NK1.1^{+}$ NK cells in the liver, and undergo relatively slow proliferation (31). Within the trNK cell subset, NK 'memory' cells can be defined by heightened expression of the chemokine receptor CXCR6 and adhesion marker CD49a, both of which facilitate migration and retention in the liver (31, 365). The exact role these markers play in sustaining an NK cell memory response is currently unknown. Both humans and mice have populations of immature NK cells with heightened CD49a and CXCR6 expression in the liver (44, 45), meaning that these data may be applicable to HCMV as well as MCMV infection.

During these experiments, I demonstrated that cNK cells decrease in frequency in the spleen, but increase in frequency in the liver during acute infection. This corresponds with an increase in CD49a expression, potentially driving migration of cNK cells to the liver. Previous research on human NK cells demonstrates that inflammatory cytokines IL-2, IL-12 and IL-15 promote CD49a expression on NK cells, indicating that an inflammatory environment in the spleen during acute infection may facilitate this migration (365). In contrast, the total population of tissue-resident NK cells in the liver decreases over the acute infection time course, which correlates with a decrease in $CD49a^{+}$ trNK cells during this time. This was previously described by Dodard *et al*, who elucidated that during acute MCMV infection, the $CD49a^{+}$ trNK cell population, but not cNK cells, undergo apoptosis in response to increased lactic acid sensitivity (39). However, there is a distinct increase in the population of trNK cells in the liver expressing CXCR6 up to day 4 post-infection in these data. This population, therefore, may drive the liver-specific cytotoxic response against acute MCMV infection.

The immature liver-resident trNK cell population was investigated to see if it facilitated a response to MCMV infection, and how this compared to the cNK cell response during acute infection time points. Previous research demonstrates that cNK and trNK cells

are functionally different (31), and that liver-resident trNK cells (otherwise known as ILC1 in the literature) have substantial cytokine production and cytotoxic capacity following stimulation and after infection with Vaccinia virus, *Francisella tularensis* (28), *Toxoplasma gondii, Salmonella enterica* and *Clostridium difficile* (446, 460). Most importantly, Weizman *et al* showed that at 36 hours post-MCMV, PR8 influenza virus, and Sendai virus infection, $Tbet^{+}Eomes^{-}$ ILC1 (trNK) cells, but not cNK cells, were activated by IL-12 secreted by cDC, and were the main source of antiviral IFN-γ in the liver. By using Hobit-deficient mice, which lack tissue-resident ILC1s but not cNK cells, the authors established that this IFN-γ was essential for controlling MCMV viral load during early acute infection (42). The research conducted in this chapter shows in further depth how the trNK and cNK cell populations differ in their antiviral response during acute MCMV infection, and further support the trNK cell population as a driver of antiviral immunity in the liver.

Across both cNK and trNK subsets, activation when measured by SSC-A was highest at day 4 post-infection, indicating a substantial systemic NK cell response (41). As observed by others, trNK cells had higher baseline SSC-A, reflecting a more granular phenotype at the pre-infection timepoint, and also had higher expression of activation markers (41). Sojka *et al* suggest that trNK cells may be more reactive as they do not express the same profile of Ly49 molecules, and so do not undergo NK cell 'licensing' in a similar way to cNK cells (41). To further support this, there was a differential amount of cytokine secretion and degranulation by NK cells between organs and NK cell subsets. cNK in the spleen were more polyfunctional than cNK cells in the liver, with a peak of polyfunctionality at day 4 post-infection. Both splenic and liver cNK cells secreted high concentrations of granzyme B at day 4 post-infection, however only splenic cNK had a significant increase of IFN-γ and CD107a expression at day 7 post infection. No other increase in cytokine production by

cNK cells was observed in the liver. These data indicate that cNK cells are the predominant NK subset responding to acute MCMV infection in the spleen, and that this response is diminished in the liver.

Liver trNK cells were vastly more polyfunctional than splenic and liver cNK cells at all time points post-infection. Liver trNK cells produced high quantities of GzB at day 0, which decreased by day 7. The liver is a tolerogenic environment (10), so this excessive GzB production may be caused by tissue processing or aberrant activation, or as suggested by Sojka *et al* increased degranulation may also be a feature of unlicensed trNK cells (41). IFN-γ and CD107a expression peaked in the liver trNK at day 4 post-infection, which was 3 days sooner than the cNK IFN-γ and CD107a expression in the spleen. Overall, a higher frequency of trNK expressed at least one marker of activation compared to cNK, although both populations were most activated at day 4 post-infection. These data are similar to previously-published data on immature, liver-resident NK cell activation following *Francisella tularensis* infection, which also reported maximum secretion of IL-2 and TNF, but not IFN-γ, between 2- and 3-days post-infection (28). These data are also in accordance to Weizman *et al*, who demonstrate that trNK-derived IFN-γ is a predominant antiviral cytokine in the liver during acute MCMV infection (42).

Previous research demonstrates that $DX5^{-}CD49a^{+}$ liver-resident NK cells in humans produce Th1-skewed cytokines following activation, and sometimes respond to stimulation with a robust cytotoxic response (41, 48, 365). Other data shows that the $CXCR6^{+}$ $DX5^{-}$ $NK1.1^{+}$ population of NK cells are less cytotoxic and respond less robustly to activation, potentially facilitating an immunotolerant and regulatory role in the liver (45). Conversely, these data show that $CD49a^{+}$ trNK cells are less responsive to acute MCMV infection, and only produce significantly more CD107a at day 4 post-infection. On the other hand, $CXCR6^{+}$

trNK cells elicit a strong IFN-γ, TNF and CD107a response in the liver during acute infection. These data correlate with the increase frequency of CXCR6^{+} trNK cells in the liver during acute infection, and imply that these CXCR6^{+} trNK cells are the primary mediators of the inflammatory response against MCMV in the liver.

It is possible that the trNK response is driven in part by antigen-specific epitope recognition. Ly49H is the antigen-specific activating receptor for MCMV expressed on NK cells, and undergoes expansion during early MCMV infection (461). However, this receptor is not expressed at high frequency on immature Eomes^{-} NK cells (459). Further research could investigate whether Ly49H expression or other antigen-specific receptors also drive cytokine secretion and degranulation during acute infection in the liver. There is also a difference between the method of MCMV infection in these studies (intravenous injection in this study, intraperitoneal infection in Weizman *et al* (42)), and the natural acquired transmission of MCMV (salivary transmission). Therefore, the NK cell response in the liver might be heightened during i.v. infection due to the circulation of peripheral blood through the liver (31), and exposed to MCMV antigens in a way that is artificial in comparison to natural infection.

From these data, we can conclude that splenic cNK cells secrete more cytokines and degranulate more than cNK cells in the liver of mice following MCMV infection, even though they are at a lower frequency than in the liver. trNK cells in the liver, especially CXCR6^{+} trNK cells, drive a robust response against MCMV that peaks at day 4 and potentially controls viral replication and induces viral latency. This is in accordance with the literature outlining how trNK cells are the source of antiviral IFN-γ in the liver during acute MCMV infection, and further builds on the how the cytotoxic profiles of these individual NK cell lineages differ through location and phenotype.

5.3.2. T cell responses to MCMV infection

I first outlined the responses of regulatory T cell populations to MCMV infection, some of which is pre-established in the literature. I observed a small but significant increase in $T_{reg,}$ T_{FR} and T_{FH} frequency at 50 days post-MCMV infection compared to 7 days post-infection in the iLN. This is somewhat in agreement with previously published results showing an increase in T_{reg} frequency during acute infection, or by chronic infection stage in the spleen and liver (265, 462, 463).

Next, I aimed to corroborate known literature of T cell phenotype during MCMV infection with observed data during acute and chronic infections. The expression of PD1, KLRG1 and NKG2A all aligned with data previously published for acute and chronic MCMV infection (307, 389, 464, 465). These data differ from observed human infection data; unlike HCMV, MCMV does not induce expansion and maintenance of terminally differentiated $KLRG1^+$ or $PD1^+$ T cells, which remain in circulation following establishment of latent infection (320). Acute MCMV infection also established proliferation of $CD62L^+CX3CR1^+CD8^+$ T cells in the lymph nodes, which are cytotoxic and can migrate to sites of inflammation but do not persist with chronic infection (450), and which have been previously described during LCMV, MCMV and HCMV infection (454, 455, 465). There was also an increase of $CXCR6^+$ T cells during acute infection, which is expressed on activated $CD8^+$ and $CD4^+$ T cells and may function towards increased T cell survival and memory cell retention in the liver (466, 467), although is not essential for effector function (468). Infection with *Listeria monocytogenes* and *Plasmodium yoelii* also induces increased CXCR6 expression on T cells (467, 468), so it is not impossible to assume that MCMV infection induces CXCR6-mediated migration to the liver.

This chapter also outlines the development of a model of CMV infection and vaccination that would replicate the loss of immunogenicity observed in human vaccine trial participants in chapter 4. From these data, it was determined that chronic MCMV infection at a dose of $1x10^6$ i.u. does not alter the vaccine immune response at one-week post-MVA boost. However, there is a trend towards loss of $CD8^+$ T cell IFN-γ secretion at three months post-vaccination. This model is limited as it only places the pathogenic burden of MCMV on the mice, and it is important to take into account that humans contact a range of pathogens and may be infected multiple times with HCMV during a lifetime with different infectious titres and at different ages, which could drive a more immunosenescent phenotype (260, 469-471). Further research could investigate whether multiple MCMV infections, or a change in the infectious dose, affects the murine response to vaccination.

5.3.3. MAIT cell responses to MCMV infection

MAIT cell activation can be MR1-dependent via presentation of vitamin B metabolites, or MR1-independent via APC-derived IL-18 and IL-12 stimulated by viral infection (89, 96). MAIT cells activated by Influenza A and HCV are cytotoxic and up-regulate CD25, CD69 and CD38 (89, 97). Contrary to other viruses, *in vivo* MCMV infection in C57BL/6J mice only transiently and somewhat minimally activates MAIT cells during acute infection, as seen through maximum up-regulation of CD69, but not CD25 expression, at day 4 post-infection. This is unusual, because MAIT cells are activated by acutely infecting viruses (influenza, Dengue virus, Zika virus) (96, 97, 103), and chronic viruses (Hepatitis C Virus) (106). Under-activation of MAIT cells implies a viral mechanism evolved by MCMV, potentially through down-regulation of pDC and monocyte IL-18 and TNF (109). MCMV has many genes that prevent the immune activation of NK cells and T cells, so it is not unlikely that genes exist

to also down-regulate the response of other immune compartments. It is possible that a lack of CD25 (IL-2 receptor α chain) expression, especially in the liver which a main site of MCMV infection, could potentially be an MCMV-mediated response to prevent IL-2-mediated activation by MAIT cells (472). Research published during this PhD demonstrates that under-activation of MAIT cells may be a herpesvirus-specific feature, and HSV-1 and MCMV can down-regulate MR1 expression on antigen-presenting cells *in vitro*, mediated partially by the *Us3* gene (447). This paper also demonstrates that MAIT cells may be activated via MR1 presentation of viral antigens during infection. The authors hypothesised that, as HSV-1 causes skin lesions, MR1 down-regulation may prevent MAIT cell activation by co-infecting commensal microbiota (447). Therefore, this may be a redundant pathway in MCMV infection as skin lesions are not part of viral pathology. I also demonstrate that MAIT cells may exert a regulatory function on NK cells following vaccination. Research published as a pre-print during this PhD demonstrates that MAIT cells negatively regulate NK cell maturation and functionality under steady state conditions (473), and these data suggest a similar response during vaccination.

In this chapter, I have determined that MCMV differentially activates unconventional immune cells dependent on their location and function. This will further contribute towards our understanding of how MCMV manipulates the immune response and how this will affect vaccine immunogenicity responses.

Chapter 6

CMV infection and the immune response to viral vector vaccination in clinical trials

Chapter 6 : CMV infection and the immune response to viral vector vaccination in clinical trials

6.1. Introduction and aims

Cytomegalovirus (CMV) infection has a seroprevalence of ~30-100% within a given population and negatively correlates with socioeconomic status (264, 267, 474). Increasing age is also associated with increased likelihood of CMV seropositivity (320, 475). In the UK and USA, seroprevalence of CMV is approximately 50% (264, 476). However, in sub-Saharan Africa, seroprevalence reaches nearly 100% by early adulthood (338, 477).

CMV infection in young adults induces an immunosenescent phenotype that is comparable to the immune profile of older individuals. T cells from older individuals have reduced antigen receptor diversity, and are dominated by populations of clonally expanded $CD4^+$ and $CD8^+$ T cells (321). These expanded populations of antigen-specific T cells accumulate in older adults as a result of lifelong exposure to chronic antigens, such as CMV (317).

There are several similarities between the immune phenotypes of older adults and CMV-seropositive younger adults. These include anergic effector and memory T cells with low expression of CD27, CD28, and CD62L (311, 318), and an increased percentage of terminally differentiated T cells expressing CD45RA, CD57 and KLRG1 (317-319) (311, 312, 320-323). $CD45RA^+$ T_{EMRA} T cells are more anergic than $CD45RA^-$ effector memory T cells (324). This anergy is likely due to the prolonged immune exertion from controlling CMV reactivation (322, 469). Consistent with a lack of CD28-mediated activation, $CD8^+$ T cells from CMV seropositive individuals can be activated via alternative signalling from NKG2D, which recognises MIC molecules up-regulated by infected cells (478). These

immunosenescent T cells also have a decreased proliferative capacity, with shortened telomeres and a reduction in the TCR variability (312, 323).

The results of research untangling the impact of cytomegalovirus infection on vaccine immunogenicity are somewhat contradictory. The majority of the research published is conducted in European countries on healthy young and older adults in influenza vaccine trials, although this is not necessarily representative of the global impact of CMV burden on vaccine responses especially as people are seasonally exposed to influenza.

Some research demonstrates that CMV seropositivity has a negative impact on vaccine immunogenicity. Within the T cell compartment, several studies define an increase in terminally differentiated $CD28^{-}CD57^{+}$ lymphocytes and a CMV-associated reduction in inflammatory cytokines including GzB, IFN-γ and TNF after stimulation with vaccine peptides or virus in older adults and CMV-seropositive younger adults (226, 328, 335, 339). Chronic background production of inflammatory cytokines including TNF and IL6 (336, 479) and GzB (226) is also associated with age and CMV infection resulting in exhaustion and poorer response upon antigen exposure. Terminally differentiated $CD8^{+}$ T cells from CMV-seropositive individuals release GzB even at rest, which in turn prevents an increase of inducible granzyme B production upon cell stimulation *in vitro* with influenza virus (226). The immunosenescent effect of CMV infection on the immune system is so potent that differentiated memory T cells for CMV are present in Gambian infants that have been exposed to CMV as young as nine months (480, 481).

B cell responses with CMV seropositivity following vaccination are less clear; some studies correlate a loss of vaccine-specific humoral response with an expansion $CD45RA^{+}CCR7^{-}CD27^{-}CD28^{-}$ $CD4^{+}$ T cells and switched memory B cell frequency in CMV^{+}

participants aged >60 years (336, 337). Bowyer *et al* (2020) also demonstrates that CMV infection reduces both antigen-specific T cell and B cell immunogenicity to vaccination (339). In a study of Gambian infants, CMV infection correlated with a reduction in IgG response to routine tetanus vaccination. However, this study did not find a CMV-associated reduction in the T cell vaccine response, or in either the cellular or humoral response to measles and diphtheria vaccination (338). Contrastingly, there is evidence in the literature that CMV infection has no effect on immune responses following vaccination (328, 340-343), or that CMV infection enhances immune response to vaccination (344-347). One study showed that CMV infection in healthy young adults, but not older adults, after seasonal influenza vaccine correlated with increased vaccine-specific antibody titres and $CD8^+$ T cell sensitivity (347).

NK cells from individuals with CMV infection also have a distinct terminally differentiated profile. CMV infection is associated with an expanded $CD57^+NKG2C^+$ population, which is proposed to be antigen-specific for CMV and functional in controlling reactivation (57, 293). This immune phenotype is unique to CMV infection, and is not measured following any other chronic herpesvirus infections such as EBV (311), and HSV. In individuals vaccinated against *Bordetella pertussis,* ebolavirus and influenza, NK cells from CMV seropositive donors have a reduction of IFN-γ secretion and CD107a expression (38, 362, 363). This loss of activation is correlated with the expansion of $CD57^+$ NK cells, which are less receptive to cytokine activation, including antigen-specific IL-2 secreted by $CD4^+$ T cells (22, 400), and have lower surface expression of the IL-2 receptor CD25 (35).

In this chapter, I investigate how CMV seropositivity impacts vaccine immune response in young adults vaccinated with single-dose, homologous and heterologous prime-boost viral vector regimens. I also compare the immune phenotype of vaccinated

young adults with regards to CMV serostatus. Finally, I assess how CMV infection affects vaccine immunogenicity in homologous and heterologous viral vector vaccination regimens in older adults.

Aims of Chapter 6

1. Analyse the phenotype and immune response (T cells, B cells and NK cells) to single dose ChAdOx1 vaccination following stratification for CMV serostatus.
2. Analyse a cohort of CMV+/CMV- participants from single dose and heterologous prime-boost vaccination regimens to determine effect of prime-boost vaccination on immunogenicity.
3. Compare the immunogenicity responses of older adults from with heterologous and homologous prime-boost vaccination when stratified for CMV serostatus.

6.2. Results

6.2.1. CMV serotyping of younger adults aged 18-55 vaccinated with a single dose, homologous, or heterologous prime-boost ChAdOx1 and MVA regimen

Three groups of younger adults (aged 18-55) in the COV001 and COV002 clinical trial conducted in the UK were selected to be CMV serotyped by ELISA. These groups received either a single dose (COV001 group 1) or homologous prime-boost (COV001 group 3 and COV002 group 5d) of ChAdOx1 nCoV-19 (table 6.1) (169). CMV serostatus was determined by commercially-available anti-CMV IgG ELISA and percentage seroprevalence in each group was calculated. Only participants who were vaccinated with ChAdOx1 nCoV-19, and not the placebo (MenACWY), were included in further analysis. In COV001 group 1, 13/44 donors were CMV seropositive, resulting in a seroprevalence of 29.55%. COV001 Group 3 had 4/10 donors CMV seropositive, and a 40% seroprevalence. COV002 Group 5d had a CMV seroprevalence of 20/49, corresponding to 40.82% of participants. These data are within the expected range for young adults living in the UK (264, 477).

Vaccination regimens for the FLU005 trial which was assessing immunogenicity of ChAdOx1 and MVA vectored vaccines against influenza A (IAV) can be found in table 6.1. CMV serotyping was conducted prior to commencement of this PhD by Dr Georgina Bowyer using the same anti-CMV IgG ELISA kit. 12/46 donors (26.1%) were CMV seropositive, with an even distribution between trial groups (Supplementary Figure 12).

Trial	Group	N	Prime	Prime dose (i.u.)	Boost	Boost dose (i.u.)	Boost date	CMV+ (n)
COV001	1	44	ChAdOx1 nCoV-19	$5x10^{10}$	N/A	N/A	N/A	13
COV001	3	10	ChAdOx1 nCoV-19	$5x10^{10}$	ChAdOx1 nCoV-19	$5x10^{10}$	+28 days	3
COV002	5d	49	ChAdOx1 nCoV-19	$5x10^{10}$	ChAdOx1 nCoV-19	$5x10^{10}$	+28 days	20
FLU005	1, 2	23	ChAdOx1 NP+M1	$2.5x10^{10}$	MVA NP+M1	$1.5x10^{8}$	+ 8 weeks/ + 52 weeks	12
FLU005	3, 4	23	MVA NP+M1	$1.5x10^{8}$	ChAdOx1 NP+M1	$2.5x10^{10}$	+ 8 weeks/ + 52 weeks	

Table 6.1. Details of COV001 groups 1 and 3, COV002 group 5d, and FLU005 groups 1-4 vaccination regimens

6.2.2. Background immunity and CMV serostatus in 18–55-year-old trial participants

Within the FLU005 trial, ELISpot data was collected from fresh PBMC samples by trial scientists, and ELISA data was collected from a selection of participants by Bryony Shaw. ELISpot and ELISA data from the COV001 and COV002 trials were collected and quality-controlled by the Oxford COVID-19 vaccine trial team. I analysed these data retrospectively by myself with regards to CMV serostatus of the participants.

Analysis was conducted on day 0 total IgG (tIgG) ELISA and IFN-γ ELISpot data from combined COV001/002 and FLU005 adults to determine if CMV infection was correlated with increased pre-existing antigen-specific T cell and antibody response to SARS-CoV-2 or influenza A. There was no significant difference in the day 0 titres of IgG, or in the day 0 T cell IFN-γ production in the COV001/002 and FLU005 trial participants regardless of CMV serostatus (Figure 6.1). Participants in the FLU005 trial, however, had substantially higher pre-existing antibody titres and ELISpot IFN-γ response to IAV NP + M1 peptides than participants in the COV001/002 trials did to S1 and S2 peptides. It is not unexpected that the level of pre-existing immunogenicity to common circulating influenza proteins is higher than to an emerging coronavirus, so the significant difference between trial groups is not relevant to this analysis.

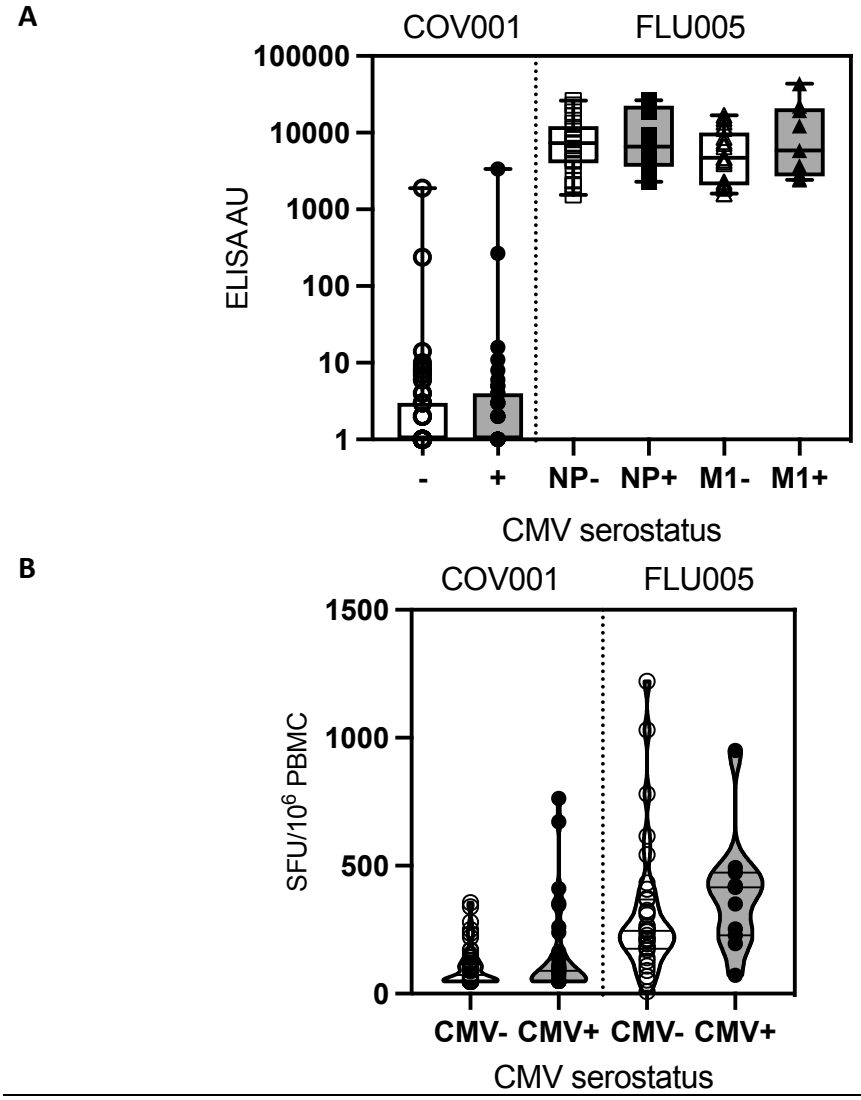


Figure 6.1. Pre-existing immunogenicity to SARS-CoV-2 and Influenza A antigens in younger adults.

Day 0 ELISpot and ELISA responses from combined COV001/002 and FLU005 groups 1-4 participants, stratified by CMV serostatus. **A)** total IgG ELISA (arbitrary units) against SARS-CoV-2 Spike antigen and Influenza A NP and M1 at day 0, **B)** IFN-γ T cell ELISpot response against SARS-CoV-2 spike peptide pools and Influenza A NP and M1 peptide pools at day 0, measured as spot forming units (SFU)/10^6 PBMCs.

Statistical analysis conducted using Kruskal-Wallis test with Dunn's multiple comparisons.

6.2.3. Stratification of the cellular immune response by CMV serostatus in single-dose, homologous, and heterologous ChAdOx1 and MVA vaccination regimens.

T cell IFN-γ ELISpot data for each COV001 and COV002 group up to day 182 post-vaccination was stratified based on CMV serostatus. To increase the number of participants analysed within the FLU005 cohort, Groups 1 and 2 (ChAdOx1 NP+M1 prime, MVA NP+M1 boost) and groups 3 and 4 (MVA NP+M1 prime, ChAdOx1 MP+M1 boost) were pooled into 'post-prime' and 'post-boost' groups, respectively. Previous analysis indicates that there is no difference in the immune response of groups 1 and 2, and groups 3 and 4, respectively (179).

Across either single-dose or homologous boost ChAdOx1 nCoV-19, there was no significant difference in the total T cell IFN-γ production measured by ELISpot spot-forming units (SFU, Figure 6.2A-C). Contrastingly, there was a more significant effect of CMV infection on T cell IFN-γ production after heterologous boosting in the FLU005 trial. In the pooled groups 1 and 2 responses (ChAdOx1 prime, MVA boost), there was a visible decrease in the IFN-γ SFU in the CMV seropositive participants at one-week post-MVA boost and an overall significant difference when comparing time point and CMV (fixed methods analysis, p=0.0038, Figure 6.2D). Furthermore, when analysing the fold change of IFN-γ production to day 0, there was a significant difference at week 1 post-boost (p=0.0008. Figure 6.2E). In the pooled groups 3 and 4 responses (MVA prime, ChAdOx1 boost), there was no significant difference between CMV serostatus and IFN-γ production at any time point post-prime or post-boost (Figure 6.2F). These data demonstrate that the immunogenicity of a single dose of ChAdOx1 is not affected by CMV serostatus, however overall T cell immunogenicity is reduced following heterologous MVA boost in CMV-seropositive donors.

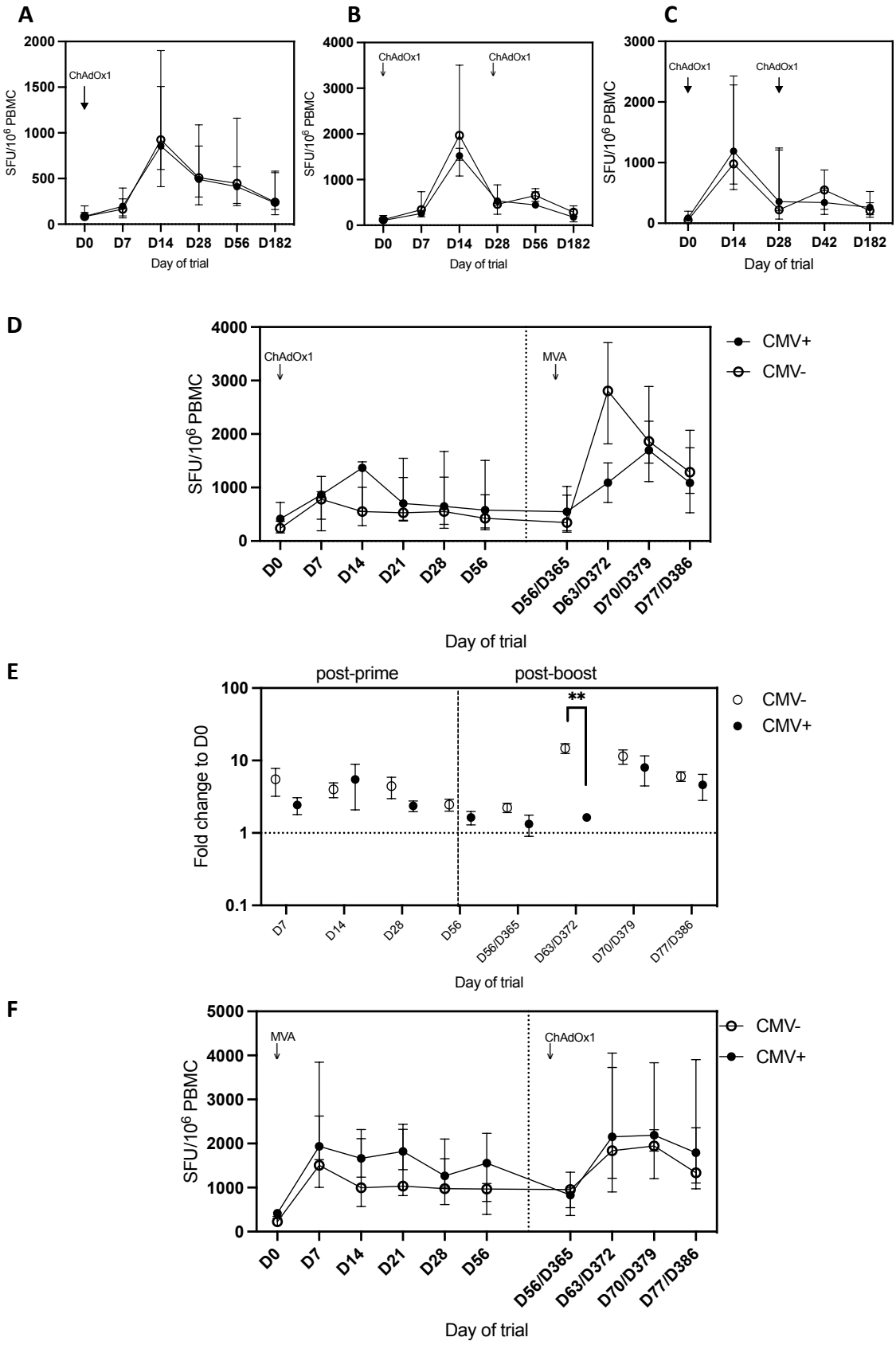


Figure 6.2. T cell IFN-γ ELISpot response following single dose, homologous and heterologous boosting stratified by CMV serostatus.

T cell IFN-γ ELISpot data from COV001 groups 1 and 3, COV002 group 5d and the FLU005 clinical trial, stratified by CMV serostatus. Data shown as T cell IFN-γ spot forming units (SFU) per million cells. **A)** COV001 group 1, **B)** COV001 group 3, **C)** COV002 group 5d. **D)** The pooled groups 1 and 2 total T cell IFN-γ ELISpot response following ChAdOx1 NP+M1 prime and MVA NP+M1 boost and **E)** fold-change to day 0 of post-prime ChAdOx1 NP+M1 and post-boost MVA NP+M1 **F)** The pooled group 3 and 4 T cell IFN-γ ELISpot response following MVA NP+M1 prime and ChAdOx1 NP+M1 boost.

Statistics conducted using mixed-effect analysis with Sidak multiple comparisons. $^{**}p<0.01$. Error bars presented as mean± SEM.

6.2.4. T cell differentiation and memory populations with CMV serostatus

26 donors from the COV001 group 1 trial, and participants from groups 1-4 of the FLU005 trial, were analysed using spectral cytometry with the panel outlined in table 2.16. It has been previously demonstrated that T cells from CMV-seropositive individuals have an enriched population of terminally differentiated $CD57^+KLRG1^+$ $CD8^+$ T cells (339). In the COV001 and FLU005 cohorts, both $CD4^+$ and $CD8^+$ T cells had a significant increase in $CD57^+KLRG1^+$ populations (COV001 $p<0.0001$ and $p=0.0003$, FLU005 $p<0.0001$ and $p=0.01$ respectively. Figure 6.3A). Furthermore, in both cohorts the proportion of $CD57^+PD1^+$ $CD4^+$ T cells were significantly increased in CMV seropositive donors (COV001 and FLU005 $p<0.0001$). Comparatively, there was a significant reduction in the percentage of $CD57^+PD1^+$ $CD8^+$ T cells in the COV001 cohort, but not in the FLU005 cohort ($p=0.019$. Figure 6.3B). This CMV-specific $CD4^+$ T cell phenotype has not previously been identified, but contributes towards the terminally differentiated and quiescent profile that CMV induced on the immune system.

$CD8^+$ T cell memory phenotype was also altered with CMV serostatus across trials. CMV seropositive COV001 participants had a significantly expanded $CD45RA^+CCR7^-$ T_{EMRA} population ($p=0.031$, Figure 6.3C). A similar yet non-significant trend was observed in the FLU005 cohort (Figure 6.3D). This was also observed in the EBL04 participants in chapter 4 (Supplementary Figure 10). T_{EMRA} expansion in CMV seropositive individuals is a known phenomenon and contributes towards the enhanced terminal phenotype induced by CMV (322, 475).

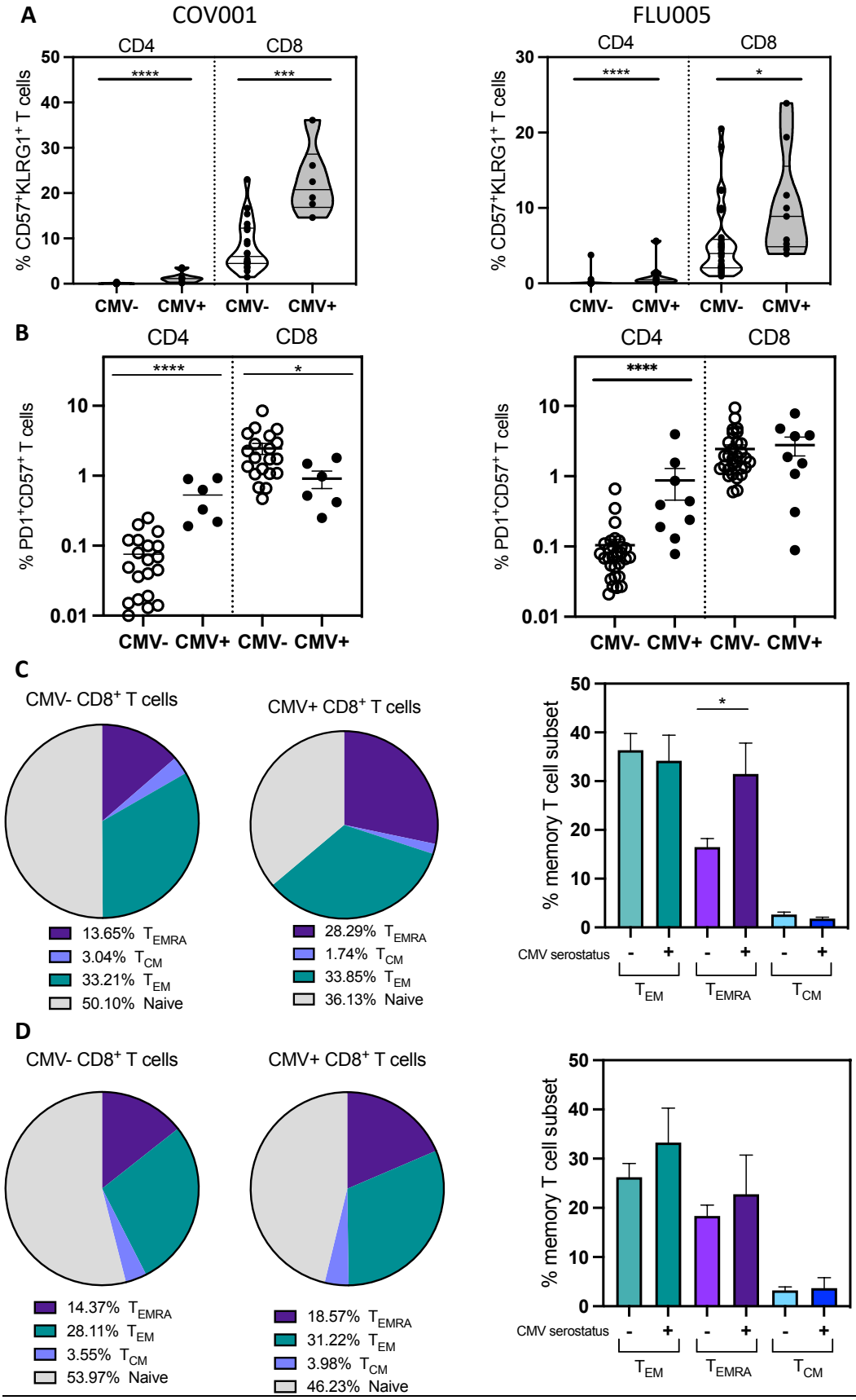


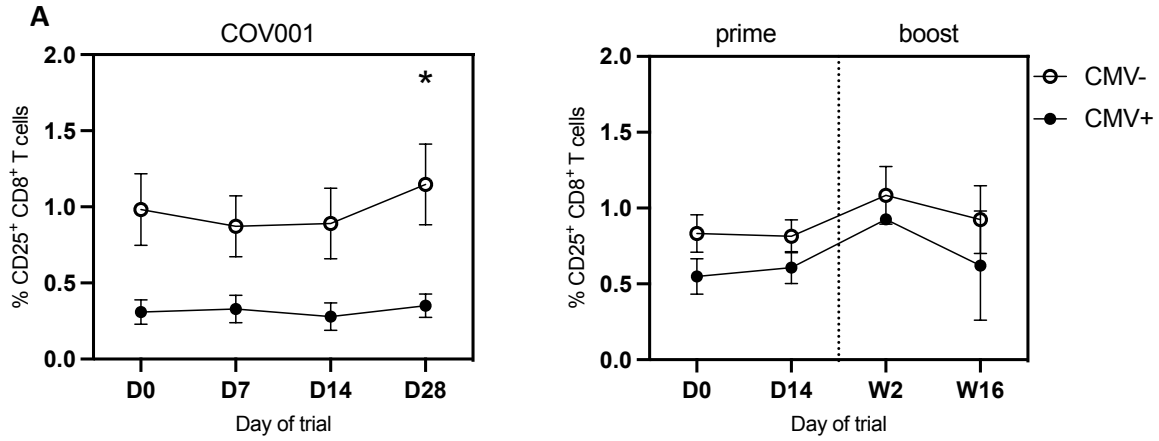
Figure 6.3. T cell terminal differentiation and memory populations with CMV infection

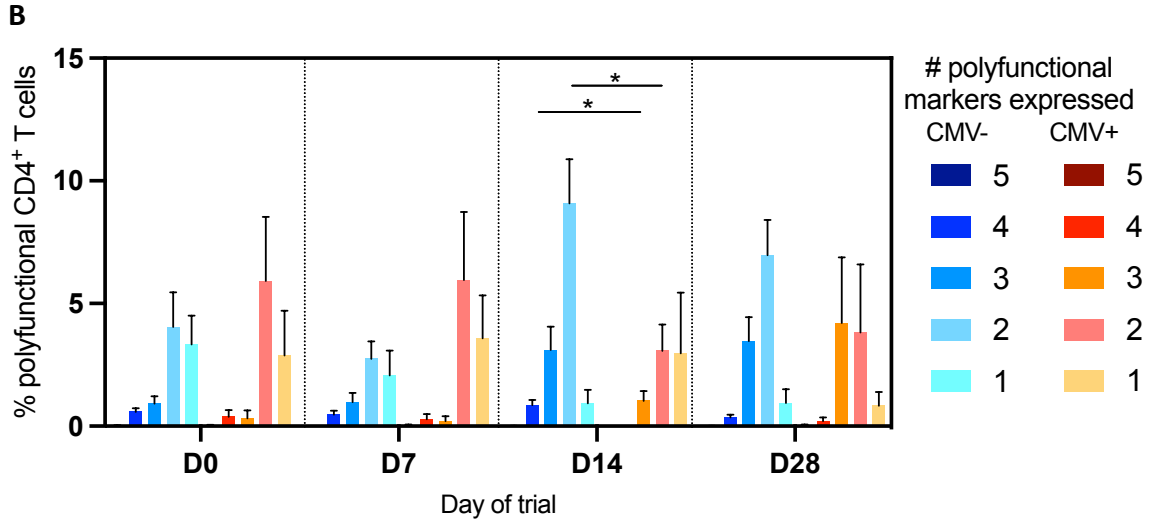
Unstimulated PBMCs from COV001 group 1 and FLU005 were analysed for expression of terminal differentiation and memory population markers. **A)** Frequency of double positive CD57 KLRG1 $CD4^+$ and $CD8^+$ T cells in the COV001 cohort and FLU005 cohort **B)** COV001 and FLU005 $PD1^+CD57^+$ $CD4^+$ and $CD8^+$ T cell frequency **C)** COV001 CD45RA/CCR7 $CD8^+$ T cell memory profile. **D)** COV001 CD45RA/CCR7 $CD8^+$ T cell memory profile.

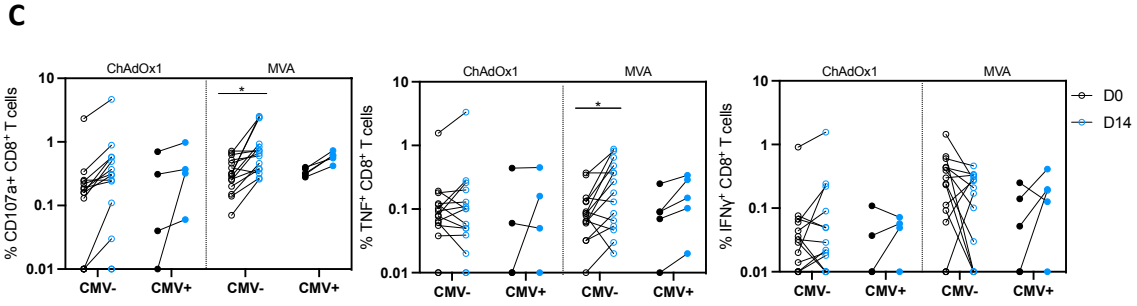
Statistics conducted using Mann-Whitney U test and mixed-effect analysis with Holm-Sidak multiple comparisons. *p<0.05, **p<0.01, ***p<0.005, ****p<0.0001. Error bars shown as mean± SEM.

6.2.5. T cell activation and functionality with CMV serostatus

T cell activation and functionality was measured with respect to CMV infection. In the COV001 cohort, $CD8^+$ T cells had significantly lower expression of CD25 in CMV seropositive individuals (p=0.035 at day 28), with a similar trend in the FLU005 cohort (Figure 6.4A). Within the COV001 cohort, there was no significant difference in the cytokine expression of $CD4^+$ T cells following peptide stimulation (data not shown). T cell polyfunctionality was assessed through Boolean gating as above; $CD69^+$ cells were measured for the expression of five different activation markers (CD25, CD107a, IFN-γ, IL-2, and TNF-α). There was no significant difference between CMV serotype on $CD8^+$ T cell polyfunctionality (data not shown). However, there were significantly fewer $CD4^+$ T cells from CMV seropositive participants expressing 2 and 4 cytokines at day 14 post-vaccination (p=0.035 and p=0.026 respectively. Figure 6.4B). Within the FLU005 cohort, groups were pooled into ChAdOx1 and MVA prime cohorts as before and the response was measured at day 14 post-prime vaccination. There was a significant increase of CD107a expression in the MVA-vaccinated CMV seronegative group, and a trend in the ChAdOx1-vaccinated CMV seronegative group (p=0.01 and p=0.08, respectively). CMV seropositive donors in either group did not have a significant increase in CD107a expression post-prime vaccination. Similarly, there was a significant increase in TNF secretion post-MVA vaccination in the CMV seronegative, but not CMV seropositive, participants (p=0.011). There was no significant change in $CD8^+$ T cell IFN-γ secretion with CMV serostatus in either vaccine group (Figure 6.4C). Post-boost vaccination time points also demonstrated a similar trend towards loss of $CD8^+$ T cell response in CMV seropositive donors, although these were non-significant (Figure 6.4D).


A
COV001
prime
boost
CMV-
CMV+
% CD25+ CD8+ T cells
2.0
1.5
1.0
0.5
0.0
*
D0
D7
D14
D28
W2
W16
Day of trial


B
% polyfunctional CD4+ T cells
15
10
5
0
*
*
D0
D7
D14
D28
Day of trial
polyfunctional markers expressed
CMV-
CMV+
5
4
3
2
1


C
ChAdOx1
MVA
% CD107a+ CD8+ T cells
% TNF+ CD8+ T cells
% IFNγ+ CD8+ T cells
10
1
0.1
0.01
*
CMV-
CMV+
D0
D14

D

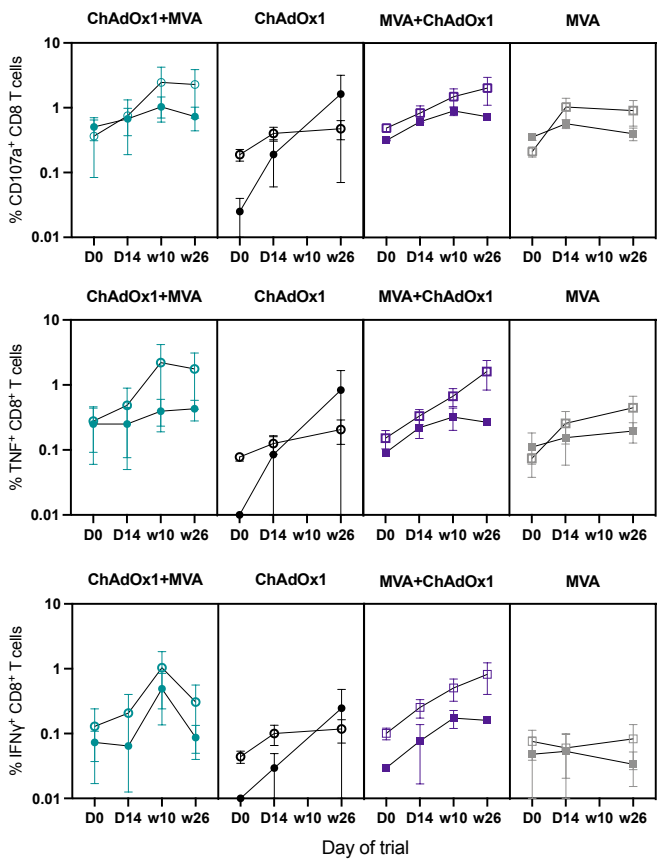


Figure 6.4. T cell activation and cytokine production with CMV serostatus

A) CD25 expression on unstimulated $CD8^+$ T cells in COV001 group 1 and FLU005 group 1 and 2 donors when stratified by CMV serostatus. **B)** COV001 polyfunctional analysis of $CD69^+CD4^+$ T cells post-vaccination conducted on expression of CD25, CD107a, IFN-γ, TNF and IL-2. **C)** Post-prime analysis of CD8+ T cells from pooled ChAdOx1 and MVA vaccinated participants from the FLU005 trial. (L-R) CD107a, TNF and IFN-γ expression stratified by CMV serostatus. **D)** Prime-boost response of Production of $CD8^+$ T cells across FLU005 trial participants. (Top-bottom) CD107a, TNF and IFN-γ expression. from Closed symbol= CMV^+, open symbol = CMV^-

Statistics conducted using mixed-effect analysis with Holm-Sidak multiple comparisons. *p<0.05. Error bars shown as mean± SEM.

6.2.6. Total IgG antibody responses to single-dose, homologous and heterologous prime-boost vaccination stratified by CMV serostatus

The total IgG antibody response from the clinical trial groups analysed in this chapter were stratified for tIgG with CMV serostatus. Antibody subclass titres of the COV001 group 1 cohort were measured by Jordan Barrett and Dr Sandra Belij-Rammerstorfer from serum samples, and analysed by myself for differences in CMV serostatus. Within single dose and homologous boost ChAdOx1 vaccine regimens, there was no significant difference between CMV infection and total IgG up to day 182 post-vaccination (Figure 6.5A-C). There was also no significant difference between CMV serostatus and the titres of IgG1, IgG3, IgA or IgM within the COV001 group 1 cohort (Figure 6.5D-G) The total IgG antibody titre against NP and M1 antigens had been determined previously for a subset of the FLU005 cohort by Bryony Shaw. As in section 6.2.3, to increase statistical power, the IgG response to prime vaccination was analysed from pooled groups 1 and 2 (ChAdOx1 NP+M1 prime, MVA NP+M1 boost) and groups 3 and 4 (MVA NP+M1 prime and ChAdOx1 NP+M1 boost) in 'post-prime' and 'post-boost' groups. There was no statistical significance between CMV serostatus and the total IgG response to either NP or M1 protein with either vaccine regimen. This is not unexpected because NP and M1 are internal antigens which generate a robust T cell response, which was the primary aim of this trial and are not designed to induce strong antibody responses (179, 229, 482) (Figure 6.5H-I). These data suggest that the IgG response to prime-boost viral vector vaccination is less affected than the T cell response by CMV infection in healthy UK adults in the COV001/002 trials.

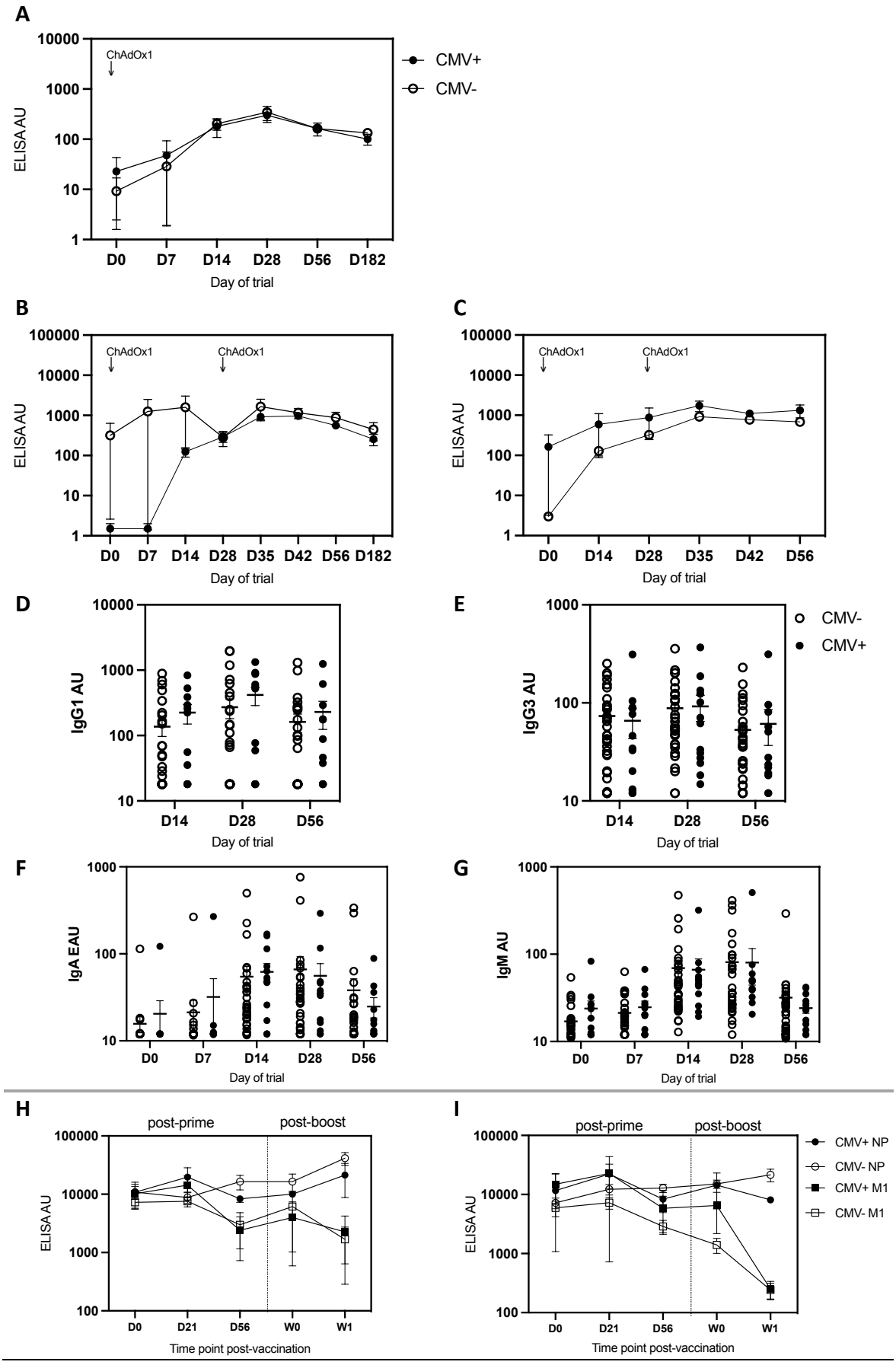

A
ChAdOx1
CMV+
CMV-
ELISA AU
Day of trial
B
C
D
IgG1 AU
E
IgG3 AU
F
IgA EAU
G
IgM AU
H
post-prime
post-boost
Time point post-vaccination
I
CMV+ NP
CMV- NP
CMV+ M1
CMV- M1

Figure 6.5. Antibody ELISA response to single dose, homologous and heterologous vaccination stratified by CMV serostatus.

ELISA data from the COV001/002 and FLU005 clinical trials, stratified by CMV serostatus. Data presented in ELISA arbitrary units (AU). **A)** COV001 group 1 **B)** COV001 group 3, **C)** COV002 group 5d. **D)** COV001 group 1 IgG1, **E)** COV001 group 1 IgG3, **F)** COV001 group 1 IgA, **G)** COV001 group 1 IgM. **H)** The pooled group 1 and 2 responses of post-prime ChAdOx1 NP+M1 and post-boost MVA NP+M1. **I)** The pooled group 3 and 4 responses of post-prime MVA NP+M1 and post-boost ChAdOx1 NP+M1.

Statistics conducted using mixed-effect analysis with Tukey multiple comparisons. Error bars shown as mean± SEM.

6.2.7. B cell memory with CMV serostatus

B cells from the COV001 cohort were analysed for differences in activation and immunoglobulin expression after vaccination with regards to CMV serostatus. There were minimal differences in the frequencies of B cell populations with CMV across the vaccine time course (Supplementary Figure 13).

6.2.8. NK cell phenotype and CMV serostatus

Previous research indicates that NK cells from CMV seropositive individuals have expanded populations of $CD57^+$, $NKG2C^+$, and $CD57^+NKG2C^+$ NK cells (293, 483). This was confirmed in chapter 4 in CMV seropositive donors from the EBL04 vaccine clinical trial. In the COV001 and FLU005 CMV seropositive donor cohort, there was a significant increase in the frequency of $CD57^+NKG2C^+$ double-positive NK cells (COV001 p=0.0003, FLU005 p=0.0021. Figure 6.6A). Within the $CD57^+$ NK cell compartment, which is expanded during CMV infection, CMV seropositive donors from COV001 had significantly less CD25 expression at days 14 and 28 post-vaccination (p=0.03 and p=0.011 respectively, Figure 6.6B). NK cells from CMV seropositive individuals in COV001 group 1 also had significantly lower activation when measured by CD69 expression at day 7 post-vaccination (p=0.0011, figure 6.6C and D). tSNE analysis was conducted on COV001 NK cells independent of CMV serostatus. NK cells across all time points had defined clusters of activated and proliferating cells (measured by Ki-67, CD107a, CD56 and CD25), which were distinct from terminally differentiated clusters ($CD57^+NKG2C^+$ NK cells), and cells with a $KLRG1^+CD69^+$ phenotype (Figure 6.6E).

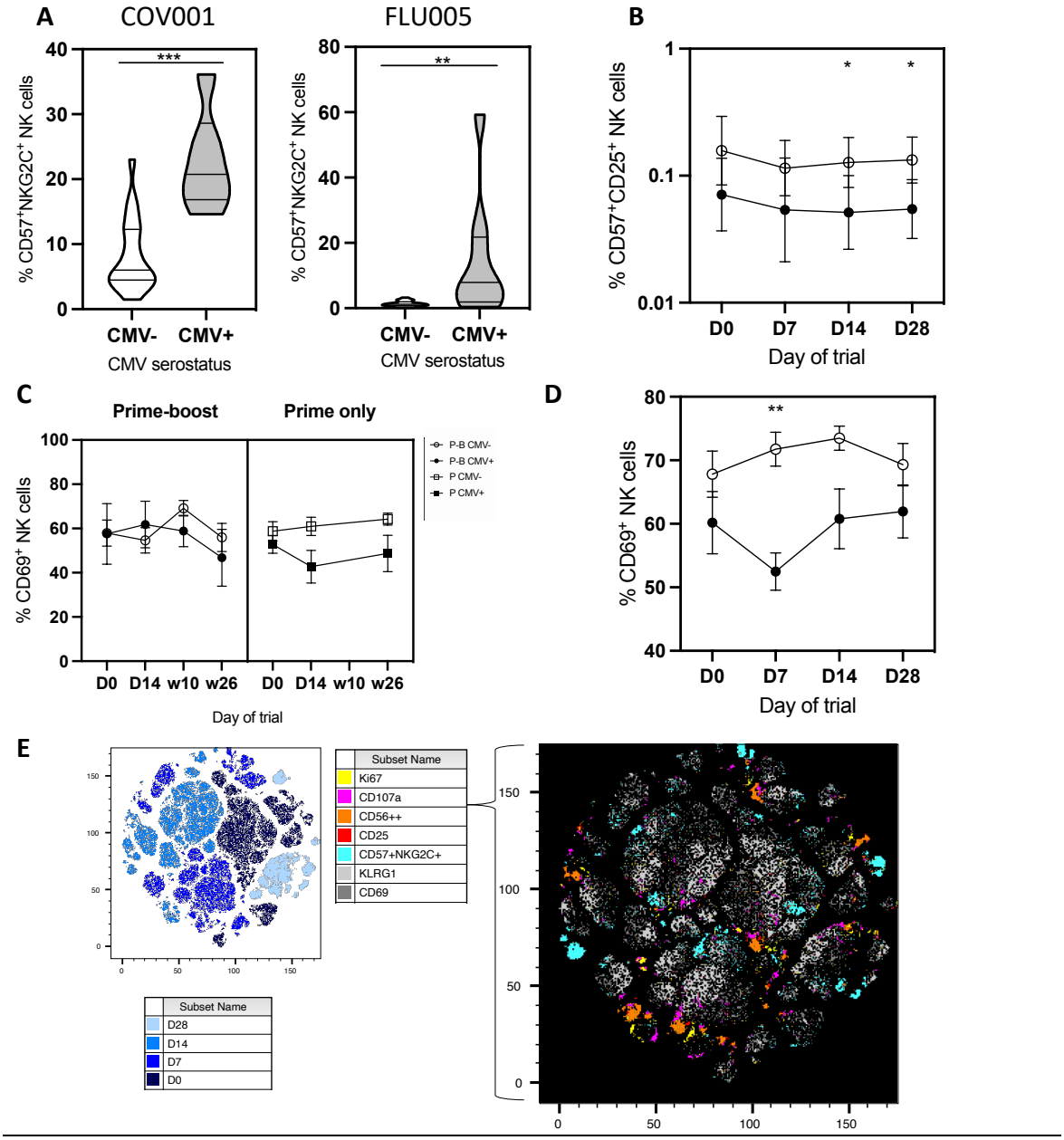


Figure 6.6. NK cell phenotype with CMV serostatus.

PBMCs from COV001 group 1 and FLU005 were left unstimulated and analysed for terminal differentiation and activation markers when stratified by CMV serostatus. **A)** NKG2C and CD57 expression on NK cells. **B)** CD57⁺ NK cell CD25 expression **C)** NK cell CD69 expression from the FLU005 cohort, **D)** NK cell CD69 expression from the COV001 group 1 cohort. **E)** tSNE analysis conducted on COV001 samples across four time points and 25,000 randomly-selected NK cells from each time point and sample. Statistics conducted using Mann-Whitney U test and mixed-effect analysis with Holm-Sidak multiple comparisons. **p*<0.05, ***p*<0.01. Error bars shown as mean± SEM or geometric mean with 95% CI

6.2.9. NK cell response to vaccination regimens and CMV serostatus

NK cell cytokine secretion and degranulation was measured in the COV001 and FLU005 clinical trial groups to assess whether CMV infection altered response to vaccine antigen.

Within the COV001 cohort, NK cells stimulated with S1 and S2 peptides had a significant increase in CD107a expression between days 7 and 28 post-vaccination in the CMV seronegative individuals (p=0.029), however this was not observed in the CMV seropositive individuals. There were no significant changes in TNF or IFN-γ secretion between CMV cohorts (Figure 6.7A). $CD69^+$ NK cells were measured for the expression of four different activation markers (CD107a, IFN-γ, IL-2, and TNF-α). Sequential 'OR' and 'Combination' gating, as described in chapter 4, elicited the proportion of cells that were expressing all activation marker combinations. At all points post-vaccination, there was no significant difference between polyfunctional cytokine production or proportion of NK cells expressing at least one cytokine with regards to CMV serostatus (Figure 6.7B).

Antigen-specific IL-2 secretion from $CD4^+$ T cells has been demonstrated to activate NK cells following vaccination and infection (400, 484). To assess whether the NK cell response to vaccination correlate with IL-2 secretion, correlations between antigen-specific $CD4^+$ T cell IL-2 secretion and expression of NK cell CD25 and Ki-67 were determined (Figure 6.7C). CMV seronegative donors had moderate correlation between IL-2 secretion and CD25 expression (goodness of fit R^2=0.52, p=0.0003) or Ki-67 expression (goodness of fit R^2=0.43, p=0.0024) at 14 days post-vaccination. Contrastingly, this correlation was not significant in the CMV seropositive cohort (CD25 R^2=0.035, p=0.72, Ki-67 R^2=0.16, p=0.39).

Due to the lack of boosting response on NK cells following heterologous vaccination in the ChAdOx1 and MVA vaccinated FLU005 cohort (Figure 4.6), participants were pooled

as above into group 1/2 and groups 3/4 for post-prime analysis. ChAdOx1-vaccinated, but not MVA-vaccinated, participants who were CMV seropositive had significantly higher expression of CD107a post-vaccination than CMV seronegative participants (p=0.0072, Figure 6.7D). There were no significant differences in TNF or IFN-γ expression across the rest of the ChAdOx1 prime vaccinated group, or within the MVA prime vaccinated group (Figure 6.7D).

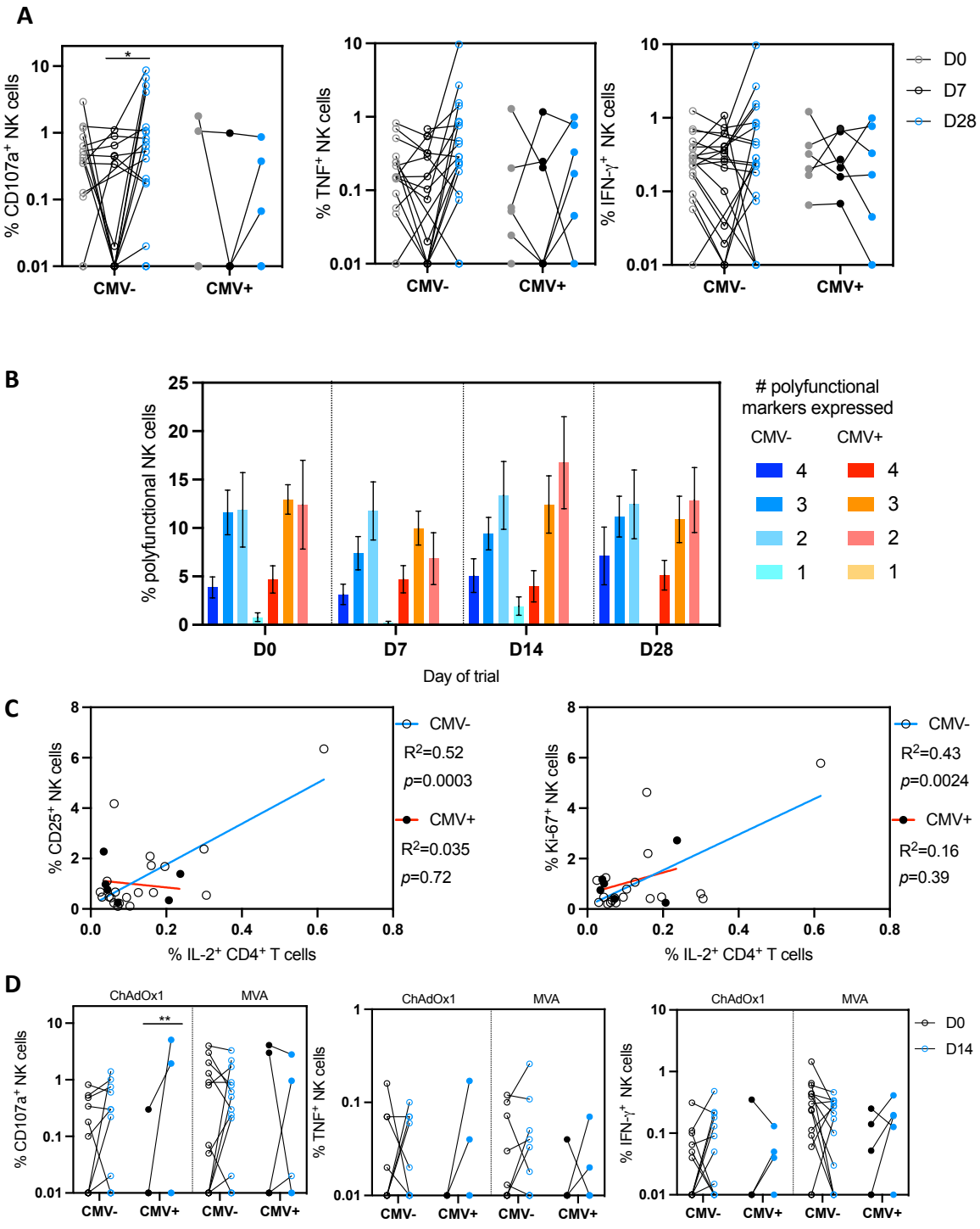

A
% CD107a+ NK cells
% TNF+ NK cells
% IFN-γ+ NK cells
CMV-
CMV+
D0
D7
D28
B
% polyfunctional NK cells
Day of trial
D0
D7
D14
D28
polyfunctional markers expressed
CMV-
CMV+
4
3
2
1
C
% CD25+ NK cells
% Ki-67+ NK cells
% IL-2+ CD4+ T cells
CMV-
R2=0.52
p=0.0003
CMV+
R2=0.035
p=0.72
R2=0.43
p=0.0024
R2=0.16
p=0.39
D
ChAdOx1
MVA
% CD107a+ NK cells
% TNF+ NK cells
% IFN-γ+ NK cells
D0
D14

Figure 6.7. Activation and cytotoxic response of NK cells to vaccine peptides when stratified by CMV serostatus.

PBMCs from COV001 group 1 and FLU005 were stimulated with respective pools of S1 and S2 peptide, NP+M1 peptide, or left unstimulated. NK cells as a population of lymphocytes were measured for production of cytokines and CD107a. Cytokine response was measured by subtracting the unstimulated cell values from stimulated cell values. COV001: **A)** Total NK cell expression of CD107a, TNF and IFN-γ at days 0, 7 and 28, stratified by CMV serostatus. **B)** Polyfunctional NK cell response across measured time points stratified by CMV serostatus. **C)** Correlation of $CD4^+$ IL-2 secretion and NK cell expression of CD25 and Ki-67 at day 14 post-vaccination, stratified by CMV serostatus. FLU005: **D)** Total NK cell production of CD107a, TNF and IFN-γ stratified by CMV serostatus in pooled post-prime groups at day 0 and day 14.

Statistics conducted using linear regression and mixed-effect analysis with Holm-Sidak multiple comparisons. *p<0.05, **p<0.01. Error bars shown as mean± SEM or geometric mean with 95% CI.

6.2.10. CMV serotype and vaccine response in older age adults

6.2.10.1.CMV serotyping COV002 and FLU005 older adults.

The COV002 clinical trial tested the ChAdOx1 nCoV-19 vaccine in older adults, aged 55-69 in group 7b and 70+ years old in group 8b. Trial participants in groups 7b and 8b were prime-boosted with a homologous dose of ChAdOx1 nCoV-19 at an interval of 28 days. FLU005 groups 5 and 6 tested the ChAdOx1 NP+M1 and MVA NP+M1 vaccines on a cohort of adults aged 50+. Group 5 received one dose of ChAdOx1 NP+M1, and group 6 received ChAdOx1 NP+M1 with an MVA NP+M1 boost dose after 8 weeks (table 6.2). CMV serotyping showed that Group 7b had a seroprevalence of 55% (22/40), and group 8b had a seroprevalence of 48.3% (29/60). FLU005 CMV serotyping was completed prior to the commencement of this D.Phil. by Dr Georgina Bowyer. Between group 5 and 6, which were not significantly different in age, 47.83% (11/23) individuals were CMV seropositive (Supplementary Figure 14).

Trial	Group	Age (years)	N	Prime	Prime dose	Boost	Boost dose	Boost date	CMV (n)
COV002	7b	55-69	40	ChAdOx1 nCoV-19	$5x10^{10}$	ChAdOx1 nCoV-19	$5x10^{10}$	28 days	22
COV002	8b	70+	60	ChAdOx1 nCoV-19	$5x10^{10}$	ChAdOx1 nCoV-19	$5x10^{10}$	28 days	29
FLU005	5	50+	11	ChAdOx1 NP+M1	$2.5x10^{10}$	N/A	N/A	N/A	11
FLU005	6	50+	12	ChAdOx1 NP+M1	$2.5x10^{10}$	MVA NP+M1	$1.5x10^{8}$	8 weeks	

Table 6.2. COV002 groups 7b and 8b and FLU005 groups 5 and 6

6.2.11. Pre-existing immunity in the older adult cohorts

As previously, COV002 ELISpot and ELISA data was collected and analysed by the Oxford COVID clinical trials team. FLU005 ELISpot data was collected during the trial, and ELISA data by Bryony Shaw. Pre-existing immunity from previous exposure either SARS-CoV-2 or influenza was determined from day 0 ELISA total IgG and ELISpot IFN-γ responses (Figure 6.8). There were no significant differences between CMV serostatus and either vaccine response, although the pre-existing immunity to Influenza A was much higher than to SARS-CoV-2 as demonstrated in younger adults.

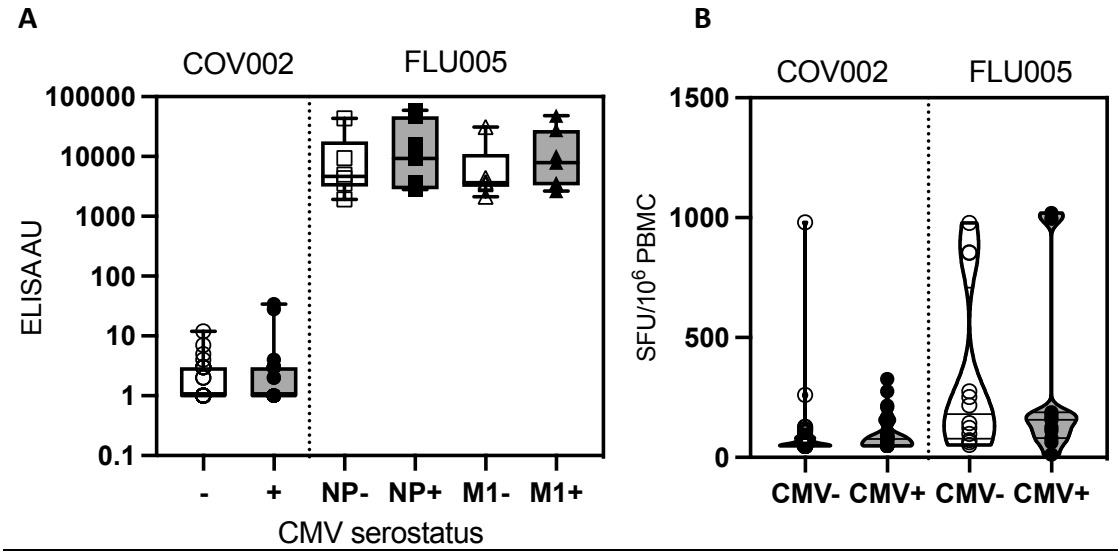


Figure 6.8. Pre-existing immune responses to SARS-CoV-2 and influenza A in older adults

The day 0 response stratified by CMV serostatus in combined COV002 groups 7b and 8b **A)** the total IgG response (ELISA arbitrary units) to SARS-CoV-2 spike protein and to Influenza A NP and M1 protein and **B)** the IFN-γ T cell response to SARS-CoV-2 S1 and S2 peptides and to Influenza A NP and M1 peptides.

6.2.12. Older adult IFN-γ ELISpot responses with CMV serostatus

COV002 Group 7b and 8b T cell IFN-γ ELISpot responses were stratified for CMV serostatus between day 0 and day 56 post prime vaccination. There was no significant difference in either group with CMV serostatus at any time point (Figure 6.9A and B). There was also no significant difference between CMV serostatus and T cell IFN-γ SFU in either FLU005 group up to day 182 post-vaccination (Figure 6.9C and D).

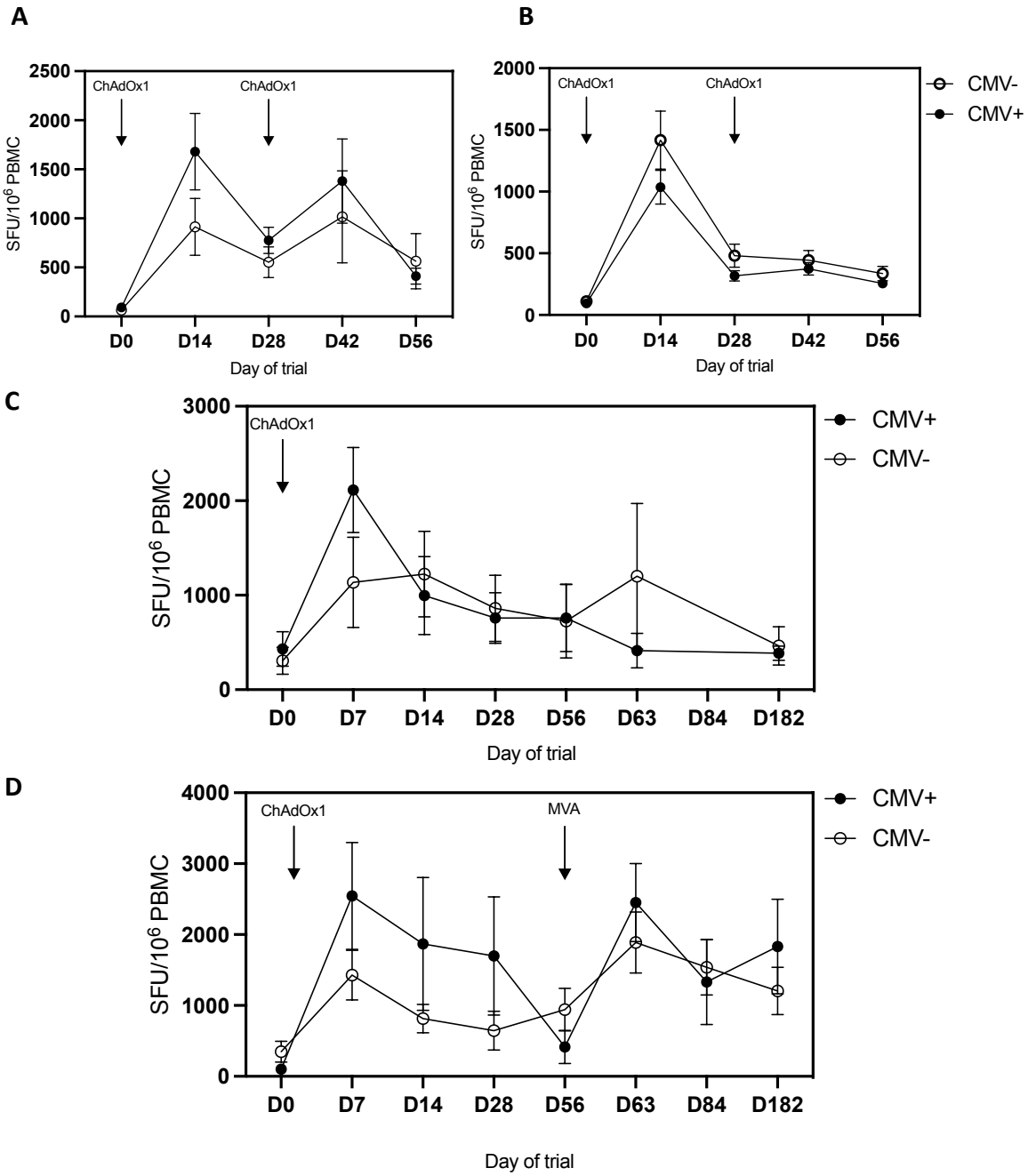


Figure 6.9. ELISpot T cell IFN-γ in COV002 trial group 7b and group 8b and FLU005 groups 5 and 6 stratified by CMV serostatus.

T cell IFN-γ was measured by ELISpot and participants stratified by CMV serostatus. IFN-γ measured in spot-forming units (SFU) per million cells and tIgG measured as ELISA arbitrary unit. **A)** COV002 group 7b, **B)** COV002 group 8b, **C)** FLU005 group 5, **D)** FLU005 group 6.

Statistics conducted using Mixed-Effects analysis with Sidak multiple comparisons. Error bars shown as mean± SEM.

6.2.13. Humoral responses to single dose, homologous and heterologous prime boost vaccination in older adults stratified by CMV serostatus

Within the COV002 cohort, the tIgG response to Spike protein was stratified by donor CMV serostatus. Interestingly, within group 7b, there was a trend towards more anti-spike tIgG correlated with CMV seropositivity (Fixed methods analysis, time point x CMV p=0.066, Figure 6.10A). This effect was not replicated within group 8b, with no significant difference between CMV serostatus and tIgG response (Figure 6.10B). Group 7b and 8b donors were further analysed for antibody isotypes by Dr Sandra Belij-Rammerstorfer and Jordan Barrett. There was no significant difference with CMV serostatus and titres of IgG1, IgA and IgM. However, there was a significant increase of IgG3 in CMV seropositive participants of group 7 at days 42 and 56 post-vaccination (day 42 p=0.041 and day 56 p=0.046, Figure 6.10C). Neither group 5 or 6 of the FLU005 trial demonstrated any difference in tIgG against NP or M1 with CMV serostatus (Figure 6.10D and E).

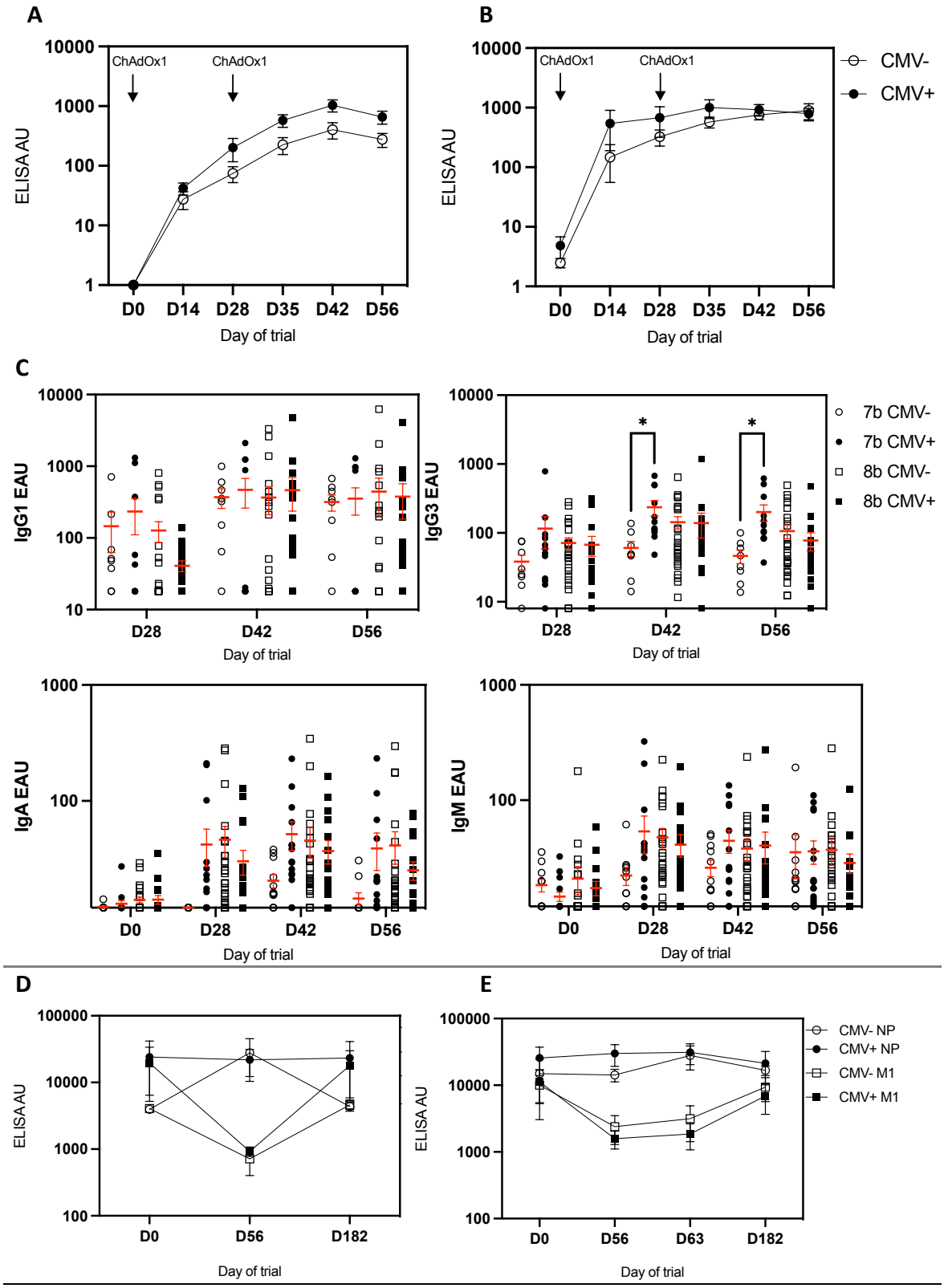


Figure 6.10. ELISpot T cell IFN-γ and tIgG ELISA responses in COV002 trial group 7b and group 8b and FLU005 groups 5 and 6

Total IgG was measured by ELISA and participants stratified by CMV serostatus. tIgG measured as ELISA arbitrary units. **A)** COV002 group 7b (aged 55-69), **B)** COV002 group

8b (aged 70+). **C)** Group 7b and group 8b isotype titres of IgG1, IgG3 IgA and IgM. **D)** FLU005 group 5 tIgG, **E)** FLU005 group 6 tIgG. Statistics conducted using mixed-effect analysis with Sidak multiple comparisons. *p<0.05. Error bars shown as mean± SEM.

6.3. Discussion

Current literature is unclear on how CMV infection affects vaccine immunogenicity, with both positive and negative effects demonstrated across clinical trials (226, 335-337, 339-341, 343, 345, 346, 348). In this chapter, I demonstrate that:

- CMV infection does not reduce antigen-specific T cell and antibody responses in single-dose or homologous ChAdOx1 vaccination, but does reduce T cell IFN-γ secretion following heterologous ChAdOx1-MVA vaccination in younger adults.
- NK cells and T cells from CMV seropositive individuals have a terminally differentiated phenotype.
- CMV seropositive older adults receiving homologous ChAdOx1 or ChAdOx1-MVA vaccination do not have reduced antigen-specific immunogenicity compared to CMV seronegative older adults.

6.3.1. NK cell phenotype and functionality

The phenotype of NK cells after CMV infection has been reasonably well detailed in the literature (485). CMV infection induces an expansion of NKG2C$^+$ NK cells with increased CD57 expression and activating KIR repertoire (293, 485). NKG2C is an activating receptor that is antigen-specific for the CMV ligand UL40 when presented on HLA-E (279, 486). NKG2C$^+$ NK cells have adaptive-like properties and are epigenetically similar to CD8$^+$ effector T cells, with reduced CD161 and lack of transcription factor signalling from Syk and PLZF (485, 487). The expanded NKG2C$^+$ population likely facilitates control of repeated CMV infection and resurgence from latency (57). CD57$^+$ NK cells have reduced expression of the cytokine receptors CD25 (IL-2Rα), IL-15R, IL-18R and IL-12R (18, 19, 34, 35, 379, 380, 396, 401, 431, 488), and reduced transcription of the *IFNG* locus (489). Therefore,

expansion of NKG2C$^+$CD57$^+$ NK cells in CMV seropositive individuals indicates that the overall NK cell population is more terminally differentiated and responsive towards CMV peptides, but less responsive to activation by cytokine stimulation than NK cells in CMV seronegative individuals.

In this analysis, I also demonstrate that CMV seropositive participants across all trial groups have a significant expansion of CD57$^+$NKG2C$^+$ NK cells, and that CD57$^+$ NK cells also have significantly reduced expression of the IL-2 receptor CD25. Furthermore, there is also reduced CD69 expression across the total NK cell population associated with CMV seropositivity. This expansion of CD57$^+$ NK cells with lower cytokine receptor expression may facilitate the loss of activation observed in NK cells following vaccination due to reduced cytokine activation. It has previously been shown that antigen-specific IL-2 from CD4$^+$ T cells activates NK cells following vaccination and infection functionality (380, 396, 488, 490). A reduction in IL-2 secretion, combined with a loss of CD25 (IL-2Rα) expression on NK cells, may facilitate a loss of NK cell activation with CMV seropositivity. A correlation between CD4 IL-2 secretion and NK cell activation was tested. CMV seronegative donors had some correlation between CD4 IL-2 secretion and NK cell CD25 and Ki-67 expression. This corresponds with IL-2 being only one of several cytokines to activate NK cells, and therefore would not be responsible for activation in its entirety. However, there was no significant correlation between CD4$^+$ T cell IL-2 secretion and NK cell activation within the CMV seropositive cohort. This suggests, therefore, that NK cell activation may be reduced in part by loss of IL-2 secretion from CD4$^+$ T cells, and reduction of CD25 expression on the expanded CD57$^+$ NK cell population.

Previous research demonstrates that CMV-seropositive donor NK cells secrete less IFN-γ after vaccination and stimulation with *Bordetella pertussis*, influenza A, and

ebolavirus antigens (362, 396, 491). This loss of cytokine secretion is potentially due to expansion of adaptive $CD57^{+}NKG2C^{+}$ NK cells which are less responsive to cytokine activation but can still be activated by ADCC through activation of CD16 (35, 487). Within this cohort of single-dose ChAdOx1 nCoV-19 vaccinees, there was a significant increase in CD107a expression at day 28 post-vaccination in the CMV seronegative individuals, but not the CMV seropositive individuals. Contrastingly, after ChAd3-MVA vaccination and single-dose ChAdOx1 NP+M1 vaccination, CD107a expression was increased in CMV-seropositive donors, either in the $NKG2C^{+}$ NK cell population or the total NK cell population, respectively. CD107a expression is facilitated by antibody-dependent activation of FcγRIII (CD16), and IL-2-mediated activation of CD25 (491). Potentially, the increase of CD107a expression is proportional to the increase of $CD57^{+}$ NK cells, which are less responsive to activation by cytokines and also secrete lower levels of inflammatory cytokines, but can respond to activation by degranulation (35). CMV seropositivity has previously been linked to no change in CD107a expression (362, 396, 491), or reduced CD107a expression (363) following stimulation with vaccine antigen or virus. These data, therefore, indicate a differential response of NK cells following vaccination. Potentially, increased degranulation may indicate an NK cell regulatory function on $CD8^{+}$ T cells; Lee *et al* demonstrates a correlation between increased IL-10 secretion and degranulation during MCMV infection (439). This response may also be facilitated in part by the vaccine encoded antigen, and further research across vaccine trials with larger group sizes will be required to establish the effect of antigen on NK cell response.

6.3.2. T cell phenotype and functionality with CMV serostatus

Previous research demonstrates an expansion of $CD57^{+}KLRG1^{+}$ T cells in CMV seropositive individuals, as well as an inactivated $CD27^{-}CD28^{-}$ phenotype and accumulation of late-differentiated $CD45RA^{+}CCR7^{-}$ T_{EMRA} memory T cells (318, 322, 339, 481). Data from young adults in both the COV001 and FLU005 cohorts exemplify these phenomena and demonstrate that CMV infection exerts a reduction in T cell activation, with noticeable CD25 downregulation on $CD8^{+}$ T cells, and increased frequency of $PD1^{+}CD57^{+}$ $CD4^{+}$ T cells correlated with CMV serostatus. This has not been previously described as a CMV-specific phenotype, but supports a CMV-driven anergic phenotype and suggests a mechanism behind lack of T cell activation. The T cell phenotype in CMV seropositive young adults in the FLU005 vaccine trial was less well defined than other trials studied. This may be due to the younger age of the cohort, potentially skewing the immune phenotypes towards a less terminally differentiated profile. Furthermore, the FLU005 samples were kept in liquid nitrogen since 2014, and defrosting may have caused death of senescent T cell populations compared to more recently collected samples.

Within CMV seropositive participants receiving a single dose of ChAdOx1 nCoV-19, there was a significant reduction in the frequency of $CD4^{+}$ T cells expressing 2 and 4 markers of activation at day 14 post-vaccination in CMV seropositive donors. Similarly, there was no significant increase in the expression of CD107a and TNF at two weeks post-vaccination in the CMV seropositive cohort receiving single dose ChAdOx1 or MVA NP+M1. There were similar trends following post-boost timepoints, however due to small sample sizes these data did not reach significance. These data support previously published results demonstrating that CMV infection reduces T cell immunogenicity following vaccination (336, 339, 479), however this is the first time it has been demonstrated across multiple

viral vectored vaccine regimens. Interestingly, reduction in immunogenicity as measured by ICS did not necessarily translate directly into reduced vaccine immunogenicity measured by T cell ELISpot; ELISpot data from a single dose of ChAdOx1 nCoV-19, ChAdOx1 NP+M1, or MVA NP+M1 elicited no significant difference in T cell IFN-γ production between serostatus. This may be due to differences in the sensitivity of both assays, but suggests that CMV does not have an overall large impact on T cell cytokine secretion following these vaccination regimens. There was also no significant difference following homologous ChAdOx1-ChAdOx1 vaccination. A significant reduction of immunogenicity was observed, however, after ChAdOx1 NP+M1 prime, MVA NP+M1 boost. This is in keeping with data presented in Bowyer *et al*, and suggests MVA boost vaccination may exacerbate CMV-mediated immunosenescence.

In this chapter, I also identify an increased seroprevalence of CMV in the older adult vaccine groups. Older adults receiving homologous ChAdOx1 and heterologous ChAdOx1 and MVA vaccine regimens did not demonstrate any loss of T cell or IgG immunogenicity with CMV seropositivity, contrary to literature published on influenza vaccination (226, 328, 335, 348, 479). Unexpectedly, in adults aged 55-69, CMV seropositivity was associated with higher titres of IgG3 following ChAdOx1 nCoV-19 prime-boost vaccination. Older adults vaccinated with ChAdOx1 nCoV-19 also have an equal T cell IFN-γ response and IgG response when compared to younger adults, demonstrated in this thesis and across vaccine immunogenicity trials (222).

The reasons for the differences observed within these viral vector trials and in contrast to other trials are unclear, but several potential explanations exist. Firstly, the ChAdOx1 vector is highly immunogenic, and single dose vaccination alone may be sufficient to overcome CMV-mediated loss of immunogenicity, even with an observable

immunosenescent T cell population. Potentially, the impact of heterologous ChAdOx1-MVA boosting may impact the immunogenicity as seen in Bowyer et al, through the mechanism of increased cell death by necroptosis as described in chapter 3. Further investigation will be needed to understand why heterologous MVA boost vaccination drives a loss of T cell immunogenicity across these two trials.

The overall maintenance of humoral and cellular functionality within these cohorts is in contrast to other trials conducted with non-viral vectored vaccines in Europe and Africa. This may potentially be due to differential burden of CMV infection between regions; it is likely that younger adults in the UK have an older age of first CMV exposure than young adults in sub-Saharan Africa, and therefore have more immune memory space to form immunogenic responses to vaccination (264). This is demonstrated within these data; approximately 40% adults aged 18-55 are CMV seropositive, compared to 88% of infants in the Gambia aged 6 months (338), and 100% of adults in the Senegalese arm of the EBL04 trial (339). In mice, the infectious dose of primary CMV infection also establishes the immunosenescent phenotype of T cells and correlates to the impairment of T cell cytotoxicity (469). Therefore, further investigation into other demographic populations with differential CMV exposure may elucidate whether multiple infections, or age of first infection, or likely a combination of environmental factors, disease burden and other co-factors determine vaccine immunogenicity.

These experiments are limited due to the sample size of vaccine cohorts, and the variability of CMV infection between groups. CMV serotyping was conducted retrospective to immunological analysis, hence the differing group sizes and number of CMV seropositive individuals within groups. The vaccine trials analysed are also not aged matched, and a younger population may have an overall less immunosenescent profile than a group of

adults with an older average age. However, the data presented in this chapter provide a further insight into the effect of CMV infection on the phenotype of the immune system, and the differential response observed following viral vector vaccination across multiple vaccine regimens.

Papers published including results presented in this chapter

Sharpe, HR., Provine, NM., Bowyer, G., Folegatti, P., Belij-Rammerstorfer, S., Flaxman, A., Makinson, R., Hill, AVS., Ewer, KJ., Pollard, AJ., Klenerman, P., Gilbert, S., Lambe, T. *CMV-associated T cell and NK cell terminal differentiation does not impact immunogenicity of ChAdOx1 vaccination.* Currently under peer review at JCI Insight.

Chapter 7

The COVID-19 pandemic and SARS-CoV-2 vaccine trials

Chapter 7 : The COVID-19 pandemic and SARS-CoV-2 vaccine trials

7.1. Introduction

The novel emerging pathogen, Severe Acute Respiratory Syndrome Coronavirus 2 (SARS-CoV-2) was identified during this D.Phil. in December 2019 from a case of unknown pulmonary infection in Wuhan, China (196). Over the subsequent months, SARS-CoV-2 spread globally and was declared a pandemic by the WHO on 11th March 2020 (200) . The resulting disease, COVID-19, ranges from asymptomatic to severe presentation and can cause long-lasting morbidity and death. The exact correlates of severity and mortality of COVID-19 patients has been difficult to delineate thus so far, and there are multiple immune phenotypes and co-morbidities which associate with severe disease (205, 211, 213).

On 23rd March 2020, the UK went into national lock down, with closure of academic research institutions including the University of Oxford. As highlighted in the previous chapters, several experiments were disrupted during this time, although efforts were made to rectify any lost data at a later stage. During the lock down and the months after, I was fortunate to be involved in pre-clinical and clinical trials work on ChAdOx1 nCoV-19 (AZD1222, now known as Vaxzevria).

This short chapter will highlight the research I assisted with during this time, and the methods learnt. Briefly, I assisted with pre-clinical trials of the ChAdOx1 nCoV-19 vaccine, and worked as a part of the Oxford COVID-19 clinical trials team undertaking sample processing and T cell immunogenicity assay set up. I also investigated the immune response to severe COVID-19 and influenza A to identify correlates of morbidity conducted on PBMCs from the most severe cohort of COVID-19 patients in the Intensive Care Unit of St George's Hospital, London. These patients were enrolled alongside a cohort of severe

influenza patients, and COVID-19 convalescent health care workers. Comparison of the immune phenotypes of two severe respiratory diseases alongside convalescent COVID-19 donors and healthy individuals will provide more insight into the immune signature that leads to severe disease and death in COVID-19, and could be used as a predictor of outcome to help streamline treatment options.

7.2. Work conducted during the pandemic

7.2.1. Pre-clinical sample processing

Starting from late March 2020, I assisted with sample processing and assay set up for pre-clinical experiments using ChAdOx1 nCoV-19 alongside Dr Alex Spencer. I primarily assisted with processing splenocytes from mouse vaccinations (Section 2.3.8). I also was trained to process blood samples from ferret and NHP vaccinations (Section 2.6.1), and ran samples on the BD Fortessa cytometer to measure T cell activation and functional response to vaccination.

7.2.2. Clinical trials sample processing

Starting from July 2020, I completed GCP training and enlisted as a clinical trials scientist. I assisted with the separation of plasma and PBMCs from human blood samples taken as part of the COV001, COV002 and COV006 clinical trials (Section 2.6.2). I also assisted with ELISpot assay set up (Section 2.6.3) conducting the Intracellular Cytokine Staining assay (section 2.6.4) and freeze-down of PBMC samples (Section 2.6.5).

7.2.3. The impact of severe influenza A and COVID-19 on the immune system

7.2.3.1. Cohort and study description

The optimised Cytek™ Aurora panel (table 2.16) was used to analyse PBMCs from individuals diagnosed with severe Influenza A or COVID-19. These individuals were recruited for an ongoing observational clinical trial AspiFlu (http://www.isrctn.com/ISRCTN51287266) conducted at St George's University Hospital, London, and University of Oxford. Samples from participants were taken at different time points, however all were taken at the peak of infection during the participant's stay in the ICU. During this assay, PBMC samples were stimulated with either SARS-CoV-2 spike peptide pools or Influenza A NP+M1 peptides respective of disease, the positive control PMA, or left unstimulated. The stimulation and staining assays were conducted by Dr Nicholas Provine, due to required training for CL3 handling. The panel was designed by myself, and I also undertook all computational and statistical analysis. Parallel staining was conducted on the COV001 group 1 cohort, as presented in chapters 4 and 6.

The main cohort of 24 individuals was split into 12 with influenza A (IAV) and 12 with COVID-19 (COV). Each cohort was equally balanced by gender (6 male, 6 female), and age matched. Within the influenza cohort, 4 individuals had subtype H1N1, 4 had H3N2, 1 had Influenza B, and 5 were unsubtyped (Supplementary Figure 15). A cohort of health care workers who had fully recovered from mild/moderate COVID-19 (cHCW n=12) were included as a control, but were not age-matched to the other donor cohorts. For the NK cell surface phenotyping analysis, a larger cohort of patients was analysed using the same surface marker panel (n=20 IAV, n=40 COVID-19, n=19 cHCW).

7.2.3.2. T cell activation and senescence

Donor T cells were analysed for changes in frequency, activation, and memory populations following the gating strategy in supplementary figure 5. There was a reduction of $CD8^+$ T cell frequency in both disease cohorts (figure 7.1A). Acute lymphopenia is a hallmark of severe COVID-19, especially within $CD8^+$ T cells (211, 213) For further analysis, samples that had fewer than 300 cells per subset were excluded.

Both $CD4^+$ and $CD8^+$ T cells were more proliferative in both disease conditions and expressed more Ki-67 than cHCW (IAV $p<0.0048$, COV $p<0.0027$, figure 7.1B). However, only IAV donors had significantly more CD69 expression than control donors, although there was still a trend towards increased expression in COVID-19 patients (IAV CD4 $p=0.018$, CD8 $p=0.019$, figure 7.1C). Interestingly, IAV donors had significantly more $CD25^+$ CD8 T cells compared to COVID-19 donors and controls ($p<0.0001$, figure 7.1D). Both cohorts displayed increased expression of the terminal differentiation marker KLRG1 on $CD8^+$ T cells than control donors, and an increased frequency of the $KLRG1^+CD57^+$ $CD8^+$ T cell population (Figure 7.1E and F).

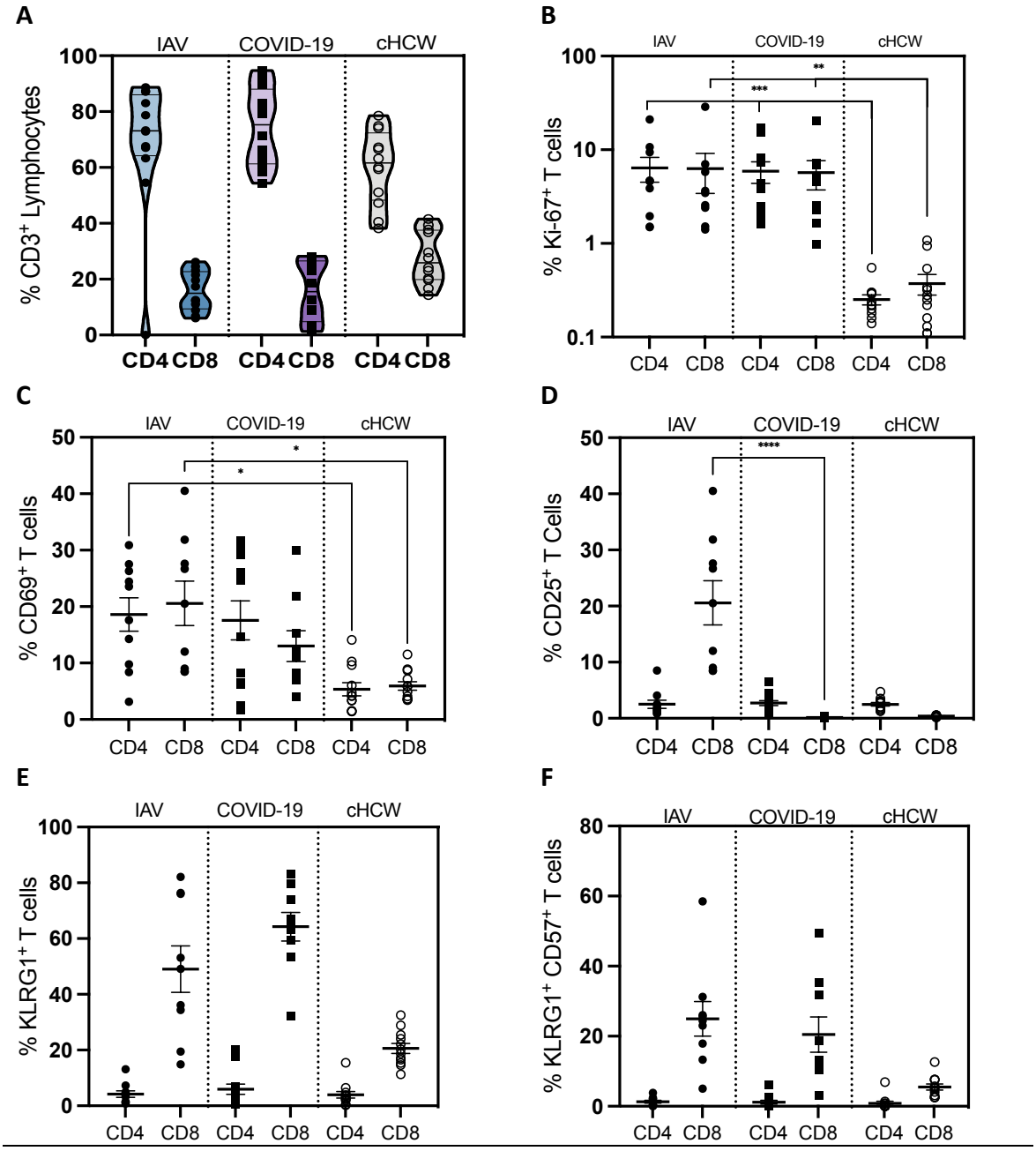


Figure 7.1. The activation and differentiation profile of T cells in IAV and COVID-19

Donor PBMCs stained for $CD8^+$ and $CD4^+$ T cells were analysed via Aurora flow cytometry. **A)** CD4:CD8 ratio, **B)** Ki-67 expression, **C)** CD69 expression, **D)** CD25 expression **E)** KLRG1, **F)** frequency of $KLRG1^+CD57^+$ T cells.

Statistics conducted by Kruskal-Wallis test with Dunn's multiple comparisons, *p<0.05, **p<0.01, ***p<0.005, ****p<0.0001. Error bars shown as mean± SEM.

7.2.3.3. T cell memory profile

The memory profile along the CD45RA/CCR7 axis was analysed in both $CD4^+$ and $CD8^+$ T cells from donors (figure 7.2). Overall, non-naïve T cells from IAV and COVID-19 donors expressed higher proportions of the terminal differentiation marker CD45RA than cHCW, demonstrated by an increase in $CD4^+CD45RA^+CCR7^-$ (T_{EMRA}) T cells in both IAV and COVID-19 donors (IAV p=0.0056, COV p=0.0007). IAV donors also had significantly more $CD8^+CD45RA^+CCR7^-$ (T_{EMRA}) T cells (p=0.0095), and COVID-19 donors had significantly more $CD4^+CCR7^+CD45RA^-$ (T_{CM}) T cells (p=0.021). Both IAV and COVID-19 patients had significantly fewer $CD8^+CD45RA^-CCR7^-$ (T_{EM}) T cells in comparison to cHCW (p<0.0053). These data demonstrate the alterations in T cell memory and terminal differentiation facilitated by severe IAV and COVID-19, leading towards fewer effector memory T cells and more terminally differentiated effector memory T cells.

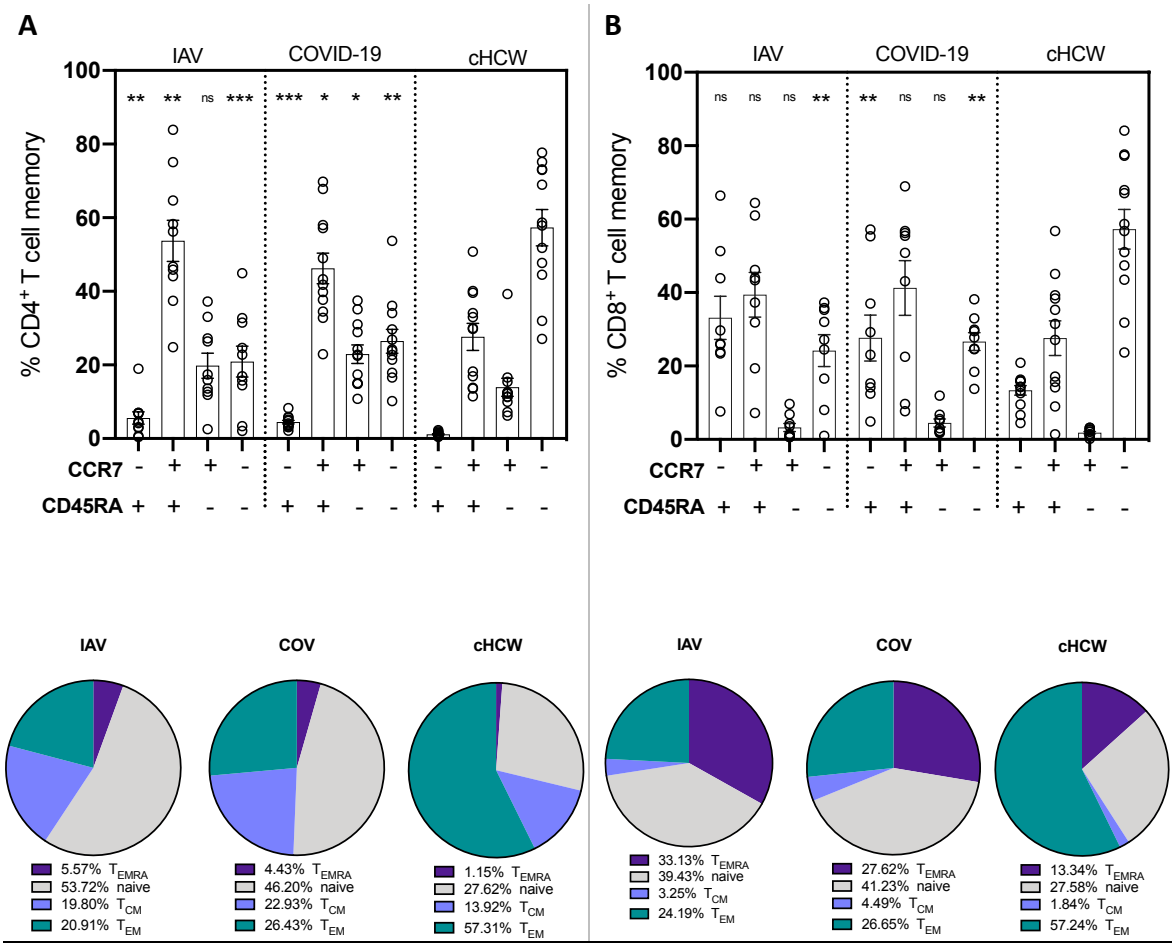


Figure 7.2. CD4⁺ and CD8⁺ T cell memory populations

Donor CD8⁺ and CD4⁺ T cells were analysed via Aurora flow cytometry for T cell memory populations. **A)** CD4⁺ T cell memory populations from COV, IAV and HC/cHCW frequency. **B)** CD8⁺ T cell memory populations from COV, IAV and HC/cHCW frequency. CCR7⁻ CD45RA⁺ = T_{EMRA}, CCR7⁺CD45RA⁺ = naïve, CCR7⁺CD45RA⁻ = T_{CM}, CCR7⁻CD45RA⁺ = T_{EM}. Statistics conducted by Kruskal-Wallis test with Dunn's multiple comparisons. Statistics above bars are in comparison to the cHCW cohort. **p*<0.05, ***p*<0.01, ***p<0.005. Error bars shown as mean± SEM.

7.2.3.4. T cell cytokine production

PBMCs were stimulated with pools of either spike glycoprotein or influenza A NP+M1 peptides. $CD4^+$ T cells from COVID-19 donors produced significantly more IL-2 (p=0.028) and expressed less CD107a (p<0.0001) than cHCW, and had a trend towards more TNF production (Figure 7.3A). $CD4^+$ T cells from IAV donors expressed significantly more TNF, IL-2 and CD107a than cHCW (p=0.019, p=0.0003, p<0.0001, respectively. Figure 7.3B). There were fewer significant differences in the $CD8^+$ T cell compartment when comparing both patient cohorts with the control group. cHCW stimulated with COV spike peptides had significantly more CD107a expression than COVID-19 donors (p=0.039, figure 7.3C). There were no significant differences between the production of any other inflammatory mediators in $CD8^+$ T cells from IAV donors and cHCW (Figure 7.3D). These data show that $CD4^+$ T cells from IAV donors are more responsive following peptide stimulation, and this lack of response in COVID-19 patients may underpin the course of disease severity.

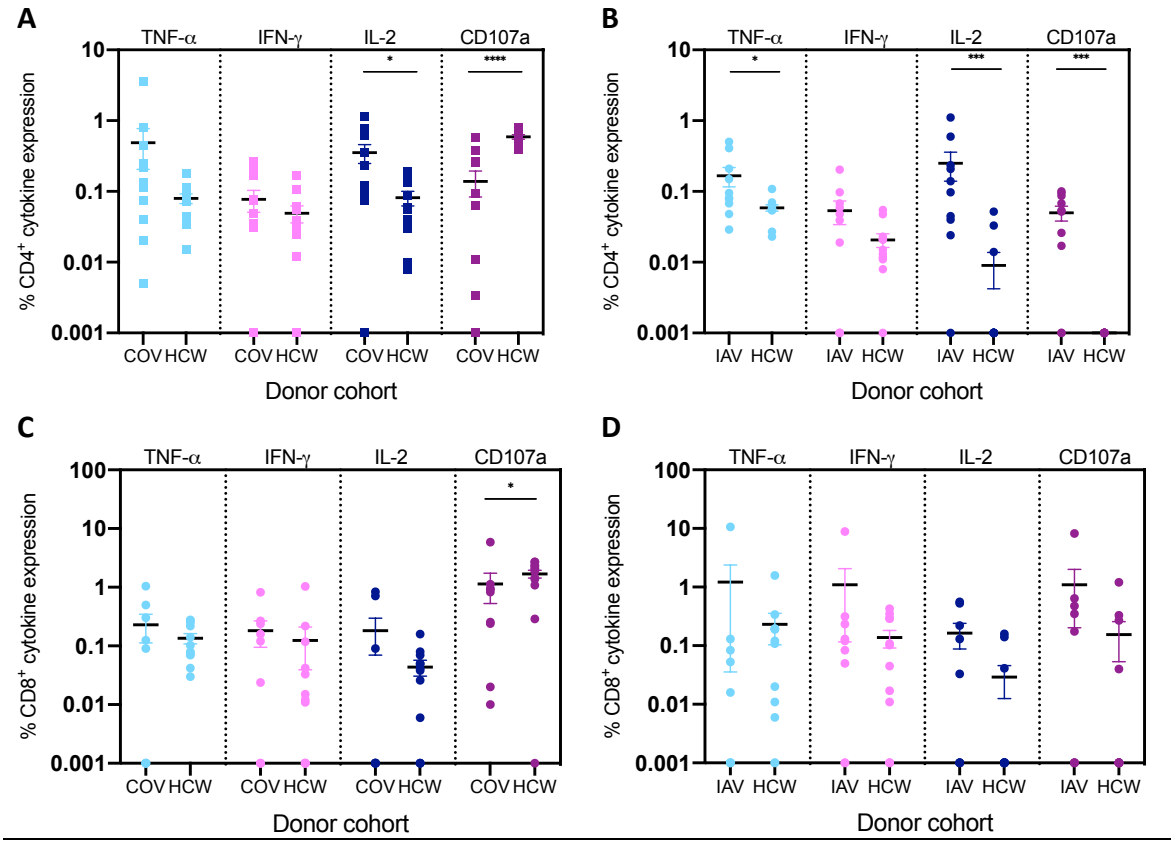


Figure 7.3. The cytokine and inflammatory marker profile of stimulated T cells from IAV and COVID-19 patients

Donor $CD8^+$ and $CD4^+$ T cells were stimulated with relevant peptides (SARS-CoV-2 spike glycoprotein S1 and S2, COVID-19 and cHCW donors, influenza A H3N2 NP+M1, IAV and cHCW donors) or left unstimulated as a control. Samples were analysed for cytokine secretion and degranulation via Aurora flow cytometry.

$CD4^+$ T cell cytokine expression from **A)** COV and cHCW donors and **B)** IAV and cHCW donors. $CD8^+$ T cell cytokine from **C)** COV and cHCW donors and **D)** IAV and cHCW donors. Statistics conducted by Mann-Whitney U test *p<0.05, **p<0.01, ***p<0.005, ****p<0.001. Error bars shown as mean± SEM.

7.2.3.5. NK cells activation and cytokine secretion during influenza A and SARS-CoV-2 infection

Within the larger cohort of patients analysed for NK cell phenotype, there was a trend towards a higher frequency of NK cells as a proportion of live lymphocytes in severe COVID-19 patients, although this is in contrast to other papers which demonstrate NK cell leukopenia with SARS-CoV-2 infection (211, 213) (Figure 7.4A). Patients with <400 NK cells per sample were not analysed further. Interestingly, NK cells from COVID-19 donors had significantly lower expression of CD69 than cHCW (p=0.049, figure 7.4B) There was also a trend towards increase KLRG1 expression, and increased $CD57^{+}NKG2C^{+}$ NK cells in both groups (figures 7.4C and D). Within the IAV cohort, but not the COV cohort, there was a significant increase in proliferation as measured by Ki-67 expression (p=0.03. Figure 7.4E), although COV donors had much wider range of values. Both cohorts had a significant increase in NK cell SSC-A, which is a measurement of cellular activation and granule formation (p<0.03, Figure 7.4F). It was not possible to perform analysis on the $CD56^{++}$ population of NK cells, as actual cell counts were very low across severe cohort donor samples.

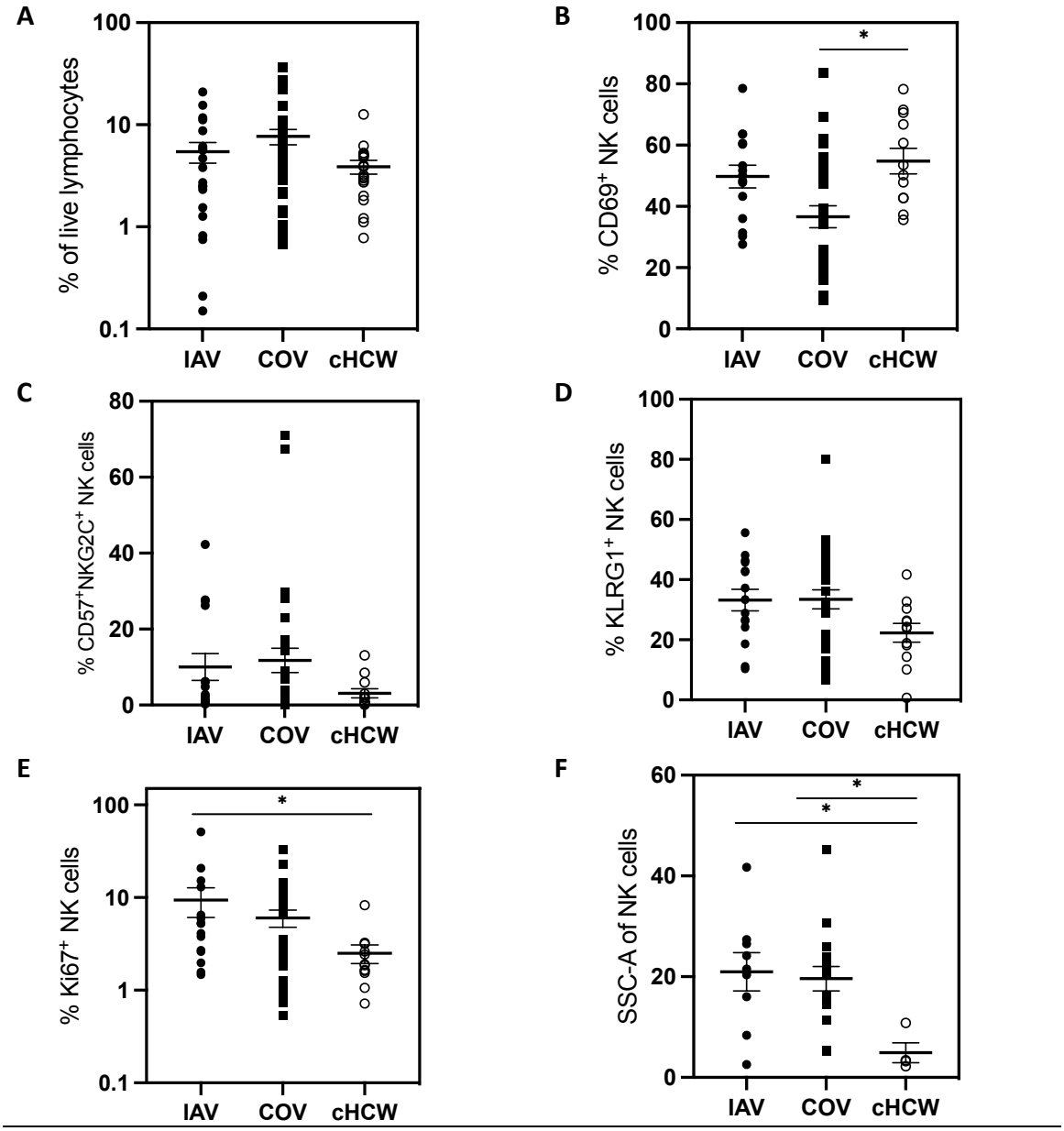


Figure 7.4. NK cell phenotype and activation in patients with severe COVID-19 and influenza A

PBMCs from individuals with severe COVID-19 (COV) or Influenza A (IAV), or convalescent healthcare workers (cHCW) **A)** Frequency of NK cells as a percentage of live lymphocytes. **B)** CD69 expression, **C)** KLRG1 expression, **D)** frequency of NKG2C^{+}CD57^{+} NK cells. **E)** NK cell Ki-67 expression, **F)** NK cell SSC-A.

Statistics were conducted using Kruskal-Wallis tests with Dunn's multiple comparisons. *p<0.05. Error bars shown as mean±SEM.

The cytokine response of the core 12 COVID-19 and 12 IAV individuals' NK cells was measured following stimulation of PBMCs with relevant peptide pools. The overall response of NK cells to peptide stimulation was broad and varied; NK cells from COVID-19 donors exhibited a trend towards more IFN-γ and CD107a than IAV donors (IFN-γ p=0.08, CD107a p=0.1 Figure 7.5A and 7.5B). Low and non-significant quantities of TNF and IL-2 were detected from NK cells during either disease (Figure 7.5C and D).

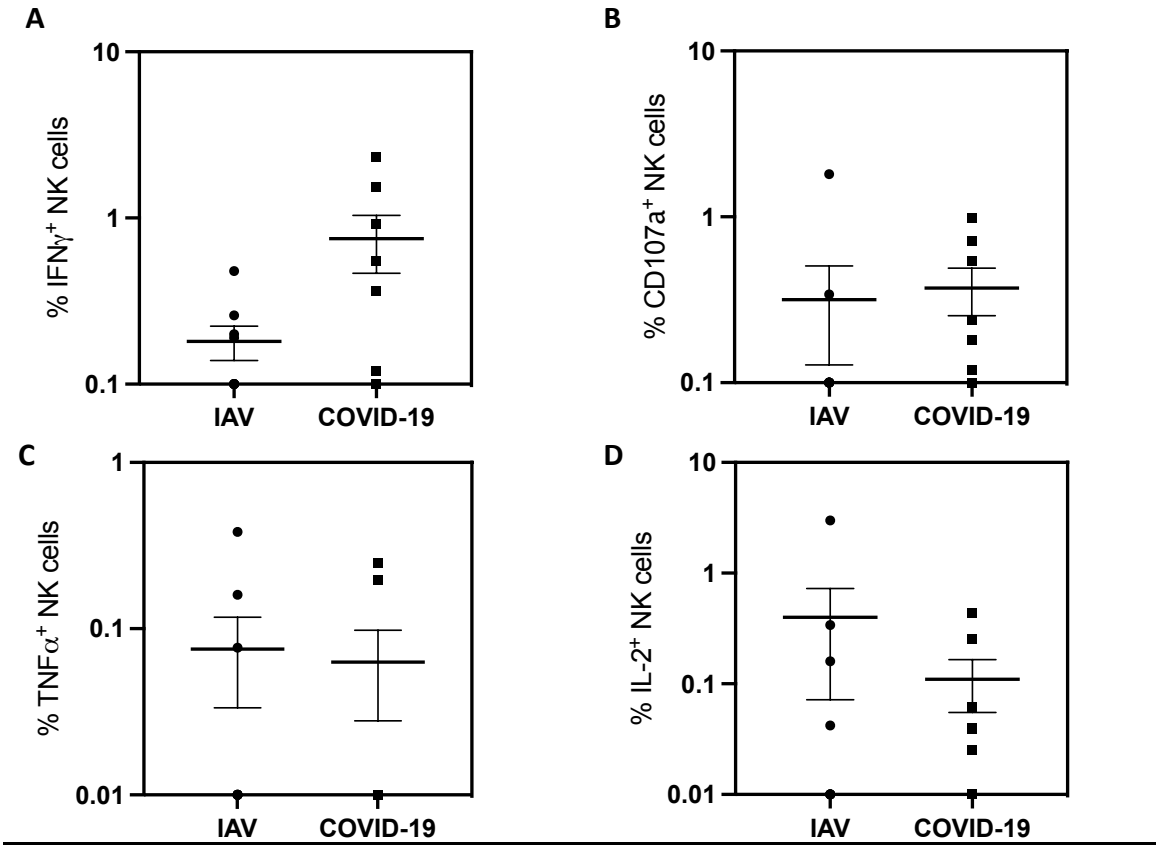


Figure 7.5. NK cell cytokine secretion and degranulation in severe COVID-19 and influenza A

Total NK cell functionality following peptide stimulation of PBMCs. **A)** IFN-γ, and **B)** CD107a, **C)** TNF, **D)** IL-2. Statistics were conducted using Mann-Whitney U test. Error bars shown as mean±SEM.

7.2.3.6. NK cell and T cell polyfunctionality in COVID-19 and IAV donors.

The polyfunctional cytokine and activation marker responses to peptide stimulation were analysed in NK cells and T cells from the COVID-19 and IAV donors. Using Boolean 'OR' gating, donor samples were analysed for cells expressing CD69 and TNF-α OR IFN-γ OR IL-2 OR CD107a (T cells and NK cells) OR CD25 (T cells only). There was a broad range of NK cells expressing more than one marker of activation across all donors in response to each peptide pool (figure 7.6A). Within the T cell compartment, a high frequency of $CD8^+$ T cells from COVID-19 patients expressed at least one marker of activation following stimulation with S1 and S2 peptides. This was significantly higher than $CD4^+$ T cells from COVID-19 patients stimulated with S1 and S2 peptides (p=0.011. Figure 7.6A).

From the 'OR' gates, Boolean 'COMBINATION' gating was applied to analyse the polyfunctionality of cells expressing multiple activation markers and cytokines after stimulation. NK cells were broadly responsive to peptide stimulation, with equal frequencies of polyfunctional cells between patient cohorts (Figure 7.6B). Similarly, there were no significant differences between polyfunctional cytokine expression in $CD8^+$ and $CD4^+$ T cells in either patient group (Figure 7.6C and D).

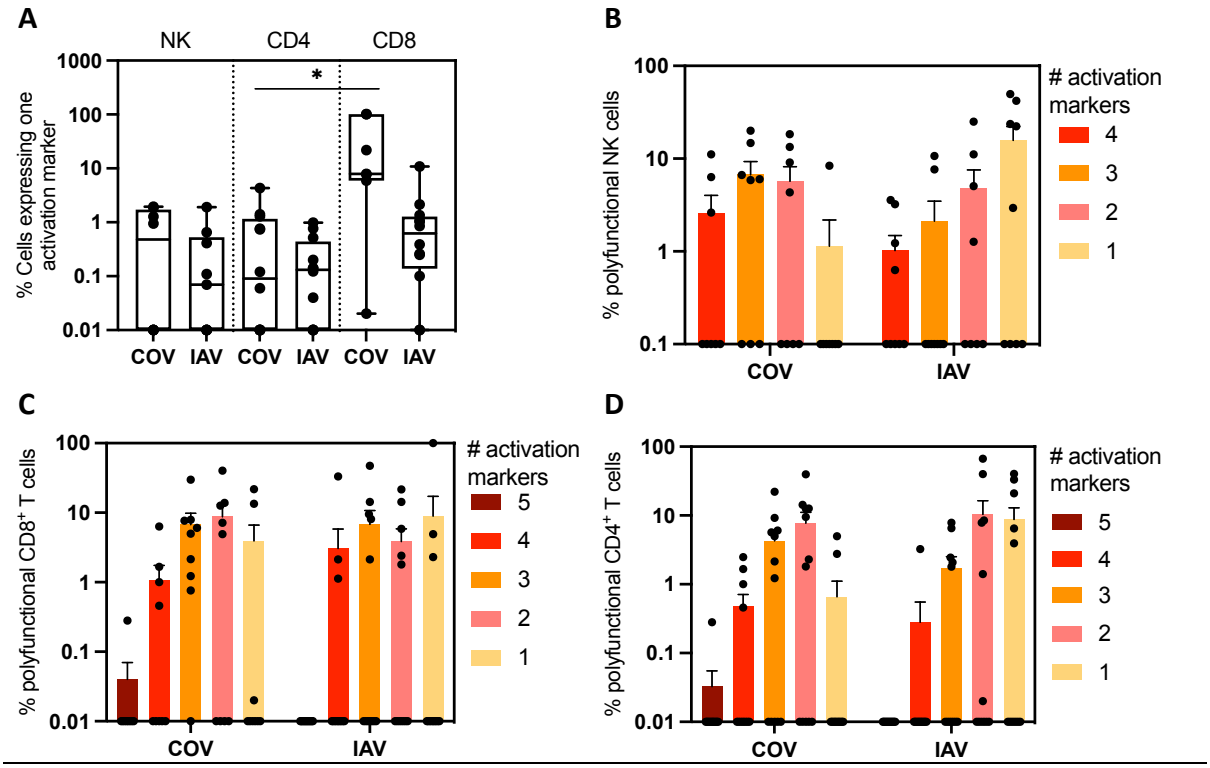


Figure 7.6. Polyfunctionality of NK cells, CD4⁺ and CD8⁺ T cells following stimulation with COVID-19 or IAV peptides

Donor CD8⁺ and CD4⁺ T cells (IAV and COVID-19 n=12) were stimulated with relevant peptides (SARS-CoV-2 spike glycoprotein S1 and S2= COVID-19, Influenza A H3N2 NP+M1= IAV) or left unstimulated as a control. Samples were analysed for cytokine secretion or degranulation via Aurora flow cytometry and Boolean analysis was conducted on activated cells for polyfunctional cytokine expression. **A)** Activated NK cells expressing at least one cytokine in response to COV or IAV peptides. **B)** The proportion of polyfunctional NK cells expressing one to four cytokines in response to COV or IAV peptides **C)** Polyfunctional CD8⁺ T cells with frequency of cytokines expression **D)** Polyfunctional CD8⁺ T cells with frequency of cytokines expression. Statistics conducted using Mixed-effects analysis with multiple comparisons. *p<0.05. Error bars shown as mean± SEM.

7.2.3.7. B cell phenotype in IAV and COVID-19 infection.

There was no significant difference in the frequency of $CD3^{-}CD19^{+}$ lymphocytes (B cells) in either disease state compared to cHCW, although IAV donors had a wider range of frequencies (Figure 7.7A). There was, however, a significant down-regulation of CD71 on the surface of B cells from both disease cohorts (IAV p=0.0004, COV p=0.0023, Figure 7.7B) when compared with healthy controls. B cell proliferation (Ki-67) was significantly higher in both cohorts of infected individuals than recovered individuals (IAV p=0.0001, COV p=0.0003, Figure 7.7C) and so was the frequency of $IgG^{+}CD27^{+}$ (switched memory) B cells (IAV p=0.005, COV p=0.003. Figure 7.7D). Comparatively, there was no change in the frequency of $IgG^{-}CD27^{+}$ unswitched memory B cells or overall IgG expression in either COVID-19 or IAV donors (Figure 7.7E and F).

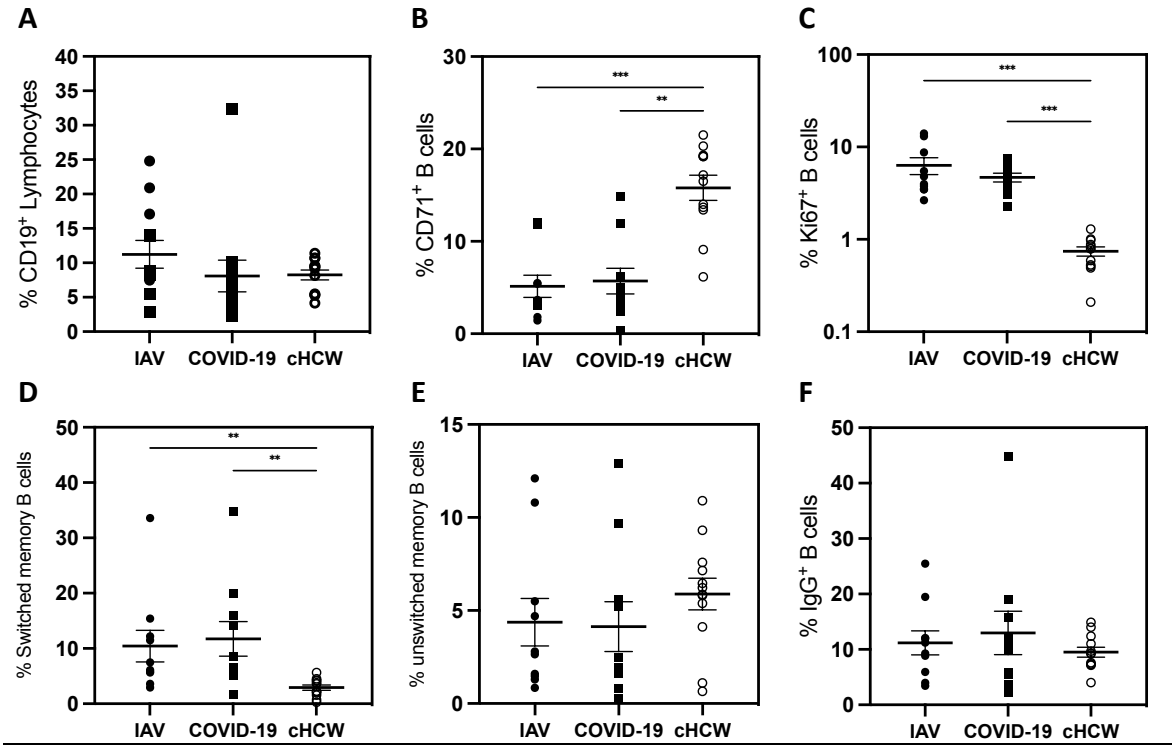


Figure 7.7. B cell activation and memory populations

Donor B cells were analysed via Aurora flow cytometry for B cell activation and memory populations. **A)** B cell frequency, **B)** B cell CD71 expression, **C)** Ki-67 expression, **D)** Switched memory (IgG^+CD27^+ B cell) frequency, **E)** IgG^-CD27^+ unswitched memory frequency, **F)** frequency of IgG^+ B cells.

Statistics conducted by Kruskal-Wallis test with Dunn's multiple comparisons. **p*<0.05, ***p*<0.01, ***p<0.005. Error bars shown as mean± SEM.

7.3. Discussion

7.3.1. SARS-CoV-2 infection and influenza A infection elicit an aberrant immune profile

Both SARS-CoV-2 and influenza A infection causes a range of disease pathology from asymptomatic to severe, and there is no clear correlation between immunopathology and disease outcome. COVID-19 has a higher mortality rate than seasonal IAV, with an approximated mortality of 6.1% of diagnosed cases (214). In this analysis, I compared PBMC samples from individuals with severe COVID-19 and influenza A to COVID-19-convalescent controls to elucidate immune phenotypes correlated with mortality.

Both COVID-19 and IAV patients had heterogeneous yet aberrant immune activation compared to healthy controls. In support of other studies, both IAV and COVID-19 patients had $CD8^+$ T cell lymphopenia (214), and had similarities in proliferation and terminal differentiation of T cells in comparison to cHCW (211, 492). However, there were some differences in our data, such as a lack of PD1, CD25 and CD69 up-regulation in COVID-19 patients, which is reported in other studies (212, 214, 493, 494). $CD4^+$ T cells from IAV patients mounted a more robust response with significantly more IL-2, TNF and CD107a expression compared to stimulated cHCW PBMCs. By comparison, $CD4^+$ T cells from COVID-19 patients only had significantly more IL-2 secretion than cHCW. This was reflected in the $CD8^+$ T cell compartment, with significantly less expression of CD107a in COVID-19 patient T cells than cHCW T cells and no other significant differences in cytokine production. Other research outlines significant increase in T cell TNF in COVID-19 donors, alongside other unmeasured cytokines including IL-6 and IL-10 (214, 495). It may be that a strong early $CD4^+$ T cell response is effective at curtailing COVID-19 disease progression, and may account for the lack of CD4/$CD8^+$ T cell responses seen in these patients (496), furthermore severe disease may reduce cytokine production including IFN-γ (495, 497). Differences in peptide

response between cohorts may be due to the recent exposure to SARS-CoV-2 in cHCW and generation of robust memory responses, compared to prior exposure to unknown strains of influenza A, which may not respond as robustly to H3N2 peptide stimulation. We also did not account for non-spike T cell responses, including to other proteins such as matrix and nucleocapsid.

In COVID-19 donors there was no reduction in NK cell frequency in contrast to other studies demonstrating NK cell-inclusive leukopenia (213, 498). Overall, NK cells from COVID-19 patients in our study expressed fewer markers of activation and proliferation (CD69 and Ki-67) than demonstrated in other studies of severe COVID-19 (499). Similarly, this cohort of IAV patients also did not show any significant up-regulation of NK cell CD69 in comparison to cHCW. Increased CD69 expression on NK cells is seen in seasonal IAV infection, but less so in H1N1 swine flu infection, particularly in the $CD56^{++}$ populations, which indicates activation but may also facilitate migration to the lungs (33, 50).

A potential explanation for lack of IAV donor NK cell cytokine secretion may be due to the variation in influenza strains within the cohort, and the use of only H3N2 peptides for stimulation, as others identify a robust NK cell response from IAV patients (33, 50). NK cells from COVID-19 patients also did not have a robust response, which supports other research (498). *In vitro* experiments by Bortolotti *et al* demonstrate that SARS-CoV-2 spike epitopes presented by lung epithelial cells on HLA-E are recognised by, and induce expression of, the inhibitory receptor NKG2A on NK cells, which correlated with a lack of CD107a expression and potential loss of functionality (500). These data suggest that SARS-CoV-2 is able to down-regulate NK cell activation and inhibit a cytotoxic response, and overall suggests that COVID-19 does not induce NK cell activation and proliferation, thus potentially slowing early antiviral control and increasing disease severity (498). As

discussed previously, some IL-2 was detected from NK cells following stimulation with peptides, however this may be captured IL-2 secreted by other immune cells and detected on the NK cell IL-2R (438).

In contrast to previous data, B cell frequency did not increase with SARS-CoV-2 infection (214, 495), however B cells from both IAV and COVID-19 patients had a higher proportion of $IgG^{+}CD27^{+}$ switched memory B cells, also described in SARS-CoV-2 infection by Hartley *et al* (501).

Overall, both severe IAV and COVID-19 patients exhibit a hyperactivated and exhausted immune phenotype across measured populations. However, COVID-19 patients lacked some important markers of activation, e.g. CD25 expression and lower CD69 expression on T cells, and had a reduced response to peptide stimulation. Other immunopathology observed in severe cases of COVID-19 is varied, but includes infiltration of monocytes and lack of type I IFNs (214), with an inflammatory response including IL-1ß, IL-16 and IL-21 (502), and increased expression of pro-inflammatory mediators including CCL2, CCL3 and CXCL3 (503). Others (492) showed a strong IFN-α response in severe patients, and others, enhanced monocyte recruitment to the lungs potentially facilitating excessive inflammation (494). This aberrant activation and lack of coordinated functional response and subsequent effector cell exhaustion may be a driving cause behind increased mortality in SARS-CoV-2 infection. This data set is limited by the single time point analysis conducted on these patients, which was taken at the peak of disease severity but will not necessarily be at the same time point post-infection. Some donors also had limited PBMC availability, thus preventing further analysis into smaller immune cell populations, e.g., $CD56^{++}$ NK cells. The cohort in this analysis contributed towards a paper (504), which further describes how MAIT cell activation is a predictor of severe COVID-19 and IAV

pathophysiology and mortality and is correlated with broad and uncoordinated pro-inflammatory responses.

Youngs, J.*, Provine, N.M.*, Lim, N.*, **Sharpe, H**.[&], Amini, A.[&], Chen, Y-L.[&], Luo, J.[&], Edmans, M., Zacharapoulou, P., Luo, J., Chen, W., Sampson, O., Paton, R., Duncan, D.A., McNaughton, A., Miao, V.N., Leaver, S., Wyncoll, D., Oxford Immunology Network Covid-19 response T cell Consortium, Oxford Protective T cell Immunology for COVID-19 (OPTIC) Clinical team, Skelly, D.T., Barnes, E., Dunachie, S., Ogg, G., Lambe, T., Pavord, I., Shalek, A.K., Thompson, C., Xue, L., Macallan, D., Goulder, P.[#], Klenerman, P.[#], Bicanic, T.[#] Identification of immunologic correlates of fatality in critically ill COVID-19 patients. PLoS Pathogens. 2021 Sep 16;17(9):e1009804. PMID: 34529726

7.4. Papers published from pre-clinical and clinical trial work outlined in this chapter

Pre-clinical

Van Doremalen, N.*, Lambe, T.*, Spencer, A., Belij-Rammerstorfer, S., Purushotham, J., Port, J., Avanzato, V., Bushmaker, T., Flaxman, A., Ulaszewska, M., Feldmann, F., Allen, E., **Sharpe, H.,** Schulz, J., Holbrook, M., Okumura, A., Meade-White, K., Perez-Perez, L., Bissett, C., Gilbride, C., Williamson, B., Rosenke, R., Long, D., Ishwarbhai, A., Kailath, R., Rose, L., Morris, S., Powers, C., Lovaglio, J., Hanley, P., Scott, D., Saturday, G., de Witt, E., Gilbert, S.C.^, Munster, V^. *ChAdOx1 nCov-19 vaccination prevents SARS-CoV-2 pneumonia in rhesus macaques.* Nature. 2020 Oct; 586(7830):578-582. PMID: 32731258.

Graham, S.P., McLean, R.K.*, Spencer, A.J.*, Belij-Rammerstorfer, S., Wright, D., Ulaszewska, M., Edwards, J.C., Hayes, J., Martini, V., Thakur, N., Conceicao, C., Dietrich, I., Shelton, H., Waters, R., Ludi, A., Wilsden, G., Browning, C., Bialy, D., Bhat, S., Stevenson-Leggett, P., Hollinghurst, P., Gilbride, C., Pulido, D., Moffat, K., **Sharpe, H.,** Allen, E., Mioulet, V., Chui, C., Newman, J., Asfor, A.S., Burman, A., Crossley, S., Huo, J., Owens, R.J., Carroll, M., Hammond, J.A., Tchilian, E., Bailey, D., Charleston, B., Gilbert, S.C., Tuthill, T.J.^, Lambe, T^. *Evaluation of the immunogenicity of prime-boost vaccination with the replication-deficient viral vectored COVID-19 vaccine candidate ChAdOx1 nCoV-19.* Npj Vaccines. 5, 69 (2020). PMID: 32793398

Spencer, A.J.*, McKay, P.F.*, Belij-Rammerstorfer, S., Ulaszewska, M., Bissett, C.D, Hu, K., Samnuan, K., **Sharpe, H.R.,** Wright, D, Gilbride, C., Truby, A., Allen, E.R., Gilbert, S.C., Shattock, R.J., Lambe, T. *Heterologous vaccination regimens with self-amplifying RNA and adenoviral COVID vaccines induce superior immune responses than single dose vaccine regimens in mice.* Nature Communications. 2021. 17;12 (1), 2893. PMID: 34001897.

Provine, N.M., Amini, A., Garner, L.C., Spencer, A.J., Dold, C., Hutchings, C., Silva Reyes, L., FitzPatrick, M.E.B., Chinnakannan, S., Oguti, B., Raymond, M., Ulaszewska, M., Troise, F., **Sharpe, H**., Lambe, T., Capone, S., Folgori, A., Barnes, E., Rollier, C.S., Pollard, A.J., Klenerman, P. *MAIT cell activation augments adenovirus vector vaccine immunogenicity.* Science. 2021 Jan 29;371(6528)521-526. PMID: 22510029

Lambe, T.*, Spencer, A.J.*, Thomas, K.M.*, Thomas, S., White, A.D., Humphries, H.E., Wright, D., Belij-Rammerstorfer, S., Thakur, N., Conceicao, C., Alden, L., Allen, L., Aram, M.,

Bewley, K., Blunt, E., Brown, P., Cavell, B.E., Cobb, R., Fotheringham, S., Gilbride, C., Harris, D.J., Ho, C., Hunter, L., Kennard, C.L., Leung, S., Lucas, V., Ngabo, D., Ryan, K., **Sharpe, H.,** Sarfas, C., Sibley, L., Slack, G., Ulaszewska, M., Wand, M., Wilbin, N., Gleeson, F.V., Bailey, D., Sharpe, S., Charlton, S., Salguero, F.J., Carroll, M., Gilbert, S.C. *ChAdOx1 nCoV-19 protection against SARS-CoV-2 in rhesus macaque and ferret challenge models.* Nature communications biology. 2021 Jul 26; 4(1):915. PMID:34312487.

Clinical trials as part of the Oxford COVID vaccine trial group

Flaxman, A., Marchevsky, N., Jenkin, D., Aboagye, J., Aley, P.K., Angus, B., Belij-Rammerstorfer, S., Bibi, S., Bittaye, M., Cappuccini, F., Cicconi, P., Clutterbuck, E.A., Davies, S., Dejnirattisai, W., Dold, C., Ewer, K.J., Folegatti, P.M., Fowler, J., Hill, A.V.S., Kerridge, S., Minassian, A.M., Mongkolsapaya, J., Mujadidi, Y.F., Plested, E., Ramasamy, M.N., Robinson, H., Sanders, H., Sheehan, E., Smith, H., Snape, M.D., Song, R., Woods, D., Screaton, G., Gilbert, S.C., Voysey, M., Pollard, A.J., Lambe, T., and the Oxford COVID Vaccine Trial Group (Including **Hannah R Sharpe**). *Reactogenicity and immunogenicity after a late second dose or a third dose of ChAdOx1 nCoV-19 in the UK: a substudy of two randomised controlled trials (COV001 and COV002).* The Lancet. 2021 Sep 11;398(10304):981-990. PMID: 34480858

Emary, K.R.W., Golubchik, T., Aley,, P.K., Ariani, C.V., Angus,, B.J., Bibi, S., Blane, B., Bonsall, D., Cicconi, P., Charlton, S., Clutterbuck, E., Collins, A.M., Cox, T., Darton, T., Dold, C., Douglas, A., Duncan, C.J.A., Ewer, K., Flaxman, A., Faust, S.N., Ferreira, D.M., Feng, S., Finn, A., Folegatti, P.M., Fuskova, M., Galiza, E., Goodman, A.L., Green, C.M., Green, C.A., Greenland, M., Hallis, B., Heath, P.T., Hay, J., Hill, H.C., Jenkin, D., Kerridge, S., Lazarus, R.,

Libri, V., Lillie, P.J., Ludden, C., Marchevsky, N.G., Minassian, A.M., McGregor, A.C., Mujadidi, Y.F., Phillips, D.J., Plested, E., Pollock, K.M., Robinson, H., Smith, A., Song, R., Snape, M.D., Sutherland, R.K., Thomson, E.C., Toshner, M., Turner, D.P.J., Vekemans, J., Villafana, T.L., Williams, C.J., Hill, A.V.S.^, Lambe, T.^, Gilbert, S. C.^, Voysey, M.^, Ramasamy, M.N.^, Pollard, A.J.^, The COVID-19 Genomics UK consortium and the Oxford COVID Vaccine Trial Group (including **Hannah R Sharpe**). *Efficacy of ChAdOx1 nCoV-19 (AZD1222) vaccine against SARS-CoV-2 VOC 202012/01 (B.1.1.7).* Lancet. 2021 Apr10; 397 (10282): 1351-1362. PMID: 33798499.

Voysey, M*. Costa Clemens, S.A*., Madhi, S.A., Weckx, L.Y.*, Folegatti, P.M.*, Aley, P.K., Angus, B., Baillie, V.L., Barnabas, S.L., Bhorat, Q.E., Bibi, S., Briner, C., Cicconi, P., Clutterbuck, E.A., Collins, A.M., Cutland, C.L., Darton, T.C., Dheda, K., Dold, C., Duncan, C.J.A., Emary, K.R.W., Ewer, K.J., Flaxman, A., Fairlie, L., Faust, S.N., Feng, S., Ferriera, D.M., Finn, A., Galiza, E., Goodman, A.L., Green, C.M., Green, C.A., Greenland, M., Hill, C., Hill, H.C., Hirsch, I., Izu, A., Jenkin, D., Joe, C.C.D., Kerridge, S., Koen, A., Kwatra, G., Lazarus, R., Libri, V., Lillie, P.J., Marchevsky, N.G., Marshall, R.P., Mendes, A.V.A., Milan, E.P., Minassian, A.M., McGregor, A., Mujadidi, Y.F., Nana, A., Padayachee, S.D., Phillips, D.J., Pittella, A., Plested, A., Pollock, K.M., Ramasamy, M.N., Ritchie, A.J., Robinson, H., Schwarzbold, A.V., Smith, A., Song, R., Snape, M.D., Sprinz, E., Sutherland, R.K., Thomson, E.C., Török, M.E., Toshner, M., Turner, D.P.J., Vekemans, J., Villafana, T.L., White, T., Williams, C.J., Douglas, A.D.^, Hill, A.V.S.^, Lambe, T.^, Gilbert, S.C.^, Pollard, A.J.^, and the Oxford COVID Vaccine Trial Group (including **Hannah R Sharpe**). *Single dose administration, and the influence of the timing of the booster dose on immunogenicity and*

efficacy of ChAdOx1 nCoV-19 (AZD1222) vaccine. Lancet. March 2021. 397, 10277. P881-891. PMID: 33617777

Barrett, J.R.*, Belij-Rammerstorfer, S.*, Dold, C.*, Ewer, K.J.*, Folegatti, P.M.*, Gilbride, C.*, Halkerston, R.*, Hill, J.*, Jenkin, D.*, Stockdale, L.*, Verheul, M.K*., Aley, P., Angus, B., Bellamy, D., Berrie, E., Bibi, S., Bittaye, M., Carroll, M.W., Cavell, B., Clutterbuck, E.A., Edwards, N., Flaxman, A., Fuskova, M., Gorringe, A., Green, C.M., Hallis, B., Kerridge, S., Lawrie, A.M., Linder, A., Liu, X., Madhavan, M., Makinson, R., Mellors, J., Minassian, A., Moore, M., Mujadidi, Y., Plested, E., Poulton, I., Ramasamy, M.N., Robinson, H., Rollier, C.S., Song, R., Snape, M.D., Tarrant, R., Taylor, S., Thomas, K.M., Voysey, M., Watson, M.E.E., Wright, D., Douglas, A., Hill, A.V.S.^, Lambe, T.^, Gilbert, S.^, Pollard., A.J.^, and the Oxford COVID Vaccine Trial Group (Including **Hannah Sharpe**). *Phase I/II trial of SARS-CoV-2 vaccine ChAdOx1 nCoV-19 with a booster dose induces multifunctional antibody responses. Nature Medicine. 2021 Feb; 27(2)279-288. PMID 33335322*

Voysey, M.*, Costa Clemens, S.A.*, Madhi, S.A.*, Weckx, L.Y.*, Folegatti, P.M.*, Aley, P.K., Angus, B., Baillie, V.L., Barnabas, S.L., Bhorat, Q.E., Bibi, S., Briner, C., Cicconi, P., Collins, A.M., Colin-Jones, R., Cutland, C.L., Darton, T.C., Dheda, K., Duncan, C.J.A., Emary, K.R.W., Ewer, K.J., Fairlie, L., Faust, S.N., Feng, S., Ferreira, D.M., Finn, A., Goodman, A.L., Green, C.M., Green, C.A., Heath, P.T., Hill, C., Hill, H., Hirsch, I., Hodgson, S.H.C., Izu, A., Jackson, S., Jenkin, D., Joe, C.C.D., Kerridge, S., Koen, A., Kwatra, G., Lazarus, R., Lawrie, A.M., Lelliott, A., Libri, V., Lillie, P.J., Mallory, R., Mendes, A.V.A., Milan, E.P., Minassian, A.M., McGregor, A., Morrison, H. Mujadidi, Y.F., Nana, A., O'Reilly, P.J., Padayachee, S.D., Pittella, A., Plested, E., Pollock, K.M., Ramasamy, M.N., Rhead, S., Schwarzbold, A.V., Singh, N.,

Smith, A., Song, R., Snape, M.D., Sprinz, E., Sutherland, R.K., Tarrant, R., Thomson, E.C., Török, M.E., Toshner, M., Turner, D.P.J., Vekemans, J., Villafana, T.L., Watson, M.E.E., Williams, C.J., Douglas, A.D.^, Hill, A.V.S.^, Lambe, T.^, Gilbert, S.C.^, Pollard, A.J.^, and the Oxford COVID Vaccine Trial Group (including **Hannah R Sharpe**) *Safety and efficacy of the ChAdOx1 nCoV-19 vaccine (AZD1222) against SARS-CoV-2: an interim analysis of four randomised controlled trials in Brazil, South Africa, and the UK.* The Lancet. 2020. DOI: 10.1016/S0140-6736(20)32661-1

Ramasamy, M.N.*, Minassian, A.M.*, Ewer, K.J.*, Flaxman, A.L.*, Folegatti, P.M.*, Owens, D.R.*, Voysey, M.*, Aley, P.K., Angus, B., Babbage, G., Belij-Rammerstorfer, S., Berry, L., Bibi, S., Bittaye, M., Cathie, K., Chappell, H., Charlton, S., Cicconi, P., Clutterbuck, E.A., Colin-Jones, R., Dold, C., Emary, K.R.W., Fedosyuk, S., Fuskova, M., Gbesemete, D., Green, C., Hallis, B., Hou, M.M., Jenkin, D., Joe, C.C.D., Kelly, E.K., Kerridge, S., Lawrie, A.M., Lelliott, A., Nwe Lwin, M., Makinson, R., Marchevsky, N.G., Mujadidi, Y., Munro, A.P.S., Pacurar, M., Rand, J., Rawlinson, T., Rhead, S., Robinson, H., Ritchie, A.J., Ross Russell, A.L., Saich, S., Singh, N., Smith, C.C., Snape, M.D., Song, R., Tarrant, R., Themistocleous, Y., Thomas, K.M., Villafana, T.L., Warren, S.C., Watson, E.E., Douglas, A.D.^, Hill, A.V.S.^, Lambe, T.^, Gilbert, S.C.^, Faust, S.N.^, Pollard, A.J.^, and the Oxford COVID Vaccine Trial Group (including **Hannah R Sharpe**) *Safety and Immunogenicity of ChAdOx1 nCoV-19 (AZD1222) vaccine administered in a prime-boost regimen in older adults (COV002): a Phase 2/3 single blind, randomised controlled trial.* Lancet. 2020 https://doi.org/10.1016/S0140-6736(20)32466-1

Folegatti, P.M.*, Ewer, K.J.*, Aley, P., Angus, B., Becker, S., Belij-Rammerstorfer, S., Bellamy, D., Bibi, S., Bittaye, M., Clutterbuck, E., Dold, C., Faust, S.N., Finn, A., Flaxman, A.L.,

Hallis, B., Heather, P., Jenkin, D., Lazarus, R., Makinson, R., Minassian, A., Pollock, K.M., Ramasamy, M.N., Robinson, H., Snape, M.D., Tarrant, R., Voysey, M., Green, C.M.^, Douglas, S.^, Hill, A.V.S.^, Lambe, T.^, Gilbert, S.^, Pollard, A.J.^, and the Oxford COVID Vaccine Trial Group (Including **Hannah R Sharpe**). *Safety and immunogenicity of the ChAdOx1 nCoV-19 vaccine against SARS-CoV-2: a preliminary report of a Phase 1/2, single-blind, randomised control trial.* The Lancet. 396, 10249, P467-478. 2020. PMID: 32702298

Chapter 8

Conclusions and future directions

Chapter 8 : Conclusions and future directions

8.1. Overview

There is a global need for vaccine platforms that are immunogenic and can be manufactured at speed and low cost. The viral vector ChAdOx1 was developed at the Jenner Institute (165), and was used in a number of early stage clinical trials prior to 2020 and these trials demonstrated both the safety and immunogenicity of this platform technology (178, 179, 181). The importance of this vaccine platform was highlighted during this D.Phil. by the ongoing SARS-CoV-2 pandemic, and the development of ChAdOx1 nCoV-19 (now known as Vaxzevria), which was demonstrated to be efficacious against preventing COVID-19 (223, 505) and over 1 billion doses have now been released worldwide (506). ChAdOx1-vectored vaccines are now in clinical trials for other pathogens including bivalent Ebola vaccines, Rift Valley fever, Chikungunya virus and Zika virus (table 1.4).

Cytomegalovirus has evolved alongside humans for millennia (262). In the vast majority of infections, CMV does not generate a substantial immunopathologic response and remains latent in the host for life. However, HCMV elicits a terminally differentiated profile on immune cells that reflects immunosenescence in older adults (312, 475). This anergy correlates with a lack of antigen-specific immunogenicity conducted in younger and older adults from the UK and sub-Saharan Africa predominantly with influenza vaccination (336-339, 479), although other trials have not described such an effect (328, 347). It is therefore important to understand how CMV affects immunogenicity and differentiation of immune cells, and what roles age, vaccine regimen or type of vaccine play in exacerbating the impact.

Due to the SARS-CoV-2 pandemic, the aims of this thesis were substantially changed and, in this thesis, I contribute in part to our understanding of how viral vectored vaccines including ChAdOx1 activate innate and adaptive immune cells in pre-clinical and clinical settings, and how infection with CMV alters the immune response to viral vector vaccination.

8.2. Summary, limitations and future directions

8.2.1. Vaccination with single dose, homologous, or heterologous viral vector vaccines alter the activation and senescence profile of NK cells in a mouse model

The work completed in chapter 3 outlines how vaccination with ChAdOx1 and/or MVA changes the activation and surface marker profile of NK cells in mice. NK cells are not frequently studied as part of vaccine responses to clinical trials, although they respond robustly and may contribute towards overall immunogenicity (363, 364, 402, 507). Here, I demonstrate that heterologous ChAdOx1-MVA vaccination activates NK cells and induces the highest frequency of $CD107a^{+}IFN\text{-}\gamma^{+}$ NK cells following stimulation, which further exemplifies how heterologous prime-boost vaccination provides a more robust immune response compared to single dose or homologous boost vaccination, and that NK cells contribute towards antigen-specific cytotoxicity. NK cell depletion reduces the frequency of $CD8^{+}$ T_{EM} cells and increases the frequency of $CD8^{+}$ T_{EFF} cells, however increases IFN-γ secretion and CD107a expression within each T cell subset following heterologous viral vector vaccination. This supports previous research that outlines how NK cells act as negative regulators of $CD8^{+}$ T cell activity during viral infection and vaccination (7, 369, 418, 508), however may also promote formation of T cell memory populations.

Vaccination regimens including MVA enhance an immature and less activated systemic NK cell profile, indicated by a reduction in $CD11b^+$ and $Ly49H^+$ NK cells. ChAdOx1 and MVA vaccination also instigate different cell death pathways following vaccination similarly to adenovirus and Vaccinia virus, the live viruses from which the vectors were derived respectively. ChAdOx1 activates the apoptosis cell death pathway, whereas MVA instigates necroptotic cell death in NK cells. This reduction in NK cell maturity and increased frequency of necroptosis has been previously described with Vaccinia virus (406, 413), but not for MVA vaccination.

The limitations of these results are that I solely used young naïve C57BL/6J mice which had no previous pathogen or vaccine exposure. This would limit the size of T cell memory populations, which will be an inaccurate reflection on memory populations in humans with a wider exposure to vaccines and pathogens. A clear future direction would be to investigate whether MVA vaccination in humans induces the same loss of NK cell maturity and potential increase in necroptosis as demonstrated in the preclinical model, as if so, this may suggest MVA transiently reduces NK cell functional capacity in the weeks following vaccination. Furthermore, these data warrant investigation into whether route of vaccination affects innate immune cell activation; as previously demonstrated, differential humoral and cellular immunogenicity can be generated by either intramuscular or intranasal Ad-vector vaccination (509, 510), and this should be further expanded into the differences in systemic and tissue-resident NK cell responses following vaccination.

8.2.2. Single dose and heterologous boost viral vector vaccinations activate NK cells and T cells

A single dose of ChAdOx1 activates NK cells and T cells up to 28 days post-vaccination in humans, and heterologous ChAdOx1 and MVA vaccination induces robust T cell responses without increasing cell senescence at 2 weeks post-boost. These data demonstrate that heterologous prime-boost vaccination enhances durability and functionality of T cell immune responses (138, 146, 166, 175, 179).

Analysis on these data was conducted retrospectively on samples across multiple trials with non-matching time points or group sizes. Therefore, direct immunogenicity comparisons cannot be made between groups in different trials. Furthermore, the vaccines studied have different transgene antigens, which may alter vaccine immunogenicity. A direction for future research is further investigation into heterologous vaccination with adenovirus and mRNA vaccines. Currently, several trials are underway to assess different combinations of heterologous vaccination in context of SARS-CoV-2 vaccination (511). From these trials, it would be interesting to investigate to what extent this prime-boost combination enhances immune responses in non-classically studied immune compartments.

8.2.3. MCMV activates tissue resident NK cells and non-classical T cells

I also began to explore the use of a MCMV as a model for HCMV in the context of vaccine immunogenicity. I undertook analysis into whether acute and chronic MCMV activates MAIT cells, and circulating and tissue-resident NK cells. The data collected in this chapter demonstrate that MCMV differentially activates MAIT cells, T cells, and different subsets of NK cells during acute infection. Unlike infection with influenza (89), MCMV does not

prominently activate MAIT cells but does activate T cells up to day 7 post-infection, indicating a MCMV may have a specific mechanism to prevent MAIT cell activation. Furthermore, MCMV infection differentially activates cNK and trNK cells in the spleen and liver. Splenic cNK cells elicit a robust response to MCMV, but it is the trNK cells in the liver that are most cytotoxic during acute infection. This gives insight into tissue-dependent viral regulation by different cell subsets.

One limitation of these studies is the use of a fixed, single inoculating dose of MCMV. This was to maintain comparisons between experiments; however, this method does not take into account multiple potential infections with different titres of virus that would occur across a natural life course in mice and humans (512, 513). This may explain why no significant difference was seen between vaccinated mice with and without chronic MCMV infection. These data also highlight some of the differences that HCMV and MCMV exert on their respective host immune systems, and demonstrate how the mouse immune system is able to undergo less terminal differentiation whilst maintaining viral latency. Possible explanations for this include differences in the level of pathogen exposure in SPF-housed animal experiences compared with a human, different lifespan with recurrent and concurrent pathogen infection and differences in immune physiology. However, the mouse model is a good tool to understand the fundamental interactions of MCMV with the immune system, which could be used to influence further vaccine design. There is much scope to follow this research with exploration into how multiple acute or chronic infections can modulate the cytotoxic response to vaccination. This could be extended into further developing the infection and vaccination model by investigating whether parameters including duration of MCMV infection and initial viral dose affects vaccine immunogenicity, and improve our understanding of cytomegalovirus and immune exhaustion.

8.2.4. CMV seropositivity induces a terminally differentiated immune phenotype and reduces heterologous vaccine immunogenicity

The immunogenicity of single dose or homologous boost of ChAdOx1 is not reduced with CMV seropositivity. This was demonstrated in trials including younger (18-55 years old) and older (55+ years old) adults and across two trials with different vaccine antigens. These data do show that CMV does have a significant burden on the immune system, demonstrated by expanded populations of terminally differentiated $KLRG1^{+}CD57^{+}$ T cells, a higher proportion of $CD45RA^{+}$ TEMRA cells, and NK cells with a $CD57^{+}$ phenotype. However, unlike other studies, CMV seropositive donors did not have significantly reduced antigen-specific T cell IFN-γ and antibody secretion following vaccination. CMV-seropositive donors did have a significant reduction in $CD4^{+}$ T cell polyfunctionality following a single dose of ChAdOx1, and a reduction of T cell-mediated immunogenicity associated with CMV seropositivity following heterologous prime-boost vaccination with ChAd-vectored vaccines and MVA. Encouragingly, these data demonstrate that CMV seropositivity is not impacting the immunogenicity of ChAdOx1 nCoV-19, which is important considering the global use of this vaccine predominantly in LMIC.

Although the trials analysed for this study were conducted on healthy adults living in the UK, the data presented within this thesis are promising towards vaccine immunogenicity across the world. It is important to consider that the global burden of CMV infection changes depending on socioeconomic status and age (264), however, these data indicate that CMV infection does not reduce immunogenicity of homologous-boosted ChAdOx1-vectored vaccines, including ChAdOx1 nCoV-19. These data also give an insight into how CMV affects immune phenotypes across a cohort of vaccine trial participants, and provide evidence for CMV screening during larger vaccine trials in the future. This would

generate more highly powered data sets to analyse in greater depth how CMV seropositivity affects T cell and antibody immunogenicity across different trials and whether varying CMV burden affects the outcome of vaccination. Given that many diseases for outbreak pathogens occur in regions of high CMV seroprevalence, future research will have to include direct comparisons between vaccine trials in the UK and in countries where the disease is endemic (for example, sub-Saharan Africa and ebolavirus, as detailed in (339)). This will also give an insight into whether the immunogenicity of different vaccine platforms are differentially affected by CMV infection.

From these data presented in this thesis and in other research, it is likely that frequency of CMV exposure, age of first infection, and burden of other endemic pathogens may each contribute in part towards alterations in vaccine immunogenicity, with no one factor being the sole driver towards impacting of immunogenicity. Endemic infections including malaria parasitaemia also impair the immune response following infection (514), therefore there will need to be further research into the combinatorial effect of CMV and other endemic pathogens in regions of targeted vaccine trials and rollout.

8.3. Final remarks

The work presented in this thesis contributes towards our understanding of viral vector vaccination and CMV infection on immune cell populations that are not traditionally studied in vaccinology. In order to develop vaccines that induce optimal immune responses, it is vital to understand how all compartments of the immune system respond and contribute towards immunogenicity and ultimately efficacy. It is also of importance to undertake research into pathogens that alter vaccine immunogenicity and how this could impact the outcome of clinical trials in target vaccine populations.

References

1. Artis D, Spits H. The biology of innate lymphoid cells. Nature. 2015;517(7534):293-301.
2. Pulendran B, S Arunachalam P, O'Hagan DT. Emerging concepts in the science of vaccine adjuvants. Nat Rev Drug Discov. 2021.
3. Dunkelberger JR, Song WC. Complement and its role in innate and adaptive immune responses. Cell Res. 2010;20(1):34-50.
4. Forrest C, Gomes A, Reeves M, Male V. NK Cell Memory to Cytomegalovirus: Implications for Vaccine Development. Vaccines (Basel). 2020;8(3).
5. Paust S, Blish CA, Reeves RK. Redefining Memory: Building the Case for Adaptive NK Cells. J Virol. 2017;91(20).
6. Min-Oo G, Kamimura Y, Hendricks DW, Nabekura T, Lanier LL. Natural killer cells: walking three paths down memory lane. Trends Immunol. 2013;34(6):251-8.
7. Waggoner SN, Cornberg M, Selin LK, Welsh RM. Natural killer cells act as rheostats modulating antiviral T cells. Nature. 2011;481(7381):394-8.
8. Zhou J, Peng H, Li K, Qu K, Wang B, Wu Y, et al. Liver-Resident NK Cells Control Antiviral Activity of Hepatic T Cells via the PD-1-PD-L1 Axis. Immunity. 2019;50(2):403-17.e4.
9. Chiossone L, Chaix J, Fuseri N, Roth C, Vivier E, Walzer T. Maturation of mouse NK cells is a 4-stage developmental program. Blood. 2009;113(22):5488-96.
10. Krueger PD, Lassen MG, Qiao H, Hahn YS. Regulation of NK cell repertoire and function in the liver. Crit Rev Immunol. 2011;31(1):43-52.
11. Hoare HL, Sullivan LC, Clements CS, Ely LK, Beddoe T, Henderson KN, et al. Subtle changes in peptide conformation profoundly affect recognition of the non-classical MHC class I molecule HLA-E by the CD94-NKG2 natural killer cell receptors. J Mol Biol. 2008;377(5):1297-303.
12. Dai KZ, Ryan JC, Naper C, Vaage JT. Identification of MHC Class Ib Ligands for Stimulatory and Inhibitory Ly49 Receptors and Induction of Potent NK Cell Alloresponses in Rats. J Immunol. 2018;200(8):2847-59.
13. Pende D, Falco M, Vitale M, Cantoni C, Vitale C, Munari E, et al. Killer Ig-Like Receptors (KIRs): Their Role in NK Cell Modulation and Developments Leading to Their Clinical Exploitation. Front Immunol. 2019;10:1179.
14. Anfossi N, André P, Guia S, Falk CS, Roetynck S, Stewart CA, et al. Human NK cell education by inhibitory receptors for MHC class I. Immunity. 2006;25(2):331-42.
15. Marquardt N, Ivarsson MA, Blom K, Gonzalez VD, Braun M, Falconer K, et al. The Human NK Cell Response to Yellow Fever Virus 17D Is Primarily Governed by NK Cell Differentiation Independently of NK Cell Education. J Immunol. 2015;195(7):3262-72.
16. Kim S, Poursine-Laurent J, Truscott SM, Lybarger L, Song YJ, Yang L, et al. Licensing of natural killer cells by host major histocompatibility complex class I molecules. Nature. 2005;436(7051):709-13.
17. Naiyer MM, Cassidy SA, Magri A, Cowton V, Chen K, Mansour S, et al. KIR2DS2 recognizes conserved peptides derived from viral helicases in the context of HLA-C. Sci Immunol. 2017;2(15).
18. Wagstaffe HR, Nielsen CM, Riley EM, Goodier MR. IL-15 Promotes Polyfunctional NK Cell Responses to Influenza by Boosting IL-12 Production. J Immunol. 2018;200(8):2738-47.

19. Nguyen KB, Salazar-Mather TP, Dalod MY, Van Deusen JB, Wei XQ, Liew FY, et al. Coordinated and distinct roles for IFN-alpha beta, IL-12, and IL-15 regulation of NK cell responses to viral infection. J Immunol. 2002;169(8):4279-87.
20. Feng Y, Daley-Bauer LP, Roback L, Potempa M, Lanier LL, Mocarski ES. Caspase-8 restricts natural killer cell accumulation during MCMV Infection. Med Microbiol Immunol. 2019;208(3-4):543-54.
21. Orange JS, Biron CA. An absolute and restricted requirement for IL-12 in natural killer cell IFN-gamma production and antiviral defense. Studies of natural killer and T cell responses in contrasting viral infections. J Immunol. 1996;156(3):1138-42.
22. Jost S, Tomezsko PJ, Rands K, Toth I, Lichterfeld M, Gandhi RT, et al. CD4+ T-cell help enhances NK cell function following therapeutic HIV-1 vaccination. J Virol. 2014;88(15):8349-54.
23. Hayakawa Y, Smyth MJ. CD27 dissects mature NK cells into two subsets with distinct responsiveness and migratory capacity. J Immunol. 2006;176(3):1517-24.
24. Martín-Fontecha A, Thomsen LL, Brett S, Gerard C, Lipp M, Lanzavecchia A, et al. Induced recruitment of NK cells to lymph nodes provides IFN-gamma for T(H)1 priming. Nat Immunol. 2004;5(12):1260-5.
25. Smyth MJ, Cretney E, Takeda K, Wiltrout RH, Sedger LM, Kayagaki N, et al. Tumor necrosis factor-related apoptosis-inducing ligand (TRAIL) contributes to interferon gamma-dependent natural killer cell protection from tumor metastasis. J Exp Med. 2001;193(6):661-70.
26. Suliman S, Geldenhuys H, Johnson JL, Hughes JE, Smit E, Murphy M, et al. Bacillus Calmette-Guérin (BCG) Revaccination of Adults with Latent Mycobacterium tuberculosis Infection Induces Long-Lived BCG-Reactive NK Cell Responses. J Immunol. 2016;197(4):1100-10.
27. Trittel S, Chambers BJ, Heise U, Guzmán CA, Riese P. Key features and homing properties of NK cells in the liver are shaped by activated iNKT cells. Sci Rep. 2019;9(1):16362.
28. Daussy C, Faure F, Mayol K, Viel S, Gasteiger G, Charrier E, et al. T-bet and Eomes instruct the development of two distinct natural killer cell lineages in the liver and in the bone marrow. J Exp Med. 2014;211(3):563-77.
29. Hayakawa Y, Andrews DM, Smyth MJ. Subset analysis of human and mouse mature NK cells. Methods Mol Biol. 2010;612:27-38.
30. Marquardt N, Béziat V, Nyström S, Hengst J, Ivarsson MA, Kekäläinen E, et al. Cutting edge: identification and characterization of human intrahepatic CD49a+ NK cells. J Immunol. 2015;194(6):2467-71.
31. Peng H, Jiang X, Chen Y, Sojka DK, Wei H, Gao X, et al. Liver-resident NK cells confer adaptive immunity in skin-contact inflammation. J Clin Invest. 2013;123(4):1444-56.
32. Silva A, Andrews DM, Brooks AG, Smyth MJ, Hayakawa Y. Application of CD27 as a marker for distinguishing human NK cell subsets. Int Immunol. 2008;20(4):625-30.
33. Jost S, Quillay H, Reardon J, Peterson E, Simmons RP, Parry BA, et al. Changes in cytokine levels and NK cell activation associated with influenza. PLoS One. 2011;6(9):e25060.
34. Fehniger TA, Cooper MA, Nuovo GJ, Cella M, Facchetti F, Colonna M, et al. CD56bright natural killer cells are present in human lymph nodes and are activated by T

cell-derived IL-2: a potential new link between adaptive and innate immunity. Blood. 2003;101(8):3052-7.
35. White MJ, Nielsen CM, McGregor RH, Riley EH, Goodier MR. Differential activation of CD57-defined natural killer cell subsets during recall responses to vaccine antigens. Immunology. 2014;142(1):140-50.
36. Vossen MT, Matmati M, Hertoghs KM, Baars PA, Gent MR, Leclercq G, et al. CD27 defines phenotypically and functionally different human NK cell subsets. J Immunol. 2008;180(6):3739-45.
37. Björkström NK, Ljunggren HG, Michaëlsson J. Emerging insights into natural killer cells in human peripheral tissues. Nat Rev Immunol. 2016;16(5):310-20.
38. Nielsen CM, White MJ, Goodier MR, Riley EM. Functional Significance of CD57 Expression on Human NK Cells and Relevance to Disease. Front Immunol. 2013;4:422.
39. Dodard G, Tata A, Erick TK, Jaime D, Miah SMS, Quatrini L, et al. Inflammation-Induced Lactate Leads to Rapid Loss of Hepatic Tissue-Resident NK Cells. Cell Rep. 2020;32(1):107855.
40. Simonetta F, Pradier A, Roosnek E. T-bet and Eomesodermin in NK Cell Development, Maturation, and Function. Front Immunol. 2016;7:241.
41. Sojka DK, Plougastel-Douglas B, Yang L, Pak-Wittel MA, Artyomov MN, Ivanova Y, et al. Tissue-resident natural killer (NK) cells are cell lineages distinct from thymic and conventional splenic NK cells. Elife. 2014;3:e01659.
42. Weizman OE, Adams NM, Schuster IS, Krishna C, Pritykin Y, Lau C, et al. ILC1 Confer Early Host Protection at Initial Sites of Viral Infection. Cell. 2017;171(4):795-808.e12.
43. Paust S, Gill HS, Wang BZ, Flynn MP, Moseman EA, Senman B, et al. Critical role for the chemokine receptor CXCR6 in NK cell-mediated antigen-specific memory of haptens and viruses. Nat Immunol. 2010;11(12):1127-35.
44. Hudspeth K, Donadon M, Cimino M, Pontarini E, Tentorio P, Preti M, et al. Human liver-resident CD56(bright)/CD16(neg) NK cells are retained within hepatic sinusoids via the engagement of CCR5 and CXCR6 pathways. J Autoimmun. 2016;66:40-50.
45. Stegmann KA, Robertson F, Hansi N, Gill U, Pallant C, Christophides T, et al. CXCR6 marks a novel subset of T-bet(lo)Eomes(hi) natural killer cells residing in human liver. Sci Rep. 2016;6:26157.
46. Cuff AO, Robertson FP, Stegmann KA, Pallett LJ, Maini MK, Davidson BR, et al. Eomeshi NK Cells in Human Liver Are Long-Lived and Do Not Recirculate but Can Be Replenished from the Circulation. J Immunol. 2016;197(11):4283-91.
47. Aw Yeang HX, Piersma SJ, Lin Y, Yang L, Malkova ON, Miner C, et al. Cutting Edge: Human CD49e- NK Cells Are Tissue Resident in the Liver. J Immunol. 2017;198(4):1417-22.
48. Harmon C, Robinson MW, Fahey R, Whelan S, Houlihan DD, Geoghegan J, et al. Tissue-resident Eomes(hi) T-bet(lo) CD56(bright) NK cells with reduced proinflammatory potential are enriched in the adult human liver. Eur J Immunol. 2016;46(9):2111-20.
49. Male V. Liver-Resident NK Cells: The Human Factor. Trends Immunol. 2017;38(5):307-9.
50. Scharenberg M, Vangeti S, Kekäläinen E, Bergman P, Al-Ameri M, Johansson N, et al. Influenza A Virus Infection Induces Hyperresponsiveness in Human Lung Tissue-Resident and Peripheral Blood NK Cells. Front Immunol. 2019;10:1116.

51. Cooper MA, Elliott JM, Keyel PA, Yang L, Carrero JA, Yokoyama WM. Cytokine-induced memory-like natural killer cells. Proc Natl Acad Sci U S A. 2009;106(6):1915-9.
52. Nabekura T, Lanier LL. Tracking the fate of antigen-specific versus cytokine-activated natural killer cells after cytomegalovirus infection. J Exp Med. 2016;213(12):2745-58.
53. Wagstaffe HR, Pickering H, Houghton J, Mooney JP, Wolf AS, Prevatt N, et al. Influenza Vaccination Primes Human Myeloid Cell Cytokine Secretion and NK Cell Function. J Immunol. 2019;203(6):1609-18.
54. Keppel MP, Yang L, Cooper MA. Murine NK cell intrinsic cytokine-induced memory-like responses are maintained following homeostatic proliferation. J Immunol. 2013;190(9):4754-62.
55. Min-Oo G, Lanier LL. Cytomegalovirus generates long-lived antigen-specific NK cells with diminished bystander activation to heterologous infection. J Exp Med. 2014;211(13):2669-80.
56. Nikzad R, Angelo LS, Aviles-Padilla K, Le DT, Singh VK, Bimler L, et al. Human natural killer cells mediate adaptive immunity to viral antigens. Sci Immunol. 2019;4(35).
57. Hammer Q, Rückert T, Borst EM, Dunst J, Haubner A, Durek P, et al. Peptide-specific recognition of human cytomegalovirus strains controls adaptive natural killer cells. Nat Immunol. 2018;19(5):453-63.
58. Saghafian-Hedengren S, Sohlberg E, Theorell J, Carvalho-Queiroz C, Nagy N, Persson JO, et al. Epstein-Barr virus coinfection in children boosts cytomegalovirus-induced differentiation of natural killer cells. J Virol. 2013;87(24):13446-55.
59. Björkström NK, Lindgren T, Stoltz M, Fauriat C, Braun M, Evander M, et al. Rapid expansion and long-term persistence of elevated NK cell numbers in humans infected with hantavirus. J Exp Med. 2011;208(1):13-21.
60. Brownlie D, Scharenberg M, Mold JE, Hård J, Kekäläinen E, Buggert M, et al. Expansions of adaptive-like NK cells with a tissue-resident phenotype in human lung and blood. Proc Natl Acad Sci U S A. 2021;118(11).
61. O'Leary JG, Goodarzi M, Drayton DL, von Andrian UH. T cell- and B cell-independent adaptive immunity mediated by natural killer cells. Nat Immunol. 2006;7(5):507-16.
62. Gillard GO, Bivas-Benita M, Hovav AH, Grandpre LE, Panas MW, Seaman MS, et al. Thy1+ NK [corrected] cells from vaccinia virus-primed mice confer protection against vaccinia virus challenge in the absence of adaptive lymphocytes. PLoS Pathog. 2011;7(8):e1002141.
63. Reeves RK, Li H, Jost S, Blass E, Schafer JL, Varner V, et al. Antigen-specific NK cell memory in rhesus macaques. Nat Immunol. 2015;16(9):927-32.
64. Lam VC, Lanier LL. NK cells in host responses to viral infections. Curr Opin Immunol. 2017;44:43-51.
65. Dou Y, Fu B, Sun R, Li W, Hu W, Tian Z, et al. Influenza vaccine induces intracellular immune memory of human NK cells. PLoS One. 2015;10(3):e0121258.
66. Smith-Garvin JE, Koretzky GA, Jordan MS. T cell activation. Annu Rev Immunol. 2009;27:591-619.
67. van der Merwe PA, Dushek O. Mechanisms for T cell receptor triggering. Nat Rev Immunol. 2011;11(1):47-55.

68. Laydon DJ, Bangham CR, Asquith B. Estimating T-cell repertoire diversity: limitations of classical estimators and a new approach. Philos Trans R Soc Lond B Biol Sci. 2015;370(1675).
69. Clark BL, Thomas PG. A Cell for the Ages: Human γδ T Cells across the Lifespan. Int J Mol Sci. 2020;21(23).
70. Guermonprez P, Valladeau J, Zitvogel L, Théry C, Amigorena S. Antigen presentation and T cell stimulation by dendritic cells. Annu Rev Immunol. 2002;20:621-67.
71. Bonilla FA, Oettgen HC. Adaptive immunity. J Allergy Clin Immunol. 2010;125(2 Suppl 2):S33-40.
72. Redmond WL, Ruby CE, Weinberg AD. The role of OX40-mediated co-stimulation in T-cell activation and survival. Crit Rev Immunol. 2009;29(3):187-201.
73. D'Cruz LM, Rubinstein MP, Goldrath AW. Surviving the crash: transitioning from effector to memory CD8+ T cell. Semin Immunol. 2009;21(2):92-8.
74. Klenerman P, Hill A. T cells and viral persistence: lessons from diverse infections. Nat Immunol. 2005;6(9):873-9.
75. Vinuesa CG, Cyster JG. How T cells earn the follicular rite of passage. Immunity. 2011;35(5):671-80.
76. Mosmann TR, Coffman RL. TH1 and TH2 cells: different patterns of lymphokine secretion lead to different functional properties. Annu Rev Immunol. 1989;7:145-73.
77. Hauben E, Roncarolo MG. Human CD4+ regulatory T cells and activation-induced tolerance. Microbes Infect. 2005;7(7-8):1023-32.
78. Craft JE. Follicular helper T cells in immunity and systemic autoimmunity. Nat Rev Rheumatol. 2012;8(6):337-47.
79. Crotty S. T follicular helper cell differentiation, function, and roles in disease. Immunity. 2014;41(4):529-42.
80. Linterman MA, Pierson W, Lee SK, Kallies A, Kawamoto S, Rayner TF, et al. Foxp3+ follicular regulatory T cells control the germinal center response. Nat Med. 2011;17(8):975-82.
81. Shulman Z, Gitlin AD, Targ S, Jankovic M, Pasqual G, Nussenzweig MC, et al. T follicular helper cell dynamics in germinal centers. Science. 2013;341(6146):673-7.
82. Schmitt EG, Williams CB. Generation and function of induced regulatory T cells. Front Immunol. 2013;4:152.
83. Veiga-Parga T, Sehrawat S, Rouse BT. Role of regulatory T cells during virus infection. Immunol Rev. 2013;255(1):182-96.
84. Long SA, Buckner JH. CD4+FOXP3+ T regulatory cells in human autoimmunity: more than a numbers game. J Immunol. 2011;187(5):2061-6.
85. Le Bourhis L, Martin E, Péguillet I, Guihot A, Froux N, Coré M, et al. Antimicrobial activity of mucosal-associated invariant T cells. Nat Immunol. 2010;11(8):701-8.
86. Gold MC, Cerri S, Smyk-Pearson S, Cansler ME, Vogt TM, Delepine J, et al. Human mucosal associated invariant T cells detect bacterially infected cells. PLoS Biol. 2010;8(6):e1000407.
87. Le Bourhis L, Mburu YK, Lantz O. MAIT cells, surveyors of a new class of antigen: development and functions. Curr Opin Immunol. 2013;25(2):174-80.
88. Ussher JE, Willberg CB, Klenerman P. MAIT cells and viruses. Immunol Cell Biol. 2018;96(6):630-41.

89. van Wilgenburg B, Scherwitzl I, Hutchinson EC, Leng T, Kurioka A, Kulicke C, et al. MAIT cells are activated during human viral infections. Nat Commun. 2016;7:11653.
90. Huang W, He W, Shi X, Ye Q, He X, Dou L, et al. Mucosal-associated invariant T-cells are severely reduced and exhausted in humans with chronic HBV infection. J Viral Hepat. 2020;27(11):1096-107.
91. Le Bourhis L, Dusseaux M, Bohineust A, Bessoles S, Martin E, Premel V, et al. MAIT cells detect and efficiently lyse bacterially-infected epithelial cells. PLoS Pathog. 2013;9(10):e1003681.
92. Provine NM, Klenerman P. MAIT Cells in Health and Disease. Annu Rev Immunol. 2020;38:203-28.
93. Wang H, Kjer-Nielsen L, Shi M, D'Souza C, Pediongco TJ, Cao H, et al. IL-23 costimulates antigen-specific MAIT cell activation and enables vaccination against bacterial infection. Sci Immunol. 2019;4(41).
94. Kjer-Nielsen L, Patel O, Corbett AJ, Le Nours J, Meehan B, Liu L, et al. MR1 presents microbial vitamin B metabolites to MAIT cells. Nature. 2012;491(7426):717-23.
95. Schneider M, Hannaway RF, Lamichhane R, de la Harpe SM, Tyndall JDA, Vernall AJ, et al. Neutrophils suppress mucosal-associated invariant T cells in humans. Eur J Immunol. 2020;50(5):643-55.
96. Loh L, Wang Z, Sant S, Koutsakos M, Jegaskanda S, Corbett AJ, et al. Human mucosal-associated invariant T cells contribute to antiviral influenza immunity via IL-18-dependent activation. Proc Natl Acad Sci U S A. 2016;113(36):10133-8.
97. van Wilgenburg B, Loh L, Chen Z, Pediongco TJ, Wang H, Shi M, et al. MAIT cells contribute to protection against lethal influenza infection in vivo. Nat Commun. 2018;9(1):4706.
98. Lal KG, Kim D, Costanzo MC, Creegan M, Leeansyah E, Dias J, et al. Dynamic MAIT cell response with progressively enhanced innateness during acute HIV-1 infection. Nat Commun. 2020;11(1):272.
99. Parrot T, Gorin JB, Ponzetta A, Maleki KT, Kammann T, Emgård J, et al. MAIT cell activation and dynamics associated with COVID-19 disease severity. Sci Immunol. 2020;5(51).
100. Preeyaa SU, Murugesan A, Sopnajothi S, Yong YK, Tan HY, Larsson M, et al. Peripheral Follicular T Helper Cells and Mucosal-Associated Invariant T Cells Represent Activated Phenotypes During the Febrile Phase of Acute Dengue Virus Infection. Viral Immunol. 2020;33(9):610-5.
101. Deschler S, Kager J, Erber J, Fricke L, Koyumdzhieva P, Georgieva A, et al. Mucosal-Associated Invariant T (MAIT) Cells Are Highly Activated and Functionally Impaired in COVID-19 Patients. Viruses. 2021;13(2).
102. Maleki KT, Tauriainen J, García M, Kerkman PF, Christ W, Dias J, et al. MAIT cell activation is associated with disease severity markers in acute hantavirus infection. Cell Rep Med. 2021;2(3):100220.
103. Paquin-Proulx D, Avelino-Silva VI, Santos BAN, Silveira Barsotti N, Siroma F, Fernandes Ramos J, et al. MAIT cells are activated in acute Dengue virus infection and after in vitro Zika virus infection. PLoS Negl Trop Dis. 2018;12(1):e0006154.
104. Flament H, Rouland M, Beaudoin L, Toubal A, Bertrand L, Lebourgeois S, et al. Outcome of SARS-CoV-2 infection is linked to MAIT cell activation and cytotoxicity. Nat Immunol. 2021;22(3):322-35.

105. Gracey E, Qaiyum Z, Almaghlouth I, Lawson D, Karki S, Avvaru N, et al. IL-7 primes IL-17 in mucosal-associated invariant T (MAIT) cells, which contribute to the Th17-axis in ankylosing spondylitis. Ann Rheum Dis. 2016;75(12):2124-32.
106. Bolte FJ, O'Keefe AC, Webb LM, Serti E, Rivera E, Liang TJ, et al. Intra-Hepatic Depletion of Mucosal-Associated Invariant T Cells in Hepatitis C Virus-Induced Liver Inflammation. Gastroenterology. 2017;153(5):1392-403.e2.
107. Cosgrove C, Ussher JE, Rauch A, Gärtner K, Kurioka A, Hühn MH, et al. Early and nonreversible decrease of CD161++ /MAIT cells in HIV infection. Blood. 2013;121(6):951-61.
108. Paquin-Proulx D, Greenspun BC, Costa EA, Segurado AC, Kallas EG, Nixon DF, et al. MAIT cells are reduced in frequency and functionally impaired in human T lymphotropic virus type 1 infection: Potential clinical implications. PLoS One. 2017;12(4):e0175345.
109. Provine NM, Amini A, Garner LC, Spencer AJ, Dold C, Hutchings C, et al. MAIT cell activation augments adenovirus vector vaccine immunogenicity. Science. 2021;371(6528):521-6.
110. Suliman S, Murphy M, Musvosvi M, Gela A, Meermeier EW, Geldenhuys H, et al. MR1-Independent Activation of Human Mucosal-Associated Invariant T Cells by Mycobacteria. J Immunol. 2019;203(11):2917-27.
111. Pieper K, Grimbacher B, Eibel H. B-cell biology and development. J Allergy Clin Immunol. 2013;131(4):959-71.
112. Strugnell RA, Wijburg OL. The role of secretory antibodies in infection immunity. Nat Rev Microbiol. 2010;8(9):656-67.
113. Wabl M, Steinberg C. Affinity maturation and class switching. Curr Opin Immunol. 1996;8(1):89-92.
114. Bournazos S, Wang TT, Dahan R, Maamary J, Ravetch JV. Signaling by Antibodies: Recent Progress. Annu Rev Immunol. 2017;35:285-311.
115. Wu YC, Kipling D, Dunn-Walters DK. The relationship between CD27 negative and positive B cell populations in human peripheral blood. Front Immunol. 2011;2:81.
116. Akkaya M, Kwak K, Pierce SK. B cell memory: building two walls of protection against pathogens. Nat Rev Immunol. 2020;20(4):229-38.
117. McHeyzer-Williams LJ, McHeyzer-Williams MG. Antigen-specific memory B cell development. Annu Rev Immunol. 2005;23:487-513.
118. Amanna IJ, Carlson NE, Slifka MK. Duration of humoral immunity to common viral and vaccine antigens. N Engl J Med. 2007;357(19):1903-15.
119. Gilbert SC. Clinical development of Modified Vaccinia virus Ankara vaccines. Vaccine. 2013;31(39):4241-6.
120. Plotkin S, Plotkin S. A Short History of Vaccination. 4 ed. Philadelphia: WB Saunders; 2004.
121. Lauring AS, Jones JO, Andino R. Rationalizing the development of live attenuated virus vaccines. Nat Biotechnol. 2010;28(6):573-9.
122. Pulendran B, Ahmed R. Immunological mechanisms of vaccination. Nat Immunol. 2011;12(6):509-17.
123. Lee J, Arun Kumar S, Jhan YY, Bishop CJ. Engineering DNA vaccines against infectious diseases. Acta Biomater. 2018;80:31-47.
124. Karch CP, Burkhard P. Vaccine technologies: From whole organisms to rationally designed protein assemblies. Biochem Pharmacol. 2016;120:1-14.

125. Bisgard KM, Rhodes P, Connelly BL, Bi D, Hahn C, Patrick S, et al. Pertussis vaccine effectiveness among children 6 to 59 months of age in the United States, 1998-2001. Pediatrics. 2005;116(2):e285-94.
126. Bisgard KM, Rhodes P, Hardy IR, Litkina IL, Filatov NN, Monisov AA, et al. Diphtheria toxoid vaccine effectiveness: A case-control study in Russia. J Infect Dis. 2000;181 Suppl 1:S184-7.
127. Sharpe HR, Gilbride C, Allen E, Belij-Rammerstorfer S, Bissett C, Ewer K, et al. The early landscape of coronavirus disease 2019 vaccine development in the UK and rest of the world. Immunology. 2020;160(3):223-32.
128. Reichmuth AM, Oberli MA, Jaklenec A, Langer R, Blankschtein D. mRNA vaccine delivery using lipid nanoparticles. Ther Deliv. 2016;7(5):319-34.
129. Blakney AK, McKay PF, Christensen D, Yus BI, Aldon Y, Follmann F, et al. Effects of cationic adjuvant formulation particle type, fluidity and immunomodulators on delivery and immunogenicity of saRNA. J Control Release. 2019;304:65-74.
130. Martin JE, Louder MK, Holman LA, Gordon IJ, Enama ME, Larkin BD, et al. A SARS DNA vaccine induces neutralizing antibody and cellular immune responses in healthy adults in a Phase I clinical trial. Vaccine. 2008;26(50):6338-43.
131. Ewer KJ, Lambe T, Rollier CS, Spencer AJ, Hill AV, Dorrell L. Viral vectors as vaccine platforms: from immunogenicity to impact. Curr Opin Immunol. 2016;41:47-54.
132. Coughlan L. Factors Which Contribute to the Immunogenicity of Non-replicating Adenoviral Vectored Vaccines. Front Immunol. 2020;11:909.
133. Capone S, D'Alise AM, Ammendola V, Colloca S, Cortese R, Nicosia A, et al. Development of chimpanzee adenoviruses as vaccine vectors: challenges and successes emerging from clinical trials. Expert Rev Vaccines. 2013;12(4):379-93.
134. Humphreys IR, Sebastian S. Novel viral vectors in infectious diseases. Immunology. 2018;153(1):1-9.
135. McConkey SJ, Reece WH, Moorthy VS, Webster D, Dunachie S, Butcher G, et al. Enhanced T-cell immunogenicity of plasmid DNA vaccines boosted by recombinant modified vaccinia virus Ankara in humans. Nat Med. 2003;9(6):729-35.
136. Ewer K, Sebastian S, Spencer AJ, Gilbert S, Hill AVS, Lambe T. Chimpanzee adenoviral vectors as vaccines for outbreak pathogens. Hum Vaccin Immunother. 2017;13(12):3020-32.
137. Cappuccini F, Bryant R, Pollock E, Carter L, Verrill C, Hollidge J, et al. Safety and immunogenicity of novel 5T4 viral vectored vaccination regimens in early stage prostate cancer: a phase I clinical trial. J Immunother Cancer. 2020;8(1).
138. Pollard AJ, Launay O, Lelievre JD, Lacabaratz C, Grande S, Goldstein N, et al. Safety and immunogenicity of a two-dose heterologous Ad26.ZEBOV and MVA-BN-Filo Ebola vaccine regimen in adults in Europe (EBOVAC2): a randomised, observer-blind, participant-blind, placebo-controlled, phase 2 trial. Lancet Infect Dis. 2021;21(4):493-506.
139. Heininger U. Efficacy of Single-Dose Ad26.COV2.S Vaccine against Covid-19. N Engl J Med. 2021.
140. RAPS. COVID-19 vaccine tracker 2021 [Available from: https://www.raps.org/news-and-articles/news-articles/2020/3/covid-19-vaccine-tracker.
141. Gurwith M, Lock M, Taylor EM, Ishioka G, Alexander J, Mayall T, et al. Safety and immunogenicity of an oral, replicating adenovirus serotype 4 vector vaccine for H5N1 influenza: a randomised, double-blind, placebo-controlled, phase 1 study. Lancet Infect Dis. 2013;13(3):238-50.

142. Sedegah M, Tamminga C, McGrath S, House B, Ganeshan H, Lejano J, et al. Adenovirus 5-vectored P. falciparum vaccine expressing CSP and AMA1. Part A: safety and immunogenicity in seronegative adults. PLoS One. 2011;6(10):e24586.
143. Matz KM, Marzi A, Feldmann H. Ebola vaccine trials: progress in vaccine safety and immunogenicity. Expert Rev Vaccines. 2019;18(12):1229-42.
144. Li Y, Wang L, Zhu T, Wu S, Feng L, Cheng P, et al. Establishing China's National Standard for the Recombinant Adenovirus Type 5 Vector-Based Ebola Vaccine (Ad5-EBOV) Virus Titer. Hum Gene Ther Clin Dev. 2018;29(4):226-32.
145. Logunov DY, Dolzhikova IV, Shcheblyakov DV, Tukhvatulin AI, Zubkova OV, Dzharullaeva AS, et al. Safety and efficacy of an rAd26 and rAd5 vector-based heterologous prime-boost COVID-19 vaccine: an interim analysis of a randomised controlled phase 3 trial in Russia. Lancet. 2021;397(10275):671-81.
146. Barnes E, Folgori A, Capone S, Swadling L, Aston S, Kurioka A, et al. Novel adenovirus-based vaccines induce broad and sustained T cell responses to HCV in man. Sci Transl Med. 2012;4(115):115ra1.
147. Ockenhouse CF, Regules J, Tosh D, Cowden J, Kathcart A, Cummings J, et al. Ad35.CS.01-RTS,S/AS01 Heterologous Prime Boost Vaccine Efficacy against Sporozoite Challenge in Healthy Malaria-Naïve Adults. PLoS One. 2015;10(7):e0131571.
148. Swadling L, Capone S, Antrobus RD, Brown A, Richardson R, Newell EW, et al. A human vaccine strategy based on chimpanzee adenoviral and MVA vectors that primes, boosts, and sustains functional HCV-specific T cell memory. Sci Transl Med. 2014;6(261):261ra153.
149. Ewer K, Rampling T, Venkatraman N, Bowyer G, Wright D, Lambe T, et al. A Monovalent Chimpanzee Adenovirus Ebola Vaccine Boosted with MVA. N Engl J Med. 2016;374(17):1635-46.
150. Tapia MD, Sow SO, Lyke KE, Haidara FC, Diallo F, Doumbia M, et al. Use of ChAd3-EBO-Z Ebola virus vaccine in Malian and US adults, and boosting of Malian adults with MVA-BN-Filo: a phase 1, single-blind, randomised trial, a phase 1b, open-label and double-blind, dose-escalation trial, and a nested, randomised, double-blind, placebo-controlled trial. Lancet Infect Dis. 2016;16(1):31-42.
151. Tiono AB, Nébié I, Anagnostou N, Coulibaly AS, Bowyer G, Lam E, et al. First field efficacy trial of the ChAd63 MVA ME-TRAP vectored malaria vaccine candidate in 5-17 months old infants and children. PLoS One. 2018;13(12):e0208328.
152. Hartnell F, Brown A, Capone S, Kopycinski J, Bliss C, Makvandi-Nejad S, et al. A Novel Vaccine Strategy Employing Serologically Different Chimpanzee Adenoviral Vectors for the Prevention of HIV-1 and HCV Coinfection. Front Immunol. 2018;9:3175.
153. Green CA, Scarselli E, Voysey M, Capone S, Vitelli A, Nicosia A, et al. Safety and immunogenicity of novel respiratory syncytial virus (RSV) vaccines based on the RSV viral proteins F, N and M2-1 encoded by simian adenovirus (PanAd3-RSV) and MVA (MVA-RSV); protocol for an open-label, dose-escalation, single-centre, phase 1 clinical trial in healthy adults. BMJ Open. 2015;5(10):e008748.
154. Folegatti PM, Bellamy D, Roberts R, Powlson J, Edwards NJ, Mair CF, et al. Safety and Immunogenicity of a Novel Recombinant Simian Adenovirus ChAdOx2 as a Vectored Vaccine. Vaccines (Basel). 2019;7(2).
155. Elizaga ML, Li SS, Kochar NK, Wilson GJ, Allen MA, Tieu HVN, et al. Safety and tolerability of HIV-1 multiantigen pDNA vaccine given with IL-12 plasmid DNA via electroporation, boosted with a recombinant vesicular stomatitis virus HIV Gag vaccine in

healthy volunteers in a randomized, controlled clinical trial. PLoS One. 2018;13(9):e0202753.
156. Henao-Restrepo AM, Longini IM, Egger M, Dean NE, Edmunds WJ, Camacho A, et al. Efficacy and effectiveness of an rVSV-vectored vaccine expressing Ebola surface glycoprotein: interim results from the Guinea ring vaccination cluster-randomised trial. Lancet. 2015;386(9996):857-66.
157. Henao-Restrepo AM, Camacho A, Longini IM, Watson CH, Edmunds WJ, Egger M, et al. Efficacy and effectiveness of an rVSV-vectored vaccine in preventing Ebola virus disease: final results from the Guinea ring vaccination, open-label, cluster-randomised trial (Ebola Ça Suffit!). Lancet. 2017;389(10068):505-18.
158. FDA. First FDA-approved vaccine for the prevention of Ebola virus disease, marking a critical milestone in public health preparedness and response 2019 [Available from: https://www.fda.gov/news-events/press-announcements/first-fda-approved-vaccine-prevention-ebola-virus-disease-marking-critical-milestone-public-health.
159. Appaiahgari MB, Vrati S. IMOJEV(®): a Yellow fever virus-based novel Japanese encephalitis vaccine. Expert Rev Vaccines. 2010;9(12):1371-84.
160. PRNewswire. Sanofi Pasteur launches IMOJEV first single-dose vaccine against Japanese encephalitis in Australia 2012 [Available from: https://www.prnewswire.com/news-releases/sanofi-pasteur-launches-imojev-first-single-dose-vaccine-against-japanese-encephalitis-in-australia-182744251.html.
161. Thomas SJ, Yoon IK. A review of Dengvaxia®: development to deployment. Hum Vaccin Immunother. 2019;15(10):2295-314.
162. EMA. Dengvaxia 2020 [updated 01.07.2021. Available from: https://www.ema.europa.eu/en/medicines/human/EPAR/dengvaxia.
163. Morris SJ, Sebastian S, Spencer AJ, Gilbert SC. Simian adenoviruses as vaccine vectors. Future Virol. 2016;11(9):649-59.
164. Guo J, Mondal M, Zhou D. Development of novel vaccine vectors: Chimpanzee adenoviral vectors. Hum Vaccin Immunother. 2018;14(7):1679-85.
165. Dicks MD, Spencer AJ, Edwards NJ, Wadell G, Bojang K, Gilbert SC, et al. A novel chimpanzee adenovirus vector with low human seroprevalence: improved systems for vector derivation and comparative immunogenicity. PLoS One. 2012;7(7):e40385.
166. Ewer KJ, O'Hara GA, Duncan CJ, Collins KA, Sheehy SH, Reyes-Sandoval A, et al. Protective CD8+ T-cell immunity to human malaria induced by chimpanzee adenovirus-MVA immunisation. Nat Commun. 2013;4:2836.
167. Borthwick N, Ahmed T, Ondondo B, Hayes P, Rose A, Ebrahimsa U, et al. Vaccine-elicited human T cells recognizing conserved protein regions inhibit HIV-1. Mol Ther. 2014;22(2):464-75.
168. Ewer KJ, Barrett JR, Belij-Rammerstorfer S, Sharpe H, Makinson R, Morter R, et al. T cell and antibody responses induced by a single dose of ChAdOx1 nCoV-19 (AZD1222) vaccine in a phase 1/2 clinical trial. Nat Med. 2020.
169. Barrett JR, Belij-Rammerstorfer S, Dold C, Ewer KJ, Folegatti PM, Gilbride C, et al. Phase 1/2 trial of SARS-CoV-2 vaccine ChAdOx1 nCoV-19 with a booster dose induces multifunctional antibody responses. Nat Med. 2020.
170. Altenburg AF, Kreijtz JH, de Vries RD, Song F, Fux R, Rimmelzwaan GF, et al. Modified vaccinia virus ankara (MVA) as production platform for vaccines against influenza and other viral respiratory diseases. Viruses. 2014;6(7):2735-61.

171. Gómez CE, Perdiguero B, García-Arriaza J, Esteban M. Clinical applications of attenuated MVA poxvirus strain. Expert Rev Vaccines. 2013;12(12):1395-416.
172. Sasso E, D'Alise AM, Zambrano N, Scarselli E, Folgori A, Nicosia A. New viral vectors for infectious diseases and cancer. Semin Immunol. 2020;50:101430.
173. Sebastian S, Flaxman A, Cha KM, Ulaszewska M, Gilbride C, Sharpe H, et al. A Multi-Filovirus Vaccine Candidate: Co-Expression of Ebola, Sudan, and Marburg Antigens in a Single Vector. Vaccines (Basel). 2020;8(2).
174. Medicines Agency E. MVABEA Ebola vaccine (MVA-BN-Filo [recombinant]) 2020 [Available from: https://www.ema.europa.eu/en/medicines/human/EPAR/mvabea.
175. Venkatraman N, Ndiaye BP, Bowyer G, Wade D, Sridhar S, Wright D, et al. Safety and immunogenicity of a heterologous prime-boost Ebola virus vaccine regimen - ChAd3-EBO-Z followed by MVA-EBO-Z in healthy adults in the UK and Senegal. J Infect Dis. 2018.
176. Fischer RJ, Purushotham JN, van Doremalen N, Sebastian S, Meade-White K, Cordova K, et al. ChAdOx1-vectored Lassa fever vaccine elicits a robust cellular and humoral immune response and protects guinea pigs against lethal Lassa virus challenge. NPJ Vaccines. 2021;6(1):32.
177. Kennedy EM, Dowall SD, Salguero FJ, Yeates P, Aram M, Hewson R. A vaccine based on recombinant modified Vaccinia Ankara containing the nucleoprotein from Lassa virus protects against disease progression in a guinea pig model. Vaccine. 2019;37(36):5404-13.
178. Antrobus RD, Coughlan L, Berthoud TK, Dicks MD, Hill AV, Lambe T, et al. Clinical assessment of a novel recombinant simian adenovirus ChAdOx1 as a vectored vaccine expressing conserved Influenza A antigens. Mol Ther. 2014;22(3):668-74.
179. Coughlan L, Sridhar S, Payne R, Edmans M, Milicic A, Venkatraman N, et al. Heterologous Two-Dose Vaccination with Simian Adenovirus and Poxvirus Vectors Elicits Long-Lasting Cellular Immunity to Influenza Virus A in Healthy Adults. EBioMedicine. 2018;29:146-54.
180. Green CA, Scarselli E, Sande CJ, Thompson AJ, de Lara CM, Taylor KS, et al. Chimpanzee adenovirus- and MVA-vectored respiratory syncytial virus vaccine is safe and immunogenic in adults. Sci Transl Med. 2015;7(300):300ra126.
181. Folegatti PM, Bittaye M, Flaxman A, Lopez FR, Bellamy D, Kupke A, et al. Safety and immunogenicity of a candidate Middle East respiratory syndrome coronavirus viral-vectored vaccine: a dose-escalation, open-label, non-randomised, uncontrolled, phase 1 trial. Lancet Infect Dis. 2020.
182. Koch T, Dahlke C, Fathi A, Kupke A, Krähling V, Okba NMA, et al. Safety and immunogenicity of a modified vaccinia virus Ankara vector vaccine candidate for Middle East respiratory syndrome: an open-label, phase 1 trial. Lancet Infect Dis. 2020;20(7):827-38.
183. Folegatti PM, Ewer KJ, Aley PK, Angus B, Becker S, Belij-Rammerstorfer S, et al. Safety and immunogenicity of the ChAdOx1 nCoV-19 vaccine against SARS-CoV-2: a preliminary report of a phase 1/2, single-blind, randomised controlled trial. Lancet. 2020;396(10249):467-78.
184. Routhu NK, Cheedarla N, Gangadhara S, Bollimpelli VS, Boddapati AK, Shiferaw A, et al. A modified vaccinia Ankara vector-based vaccine protects macaques from SARS-CoV-2 infection, immune pathology, and dysfunction in the lungs. Immunity. 2021;54(3):542-56.e9.

185. Chiuppesi F, Salazar MD, Contreras H, Nguyen VH, Martinez J, Park Y, et al. Development of a multi-antigenic SARS-CoV-2 vaccine candidate using a synthetic poxvirus platform. Nat Commun. 2020;11(1):6121.
186. von Delft A, Donnison TA, Lourenço J, Hutchings C, Mullarkey CE, Brown A, et al. The generation of a simian adenoviral vectored HCV vaccine encoding genetically conserved gene segments to target multiple HCV genotypes. Vaccine. 2018;36(2):313-21.
187. Cavenaugh JS, Awi D, Mendy M, Hill AV, Whittle H, McConkey SJ. Partially randomized, non-blinded trial of DNA and MVA therapeutic vaccines based on hepatitis B virus surface protein for chronic HBV infection. PLoS One. 2011;6(2):e14626.
188. Busquets N, Lorenzo G, López-Gil E, Rivas R, Solanes D, Galindo-Cardiel I, et al. Efficacy assessment of an MVA vectored Rift Valley Fever vaccine in lambs. Antiviral Res. 2014;108:165-72.
189. Weger-Lucarelli J, Chu H, Aliota MT, Partidos CD, Osorio JE. A novel MVA vectored Chikungunya virus vaccine elicits protective immunity in mice. PLoS Negl Trop Dis. 2014;8(7):e2970.
190. Folegatti PM, Harrison K, Preciado-Llanes L, Lopez FR, Bittaye M, Kim YC, et al. A single dose of ChAdOx1 Chik vaccine induces neutralizing antibodies against four chikungunya virus lineages in a phase 1 clinical trial. Nat Commun. 2021;12(1):4636.
191. López-Camacho C, Kim YC, Abbink P, Larocca RA, Huiskonen JT, Barouch DH, et al. Assessment of Immunogenicity and Efficacy of a Zika Vaccine Using Modified Vaccinia Ankara Virus as Carriers. Pathogens. 2019;8(4).
192. Wilkie M, Satti I, Minhinnick A, Harris S, Riste M, Ramon RL, et al. A phase I trial evaluating the safety and immunogenicity of a candidate tuberculosis vaccination regimen, ChAdOx1 85A prime - MVA85A boost in healthy UK adults. Vaccine. 2020;38(4):779-89.
193. Tameris MD, Hatherill M, Landry BS, Scriba TJ, Snowden MA, Lockhart S, et al. Safety and efficacy of MVA85A, a new tuberculosis vaccine, in infants previously vaccinated with BCG: a randomised, placebo-controlled phase 2b trial. Lancet. 2013;381(9871):1021-8.
194. Nemes E, Hesseling AC, Tameris M, Mauff K, Downing K, Mulenga H, et al. Safety and Immunogenicity of Newborn MVA85A Vaccination and Selective, Delayed Bacille Calmette-Guerin for Infants of Human Immunodeficiency Virus-Infected Mothers: A Phase 2 Randomized, Controlled Trial. Clin Infect Dis. 2018;66(4):554-63.
195. O'Hara GA, Duncan CJ, Ewer KJ, Collins KA, Elias SC, Halstead FD, et al. Clinical assessment of a recombinant simian adenovirus ChAd63: a potent new vaccine vector. J Infect Dis. 2012;205(5):772-81.
196. Zhu N, Zhang D, Wang W, Li X, Yang B, Song J, et al. A Novel Coronavirus from Patients with Pneumonia in China, 2019. N Engl J Med. 2020;382(8):727-33.
197. Drosten C, Günther S, Preiser W, van der Werf S, Brodt HR, Becker S, et al. Identification of a novel coronavirus in patients with severe acute respiratory syndrome. N Engl J Med. 2003;348(20):1967-76.
198. Chan-Yeung M, Xu RH. SARS: epidemiology. Respirology. 2003;8 Suppl:S9-14.
199. Zhou P, Yang XL, Wang XG, Hu B, Zhang L, Zhang W, et al. A pneumonia outbreak associated with a new coronavirus of probable bat origin. Nature. 2020;579(7798):270-3.
200. WHO.int. WHO Director-General's opening remarks at the media briefing on COVID-19 - 11 March 2020 2020 [Available from:

https://www.who.int/dg/speeches/detail/who-director-general-s-opening-remarks-at-the-media-briefing-on-covid-19---11-march-2020.
201. Domingo JL, Marquès M, Rovira J. Influence of airborne transmission of SARS-CoV-2 on COVID-19 pandemic. A review. Environ Res. 2020;188:109861.
202. Huang C, Wang Y, Li X, Ren L, Zhao J, Hu Y, et al. Clinical features of patients infected with 2019 novel coronavirus in Wuhan, China. Lancet. 2020;395(10223):497-506.
203. Martines RB, Ritter JM, Matkovic E, Gary J, Bollweg BC, Bullock H, et al. Pathology and Pathogenesis of SARS-CoV-2 Associated with Fatal Coronavirus Disease, United States. Emerg Infect Dis. 2020;26(9):2005-15.
204. Wu Z, McGoogan JM. Characteristics of and Important Lessons From the Coronavirus Disease 2019 (COVID-19) Outbreak in China: Summary of a Report of 72 314 Cases From the Chinese Center for Disease Control and Prevention. JAMA. 2020;323(13):1239-42.
205. Takahashi T, Ellingson MK, Wong P, Israelow B, Lucas C, Klein J, et al. Sex differences in immune responses that underlie COVID-19 disease outcomes. Nature. 2020;588(7837):315-20.
206. Zhou F, Yu T, Du R, Fan G, Liu Y, Liu Z, et al. Clinical course and risk factors for mortality of adult inpatients with COVID-19 in Wuhan, China: a retrospective cohort study. Lancet. 2020;395(10229):1054-62.
207. Wrapp D, Wang N, Corbett KS, Goldsmith JA, Hsieh CL, Abiona O, et al. Cryo-EM structure of the 2019-nCoV spike in the prefusion conformation. Science. 2020;367(6483):1260-3.
208. Yan R, Zhang Y, Li Y, Xia L, Guo Y, Zhou Q. Structural basis for the recognition of SARS-CoV-2 by full-length human ACE2. Science. 2020;367(6485):1444-8.
209. Carvalho T, Krammer F, Iwasaki A. The first 12 months of COVID-19: a timeline of immunological insights. Nat Rev Immunol. 2021;21(4):245-56.
210. Del Valle DM, Kim-Schulze S, Huang HH, Beckmann ND, Nirenberg S, Wang B, et al. An inflammatory cytokine signature predicts COVID-19 severity and survival. Nat Med. 2020;26(10):1636-43.
211. Mathew D, Giles JR, Baxter AE, Oldridge DA, Greenplate AR, Wu JE, et al. Deep immune profiling of COVID-19 patients reveals distinct immunotypes with therapeutic implications. Science. 2020;369(6508).
212. Laing AG, Lorenc A, Del Molino Del Barrio I, Das A, Fish M, Monin L, et al. A dynamic COVID-19 immune signature includes associations with poor prognosis. Nat Med. 2020;26(10):1623-35.
213. Kuri-Cervantes L, Pampena MB, Meng W, Rosenfeld AM, Ittner CAG, Weisman AR, et al. Comprehensive mapping of immune perturbations associated with severe COVID-19. Sci Immunol. 2020;5(49).
214. Hadjadj J, Yatim N, Barnabei L, Corneau A, Boussier J, Smith N, et al. Impaired type I interferon activity and inflammatory responses in severe COVID-19 patients. Science. 2020;369(6504):718-24.
215. Atyeo C, Fischinger S, Zohar T, Slein MD, Burke J, Loos C, et al. Distinct Early Serological Signatures Track with SARS-CoV-2 Survival. Immunity. 2020;53(3):524-32.e4.
216. Garcia-Beltran WF, Lam EC, Astudillo MG, Yang D, Miller TE, Feldman J, et al. COVID-19-neutralizing antibodies predict disease severity and survival. Cell. 2021;184(2):476-88.e11.

217. Iyer AS, Jones FK, Nodoushani A, Kelly M, Becker M, Slater D, et al. Persistence and decay of human antibody responses to the receptor binding domain of SARS-CoV-2 spike protein in COVID-19 patients. Sci Immunol. 2020;5(52).
218. Chandrashekar A, Liu J, Martinot AJ, McMahan K, Mercado NB, Peter L, et al. SARS-CoV-2 infection protects against rechallenge in rhesus macaques. Science. 2020;369(6505):812-7.
219. Anderson EM, Goodwin EC, Verma A, Arevalo CP, Bolton MJ, Weirick ME, et al. Seasonal human coronavirus antibodies are boosted upon SARS-CoV-2 infection but not associated with protection. Cell. 2021;184(7):1858-64.e10.
220. Wajnberg A, Amanat F, Firpo A, Altman DR, Bailey MJ, Mansour M, et al. Robust neutralizing antibodies to SARS-CoV-2 infection persist for months. Science. 2020;370(6521):1227-30.
221. van Doremalen N, Lambe T, Spencer A, Belij-Rammerstorfer S, Purushotham JN, Port JR, et al. ChAdOx1 nCoV-19 vaccine prevents SARS-CoV-2 pneumonia in rhesus macaques. Nature. 2020;586(7830):578-82.
222. Ramasamy MN, Minassian AM, Ewer KJ, Flaxman AL, Folegatti PM, Owens DR, et al. Safety and immunogenicity of ChAdOx1 nCoV-19 vaccine administered in a prime-boost regimen in young and old adults (COV002): a single-blind, randomised, controlled, phase 2/3 trial. Lancet. 2021;396(10267):1979-93.
223. Voysey M, Clemens SAC, Madhi SA, Weckx LY, Folegatti PM, Aley PK, et al. Safety and efficacy of the ChAdOx1 nCoV-19 vaccine (AZD1222) against SARS-CoV-2: an interim analysis of four randomised controlled trials in Brazil, South Africa, and the UK. Lancet. 2021;397(10269):99-111.
224. Agency EM. Vaxzevria (previously COVID-19 Vaccine AstraZeneca) 2021 [Available from: https://www.ema.europa.eu/en/medicines/human/EPAR/vaxzevria-previously-covid-19-vaccine-astrazeneca.
225. WHO. Interim recommendations for use of the ChAdOx1-S [recombinant] vaccine against COVID-19 (AstraZeneca COVID-19 vaccine AZD1222, SII Covishield, SK Bioscience). 2021.
226. Merani S, Pawelec G, Kuchel GA, McElhaney JE. Impact of Aging and Cytomegalovirus on Immunological Response to Influenza Vaccination and Infection. Front Immunol. 2017;8:784.
227. Coughlan L, Mullarkey C, Gilbert S. Adenoviral vectors as novel vaccines for influenza. J Pharm Pharmacol. 2015;67(3):382-99.
228. He CQ, Han GZ, Wang D, Liu W, Li GR, Liu XP, et al. Homologous recombination evidence in human and swine influenza A viruses. Virology. 2008;380(1):12-20.
229. Jansen JM, Gerlach T, Elbahesh H, Rimmelzwaan GF, Saletti G. Influenza virus-specific CD4+ and CD8+ T cell-mediated immunity induced by infection and vaccination. J Clin Virol. 2019;119:44-52.
230. Grant EJ, Quiñones-Parra SM, Clemens EB, Kedzierska K. Human influenza viruses and CD8(+) T cell responses. Curr Opin Virol. 2016;16:132-42.
231. Wang Z, Wan Y, Qiu C, Quiñones-Parra S, Zhu Z, Loh L, et al. Recovery from severe H7N9 disease is associated with diverse response mechanisms dominated by $CD8^+$ T cells. Nat Commun. 2015;6:6833.
232. van de Sandt CE, Hillaire ML, Geelhoed-Mieras MM, Osterhaus AD, Fouchier RA, Rimmelzwaan GF. Human Influenza A Virus-Specific CD8+ T-Cell Response Is Long-lived. J Infect Dis. 2015;212(1):81-5.

233. Valkenburg SA, Venturi V, Dang TH, Bird NL, Doherty PC, Turner SJ, et al. Early priming minimizes the age-related immune compromise of CD8$^+$ T cell diversity and function. PLoS Pathog. 2012;8(2):e1002544.
234. Trzonkowski P, Myśliwska J, Szmit E, Wieckiewicz J, Lukaszuk K, Brydak LB, et al. Association between cytomegalovirus infection, enhanced proinflammatory response and low level of anti-hemagglutinins during the anti-influenza vaccination--an impact of immunosenescence. Vaccine. 2003;21(25-26):3826-36.
235. Berthoud TK, Hamill M, Lillie PJ, Hwenda L, Collins KA, Ewer KJ, et al. Potent CD8+ T-cell immunogenicity in humans of a novel heterosubtypic influenza A vaccine, MVA-NP+M1. Clin Infect Dis. 2011;52(1):1-7.
236. Lee LY, Ha dL, Simmons C, de Jong MD, Chau NV, Schumacher R, et al. Memory T cells established by seasonal human influenza A infection cross-react with avian influenza A (H5N1) in healthy individuals. J Clin Invest. 2008;118(10):3478-90.
237. Negredo A, Palacios G, Vázquez-Morón S, González F, Dopazo H, Molero F, et al. Discovery of an ebolavirus-like filovirus in europe. PLoS Pathog. 2011;7(10):e1002304.
238. Goldstein T, Anthony SJ, Gbakima A, Bird BH, Bangura J, Tremeau-Bravard A, et al. The discovery of Bombali virus adds further support for bats as hosts of ebolaviruses. Nat Microbiol. 2018.
239. Towner JS, Sealy TK, Khristova ML, Albariño CG, Conlan S, Reeder SA, et al. Newly discovered ebola virus associated with hemorrhagic fever outbreak in Uganda. PLoS Pathog. 2008;4(11):e1000212.
240. Boisen ML, Hartnett JN, Goba A, Vandi MA, Grant DS, Schieffelin JS, et al. Epidemiology and Management of the 2013-16 West African Ebola Outbreak. Annu Rev Virol. 2016;3(1):147-71.
241. Feldmann H, Geisbert TW. Ebola haemorrhagic fever. Lancet. 2011;377(9768):849-62.
242. Holmes EC, Dudas G, Rambaut A, Andersen KG. The evolution of Ebola virus: Insights from the 2013-2016 epidemic. Nature. 2016;538(7624):193-200.
243. Baize S, Leroy EM, Georges-Courbot MC, Capron M, Lansoud-Soukate J, Debré P, et al. Defective humoral responses and extensive intravascular apoptosis are associated with fatal outcome in Ebola virus-infected patients. Nat Med. 1999;5(4):423-6.
244. Baize S, Leroy EM, Georges AJ, Georges-Courbot MC, Capron M, Bedjabaga I, et al. Inflammatory responses in Ebola virus-infected patients. Clin Exp Immunol. 2002;128(1):163-8.
245. Leroy EM, Baize S, Volchkov VE, Fisher-Hoch SP, Georges-Courbot MC, Lansoud-Soukate J, et al. Human asymptomatic Ebola infection and strong inflammatory response. Lancet. 2000;355(9222):2210-5.
246. Wauquier N, Becquart P, Padilla C, Baize S, Leroy EM. Human fatal zaire ebola virus infection is associated with an aberrant innate immunity and with massive lymphocyte apoptosis. PLoS Negl Trop Dis. 2010;4(10).
247. Reed DS, Hensley LE, Geisbert JB, Jahrling PB, Geisbert TW. Depletion of peripheral blood T lymphocytes and NK cells during the course of ebola hemorrhagic Fever in cynomolgus macaques. Viral Immunol. 2004;17(3):390-400.
248. Marzi A, Engelmann F, Feldmann F, Haberthur K, Shupert WL, Brining D, et al. Antibodies are necessary for rVSV/ZEBOV-GP-mediated protection against lethal Ebola virus challenge in nonhuman primates. Proc Natl Acad Sci U S A. 2013;110(5):1893-8.

249. Sullivan NJ, Hensley L, Asiedu C, Geisbert TW, Stanley D, Johnson J, et al. CD8+ cellular immunity mediates rAd5 vaccine protection against Ebola virus infection of nonhuman primates. Nat Med. 2011;17(9):1128-31.
250. Wauquier N, Becquart P, Gasquet C, Leroy EM. Immunoglobulin G in Ebola outbreak survivors, Gabon. Emerg Infect Dis. 2009;15(7):1136-7.
251. Sobarzo A, Ochayon DE, Lutwama JJ, Balinandi S, Guttman O, Marks RS, et al. Persistent immune responses after Ebola virus infection. N Engl J Med. 2013;369(5):492-3.
252. Ledgerwood JE, DeZure AD, Stanley DA, Coates EE, Novik L, Enama ME, et al. Chimpanzee Adenovirus Vector Ebola Vaccine. N Engl J Med. 2017;376(10):928-38.
253. De Santis O, Audran R, Pothin E, Warpelin-Decrausaz L, Vallotton L, Wuerzner G, et al. Safety and immunogenicity of a chimpanzee adenovirus-vectored Ebola vaccine in healthy adults: a randomised, double-blind, placebo-controlled, dose-finding, phase 1/2a study. Lancet Infect Dis. 2016;16(3):311-20.
254. Huttner A, Dayer JA, Yerly S, Combescure C, Auderset F, Desmeules J, et al. The effect of dose on the safety and immunogenicity of the VSV Ebola candidate vaccine: a randomised double-blind, placebo-controlled phase 1/2 trial. Lancet Infect Dis. 2015;15(10):1156-66.
255. Li JX, Hou LH, Meng FY, Wu SP, Hu YM, Liang Q, et al. Immunity duration of a recombinant adenovirus type-5 vector-based Ebola vaccine and a homologous prime-boost immunisation in healthy adults in China: final report of a randomised, double-blind, placebo-controlled, phase 1 trial. Lancet Glob Health. 2017;5(3):e324-e34.
256. Ledgerwood JE, Costner P, Desai N, Holman L, Enama ME, Yamshchikov G, et al. A replication defective recombinant Ad5 vaccine expressing Ebola virus GP is safe and immunogenic in healthy adults. Vaccine. 2010;29(2):304-13.
257. Lambe T, Bowyer G, Ewer KJ. A review of Phase I trials of Ebola virus vaccines: what can we learn from the race to develop novel vaccines? Philos Trans R Soc Lond B Biol Sci. 2017;372(1721).
258. Zhu FC, Hou LH, Li JX, Wu SP, Liu P, Zhang GR, et al. Safety and immunogenicity of a novel recombinant adenovirus type-5 vector-based Ebola vaccine in healthy adults in China: preliminary report of a randomised, double-blind, placebo-controlled, phase 1 trial. Lancet. 2015;385(9984):2272-9.
259. Marzi A, Robertson SJ, Haddock E, Feldmann F, Hanley PW, Scott DP, et al. EBOLA VACCINE. VSV-EBOV rapidly protects macaques against infection with the 2014/15 Ebola virus outbreak strain. Science. 2015;349(6249):739-42.
260. Dupont L, Reeves MB. Cytomegalovirus latency and reactivation: recent insights into an age old problem. Rev Med Virol. 2016;26(2):75-89.
261. van Beurden S, Engelsma M. Herpesviruses of Fish, Amphibians and Invertebrates. Herpesviridae: A Look into this Unique Family of Viruses. 1: IntechOpen; 2011. p. 217-42.
262. Murthy S, O'Brien K, Agbor A, Angedakin S, Arandjelovic M, Ayimisin EA, et al. Cytomegalovirus distribution and evolution in hominines. Virus Evol. 2019;5(2):vez015.
263. Borie R, Cadranel J, Guihot A, Marcelin AG, Galicier L, Couderc LJ. Pulmonary manifestations of human herpesvirus-8 during HIV infection. Eur Respir J. 2013;42(4):1105-18.
264. Zuhair M, Smit GSA, Wallis G, Jabbar F, Smith C, Devleesschauwer B, et al. Estimation of the worldwide seroprevalence of cytomegalovirus: A systematic review and meta-analysis. Rev Med Virol. 2019;29(3):e2034.

265. Almanan M, Raynor J, Sholl A, Wang M, Chougnet C, Cardin RD, et al. Tissue-specific control of latent CMV reactivation by regulatory T cells. PLoS Pathog. 2017;13(8):e1006507.
266. Stern A, Papanicolaou GA. CMV Prevention and Treatment in Transplantation: What's New in 2019. Curr Infect Dis Rep. 2019;21(11):45.
267. Bates M, Brantsaeter AB. Human cytomegalovirus (CMV) in Africa: a neglected but important pathogen. J Virus Erad. 2016;2(3):136-42.
268. Malik A, Adland E, Laker L, Kløverpris H, Fardoos R, Roider J, et al. Immunodominant cytomegalovirus-specific CD8+ T-cell responses in sub-Saharan African populations. PLoS One. 2017;12(12):e0189612.
269. Schaftenaar E, Verjans GM, Getu S, McIntyre JA, Struthers HE, Osterhaus AD, et al. High seroprevalence of human herpesviruses in HIV-infected individuals attending primary healthcare facilities in rural South Africa. PLoS One. 2014;9(6):e99243.
270. Kabagenyi J, Natukunda A, Nassuuna J, Sanya RE, Nampijja M, Webb EL, et al. Urban-rural differences in immune responses to mycobacterial and tetanus vaccine antigens in a tropical setting: A role for helminths? Parasitol Int. 2020;78:102132.
271. Lopman BA, Pitzer VE, Sarkar R, Gladstone B, Patel M, Glasser J, et al. Understanding reduced rotavirus vaccine efficacy in low socio-economic settings. PLoS One. 2012;7(8):e41720.
272. Serazin AC, Shackelton LA, Wilson C, Bhan MK. Improving the performance of enteric vaccines in the developing world. Nat Immunol. 2010;11(9):769-73.
273. Reddehase MJ, Lemmermann NAW. Mouse Model of Cytomegalovirus Disease and Immunotherapy in the Immunocompromised Host: Predictions for Medical Translation that Survived the "Test of Time". Viruses. 2018;10(12).
274. Kuijpers TW, Baars PA, Dantin C, van den Burg M, van Lier RA, Roosnek E. Human NK cells can control CMV infection in the absence of T cells. Blood. 2008;112(3):914-5.
275. Biron CA, Byron KS, Sullivan JL. Severe herpesvirus infections in an adolescent without natural killer cells. N Engl J Med. 1989;320(26):1731-5.
276. Ali AK, Komal AK, Almutairi SM, Lee SH. Natural Killer Cell-Derived IL-10 Prevents Liver Damage During Sustained Murine Cytomegalovirus Infection. Front Immunol. 2019;10:2688.
277. Seidel E, Dassa L, Schuler C, Oiknine-Djian E, Wolf DG, Le-Trilling VTK, et al. The human cytomegalovirus protein UL147A downregulates the most prevalent MICA allele: MICA*008, to evade NK cell-mediated killing. PLoS Pathog. 2021;17(5):e1008807.
278. Dunn C, Chalupny NJ, Sutherland CL, Dosch S, Sivakumar PV, Johnson DC, et al. Human cytomegalovirus glycoprotein UL16 causes intracellular sequestration of NKG2D ligands, protecting against natural killer cell cytotoxicity. J Exp Med. 2003;197(11):1427-39.
279. Prod'homme V, Tomasec P, Cunningham C, Lemberg MK, Stanton RJ, McSharry BP, et al. Human cytomegalovirus UL40 signal peptide regulates cell surface expression of the NK cell ligands HLA-E and gpUL18. J Immunol. 2012;188(6):2794-804.
280. Wang EC, McSharry B, Retiere C, Tomasec P, Williams S, Borysiewicz LK, et al. UL40-mediated NK evasion during productive infection with human cytomegalovirus. Proc Natl Acad Sci U S A. 2002;99(11):7570-5.
281. Tomasec P, Wang EC, Davison AJ, Vojtesek B, Armstrong M, Griffin C, et al. Downregulation of natural killer cell-activating ligand CD155 by human cytomegalovirus UL141. Nat Immunol. 2005;6(2):181-8.

282. Prod'homme V, Sugrue DM, Stanton RJ, Nomoto A, Davies J, Rickards CR, et al. Human cytomegalovirus UL141 promotes efficient downregulation of the natural killer cell activating ligand CD112. J Gen Virol. 2010;91(Pt 8):2034-9.
283. Arnon TI, Achdout H, Levi O, Markel G, Saleh N, Katz G, et al. Inhibition of the NKp30 activating receptor by pp65 of human cytomegalovirus. Nat Immunol. 2005;6(5):515-23.
284. Dokun AO, Kim S, Smith HR, Kang HS, Chu DT, Yokoyama WM. Specific and nonspecific NK cell activation during virus infection. Nat Immunol. 2001;2(10):951-6.
285. Wiedemann GM, Grassmann S, Lau CM, Rapp M, Villarino AV, Friedrich C, et al. Divergent Role for STAT5 in the Adaptive Responses of Natural Killer Cells. Cell Rep. 2020;33(11):108498.
286. Sun JC, Madera S, Bezman NA, Beilke JN, Kaplan MH, Lanier LL. Proinflammatory cytokine signaling required for the generation of natural killer cell memory. J Exp Med. 2012;209(5):947-54.
287. Parikh BA, Bern MD, Piersma SJ, Yang L, Beckman DL, Poursine-Laurent J, et al. Control of Viral Infection by Natural Killer Cell Inhibitory Receptors. Cell Rep. 2020;32(4):107969.
288. Andrews DM, Scalzo AA, Yokoyama WM, Smyth MJ, Degli-Esposti MA. Functional interactions between dendritic cells and NK cells during viral infection. Nat Immunol. 2003;4(2):175-81.
289. Grassmann S, Pachmayr LO, Leube J, Mihatsch L, Andrae I, Flommersfeld S, et al. Distinct Surface Expression of Activating Receptor Ly49H Drives Differential Expansion of NK Cell Clones upon Murine Cytomegalovirus Infection. Immunity. 2019.
290. Lee S, Doualeh M, Affandi JS, Makwana N, Irish A, Price P. Functional and clinical consequences of changes to natural killer cell phenotypes driven by chronic cytomegalovirus infections. J Med Virol. 2019;91(6):1120-7.
291. Heath J, Newhook N, Comeau E, Gallant M, Fudge N, Grant M. NKG2C(+)CD57(+) Natural Killer Cell Expansion Parallels Cytomegalovirus-Specific CD8(+) T Cell Evolution towards Senescence. J Immunol Res. 2016;2016:7470124.
292. Hendricks DW, Balfour HH, Dunmire SK, Schmeling DO, Hogquist KA, Lanier LL. Cutting edge: NKG2C(hi)CD57+ NK cells respond specifically to acute infection with cytomegalovirus and not Epstein-Barr virus. J Immunol. 2014;192(10):4492-6.
293. Lopez-Vergès S, Milush JM, Schwartz BS, Pando MJ, Jarjoura J, York VA, et al. Expansion of a unique CD57^{+}NKG2Chi natural killer cell subset during acute human cytomegalovirus infection. Proc Natl Acad Sci U S A. 2011;108(36):14725-32.
294. Braud VM, Allan DS, O'Callaghan CA, Söderström K, D'Andrea A, Ogg GS, et al. HLA-E binds to natural killer cell receptors CD94/NKG2A, B and C. Nature. 1998;391(6669):795-9.
295. Muntasell A, Vilches C, Angulo A, López-Botet M. Adaptive reconfiguration of the human NK-cell compartment in response to cytomegalovirus: a different perspective of the host-pathogen interaction. Eur J Immunol. 2013;43(5):1133-41.
296. Rölle A, Pollmann J, Ewen EM, Le VT, Halenius A, Hengel H, et al. IL-12-producing monocytes and HLA-E control HCMV-driven NKG2C+ NK cell expansion. J Clin Invest. 2014;124(12):5305-16.
297. Béziat V, Liu LL, Malmberg JA, Ivarsson MA, Sohlberg E, Björklund AT, et al. NK cell responses to cytomegalovirus infection lead to stable imprints in the human KIR repertoire and involve activating KIRs. Blood. 2013;121(14):2678-88.

298. van der Ploeg K, Chang C, Ivarsson MA, Moffett A, Wills MR, Trowsdale J. Modulation of Human Leukocyte Antigen-C by Human Cytomegalovirus Stimulates KIR2DS1 Recognition by Natural Killer Cells. Front Immunol. 2017;8:298.
299. Klenerman P, Oxenius A. T cell responses to cytomegalovirus. Nat Rev Immunol. 2016;16(6):367-77.
300. Jones M, Ladell K, Wynn KK, Stacey MA, Quigley MF, Gostick E, et al. IL-10 restricts memory T cell inflation during cytomegalovirus infection. J Immunol. 2010;185(6):3583-92.
301. Hengel H, Koopmann JO, Flohr T, Muranyi W, Goulmy E, Hämmerling GJ, et al. A viral ER-resident glycoprotein inactivates the MHC-encoded peptide transporter. Immunity. 1997;6(5):623-32.
302. Jost NH, Abel S, Hutzler M, Sparwasser T, Zimmermann A, Roers A, et al. Regulatory T cells and T-cell-derived IL-10 interfere with effective anti-cytomegalovirus immune response. Immunol Cell Biol. 2014;92(10):860-71.
303. Pande NT, Powers C, Ahn K, Früh K. Rhesus cytomegalovirus contains functional homologues of US2, US3, US6, and US11. J Virol. 2005;79(9):5786-98.
304. Chen KC, Stanton RJ, Banat JJ, Wills MR. Leukocyte Immunoglobulin-Like Receptor 1-Expressing Human Natural Killer Cell Subsets Differentially Recognize Isolates of Human Cytomegalovirus through the Viral Major Histocompatibility Complex Class I Homolog UL18. J Virol. 2016;90(6):3123-37.
305. Karrer U, Sierro S, Wagner M, Oxenius A, Hengel H, Koszinowski UH, et al. Memory inflation: continuous accumulation of antiviral CD8+ T cells over time. J Immunol. 2003;170(4):2022-9.
306. Karrer U, Wagner M, Sierro S, Oxenius A, Hengel H, Dumrese T, et al. Expansion of protective CD8+ T-cell responses driven by recombinant cytomegaloviruses. J Virol. 2004;78(5):2255-64.
307. Snyder CM, Cho KS, Bonnett EL, van Dommelen S, Shellam GR, Hill AB. Memory inflation during chronic viral infection is maintained by continuous production of short-lived, functional T cells. Immunity. 2008;29(4):650-9.
308. Trgovcich J, Kincaid M, Thomas A, Griessl M, Zimmerman P, Dwivedi V, et al. Cytomegalovirus Reinfections Stimulate CD8 T-Memory Inflation. PLoS One. 2016;11(11):e0167097.
309. Baumann NS, Welten SPM, Torti N, Pallmer K, Borsa M, Barnstorf I, et al. Early primed KLRG1- CMV-specific T cells determine the size of the inflationary T cell pool. PLoS Pathog. 2019;15(5):e1007785.
310. Sylwester AW, Mitchell BL, Edgar JB, Taormina C, Pelte C, Ruchti F, et al. Broadly targeted human cytomegalovirus-specific CD4+ and CD8+ T cells dominate the memory compartments of exposed subjects. J Exp Med. 2005;202(5):673-85.
311. Khan N, Hislop A, Gudgeon N, Cobbold M, Khanna R, Nayak L, et al. Herpesvirus-specific CD8 T cell immunity in old age: cytomegalovirus impairs the response to a coresident EBV infection. J Immunol. 2004;173(12):7481-9.
312. Karrer U, Mekker A, Wanke K, Tchang V, Haeberli L. Cytomegalovirus and immune senescence: culprit or innocent bystander? Exp Gerontol. 2009;44(11):689-94.
313. Redeker A, Welten SP, Arens R. Viral inoculum dose impacts memory T-cell inflation. Eur J Immunol. 2014;44(4):1046-57.
314. Klenerman P. The (gradual) rise of memory inflation. Immunol Rev. 2018;283(1):99-112.

315. Lee LN, Bolinger B, Banki Z, de Lara C, Highton AJ, Colston JM, et al. Adenoviral vaccine induction of CD8+ T cell memory inflation: Impact of co-infection and infection order. PLoS Pathog. 2017;13(12):e1006782.
316. Bolinger B, Sims S, O'Hara G, de Lara C, Tchilian E, Firner S, et al. A new model for CD8+ T cell memory inflation based upon a recombinant adenoviral vector. J Immunol. 2013;190(8):4162-74.
317. Khan N, Shariff N, Cobbold M, Bruton R, Ainsworth JA, Sinclair AJ, et al. Cytomegalovirus seropositivity drives the CD8 T cell repertoire toward greater clonality in healthy elderly individuals. J Immunol. 2002;169(4):1984-92.
318. Wikby A, Johansson B, Olsson J, Löfgren S, Nilsson BO, Ferguson F. Expansions of peripheral blood CD8 T-lymphocyte subpopulations and an association with cytomegalovirus seropositivity in the elderly: the Swedish NONA immune study. Exp Gerontol. 2002;37(2-3):445-53.
319. Morley JK, Batliwalla FM, Hingorani R, Gregersen PK. Oligoclonal CD8+ T cells are preferentially expanded in the CD57+ subset. J Immunol. 1995;154(11):6182-90.
320. Ouyang Q, Wagner WM, Voehringer D, Wikby A, Klatt T, Walter S, et al. Age-associated accumulation of CMV-specific CD8+ T cells expressing the inhibitory killer cell lectin-like receptor G1 (KLRG1). Exp Gerontol. 2003;38(8):911-20.
321. Pawelec G, Gouttefangeas C. T-cell dysregulation caused by chronic antigenic stress: the role of CMV in immunosenescence? Aging Clin Exp Res. 2006;18(2):171-3.
322. Derhovanessian E, Maier AB, Hähnel K, Beck R, de Craen AJ, Slagboom EP, et al. Infection with cytomegalovirus but not herpes simplex virus induces the accumulation of late-differentiated CD4+ and CD8+ T-cells in humans. J Gen Virol. 2011;92(Pt 12):2746-56.
323. Tu W, Rao S. Mechanisms Underlying T Cell Immunosenescence: Aging and Cytomegalovirus Infection. Front Microbiol. 2016;7:2111.
324. Appay V, Dunbar PR, Callan M, Klenerman P, Gillespie GM, Papagno L, et al. Memory CD8+ T cells vary in differentiation phenotype in different persistent virus infections. Nat Med. 2002;8(4):379-85.
325. Ouyang Q, Wagner WM, Zheng W, Wikby A, Remarque EJ, Pawelec G. Dysfunctional CMV-specific CD8(+) T cells accumulate in the elderly. Exp Gerontol. 2004;39(4):607-13.
326. Moro-García MA, Alonso-Arias R, López-Vázquez A, Suárez-García FM, Solano-Jaurrieta JJ, Baltar J, et al. Relationship between functional ability in older people, immune system status, and intensity of response to CMV. Age (Dordr). 2012;34(2):479-95.
327. McElhaney JE, Ewen C, Zhou X, Kane KP, Xie D, Hager WD, et al. Granzyme B: Correlates with protection and enhanced CTL response to influenza vaccination in older adults. Vaccine. 2009;27(18):2418-25.
328. Merani S, Kuchel GA, Kleppinger A, McElhaney JE. Influenza vaccine-mediated protection in older adults: Impact of influenza infection, cytomegalovirus serostatus and vaccine dosage. Exp Gerontol. 2018;107:116-25.
329. Cicin-Sain L, Brien JD, Uhrlaub JL, Drabig A, Marandu TF, Nikolich-Zugich J. Cytomegalovirus infection impairs immune responses and accentuates T-cell pool changes observed in mice with aging. PLoS Pathog. 2012;8(8):e1002849.
330. Barton ES, White DW, Cathelyn JS, Brett-McClellan KA, Engle M, Diamond MS, et al. Herpesvirus latency confers symbiotic protection from bacterial infection. Nature. 2007;447(7142):326-9.

331. Lelic A, Verschoor CP, Ventresca M, Parsons R, Evelegh C, Bowdish D, et al. The polyfunctionality of human memory CD8+ T cells elicited by acute and chronic virus infections is not influenced by age. PLoS Pathog. 2012;8(12):e1003076.
332. Müller J, Tanner R, Matsumiya M, Snowden MA, Landry B, Satti I, et al. Cytomegalovirus infection is a risk factor for tuberculosis disease in infants. JCI Insight. 2019;4(23).
333. Smithey MJ, Li G, Venturi V, Davenport MP, Nikolich-Žugich J. Lifelong persistent viral infection alters the naive T cell pool, impairing CD8 T cell immunity in late life. J Immunol. 2012;189(11):5356-66.
334. Ouyang Q, Wagner WM, Wikby A, Walter S, Aubert G, Dodi AI, et al. Large numbers of dysfunctional CD8+ T lymphocytes bearing receptors for a single dominant CMV epitope in the very old. J Clin Immunol. 2003;23(4):247-57.
335. Haq K, Fulop T, Tedder G, Gentleman B, Garneau H, Meneilly GS, et al. Cytomegalovirus Seropositivity Predicts a Decline in the T Cell But Not the Antibody Response to Influenza in Vaccinated Older Adults Independent of Type 2 Diabetes Status. J Gerontol A Biol Sci Med Sci. 2017;72(9):1163-70.
336. Derhovanessian E, Theeten H, Hähnel K, Van Damme P, Cools N, Pawelec G. Cytomegalovirus-associated accumulation of late-differentiated CD4 T-cells correlates with poor humoral response to influenza vaccination. Vaccine. 2013;31(4):685-90.
337. Frasca D, Diaz A, Romero M, Landin AM, Blomberg BB. Cytomegalovirus (CMV) seropositivity decreases B cell responses to the influenza vaccine. Vaccine. 2015;33(12):1433-9.
338. Cox M, Adetifa JU, Noho-Konteh F, Njie-Jobe J, Sanyang LC, Drammeh A, et al. Limited Impact of Human Cytomegalovirus Infection in African Infants on Vaccine-Specific Responses Following Diphtheria-Tetanus-Pertussis and Measles Vaccination. Front Immunol. 2020;11:1083.
339. Bowyer G, Sharpe H, Venkatraman N, Ndiaye PB, Wade D, Brenner N, et al. Reduced Ebola vaccine responses in CMV+ young adults is associated with expansion of CD57+KLRG1+ T cells. J Exp Med. 2020;217(7).
340. den Elzen WP, Vossen AC, Cools HJ, Westendorp RG, Kroes AC, Gussekloo J. Cytomegalovirus infection and responsiveness to influenza vaccination in elderly residents of long-term care facilities. Vaccine. 2011;29(29-30):4869-74.
341. van den Berg SPH, Wong A, Hendriks M, Jacobi RHJ, van Baarle D, van Beek J. Negative Effect of Age, but Not of Latent Cytomegalovirus Infection on the Antibody Response to a Novel Influenza Vaccine Strain in Healthy Adults. Front Immunol. 2018;9:82.
342. Strindhall J, Ernerudh J, Mörner A, Waalen K, Löfgren S, Matussek A, et al. Humoral response to influenza vaccination in relation to pre-vaccination antibody titres, vaccination history, cytomegalovirus serostatus and CD4/CD8 ratio. Infect Dis (Lond). 2016;48(6):436-42.
343. Wald A, Selke S, Magaret A, Boeckh M. Impact of human cytomegalovirus (CMV) infection on immune response to pandemic 2009 H1N1 influenza vaccine in healthy adults. J Med Virol. 2013;85(9):1557-60.
344. Miles DJ, Sanneh M, Holder B, Crozier S, Nyamweya S, Touray ES, et al. Cytomegalovirus infection induces T-cell differentiation without impairing antigen-specific responses in Gambian infants. Immunology. 2008;124(3):388-400.

345. Holder B, Miles DJ, Kaye S, Crozier S, Mohammed NI, Duah NO, et al. Epstein-Barr virus but not cytomegalovirus is associated with reduced vaccine antibody responses in Gambian infants. PLoS One. 2010;5(11):e14013.
346. O'Connor D, Trück J, Lazarus R, Clutterbuck EA, Voysey M, Jeffery K, et al. The effect of chronic cytomegalovirus infection on pneumococcal vaccine responses. J Infect Dis. 2014;209(10):1635-41.
347. Furman D, Jojic V, Sharma S, Shen-Orr SS, Angel CJ, Onengut-Gumuscu S, et al. Cytomegalovirus infection enhances the immune response to influenza. Sci Transl Med. 2015;7(281):281ra43.
348. McElhaney JE, Garneau H, Camous X, Dupuis G, Pawelec G, Baehl S, et al. Predictors of the antibody response to influenza vaccination in older adults with type 2 diabetes. BMJ Open Diabetes Res Care. 2015;3(1):e000140.
349. Martin MD, Badovinac VP. Defining Memory CD8 T Cell. Front Immunol. 2018;9:2692.
350. McCarron MJ, Park PW, Fooksman DR. CD138 mediates selection of mature plasma cells by regulating their survival. Blood. 2017;129(20):2749-59.
351. Romee R, Foley B, Lenvik T, Wang Y, Zhang B, Ankarlo D, et al. NK cell CD16 surface expression and function is regulated by a disintegrin and metalloprotease-17 (ADAM17). Blood. 2013;121(18):3599-608.
352. Dutton RW, Bradley LM, Swain SL. T cell memory. Annu Rev Immunol. 1998;16:201-23.
353. Hendriks J, Gravestein LA, Tesselaar K, van Lier RA, Schumacher TN, Borst J. CD27 is required for generation and long-term maintenance of T cell immunity. Nat Immunol. 2000;1(5):433-40.
354. Carrasco J, Godelaine D, Van Pel A, Boon T, van der Bruggen P. CD45RA on human CD8 T cells is sensitive to the time elapsed since the last antigenic stimulation. Blood. 2006;108(9):2897-905.
355. Van Acker HH, Capsomidis A, Smits EL, Van Tendeloo VF. CD56 in the Immune System: More Than a Marker for Cytotoxicity? Front Immunol. 2017;8:892.
356. Zimmermann M, Rose N, Lindner JM, Kim H, Gonçalves AR, Callegari I, et al. Antigen Extraction and B Cell Activation Enable Identification of Rare Membrane Antigen Specific Human B Cells. Front Immunol. 2019;10:829.
357. Tangye SG, Good KL. Human IgM+CD27+ B cells: memory B cells or "memory" B cells? J Immunol. 2007;179(1):13-9.
358. Kaiser BK, Pizarro JC, Kerns J, Strong RK. Structural basis for NKG2A/CD94 recognition of HLA-E. Proc Natl Acad Sci U S A. 2008;105(18):6696-701.
359. Sage PT, Francisco LM, Carman CV, Sharpe AH. The receptor PD-1 controls follicular regulatory T cells in the lymph nodes and blood. Nat Immunol. 2013;14(2):152-61.
360. Alharbi NK, Padron-Regalado E, Thompson CP, Kupke A, Wells D, Sloan MA, et al. ChAdOx1 and MVA based vaccine candidates against MERS-CoV elicit neutralising antibodies and cellular immune responses in mice. Vaccine. 2017;35(30):3780-8.
361. He XS, Draghi M, Mahmood K, Holmes TH, Kemble GW, Dekker CL, et al. T cell-dependent production of IFN-gamma by NK cells in response to influenza A virus. J Clin Invest. 2004;114(12):1812-9.

362. Goodier MR, Rodriguez-Galan A, Lusa C, Nielsen CM, Darboe A, Moldoveanu AL, et al. Influenza Vaccination Generates Cytokine-Induced Memory-like NK Cells: Impact of Human Cytomegalovirus Infection. J Immunol. 2016;197(1):313-25.
363. Wagstaffe HR, Susannini G, Thiébaut R, Richert L, Lévy Y, Bockstal V, et al. Durable natural killer cell responses after heterologous two-dose Ebola vaccination. NPJ Vaccines. 2021;6(1):19.
364. Palgen JL, Tchitchek N, Huot N, Elhmouzi-Younes J, Lefebvre C, Rosenbaum P, et al. NK cell immune responses differ after prime and boost vaccination. J Leukoc Biol. 2019;105(5):1055-73.
365. Hydes T, Noll A, Salinas-Riester G, Abuhilal M, Armstrong T, Hamady Z, et al. IL-12 and IL-15 induce the expression of CXCR6 and CD49a on peripheral natural killer cells. Immun Inflamm Dis. 2018;6(1):34-46.
366. Robbins SH, Nguyen KB, Takahashi N, Mikayama T, Biron CA, Brossay L. Cutting edge: inhibitory functions of the killer cell lectin-like receptor G1 molecule during the activation of mouse NK cells. J Immunol. 2002;168(6):2585-9.
367. Bukowski JF, Woda BA, Welsh RM. Pathogenesis of murine cytomegalovirus infection in natural killer cell-depleted mice. J Virol. 1984;52(1):119-28.
368. Soderquest K, Walzer T, Zafirova B, Klavinskis LS, Polić B, Vivier E, et al. Cutting edge: CD8+ T cell priming in the absence of NK cells leads to enhanced memory responses. J Immunol. 2011;186(6):3304-8.
369. Arapović J, Arapović M, Golemac M, Traven L, Tomac J, Rumora D, et al. The specific NK cell response in concert with perforin prevents CD8(+) T cell-mediated immunopathology after mouse cytomegalovirus infection. Med Microbiol Immunol. 2015;204(3):335-44.
370. Deniz G, Erten G, Kücüksezer UC, Kocacik D, Karagiannidis C, Aktas E, et al. Regulatory NK cells suppress antigen-specific T cell responses. J Immunol. 2008;180(2):850-7.
371. Cook KD, Whitmire JK. The depletion of NK cells prevents T cell exhaustion to efficiently control disseminating virus infection. J Immunol. 2013;190(2):641-9.
372. Mullarkey CE, Boyd A, van Laarhoven A, Lefevre EA, Veronica Carr B, Baratelli M, et al. Improved adjuvanting of seasonal influenza vaccines: preclinical studies of MVA-NP+M1 coadministration with inactivated influenza vaccine. Eur J Immunol. 2013;43(7):1940-52.
373. Bowyer G, Rampling T, Powlson J, Morter R, Wright D, Hill AVS, et al. Activation-induced Markers Detect Vaccine-Specific CD4$^+$ T Cell Responses Not Measured by Assays Conventionally Used in Clinical Trials. Vaccines (Basel). 2018;6(3).
374. Teigler JE, Penaloza-MacMaster P, Obeng R, Provine NM, Larocca RA, Borducchi EN, et al. Hexon hypervariable region-modified adenovirus type 5 (Ad5) vectors display reduced hepatotoxicity but induce T lymphocyte phenotypes similar to Ad5 vectors. Clin Vaccine Immunol. 2014;21(8):1137-44.
375. Jain N, Nguyen H, Chambers C, Kang J. Dual function of CTLA-4 in regulatory T cells and conventional T cells to prevent multiorgan autoimmunity. Proc Natl Acad Sci U S A. 2010;107(4):1524-8.
376. Blank CU, Haining WN, Held W, Hogan PG, Kallies A, Lugli E, et al. Defining 'T cell exhaustion'. Nat Rev Immunol. 2019;19(11):665-74.

377. Penaloza-MacMaster P, Alayo QA, Ra J, Provine NM, Larocca R, Lee B, et al. Inhibitory receptor expression on memory CD8 T cells following Ad vector immunization. Vaccine. 2016;34(41):4955-63.
378. Loftus RM, Assmann N, Kedia-Mehta N, O'Brien KL, Garcia A, Gillespie C, et al. Amino acid-dependent cMyc expression is essential for NK cell metabolic and functional responses in mice. Nat Commun. 2018;9(1):2341.
379. Ferlazzo G, Pack M, Thomas D, Paludan C, Schmid D, Strowig T, et al. Distinct roles of IL-12 and IL-15 in human natural killer cell activation by dendritic cells from secondary lymphoid organs. Proc Natl Acad Sci U S A. 2004;101(47):16606-11.
380. Stegmann KA, De Souza JB, Riley EM. IL-18-induced expression of high-affinity IL-2R on murine NK cells is essential for NK-cell IFN-γ production during murine Plasmodium yoelii infection. Eur J Immunol. 2015;45(12):3431-40.
381. Arase H, Mocarski ES, Campbell AE, Hill AB, Lanier LL. Direct recognition of cytomegalovirus by activating and inhibitory NK cell receptors. Science. 2002;296(5571):1323-6.
382. Lu L, Ikizawa K, Hu D, Werneck MB, Wucherpfennig KW, Cantor H. Regulation of activated CD4+ T cells by NK cells via the Qa-1-NKG2A inhibitory pathway. Immunity. 2007;26(5):593-604.
383. Vance RE, Jamieson AM, Raulet DH. Recognition of the class Ib molecule Qa-1(b) by putative activating receptors CD94/NKG2C and CD94/NKG2E on mouse natural killer cells. J Exp Med. 1999;190(12):1801-12.
384. Vossenkamper A, Warnes G. A Flow Cytometric Immunophenotyping Approach to the Detection of Regulated Cell Death Processes. Journal of Immunological Sciences. 2018;25:6-12.
385. Walzer T, Bléry M, Chaix J, Fuseri N, Chasson L, Robbins SH, et al. Identification, activation, and selective in vivo ablation of mouse NK cells via NKp46. Proc Natl Acad Sci U S A. 2007;104(9):3384-9.
386. Rose DL, Reagin KL, Oliva KE, Tompkins SM, Klonowski KD. Enhanced generation of influenza-specific tissue resident memory CD8 T cells in NK-depleted mice. Sci Rep. 2021;11(1):8969.
387. Xu H, Andersson AM, Ragonnaud E, Boilesen D, Tolver A, Jensen BAH, et al. Mucosal Vaccination with Heterologous Viral Vectored Vaccine Targeting Subdominant SIV Accessory Antigens Strongly Inhibits Early Viral Replication. EBioMedicine. 2017;18:204-15.
388. Sharpe AH, Pauken KE. The diverse functions of the PD1 inhibitory pathway. Nat Rev Immunol. 2018;18(3):153-67.
389. Parry HM, Dowell AC, Zuo J, Verma K, Kinsella FAM, Begum J, et al. PD-1 is imprinted on cytomegalovirus-specific CD4+ T cells and attenuates Th1 cytokine production whilst maintaining cytotoxicity. PLoS Pathog. 2021;17(3):e1009349.
390. Larocca RA, Provine NM, Aid M, Iampietro MJ, Borducchi EN, Badamchi-Zadeh A, et al. Adenovirus serotype 5 vaccine vectors trigger IL-27-dependent inhibitory CD4. Sci Immunol. 2016;1(5).
391. Lin PH, Wong WI, Wang YL, Hsieh MP, Lu CW, Liang CY, et al. Vaccine-induced antigen-specific regulatory T cells attenuate the antiviral immunity against acute influenza virus infection. Mucosal Immunol. 2018;11(4):1239-53.

392. Timothy AA, Tokanovic A, Snibson KJ, Edwards SJ, Pearse MJ, Scheerlinck JP, et al. ISCOMATRIX™ adjuvant reduces mucosal tolerance for effective pulmonary vaccination against influenza. Hum Vaccin Immunother. 2015;11(2):377-85.
393. Zhu J, Huang X, Yang Y. A critical role for type I IFN-dependent NK cell activation in innate immune elimination of adenoviral vectors in vivo. Mol Ther. 2008;16(7):1300-7.
394. Zhu J, Huang X, Yang Y. NKG2D is required for NK cell activation and function in response to E1-deleted adenovirus. J Immunol. 2010;185(12):7480-6.
395. Williams KJ, Qiu X, Fernando L, Jones SM, Alimonti JB. VSVΔG/EBOV GP-induced innate protection enhances natural killer cell activity to increase survival in a lethal mouse adapted Ebola virus infection. Viral Immunol. 2015;28(1):51-61.
396. Nielsen CM, White MJ, Bottomley C, Lusa C, Rodríguez-Galán A, Turner SE, et al. Impaired NK Cell Responses to Pertussis and H1N1 Influenza Vaccine Antigens in Human Cytomegalovirus-Infected Individuals. J Immunol. 2015;194(10):4657-67.
397. Li T, Wang J, Wang Y, Chen Y, Wei H, Sun R, et al. Respiratory Influenza Virus Infection Induces Memory-like Liver NK Cells in Mice. J Immunol. 2017;198(3):1242-52.
398. Milo I, Blecher-Gonen R, Barnett-Itzhaki Z, Bar-Ziv R, Tal O, Gurevich I, et al. The bone marrow is patrolled by NK cells that are primed and expand in response to systemic viral activation. Eur J Immunol. 2018;48(7):1137-52.
399. Sun JC, Beilke JN, Lanier LL. Adaptive immune features of natural killer cells. Nature. 2009;457(7229):557-61.
400. Horowitz A, Behrens RH, Okell L, Fooks AR, Riley EM. NK cells as effectors of acquired immune responses: effector CD4+ T cell-dependent activation of NK cells following vaccination. J Immunol. 2010;185(5):2808-18.
401. Nielsen CM, Wolf AS, Goodier MR, Riley EM. Synergy between Common γ Chain Family Cytokines and IL-18 Potentiates Innate and Adaptive Pathways of NK Cell Activation. Front Immunol. 2016;7:101.
402. Collignon C, Bol V, Chalon A, Surendran N, Morel S, van den Berg RA, et al. Innate Immune Responses to Chimpanzee Adenovirus Vector 155 Vaccination in Mice and Monkeys. Front Immunol. 2020;11:579872.
403. Sánchez-Puig JM, Sánchez L, Roy G, Blasco R. Susceptibility of different leukocyte cell types to Vaccinia virus infection. Virol J. 2004;1:10.
404. Dicks MD, Spencer AJ, Coughlan L, Bauza K, Gilbert SC, Hill AV, et al. Differential immunogenicity between HAdV-5 and chimpanzee adenovirus vector ChAdOx1 is independent of fiber and penton RGD loop sequences in mice. Sci Rep. 2015;5:16756.
405. Schroers R, Hildebrandt Y, Hasenkamp J, Glass B, Lieber A, Wulf G, et al. Gene transfer into human T lymphocytes and natural killer cells by Ad5/F35 chimeric adenoviral vectors. Exp Hematol. 2004;32(6):536-46.
406. Hatfield SD, Daniels KA, O'Donnell CL, Waggoner SN, Welsh RM. Weak vaccinia virus-induced NK cell regulation of CD4 T cells is associated with reduced NK cell differentiation and cytolytic activity. Virology. 2018;519:131-44.
407. Martinez J, Huang X, Yang Y. Direct action of type I IFN on NK cells is required for their activation in response to vaccinia viral infection in vivo. J Immunol. 2008;180(3):1592-7.
408. Arlettaz L, Villard J, de Rham C, Degermann S, Chapuis B, Huard B, et al. Activating CD94:NKG2C and inhibitory CD94:NKG2A receptors are expressed by distinct subsets of committed CD8+ TCR alphabeta lymphocytes. Eur J Immunol. 2004;34(12):3456-64.

409. Simpson J, Loh Z, Ullah MA, Lynch JP, Werder RB, Collinson N, et al. Respiratory Syncytial Virus Infection Promotes Necroptosis and HMGB1 Release by Airway Epithelial Cells. Am J Respir Crit Care Med. 2020;201(11):1358-71.
410. Cho YS, Challa S, Moquin D, Genga R, Ray TD, Guildford M, et al. Phosphorylation-driven assembly of the RIP1-RIP3 complex regulates programmed necrosis and virus-induced inflammation. Cell. 2009;137(6):1112-23.
411. Benedict CA, Norris PS, Prigozy TI, Bodmer JL, Mahr JA, Garnett CT, et al. Three adenovirus E3 proteins cooperate to evade apoptosis by tumor necrosis factor-related apoptosis-inducing ligand receptor-1 and -2. J Biol Chem. 2001;276(5):3270-8.
412. Guo H, Omoto S, Harris PA, Finger JN, Bertin J, Gough PJ, et al. Herpes simplex virus suppresses necroptosis in human cells. Cell Host Microbe. 2015;17(2):243-51.
413. Koehler HS, Jacobs BL. Subversion of Programed Cell Death by Poxviruses. Curr Top Microbiol Immunol. 2021.
414. Liu Z, Nailwal H, Rector J, Rahman MM, Sam R, McFadden G, et al. A class of viral inducer of degradation of the necroptosis adaptor RIPK3 regulates virus-induced inflammation. Immunity. 2021;54(2):247-58.e7.
415. Veyer DL, Carrara G, Maluquer de Motes C, Smith GL. Vaccinia virus evasion of regulated cell death. Immunol Lett. 2017;186:68-80.
416. Omoto S, Guo H, Talekar GR, Roback L, Kaiser WJ, Mocarski ES. Suppression of RIP3-dependent necroptosis by human cytomegalovirus. J Biol Chem. 2015;290(18):11635-48.
417. Cook KD, Waggoner SN, Whitmire JK. NK cells and their ability to modulate T cells during virus infections. Crit Rev Immunol. 2014;34(5):359-88.
418. Blass E, Aid M, Martinot AJ, Larocca RA, Kang ZH, Badamchi-Zadeh A, et al. Adenovirus Vector Vaccination Impacts NK Cell Rheostat Function following Lymphocytic Choriomeningitis Virus Infection. J Virol. 2018;92(11).
419. Lang PA, Lang KS, Xu HC, Grusdat M, Parish IA, Recher M, et al. Natural killer cell activation enhances immune pathology and promotes chronic infection by limiting CD8+ T-cell immunity. Proc Natl Acad Sci U S A. 2012;109(4):1210-5.
420. Ivanova DL, Krempels R, Denton SL, Fettel KD, Saltz GM, Rach D, et al. NK Cells Negatively Regulate CD8 T Cells to Promote Immune Exhaustion and Chronic. Front Cell Infect Microbiol. 2020;10:313.
421. Perona-Wright G, Mohrs K, Szaba FM, Kummer LW, Madan R, Karp CL, et al. Systemic but not local infections elicit immunosuppressive IL-10 production by natural killer cells. Cell Host Microbe. 2009;6(6):503-12.
422. Wang H, Li J, Dong X, Zhou X, Zhao L, Wang X, et al. NK Cells Contribute to Protective Memory T Cell Mediated Immunity to. Front Cell Infect Microbiol. 2020;10:296.
423. Habib S, El Andaloussi A, Hisham A, Ismail N. NK Cell-Mediated Regulation of Protective Memory Responses against Intracellular Ehrlichial Pathogens. PLoS One. 2016;11(4):e0153223.
424. Byrne P, McGuirk P, Todryk S, Mills KH. Depletion of NK cells results in disseminating lethal infection with Bordetella pertussis associated with a reduction of antigen-specific Th1 and enhancement of Th2, but not Tr1 cells. Eur J Immunol. 2004;34(9):2579-88.

425. Rydyznski C, Daniels KA, Karmele EP, Brooks TR, Mahl SE, Moran MT, et al. Generation of cellular immune memory and B-cell immunity is impaired by natural killer cells. Nat Commun. 2015;6:6375.
426. Stanley DA, Honko AN, Asiedu C, Trefry JC, Lau-Kilby AW, Johnson JC, et al. Chimpanzee adenovirus vaccine generates acute and durable protective immunity against ebolavirus challenge. Nat Med. 2014;20(10):1126-9.
427. Geddes L. How effective are COVID-19 vaccines in the real world? 2021 [Available from: https://www.gavi.org/vaccineswork/how-effective-are-covid-19-vaccines-real-world.
428. Warimwe GM, Lorenzo G, Lopez-Gil E, Reyes-Sandoval A, Cottingham MG, Spencer AJ, et al. Immunogenicity and efficacy of a chimpanzee adenovirus-vectored Rift Valley fever vaccine in mice. Virol J. 2013;10:349.
429. Alharbi NK, Qasim I, Almasoud A, Aljami HA, Alenazi MW, Alhafufi A, et al. Humoral Immunogenicity and Efficacy of a Single Dose of ChAdOx1 MERS Vaccine Candidate in Dromedary Camels. Sci Rep. 2019;9(1):16292.
430. Tseng CT, Sbrana E, Iwata-Yoshikawa N, Newman PC, Garron T, Atmar RL, et al. Immunization with SARS coronavirus vaccines leads to pulmonary immunopathology on challenge with the SARS virus. PLoS One. 2012;7(4):e35421.
431. Wagstaffe HR, Clutterbuck EA, Bockstal V, Stoop JN, Luhn K, Douoguih M, et al. Ebola virus glycoprotein stimulates IL-18-dependent natural killer cell responses. J Clin Invest. 2020;130(7):3936-46.
432. McMichael AJ, Gotch FM, Noble GR, Beare PA. Cytotoxic T-cell immunity to influenza. N Engl J Med. 1983;309(1):13-7.
433. Wei CJ, Boyington JC, McTamney PM, Kong WP, Pearce MB, Xu L, et al. Induction of broadly neutralizing H1N1 influenza antibodies by vaccination. Science. 2010;329(5995):1060-4.
434. Epstein SL, Kong WP, Misplon JA, Lo CY, Tumpey TM, Xu L, et al. Protection against multiple influenza A subtypes by vaccination with highly conserved nucleoprotein. Vaccine. 2005;23(46-47):5404-10.
435. Del Campo J, Pizzorno A, Djebali S, Bouley J, Haller M, Pérez-Vargas J, et al. OVX836 a recombinant nucleoprotein vaccine inducing cellular responses and protective efficacy against multiple influenza A subtypes. NPJ Vaccines. 2019;4:4.
436. Schneider J, Gilbert SC, Hannan CM, Dégano P, Prieur E, Sheu EG, et al. Induction of CD8+ T cells using heterologous prime-boost immunisation strategies. Immunol Rev. 1999;170:29-38.
437. Portevin D, Young D. Natural killer cell cytokine response to M. bovis BCG Is associated with inhibited proliferation, increased apoptosis and ultimate depletion of NKp44(+)CD56(bright) cells. PLoS One. 2013;8(7):e68864.
438. Kim M, Kim TJ, Kim HM, Doh J, Lee KM. Multi-cellular natural killer (NK) cell clusters enhance NK cell activation through localizing IL-2 within the cluster. Sci Rep. 2017;7:40623.
439. Lee SH, Kim KS, Fodil-Cornu N, Vidal SM, Biron CA. Activating receptors promote NK cell expansion for maintenance, IL-10 production, and CD8 T cell regulation during viral infection. J Exp Med. 2009;206(10):2235-51.
440. Davis ZB, Cooley SA, Cichocki F, Felices M, Wangen R, Luo X, et al. Adaptive Natural Killer Cell and Killer Cell Immunoglobulin-Like Receptor-Expressing T Cell Responses are Induced by Cytomegalovirus and Are Associated with Protection against

Cytomegalovirus Reactivation after Allogeneic Donor Hematopoietic Cell Transplantation. Biol Blood Marrow Transplant. 2015;21(9):1653-62.
441. Fodil-Cornu N, Lee SH, Belanger S, Makrigiannis AP, Biron CA, Buller RM, et al. Ly49h-deficient C57BL/6 mice: a new mouse cytomegalovirus-susceptible model remains resistant to unrelated pathogens controlled by the NK gene complex. J Immunol. 2008;181(9):6394-405.
442. Brisse E, Imbrechts M, Put K, Avau A, Mitera T, Berghmans N, et al. Mouse Cytomegalovirus Infection in BALB/c Mice Resembles Virus-Associated Secondary Hemophagocytic Lymphohistiocytosis and Shows a Pathogenesis Distinct from Primary Hemophagocytic Lymphohistiocytosis. J Immunol. 2016;196(7):3124-34.
443. Jouand N, Bressollette-Bodin C, Gérard N, Giral M, Guérif P, Rodallec A, et al. HCMV triggers frequent and persistent UL40-specific unconventional HLA-E-restricted CD8 T-cell responses with potential autologous and allogeneic peptide recognition. PLoS Pathog. 2018;14(4):e1007041.
444. Li H, Hou Y, Zhang S, Zhou Y, Wang D, Tao S, et al. CD49a regulates the function of human decidual natural killer cells. Am J Reprod Immunol. 2019;81(4):e13101.
445. Martrus G, Goebels H, Langeneckert AE, Kah J, Flomm F, Ziegler AE, et al. CD49a Expression Identifies a Subset of Intrahepatic Macrophages in Humans. Front Immunol. 2019;10:1247.
446. Klose CSN, Flach M, Möhle L, Rogell L, Hoyler T, Ebert K, et al. Differentiation of type 1 ILCs from a common progenitor to all helper-like innate lymphoid cell lineages. Cell. 2014;157(2):340-56.
447. McSharry BP, Samer C, McWilliam HEG, Ashley CL, Yee MB, Steain M, et al. Virus-Mediated Suppression of the Antigen Presentation Molecule MR1. Cell Rep. 2020;30(9):2948-62.e4.
448. Sciumè G, De Angelis G, Benigni G, Ponzetta A, Morrone S, Santoni A, et al. CX3CR1 expression defines 2 KLRG1+ mouse NK-cell subsets with distinct functional properties and positioning in the bone marrow. Blood. 2011;117(17):4467-75.
449. Gerlach C, Moseman EA, Loughhead SM, Alvarez D, Zwijnenburg AJ, Waanders L, et al. The Chemokine Receptor CX3CR1 Defines Three Antigen-Experienced CD8 T Cell Subsets with Distinct Roles in Immune Surveillance and Homeostasis. Immunity. 2016;45(6):1270-84.
450. Böttcher JP, Beyer M, Meissner F, Abdullah Z, Sander J, Höchst B, et al. Functional classification of memory CD8(+) T cells by CX3CR1 expression. Nat Commun. 2015;6:8306.
451. Rapaport AS, Schriewer J, Gilfillan S, Hembrador E, Crump R, Plougastel BF, et al. The Inhibitory Receptor NKG2A Sustains Virus-Specific CD8^{+} T Cells in Response to a Lethal Poxvirus Infection. Immunity. 2015;43(6):1112-24.
452. Wein AN, McMaster SR, Takamura S, Dunbar PR, Cartwright EK, Hayward SL, et al. CXCR6 regulates localization of tissue-resident memory CD8 T cells to the airways. J Exp Med. 2019;216(12):2748-62.
453. Latta M, Mohan K, Issekutz TB. CXCR6 is expressed on T cells in both T helper type 1 (Th1) inflammation and allergen-induced Th2 lung inflammation but is only a weak mediator of chemotaxis. Immunology. 2007;121(4):555-64.
454. Batista NV, Chang YH, Chu KL, Wang KC, Girard M, Watts TH. T Cell-Intrinsic CX3CR1 Marks the Most Differentiated Effector CD4. Immunohorizons. 2020;4(11):701-12.

455. Gordon CL, Lee LN, Swadling L, Hutchings C, Zinser M, Highton AJ, et al. Induction and Maintenance of CX3CR1-Intermediate Peripheral Memory CD8. Cell Rep. 2018;23(3):768-82.
456. Kjer-Nielsen L, Corbett AJ, Chen Z, Liu L, Mak JY, Godfrey DI, et al. An overview on the identification of MAIT cell antigens. Immunol Cell Biol. 2018;96(6):573-87.
457. Howson LJ, Salio M, Cerundolo V. MR1-Restricted Mucosal-Associated Invariant T Cells and Their Activation during Infectious Diseases. Front Immunol. 2015;6:303.
458. Fogel LA, Sun MM, Geurs TL, Carayannopoulos LN, French AR. Markers of nonselective and specific NK cell activation. J Immunol. 2013;190(12):6269-76.
459. Gordon SM, Chaix J, Rupp LJ, Wu J, Madera S, Sun JC, et al. The transcription factors T-bet and Eomes control key checkpoints of natural killer cell maturation. Immunity. 2012;36(1):55-67.
460. Abt MC, Lewis BB, Caballero S, Xiong H, Carter RA, Sušac B, et al. Innate Immune Defenses Mediated by Two ILC Subsets Are Critical for Protection against Acute Clostridium difficile Infection. Cell Host Microbe. 2015;18(1):27-37.
461. Smith HR, Heusel JW, Mehta IK, Kim S, Dorner BG, Naidenko OV, et al. Recognition of a virus-encoded ligand by a natural killer cell activation receptor. Proc Natl Acad Sci U S A. 2002;99(13):8826-31.
462. Lindenberg M, Solmaz G, Puttur F, Sparwasser T. Mouse cytomegalovirus infection overrules T regulatory cell suppression on natural killer cells. Virol J. 2014;11:145.
463. Popovic B, Golemac M, Podlech J, Zeleznjak J, Bilic-Zulle L, Lukic ML, et al. IL-33/ST2 pathway drives regulatory T cell dependent suppression of liver damage upon cytomegalovirus infection. PLoS Pathog. 2017;13(4):e1006345.
464. Blackburn SD, Shin H, Haining WN, Zou T, Workman CJ, Polley A, et al. Coregulation of CD8+ T cell exhaustion by multiple inhibitory receptors during chronic viral infection. Nat Immunol. 2009;10(1):29-37.
465. Hertoghs KM, Moerland PD, van Stijn A, Remmerswaal EB, Yong SL, van de Berg PJ, et al. Molecular profiling of cytomegalovirus-induced human CD8+ T cell differentiation. J Clin Invest. 2010;120(11):4077-90.
466. Pallett LJ, Davies J, Colbeck EJ, Robertson F, Hansi N, Easom NJW, et al. IL-2. J Exp Med. 2017;214(6):1567-80.
467. Tse SW, Radtke AJ, Espinosa DA, Cockburn IA, Zavala F. The chemokine receptor CXCR6 is required for the maintenance of liver memory $CD8^+$ T cells specific for infectious pathogens. J Infect Dis. 2014;210(9):1508-16.
468. Heesch K, Raczkowski F, Schumacher V, Hünemörder S, Panzer U, Mittrücker HW. The function of the chemokine receptor CXCR6 in the T cell response of mice against Listeria monocytogenes. PLoS One. 2014;9(5):e97701.
469. Redeker A, Remmerswaal EBM, van der Gracht ETI, Welten SPM, Höllt T, Koning F, et al. The Contribution of Cytomegalovirus Infection to Immune Senescence Is Set by the Infectious Dose. Front Immunol. 2017;8:1953.
470. Della Chiesa M, Pesce S, Muccio L, Carlomagno S, Sivori S, Moretta A, et al. Features of Memory-Like and PD-1(+) Human NK Cell Subsets. Front Immunol. 2016;7:351.
471. Wilkinson GW, Davison AJ, Tomasec P, Fielding CA, Aicheler R, Murrell I, et al. Human cytomegalovirus: taking the strain. Med Microbiol Immunol. 2015;204(3):273-84.

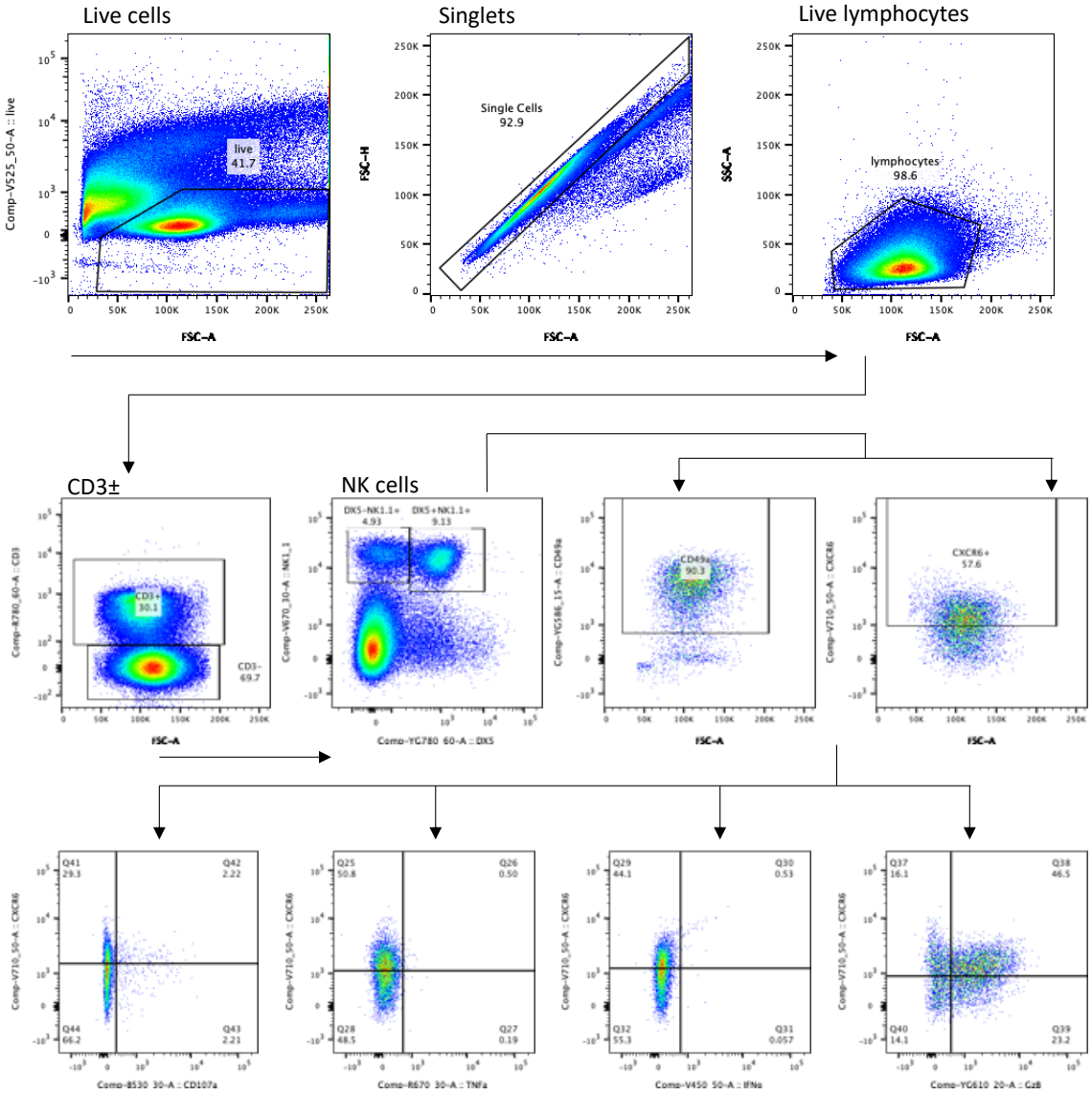
472. Tao H, Pan Y, Chu S, Li L, Xie J, Wang P, et al. Differential controls of MAIT cell effector polarization by mTORC1/mTORC2 via integrating cytokine and costimulatory signals. Nat Commun. 2021;12(1):2029.
473. Petley EV, Koay H-F, Henderson MA, Sek K, Todd KL, Keam SP, et al. MAIT cells regulate NK cell mediated tumour immunity. ResearchSquare PREPRINT. 2020.
474. Manicklal S, Emery VC, Lazzarotto T, Boppana SB, Gupta RK. The "silent" global burden of congenital cytomegalovirus. Clin Microbiol Rev. 2013;26(1):86-102.
475. Mekker A, Tchang VS, Haeberli L, Oxenius A, Trkola A, Karrer U. Immune senescence: relative contributions of age and cytomegalovirus infection. PLoS Pathog. 2012;8(8):e1002850.
476. Staras SA, Dollard SC, Radford KW, Flanders WD, Pass RF, Cannon MJ. Seroprevalence of cytomegalovirus infection in the United States, 1988-1994. Clin Infect Dis. 2006;43(9):1143-51.
477. Adland E, Klenerman P, Goulder P, Matthews PC. Ongoing burden of disease and mortality from HIV/CMV coinfection in Africa in the antiretroviral therapy era. Front Microbiol. 2015;6:1016.
478. Groh V, Rhinehart R, Randolph-Habecker J, Topp MS, Riddell SR, Spies T. Costimulation of CD8alphabeta T cells by NKG2D via engagement by MIC induced on virus-infected cells. Nat Immunol. 2001;2(3):255-60.
479. Derhovanessian E, Maier AB, Hähnel K, McElhaney JE, Slagboom EP, Pawelec G. Latent infection with cytomegalovirus is associated with poor memory CD4 responses to influenza A core proteins in the elderly. J Immunol. 2014;193(7):3624-31.
480. Miles DJ, van der Sande M, Jeffries D, Kaye S, Ojuola O, Sanneh M, et al. Maintenance of large subpopulations of differentiated CD8 T-cells two years after cytomegalovirus infection in Gambian infants. PLoS One. 2008;3(8):e2905.
481. Miles DJ, van der Sande M, Jeffries D, Kaye S, Ismaili J, Ojuola O, et al. Cytomegalovirus infection in Gambian infants leads to profound CD8 T-cell differentiation. J Virol. 2007;81(11):5766-76.
482. McMahon M, Asthagiri Arunkumar G, Liu WC, Stadlbauer D, Albrecht RA, Pavot V, et al. Vaccination With Viral Vectors Expressing Chimeric Hemagglutinin, NP and M1 Antigens Protects Ferrets Against Influenza Virus Challenge. Front Immunol. 2019;10:2005.
483. Goodier MR, Jonjić S, Riley EM, Juranić Lisnić V. CMV and natural killer cells: shaping the response to vaccination. Eur J Immunol. 2018;48(1):50-65.
484. Bihl F, Pecheur J, Bréart B, Poupon G, Cazareth J, Julia V, et al. Primed antigen-specific CD4+ T cells are required for NK cell activation in vivo upon Leishmania major infection. J Immunol. 2010;185(4):2174-81.
485. Gumá M, Angulo A, Vilches C, Gómez-Lozano N, Malats N, López-Botet M. Imprint of human cytomegalovirus infection on the NK cell receptor repertoire. Blood. 2004;104(12):3664-71.
486. Heatley SL, Pietra G, Lin J, Widjaja JM, Harpur CM, Lester S, et al. Polymorphism in human cytomegalovirus UL40 impacts on recognition of human leukocyte antigen-E (HLA-E) by natural killer cells. J Biol Chem. 2013;288(12):8679-90.
487. Schlums H, Cichocki F, Tesi B, Theorell J, Beziat V, Holmes TD, et al. Cytomegalovirus infection drives adaptive epigenetic diversification of NK cells with altered signaling and effector function. Immunity. 2015;42(3):443-56.

488. Freeman BE, Raué HP, Hill AB, Slifka MK. Cytokine-Mediated Activation of NK Cells during Viral Infection. J Virol. 2015;89(15):7922-31.
489. Luetke-Eversloh M, Hammer Q, Durek P, Nordström K, Gasparoni G, Pink M, et al. Human cytomegalovirus drives epigenetic imprinting of the IFNG locus in NKG2Chi natural killer cells. PLoS Pathog. 2014;10(10):e1004441.
490. Horowitz A, Hafalla JC, King E, Lusingu J, Dekker D, Leach A, et al. Antigen-specific IL-2 secretion correlates with NK cell responses after immunization of Tanzanian children with the RTS,S/AS01 malaria vaccine. J Immunol. 2012;188(10):5054-62.
491. Darboe A, Danso E, Clarke E, Umesi A, Touray E, Wegmuller R, et al. Enhancement of cytokine-driven NK cell IFN-γ production after vaccination of HCMV infected Africans. Eur J Immunol. 2017;47(6):1040-50.
492. Zhang JY, Wang XM, Xing X, Xu Z, Zhang C, Song JW, et al. Single-cell landscape of immunological responses in patients with COVID-19. Nat Immunol. 2020;21(9):1107-18.
493. Diao B, Wang C, Tan Y, Chen X, Liu Y, Ning L, et al. Reduction and Functional Exhaustion of T Cells in Patients With Coronavirus Disease 2019 (COVID-19). Front Immunol. 2020;11:827.
494. Song JW, Zhang C, Fan X, Meng FP, Xu Z, Xia P, et al. Immunological and inflammatory profiles in mild and severe cases of COVID-19. Nat Commun. 2020;11(1):3410.
495. Chen G, Wu D, Guo W, Cao Y, Huang D, Wang H, et al. Clinical and immunological features of severe and moderate coronavirus disease 2019. J Clin Invest. 2020;130(5):2620-9.
496. Sette A, Crotty S. Adaptive immunity to SARS-CoV-2 and COVID-19. Cell. 2021;184(4):861-80.
497. Remy KE, Mazer M, Striker DA, Ellebedy AH, Walton AH, Unsinger J, et al. Severe immunosuppression and not a cytokine storm characterizes COVID-19 infections. JCI Insight. 2020;5(17).
498. Zheng M, Gao Y, Wang G, Song G, Liu S, Sun D, et al. Functional exhaustion of antiviral lymphocytes in COVID-19 patients. Cell Mol Immunol. 2020;17(5):533-5.
499. Maucourant C, Filipovic I, Ponzetta A, Aleman S, Cornillet M, Hertwig L, et al. Natural killer cell immunotypes related to COVID-19 disease severity. Sci Immunol. 2020;5(50).
500. Bortolotti D, Gentili V, Rizzo S, Rotola A, Rizzo R. SARS-CoV-2 Spike 1 Protein Controls Natural Killer Cell Activation via the HLA-E/NKG2A Pathway. Cells. 2020;9(9).
501. Hartley GE, Edwards ESJ, Aui PM, Varese N, Stojanovic S, McMahon J, et al. Rapid generation of durable B cell memory to SARS-CoV-2 spike and nucleocapsid proteins in COVID-19 and convalescence. Sci Immunol. 2020;5(54).
502. Lucas C, Wong P, Klein J, Castro TBR, Silva J, Sundaram M, et al. Longitudinal analyses reveal immunological misfiring in severe COVID-19. Nature. 2020;584(7821):463-9.
503. Chua RL, Lukassen S, Trump S, Hennig BP, Wendisch D, Pott F, et al. COVID-19 severity correlates with airway epithelium-immune cell interactions identified by single-cell analysis. Nat Biotechnol. 2020;38(8):970-9.
504. Youngs J, Provine NM, Lim N, Sharpe HR, Amini A, Chen YL, et al. Identification of immune correlates of fatal outcomes in critically ill COVID-19 patients. PLoS Pathog. 2021;17(9):e1009804.

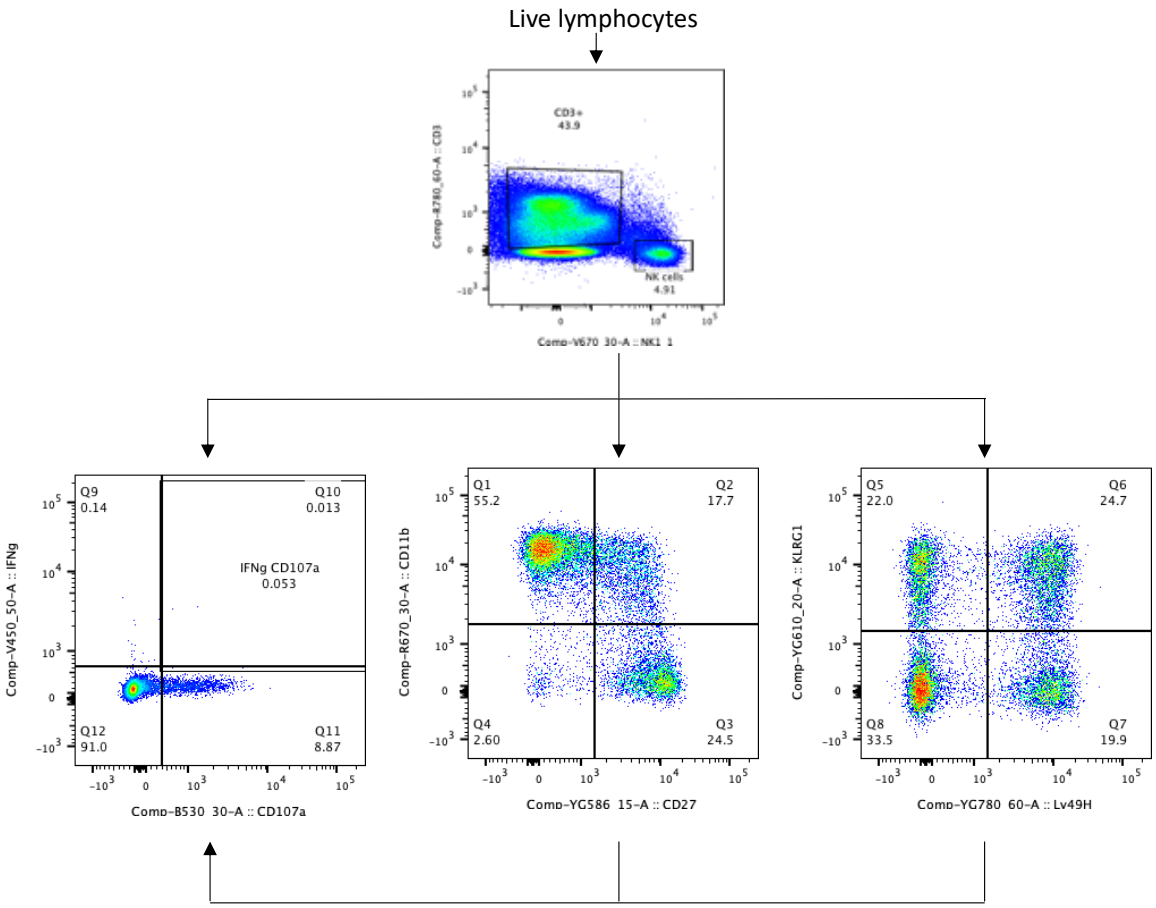
505. Voysey M, Costa Clemens SA, Madhi SA, Weckx LY, Folegatti PM, Aley PK, et al. Single-dose administration and the influence of the timing of the booster dose on immunogenicity and efficacy of ChAdOx1 nCoV-19 (AZD1222) vaccine: a pooled analysis of four randomised trials. Lancet. 2021;397(10277):881-91.
506. University O. Oxford vaccine reaches one billion dose released. 2021.
507. Wagstaffe HR, Clutterbuck EA, Bockstal V, Stoop JN, Luhn K, Douoguih M, et al. Antibody-Dependent Natural Killer Cell Activation after Ebola Vaccination. J Infect Dis. 2019.
508. Sun P, Williams M, Nagabhushana N, Jani V, Defang G, Morrison BJ. NK Cells Activated through Antibody-Dependent Cell Cytotoxicity and Armed with Degranulation/IFN-γ Production Suppress Antibody-dependent Enhancement of Dengue Viral Infection. Sci Rep. 2019;9(1):1109.
509. Matchett WE, Anguiano-Zarate SS, Barry MA. Comparison of systemic and mucosal immunization with replicating Single cycle Adenoviruses. Glob Vaccines Immunol. 2018;3(1).
510. Kim MH, Kim HJ, Chang J. Superior immune responses induced by intranasal immunization with recombinant adenovirus-based vaccine expressing full-length Spike protein of Middle East respiratory syndrome coronavirus. PLoS One. 2019;14(7):e0220196.
511. Shaw RH, Stuart A, Greenland M, Liu X, Nguyen Van-Tam JS, Snape MD, et al. Heterologous prime-boost COVID-19 vaccination: initial reactogenicity data. Lancet. 2021;397(10289):2043-6.
512. Gorman S, Harvey NL, Moro D, Lloyd ML, Voigt V, Smith LM, et al. Mixed infection with multiple strains of murine cytomegalovirus occurs following simultaneous or sequential infection of immunocompetent mice. J Gen Virol. 2006;87(Pt 5):1123-32.
513. Goüy de Bellocq J, Baird SJ, Albrechtová J, Sobeková K, Piálek J. Murine cytomegalovirus is not restricted to the house mouse Mus musculus domesticus: prevalence and genetic diversity in the European house mouse hybrid zone. J Virol. 2015;89(1):406-14.
514. Ryg-Cornejo V, Ioannidis LJ, Ly A, Chiu CY, Tellier J, Hill DL, et al. Severe Malaria Infections Impair Germinal Center Responses by Inhibiting T Follicular Helper Cell Differentiation. Cell Rep. 2016;14(1):68-81.

Appendix

Circulating and tissue resident NK cells

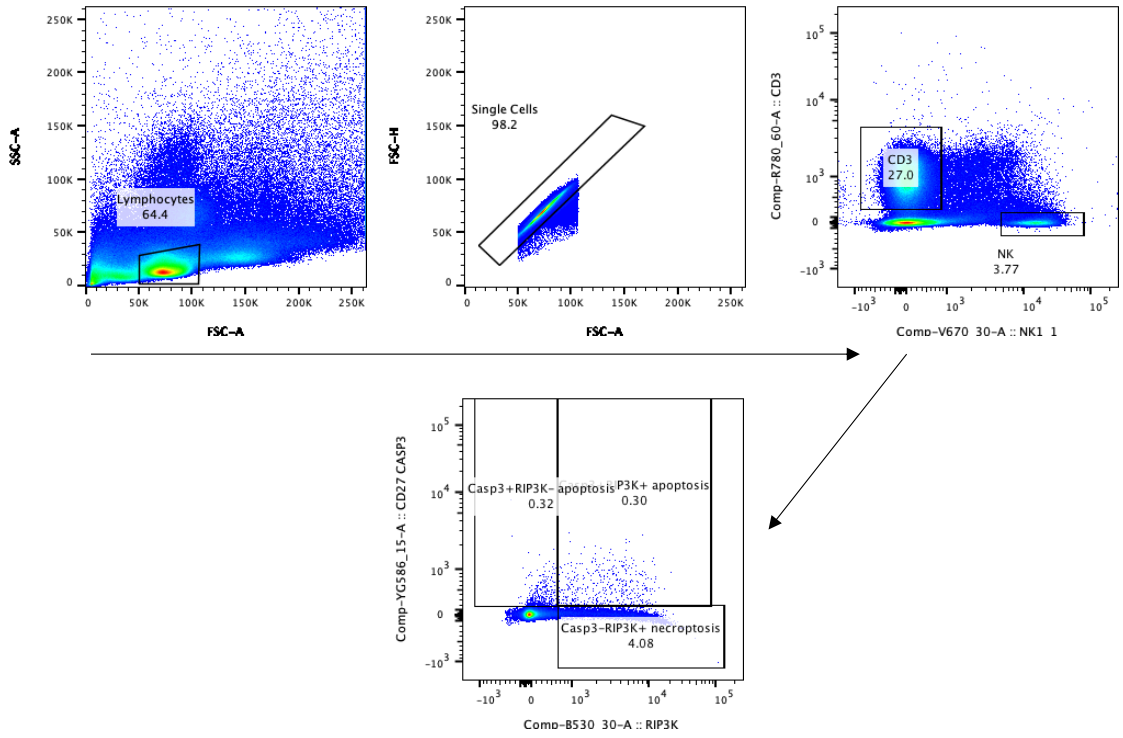


Supplementary Figure 1. Gating strategy for circulating and tissue resident NK cells



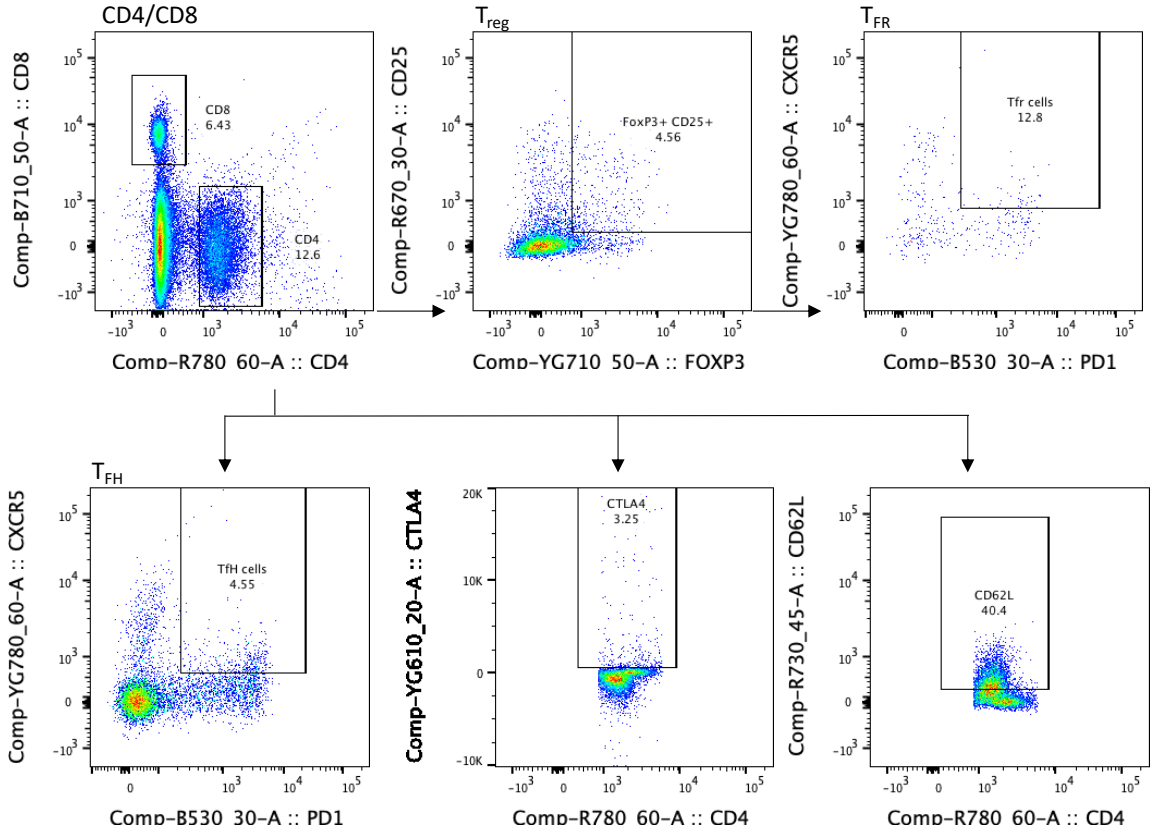
Supplementary Figure 2. Gating strategy for NK cell maturation and activation

Apoptosis and necroptosis



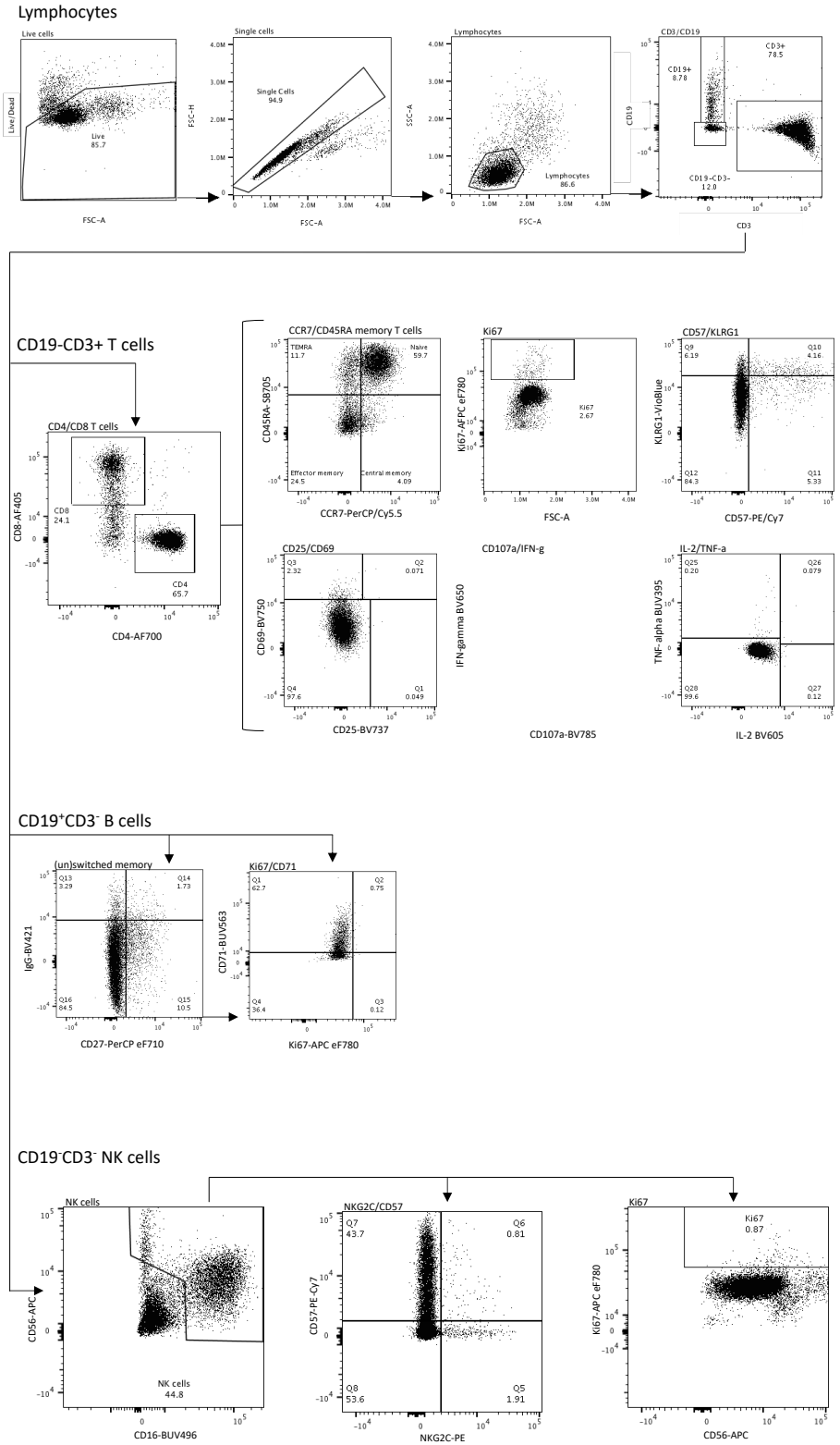
Supplementary Figure 3. Gating strategy for apoptosis and necroptosis

Regulatory T cells and T cell phenotyping

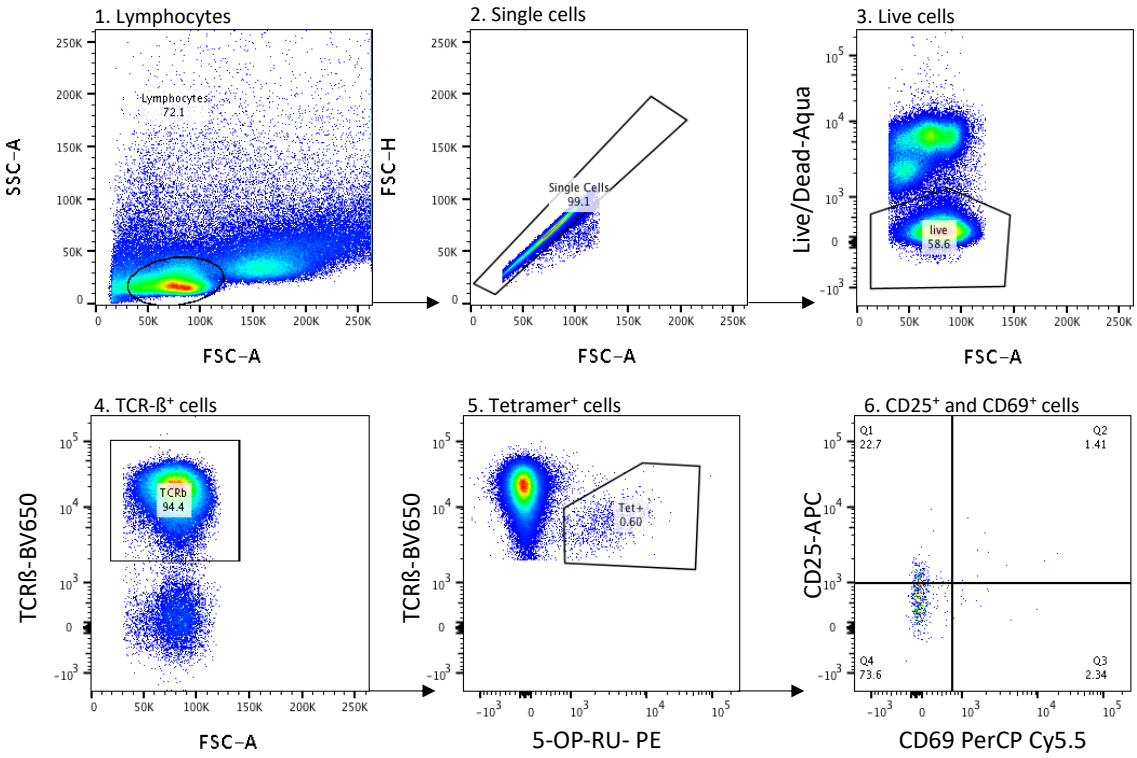


Supplementary Figure 4. Gating strategy for regulatory T cells and T cell phenotyping

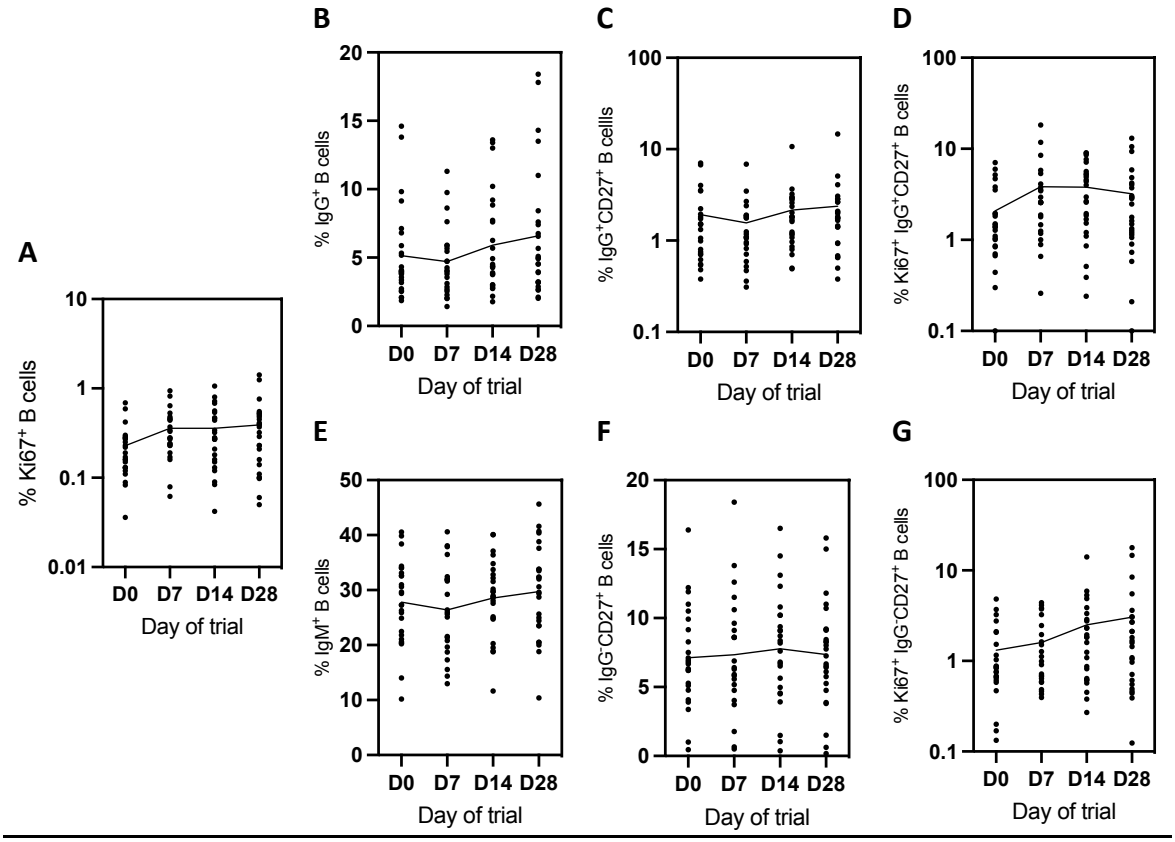
FlowJo gating for Aurora cytometry analysis



Supplementary Figure 5. Gating strategy for Aurora flow cytometry (as published in Ewer *et al* 2020).



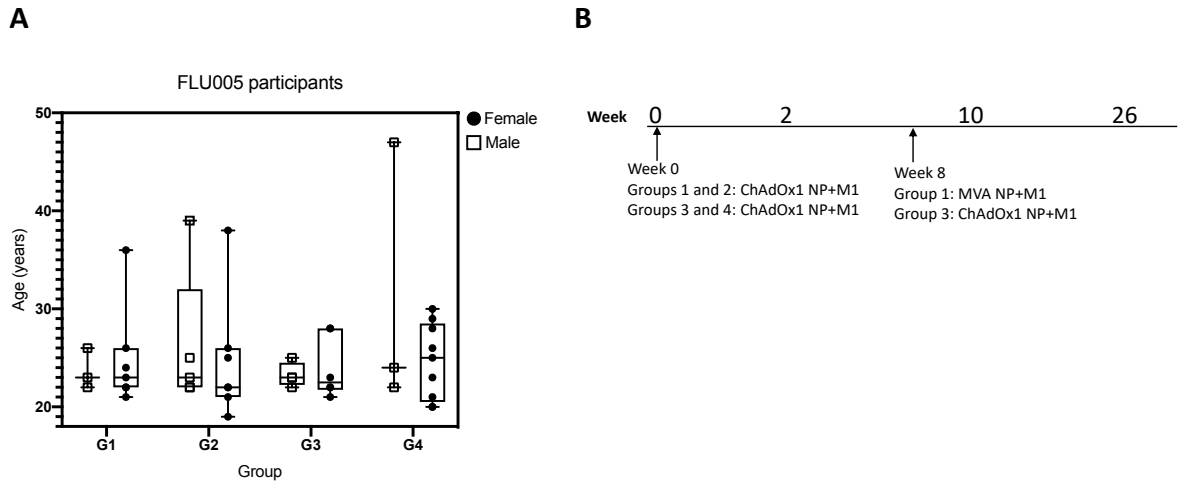
Supplementary Figure 6. Gating strategy for mouse MAIT cells



Supplementary Figure 7. B cell activation, memory populations and class switching following vaccination with ChAdOx1 nCoV-19.

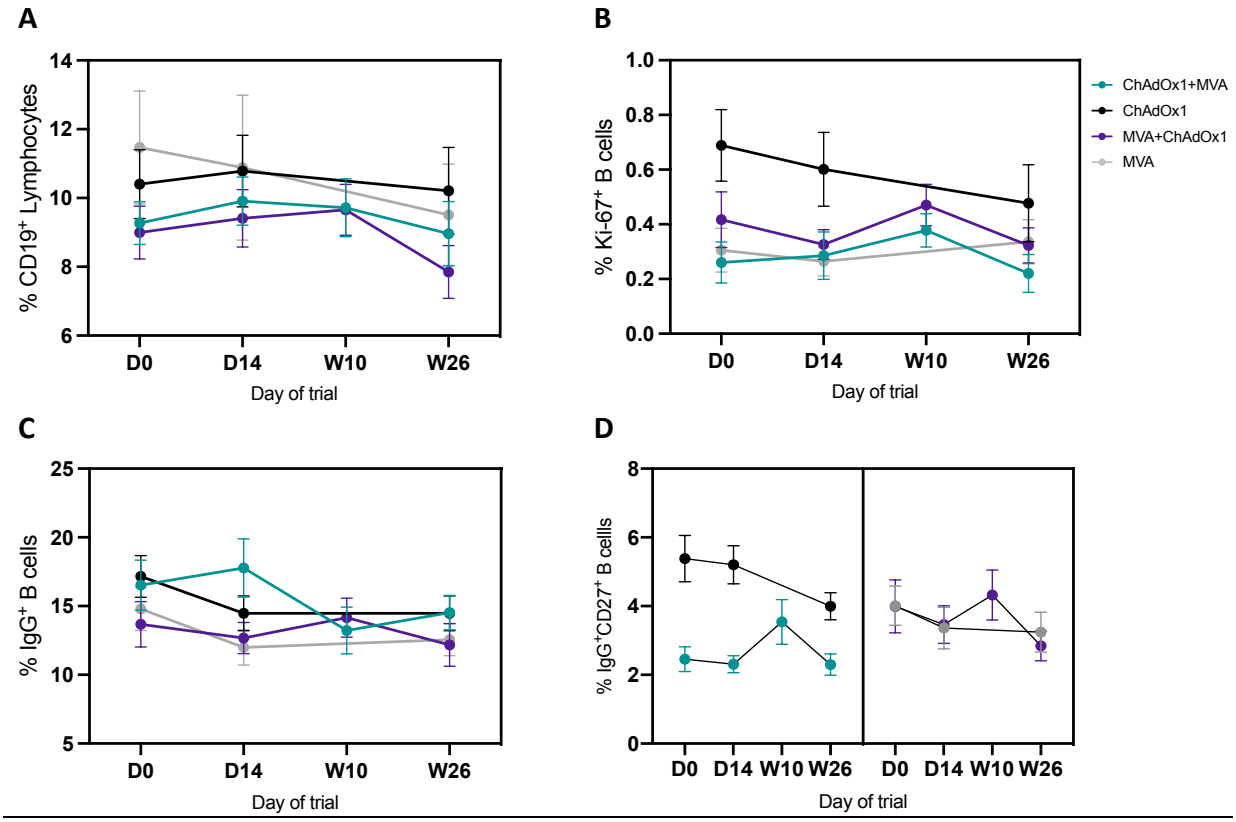
PBMCs from 26 donors vaccinated with ChAdOx1 nCoV-19 were analysed by multi-parameter flow cytometry. B cells were analysed for changes in frequency expression and activation phenotype, including **A)** Ki-67 expression, and **B)** IgG^+ B cell frequency, **C)** IgG^+CD27^+ switched memory B cell frequency, **D)** Ki-67 expression on IgG^+CD27^+ B cells, **E)** IgM^+ B cell frequency, **F)** IgM^+CD27^+ unswitched memory B cell frequency, G) Ki-67 expression on IgG^+CD27^+ B cells, all at 0-, 7-, 14-, and 28-days post-vaccination. Analysis conducted on unstimulated PBMCs.

Statistics conducted using Kruskal-Wallis test with Dunn's multiple comparisons. Error bars shown as mean± SEM.



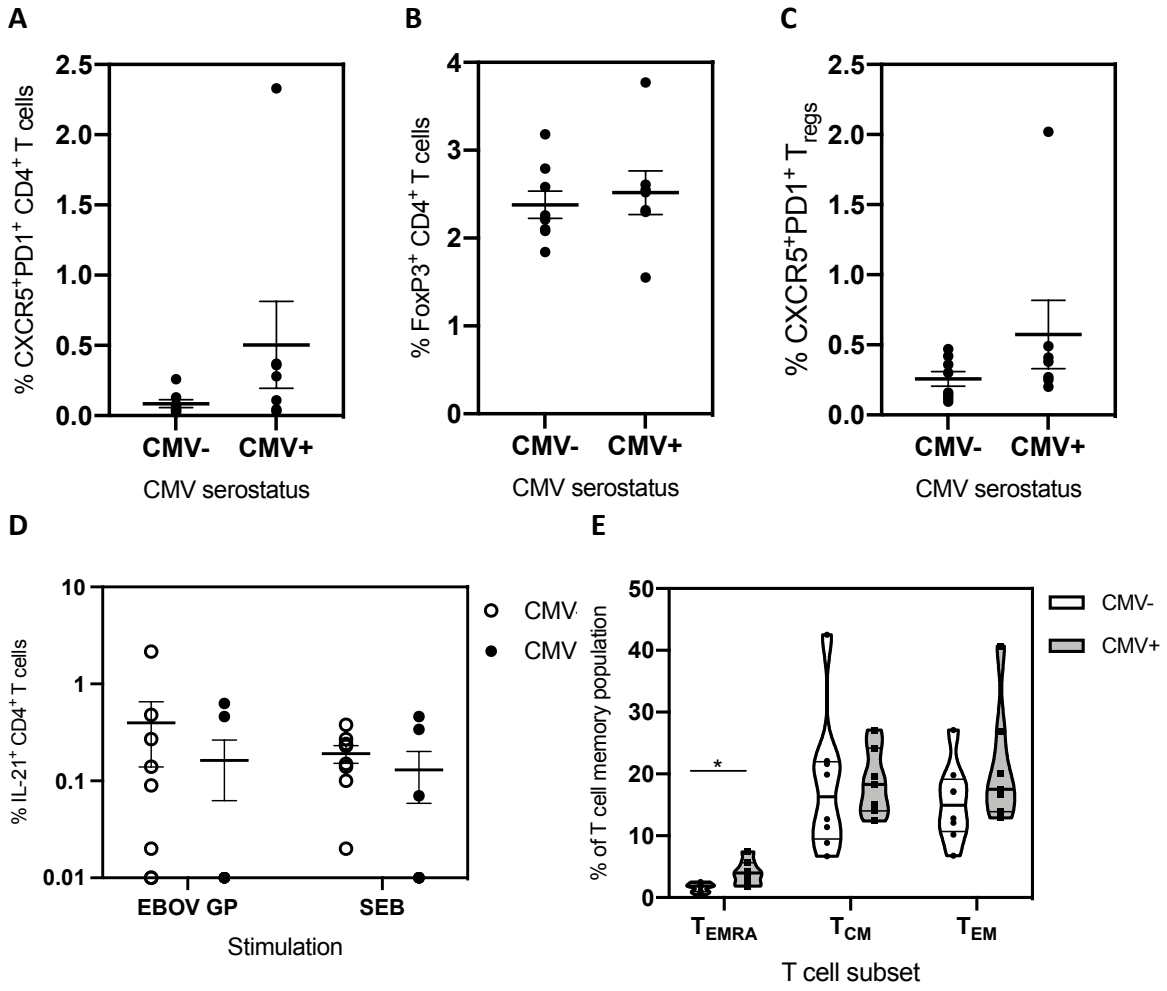
Supplementary Figure 8. Participant details and vaccine schedule for groups 1-4 of the FLU005 vaccine trial

Participants from the FLU005 trial in groups 1-4 were aged between 18-50. **A)** Distribution of age and sex between groups. **B)** The timeline of vaccinations, and time points (displayed in weeks) included in this analysis.



Supplementary Figure 9. B cell phenotype following single dose and heterologous ChAdOx1 and MVA vaccination.

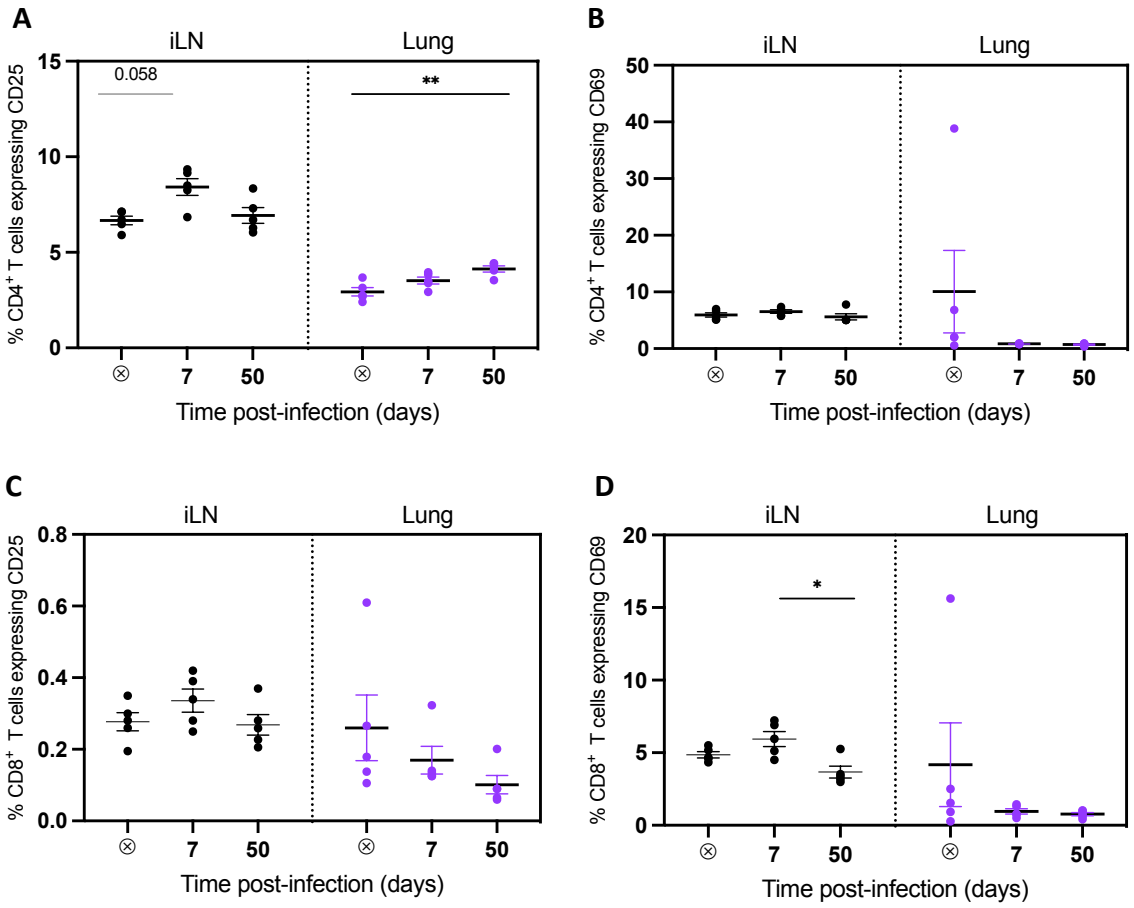
PBMCs from individuals vaccinated as part of the FLU005 vaccine trial were analysed by multi-parameter flow cytometry (Groups 1, 3, 4 n=10, group 2 n=9). B cells were analysed for changes in frequency expression and activation phenotype, including **A)** total frequency of $CD19^+$ B cells, **B)** expression of Ki-67, **C)** IgG^+ B cells, and **D)** switched memory IgG^+CD27^+ B cell at days 0 and 14, and weeks 10 (groups 1 and 3) and 26 post-vaccination. Statistics conducted using Kruskal-Wallis test with Dunn's multiple comparisons. Error bars shown as mean± SEM.



Supplementary Figure 10. T regulatory populations and T cell memory phenotypes in CMV infection

PBMCs from group 2 participants of the EBL04 clinical trial (n=16, time point day 7) were stimulated with either EBOV-GP, SEB, CMV pp65 or left unstimulated as a control. Frequencies of **A)** $CXCR5^+PD1^+$ $CD4^+$ T cells (T_{FH}), **B)** $FoxP3^+$ $CD4^+$ T cells (T_{reg}), and **C)** $CXCR5^+PD1^+FoxP3^+$ $CD4^+$ T cells (T_{FR}). **D)** Secretion of IL-21 by T_{regs} following stimulation with EBOV GP and SEB, **E)** $CD8^+$ T cell memory compartments. T_{EMRA} = $CD45RA^+CCR7^-$, T_{CM} = $CD45RA^-CCR7^+$, T_{EM}=$CD45RA^-CCR7^-$.

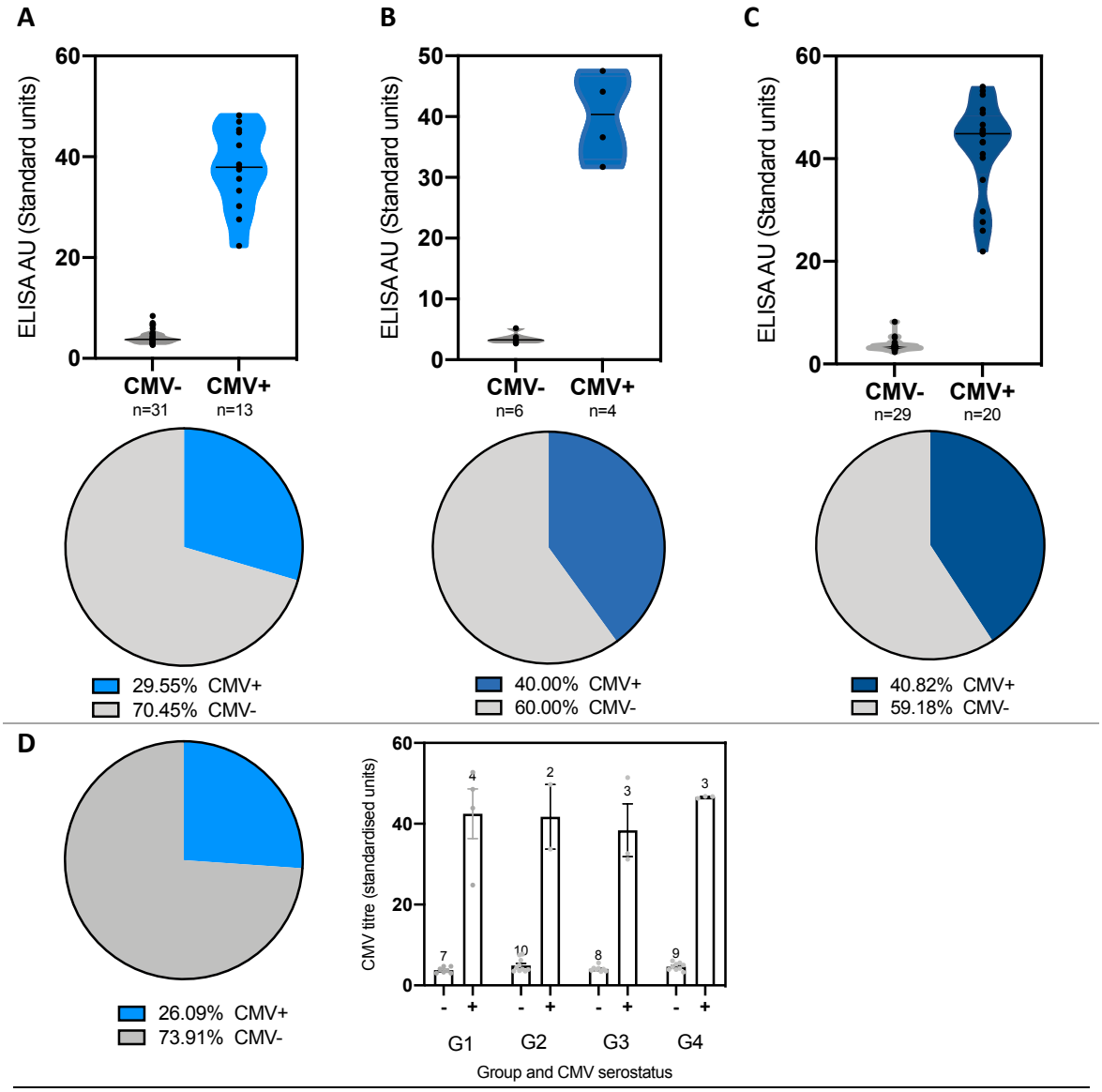
Statistics conducted using Mann-Whitney U test, *p<0.05. Error bars shown as mean± SEM.



Supplementary Figure 11. 50-day and 7-day MCMV infection on CD4⁺ and CD8⁺ T cell CD25 and CD69 expression

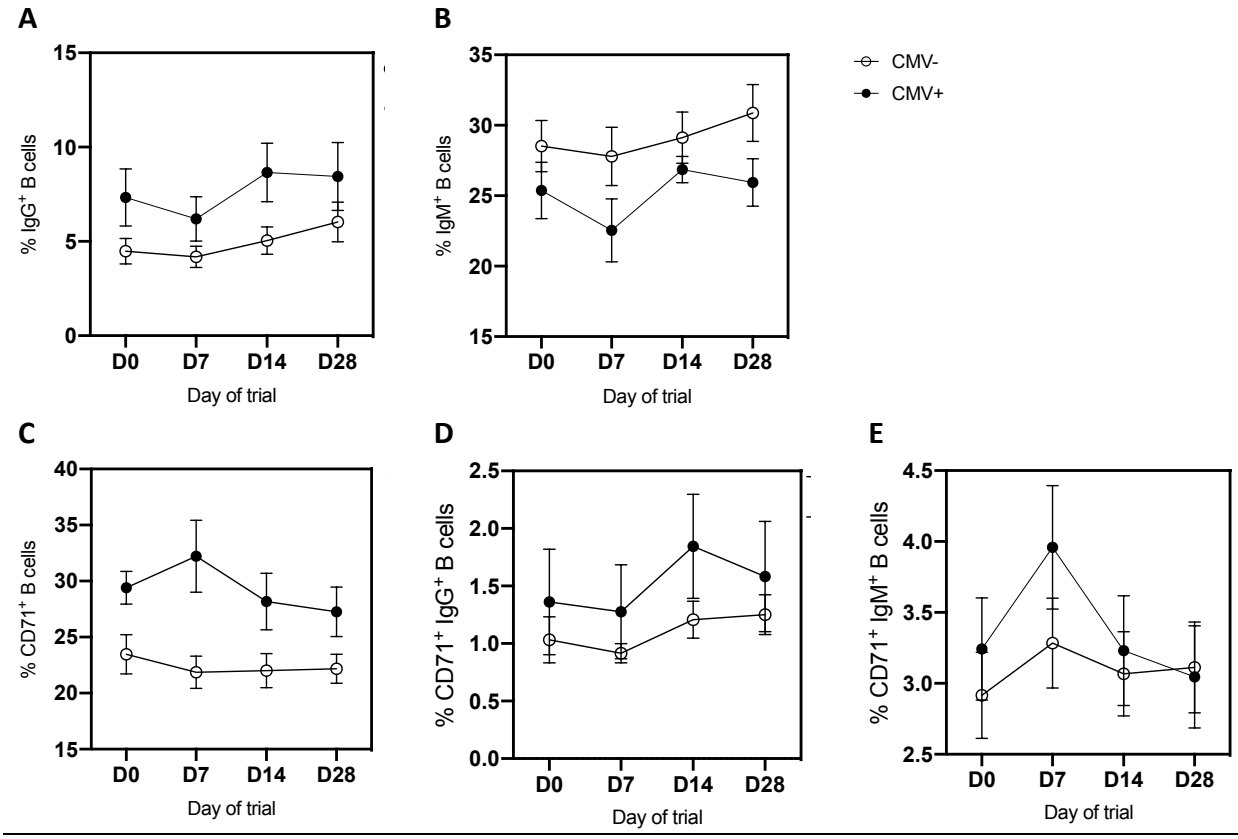
Mice (n=5 per group) were infected with 1x10^6 i.u. MCMV for a chronic (50 days) and acute (7 days) duration or left uninfected as a control (⊗). Inguinal lymph nodes (iLN) and lungs were harvested. CD4⁺ T cells were measured for **A)** CD25, and **B)** CD69 expression, and CD8⁺ T cells were measured **for C)** CD25, and **D)** CD69 expression at days 0 (uninfected), 7 and 50 post infection.

Statistics conducted using Kruskal-Wallis test with Dunn's multiple comparisons, *p<0.05, **p<0.01. Error bars shown as mean± SEM.



Supplementary Figure 12. CMV serotyping of COV001, COV002 and FLU005 younger adults

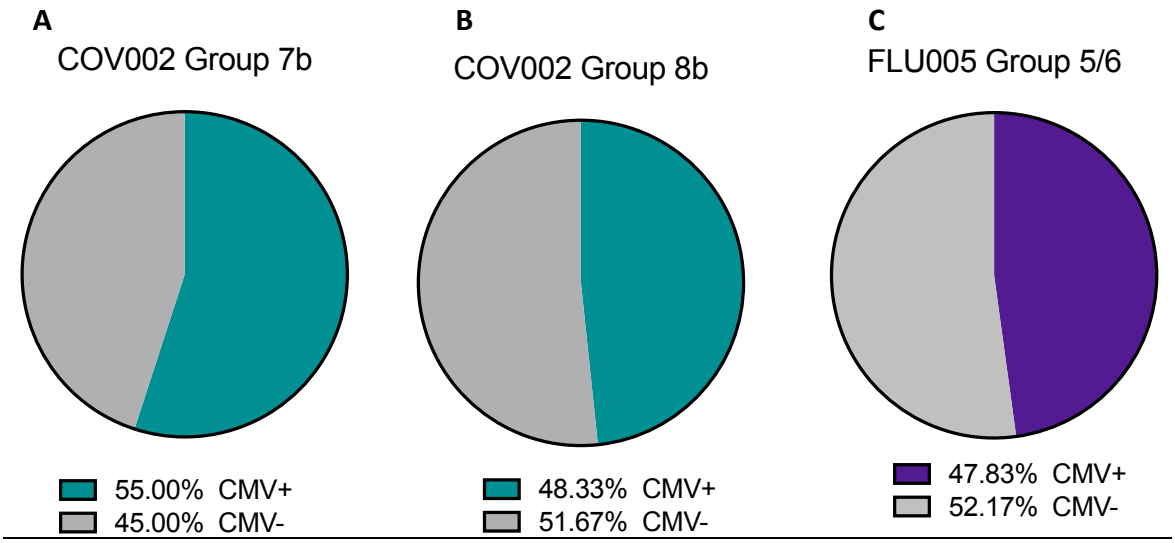
Donors from groups 1 and 3 of the COV001 clinical trial, and group 5d of the COV002 clinical trial were serotyped for CMV by anti-CMV IgG ELISA. **A)** 13/44 donors of COV001 group 1 were CMV seropositive corresponding to 37.5% of the cohort. **B)** 4/10 donors of COV001 group 3 were CMV seropositive corresponding to 40% of the cohort, **C)** 20/49 donors of the COV002 group 5d cohort were CMV seropositive, corresponding to 40.8%. **D)** 12/46 donors from the FLU005 trial were CMV seropositive, corresponding to 26.1% of the cohort. CMV seropositivity was equally distributed across groups 1-4. Data shown as standardised ELISA arbitrary units (ELISA AU).



Supplementary Figure 13. B cell population frequencies stratified by CMV serostatus in COV001 vaccinees.

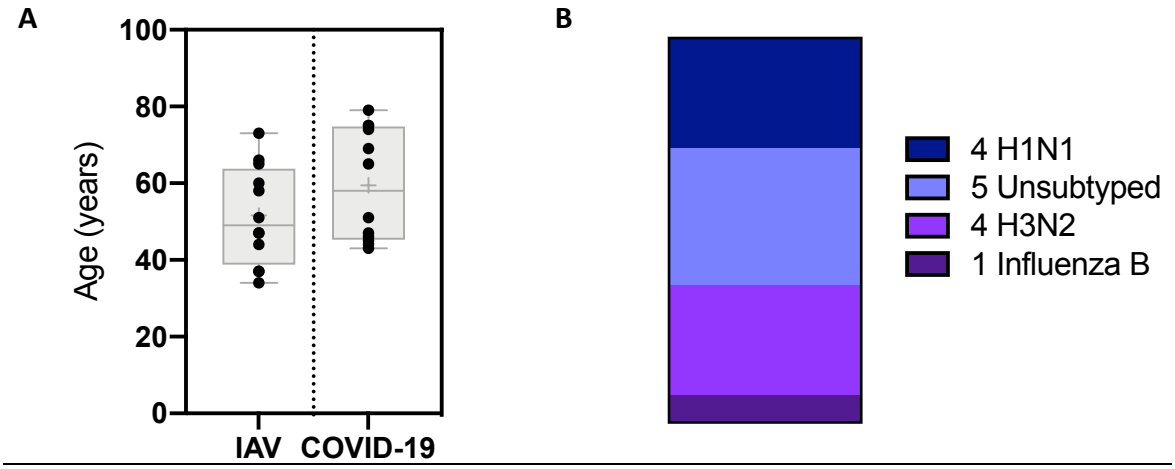
Unstimulated PBMCs from 26 donors from COV001 group 1 were analysed for frequency of B cell populations with regards to CMV infection across post-vaccine time points. **A)** Frequency of IgG^+ B cells, **B)** frequency of IgM^+ B cells. **C)** Frequency of $CD71^+$ B cells. Expression of CD71 on **D)** IgG^+ B cells and **E)** IgM^+ B cells

Statistics conducted using mixed-effect analysis with Sidak multiple comparisons. Error bars shown as mean± SEM.



Supplementary Figure 14. COV002 Groups 7b and 8b and FLU005 groups 5 and 6 CMV titres and seroprevalence

Pie charts showing the distribution of CMV seroprevalence in **A)** COV002 group 7b, **B)** COV002 group 8b, **C)** FLU005 groups 5 and 6.



Supplementary Figure 15. Summary of patient information from IAVCoV study

A) Age range (years) of patients with severe Influenza A or COVID-19 (n=12 in each group), **B)** Different subtypes of influenza diagnosed in study.